frontiers | Research Topics

Overcoming physiologic barriers to treatments for hematologic malignancies by molecularly targeting the tumor microenvironment

Edited by
Lili Feng, Qin Wang and Arif Gulzar

Coordinator by
Chen Wang and Yang-Bao Miao

Published in
Frontiers in Pharmacology
Frontiers in Oncology
Frontiers in Bioengineering and Biotechnology

ISSN 1664-8714
ISBN 978-2-8325-4360-3
DOI 10.3389/978-2-8325-4360-3

About Frontiers

Frontiers is more than just an open access publisher of scholarly articles: it is a pioneering approach to the world of academia, radically improving the way scholarly research is managed. The grand vision of Frontiers is a world where all people have an equal opportunity to seek, share and generate knowledge. Frontiers provides immediate and permanent online open access to all its publications, but this alone is not enough to realize our grand goals.

Frontiers journal series

The Frontiers journal series is a multi-tier and interdisciplinary set of open-access, online journals, promising a paradigm shift from the current review, selection and dissemination processes in academic publishing. All Frontiers journals are driven by researchers for researchers; therefore, they constitute a service to the scholarly community. At the same time, the *Frontiers journal series* operates on a revolutionary invention, the tiered publishing system, initially addressing specific communities of scholars, and gradually climbing up to broader public understanding, thus serving the interests of the lay society, too.

Dedication to quality

Each Frontiers article is a landmark of the highest quality, thanks to genuinely collaborative interactions between authors and review editors, who include some of the world's best academicians. Research must be certified by peers before entering a stream of knowledge that may eventually reach the public - and shape society; therefore, Frontiers only applies the most rigorous and unbiased reviews. Frontiers revolutionizes research publishing by freely delivering the most outstanding research, evaluated with no bias from both the academic and social point of view. By applying the most advanced information technologies, Frontiers is catapulting scholarly publishing into a new generation.

What are Frontiers Research Topics?

Frontiers Research Topics are very popular trademarks of the *Frontiers journals series*: they are collections of at least ten articles, all centered on a particular subject. With their unique mix of varied contributions from Original Research to Review Articles, Frontiers Research Topics unify the most influential researchers, the latest key findings and historical advances in a hot research area.

Find out more on how to host your own Frontiers Research Topic or contribute to one as an author by contacting the Frontiers editorial office: frontiersin.org/about/contact

Overcoming physiologic barriers to treatments for hematologic malignancies by molecularly targeting the tumor microenvironment

Topic editors
Lili Feng — Harbin Engineering University, China
Qin Wang — Southwest Jiaotong University, China
Arif Gulzar — University of Queensland, Australia

Topic Coordinators
Chen Wang — Guangxi Medical University Cancer Hospital, China
Yang-Bao Miao — School of Medicine of University of Electronic Science and Technology of China, China

Citation
Feng, L., Wang, Q., Gulzar, A., Wang, C., Miao, Y.-B., eds. (2024). *Overcoming physiologic barriers to treatments for hematologic malignancies by molecularly targeting the tumor microenvironment*. Lausanne: Frontiers Media SA.
doi: 10.3389/978-2-8325-4360-3

Table of contents

frontiers | Frontiers in Pharmacology

TYPE Original Research
PUBLISHED 05 December 2022
DOI 10.3389/fphar.2022.1076096

OPEN ACCESS

EDITED BY
Qin Wang,
Southwest Jiaotong University, China

REVIEWED BY
Yuhong Jiang,
Southwest Jiaotong University, China
Wang Xiaoxia,
Second Hospital of Shanxi Medical University, China
Xuehua Jiang,
Sichuan University, China

*CORRESPONDENCE
Rong Xiao,
wangxipo126@126.com
Lin He,
helin514@126.com

†These authors have contributed equally to this work

SPECIALTY SECTION
This article was submitted to Pharmacology of Anti-Cancer Drugs, a section of the journal Frontiers in Pharmacology

RECEIVED 21 October 2022
ACCEPTED 18 November 2022
PUBLISHED 05 December 2022

CITATION
Wang X, Dai J, Xia J, Ye Z, Huang X, Cao W, Xiao R and He L (2022), Pomalidomide enhances the maturation of dendritic cells derived from healthy donors and multiple myeloma patients.
Front. Pharmacol. 13:1076096.
doi: 10.3389/fphar.2022.1076096

Pomalidomide enhances the maturation of dendritic cells derived from healthy donors and multiple myeloma patients

Xi Wang[1†], Jingying Dai[1†], Jingyi Xia[1], Zichen Ye[1], Xiaobing Huang[1], Wanjun Cao[2], Rong Xiao[1*] and Lin He[1*]

[1]Sichuan Academy of Medical Sciences and Sichuan Provincial People's Hospital, School of Medicine, University of Electronic Science and Technology of China, Chengdu, China, [2]Department of Pharmacy, Nanchong Central Hospital, Nanchong, China

Objective: To explore the effect of pomalidomide on the maturation of monocyte-derived dendritic cells (moDCs) from healthy donors (HDs) and multiple myeloma (MM) patients.

Methods: MoDCs were generated by the incubation of monocytes from peripheral blood mononuclear cells (PBMCs) for 7 days in a medium consisting of 800 U/ml granulocyte-macrophage colony stimulating factor (GM-CSF), 500 U/ml interleukin-4 (IL-4), RPMI 1,640 medium, 5% human serum, 100 U/ml penicillin and 0.1 mg/ml streptomycin. Meanwhile, the incubation system was administrated with 10 μM pomalidomide or 1 × PBS as the control group. On the eighth day, cells were harvested and analyzed by flow cytometry. The $CD80^+CD86^+$ cell population in total cells was gated as moDCs in the FACS analyzing system. After that, the expression of CD40 and HLA-DR on moDCs was analyzed. Meanwhile, the supernatant from the incubation system was evaluated for the secretion of cytokines interleukin-12 (IL-12), tumor necrosis factor-α (TNF-α), and macrophage inflammatory protein 1α (MIP-1α) by enzyme-linked immunosorbent assay (ELISA).

Results: When analyzing all the HD-moDCs together (n = 15), pomalidomide significantly increased the mean fluorescence intensity (MFI) of CD40 expression and HLA-DR expression on moDCs compared with the control group (p = 0.003, p = 0.040). Meanwhile, the proportion of $CD40^+$ moDCs and $HLA\text{-}DR^+$ moDCs in total moDCs was significantly higher in the pomalidomide group than in the control group (p = 0.008, p = 0.032). When analyzing all MM patient-moDCs together (n = 11), pomalidomide significantly increased the MFI of CD40 expression and HLA-DR expression on moDCs compared with the control group (p = 0.047, p = 0.006). Meanwhile, the proportion of $HLA\text{-}DR^+$ moDCs in total DCs was significantly higher in the pomalidomide group than in the control group (p < 0.001). Moreover, HD-moDCs (n = 8) treated with pomalidomide secreted 192% IL-12, 110% TNF-α, and 112% MIP-1α of the untreated moDCs (p = 0.020, p = 0.006, p = 0.055). However, when analyzing MM patient-moDCs (n = 10) together, the secretion of IL-12, TNF-α and MIP-1α from moDCs showed no significant difference

between the pomalidomide group and the control group (p = 0.458, p = 0.377, p = 0.248).

Conclusion: *In vitro*, 10 μM pomalidomide enhances the maturation of moDCs derived from both HDs and MM patients. Pomalidomide shows potential to be applied as a DC adjuvant for DC-based immunotherapy, such as the DC vaccine and DC cell therapy in MM.

KEYWORDS

pomalidomide, multiple myeloma, monocyte-derived dendritic cells, maturation, DC adjuvant

Introduction

Multiple myeloma is a malignant disease with plasma cell origin, and the incidence of which ranks second in the hematological malignancies (Pinto et al., 2020). MM is still an incurable disease with high recurrence. The pathogenesis of MM is closely relevant to the chromosome deletion, the gene abnormity, and the change of immune microenvironment. Furthermore, immune disorders occur in the early stage of MM (Walker et al., 2018). The immunotherapy strategy which aims to reverse the immune disorders and improve the patients' anti-myeloma immunity can effectively eliminate cancer cells *in vivo* by improving immune surveillance, activation and killing. Thus, immunotherapy is able to achieve a favorable clinical efficacy. Dendritic cells (DCs) play an essential role in initiating the anti-cancer immune response. As the most critical antigen-presenting cell (APC), DCs present major histocompatibility complex (MHC) molecules and tumor antigens to prime naïve T cells. Meanwhile, DCs provide costimulatory signals to T cells for the further activation of T cells (Wang et al., 2016). Thus, DCs act as the most critical first-step in initiating the anti-cancer specific immune response.

It has been found that MM patients show significant immunodeficiency. The immunodeficient DCs of MM patients is one of the main reasons why specific anti-tumor immunity can't be normally and effectively activated (Li and Wang, 2019; Tamura et al., 2019), which leads to the occurrence and development of MM. Therefore, reversing the severe immunodeficiency of DCs in MM patients to improve the activity and maturity of DCs is one of the critical problems to be solved. In recent years, the generation of autologous DCs of MM patients *in vitro* with enhanced activity and maturity has been applied for DC cell therapy in MM patients. This immunotherapy strategy is the frontier research field worldwide with a promising translational future. Although DC immunotherapy has been developing in the past decades, the techniques of *in vitro* generation of DC, which to a certain extent enhance the activity and maturity of patient DC still show a distance from achieving significant clinical efficacy with successful generation of ideally active and mature DC of patients. Therefore, improving the activity and maturity of DCs of MM patients generated *in vitro* to a normal or significantly enhanced level becomes the essential issue to be solved in DC immunotherapy for MM.

Pomalidomide is the third generation of immunomodulatory drugs (IMiDs) as an analogue of thalidomide and lenalidomide. Pomalidomide has not only been approved for treating relapsed/refractory MM due to its direct anti-tumor effect (Rajkumar and Kumar, 2016) but also shows a significant immunomodulatory effect on immune cells. On the one hand, pomalidomide exerts the direct anti-myeloma effect by up-regulating the expression of $P21^{waf1}$ (Escoubet-Lozach et al., 2009), down-regulating the expression of C/EBP β (Li et al., 2011) or activating the caspase 8 (Mitsiades et al., 2002). On the other hand, it has been demonstrated that a combination of pomalidomide and low-dose dexamethasone can activate T cell function by increasing the release of interferon γ (IFN-γ), TNF-α, interleukin-2 (IL-2) derived from the T cells of relapsed/refractory MM patients. In addition, the release of TNF-α, IFN-γ, perforin and granzyme from the NK cells, the expression of CD16, adhesion molecule CD11a on NK cell surface, and the antibody-dependent cell-mediated cytotoxicity effect (ADCC) of NK cells were all enhanced with this regimen (Sehgal et al., 2015). It has been demonstrated that 10 μM pomalidomide inhibits regulatory T cells (Tregs) of HDs *in vitro* based on downregulation of the Foxp3 gene's expression. Detailly, the proportion of $CTLA\text{-}4^{+}FOXP3^{+}$ cells in PBMCs is decreased (Galustian et al., 2009; Bila et al., 2021). Moreover, Henry et al. (2013) have demonstrated that 10 μM pomalidomide significantly increases the antigen uptake of DCs. However, the immunomodulatory effect of pomalidomide on human DCs has not been deeply investigated and clarified. Therefore, we investigated the immunomodulatory effect of pomalidomide on moDCs derived from HDs and MM patients, focusing on the maturation of moDCs in this study.

Materials and methods

Donors

The study has gained approval from the Ethics Committee of the Sichuan Provincial People's Hospital. All the donors enrolled in this study have read and signed

the informed consents. This study included 15 HD donors (10 females and 5 males) and 11 MM patient donors (4 females and 7 males). All the donors should be 18–70 years old. MM patient donors should achieve partial response (PR) or complete response (CR) after treatment. The patient donors should not have immune-related diseases. In addition, the patient donors should not be undergoing chemotherapy at the time of peripheral blood donation.

Materials

Pomalidomide and human AB serum were purchased from Sigma, United States. RPMI 1,640 medium was purchased from Gibco, United States. GM-CSF and IL-4 were purchased from Novoprotein, China. Penicillin-streptomycin solution was purchased from Hyclone, United States. Human Lymphocyte separation medium (Ficoll) was purchased from GE Lifesciences, United States. 1×PBS and DMSO were purchased from Solarbio, China. FITC anti-human CD80 mAb, PE anti-human CD86 mAb, APC anti-human CD40 mAb and Pacific Blue anti-human HLA-DR mAb were all purchased from Biolegend, China.

Acquisition of peripheral blood mononuclear cells

16 ml of peripheral blood was gained from HDs (n = 15) and MM patients (n = 11) after the donors read and signed the informed consents. PBMCs were isolated by density gradient centrifugation. Specifically, equal volume of 1 × PBS was used to dilute the peripheral blood. Then the diluted peripheral blood was slowly added to the top of Ficoll for 30 min of centrifugation (400 × g). PBMCs were collected and washed with 1 × PBS for 3 times.

Dendritic cell generation

PBMCs were evenly divided into two groups and cultured at 5 × 10^6 cells/ml in RPMI 1,640 medium at 37°C in air containing 5% CO2. After 3 h of incubation, monocytes were isolated by adhesion, which were cultured in a medium consisting of 800 U/ml GM-CSF, 500 U/ml IL-4, RPMI 1,640 medium, 5% human serum, 100 U/ml penicillin and 0.1 mg/ml streptomycin for 7 days at 37°C in air containing 5% CO_2. 10 μM pomalidomide was given to one group while 1 × PBS was given to the other group as the control group. On the eighth day, moDCs were harvested. Moreover, the morphology of moDCs was observed by the inverted microscope.

Immunophenotyping by flow cytometry

The expression of DC maturation-related surface makers CD40, HLA-DR, CD80, and CD86 were analyzed by flow cytometry. Pomalidomide or 1 × PBS treated moDCs were resuspended in 100 μl cold 1 × PBS, which was then co-incubated with APC-labeled CD40 mAb, Pacific Blue-labeled HLA-DR mAb, FITC-labeled CD80 mAb and PE-labeled CD86 mAb for 30 min at 4°C. Then cells were washed with cold 1 × PBS twice. At last, the cells were resuspended in 200 μl 1 × PBS for detection by flow cytometer.

The technique for generating moDCs in this study is a usually used and efficient technique, which can successfully generate moDCs from PBMCs (Büll et al., 2017; Sung, 2019). After the process for generating moDCs, there should be a big amount of moDCs in the harvested cells. CD80 and CD86 are typical surface markers of DCs, which are usually used for defining DCs (Xue et al., 2016; Liu et al., 2018). And we found that the $CD80^+$ $CD86^+$ cell population accounted for 74.0%–99.6% of the total cells (removal of adhered cells, cell debris and dead cells). Therefore, the $CD80^+$ $CD86^+$ cell population was regarded as moDCs in this study. Then, the expression of CD40 and HLA-DR on moDCs was analyzed. To be specific, the proportion of $CD40^+$ moDCs and $HLA\text{-}DR^+$ moDCs in total moDCs as well as the MFI of CD40 and HLA-DR on moDCs were analyzed respectively. Data was analyzed by FlowJo 10.4 software (Figure 1).

Cytokine assays by ELISA

The secretion of DC maturation/activity-related cytokines IL-12, TNF-α and MIP-1α was analyzed by ELISA. Supernatant from the incubation system of pomalidomide or 1 × PBS treated moDCs was collected by centrifugation. The concentration of the cytokines IL-12, TNF-α, and MIP-1α in the supernatant was detected by the SEA ELISA kit following the manufacturer's directions. Supernatant from the incubation system of 8 HD-moDCs and 11 MM patient-moDCs were evaluated. The other supernatant samples were not able to be evaluated as a result of the amount, contamination and experimental mistakes.

Statistical analysis

Statistical analysis was performed with SPSS 17.0 software. Graphs were generated by Graphpad Prism 8.3.0 software. The normality of data distribution was determined with the Kolmogorov-Smirnov normality test. Paired t-test was used to compare whether there were differences in the expression of cytokines secreted by moDCs and the expression of DC maturation-related surface makers on moDCs administrated with or without pomalidomide. Independent t-test was used to compare whether there were differences in moDCs between

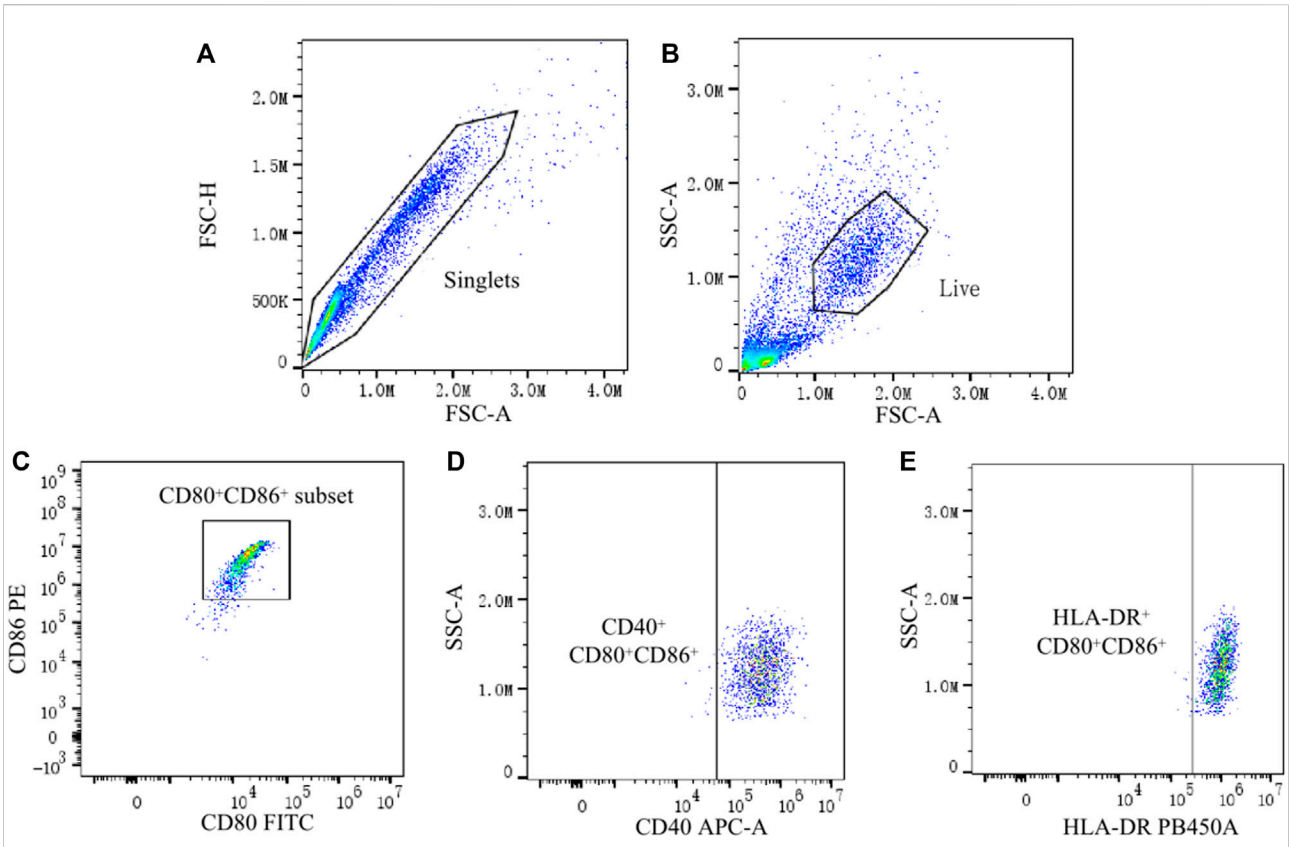

FIGURE 1
Analysis of CD40 and HLA-DR expression on moDCs by flow cytometry. **(A)** Single cells were gated by the Forward Scatter area (FSC-A) and Forward Scatter height (FSC-H). **(B)** Live cells from the single cells were further gated by the FSC-A and Side Scatter area (SSC-A). **(C)** $CD80^+$ $CD86^+$ cells (moDCs) were gated from live cells. **(D,E)** Finally, the expression of CD40 and HLA-DR on $CD80^+$ $CD86^+$ cells were analyzed.

the MM patient group and the HD group. Differences were considered to be significant if the p-value was<0.05 ($^*p < 0.05$, $^{**}p < 0.01$, $^{***}p < 0.001$). All data was expressed as Mean ± Standard Deviation (SD).

Results

The morphology of moDCs

On the eighth day, the morphology of moDCs was observed by the inverted microscope. As shown in Figure 2, the morphology of moDCs is large and irregular. There are apparent protrusions on the surface of moDCs.

The comparison of MM patient-moDCs and HD-moDCs

We firstly compared the proportion of $CD80^+$ $CD86^+$ cells in total cells between the MM patient group and the HD group. It was found that the proportion of $CD80^+$ $CD86^+$ cells in total cells in the HD group was higher than that in the MM patient group, but the difference was not statistically significant (93.49% ± 6.44% vs. 77.04% ± 29.17%, $p = 0.094$) (Figure 3).

The effect of pomalidomide on HD-moDCs

In this study, the differences of HD-moDCs ($n = 15$) between the pomalidomide group and the control group were analyzed. It was found that there was no significant difference in the proportion of $CD80^+$ $CD86^+$ cells in total cells between the pomalidomide group and the control group (95.42% ± 4.50% vs. 93.49% ± 6.44%, $p = 0.287$) (Figure 4). However, the proportion of $CD40^+$ moDCs in total moDCs in the pomalidomide group was significantly higher than that in the control group (96.85% ± 3.08% vs. 93.83% ± 5.67%, $p = 0.008$), and the MFI of CD40 expressed on moDCs in pomalidomide group was also significantly higher than that in the control group ($6.70 \times 10^5 \pm 2.63 \times 10^5$ vs. $5.33 \times 10^5 \pm 1.56 \times 10^5$, $p = 0.003$) (Figure 5). The proportion of $HLA\text{-}DR^+$ moDCs in total moDCs in the pomalidomide group was

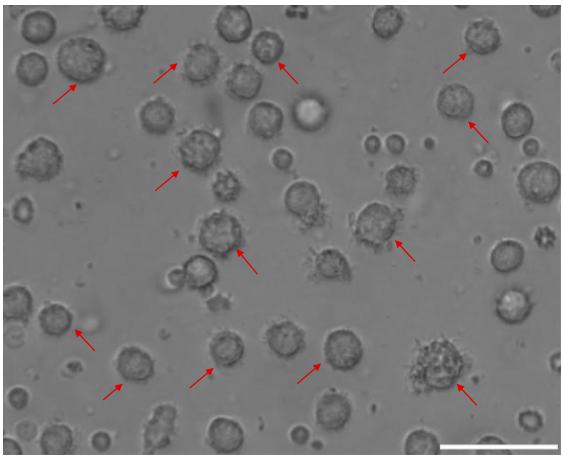

FIGURE 2
The morphology of moDCs. MoDCs are shown by the red arrow (100 μm).

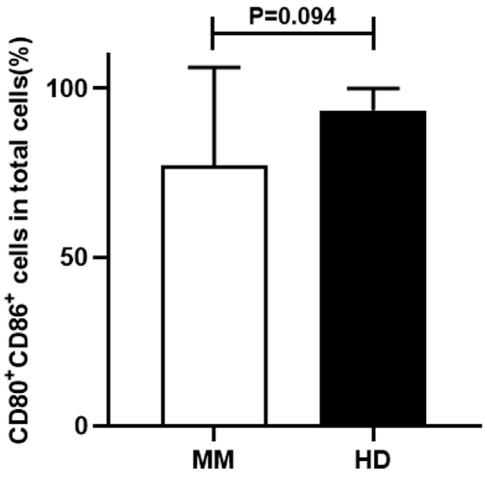

FIGURE 3
The comparison of the proportion of CD80$^+$ CD86$^+$ cells in total cells between the MM patient group and the HD group.

significantly higher than that in the control group (97.73% ± 1.56% vs. 93.36% ± 8.22%, $p = 0.032$), and the MFI of HLA-DR expressed on moDCs in pomalidomide group was also significantly higher than that in the control group ($7.49 \times 10^5 \pm 2.32 \times 10^5$ vs. $6.76 \times 10^5 \pm 2.84 \times 10^5$, $p = 0.040$) (Figure 5). In conclusion, pomalidomide significantly increases the expression of CD40 (costimulatory molecule) and HLA-DR (MHC-II molecular) on HD-moDCs. CD40 and HLA-DR are DC maturation-related surface markers. The results indicate that pomalidomide significantly enhances the maturation of moDCs derived from HDs.

The effect of pomalidomide on MM patient-moDCs

In this study, the differences of MM patient-moDCs ($n = 11$) between the pomalidomide group and the control group were analyzed. It was found that the proportion of CD80$^+$ CD86$^+$ cells in total cells in the pomalidomide group was significantly higher than that in the control group (85.68% ± 29.17% vs. 77.04% ± 19.42%, $p = 0.039$) (Figure 6). There was no significant difference in the proportion of CD40$^+$ moDCs in total moDCs between the pomalidomide group and the control group (97.4% ± 3.08% vs. 96.75% ± 4.18%, $p = 0.443$), but the MFI of CD40 expressed on moDCs was significantly higher in pomalidomide group than that in the control group ($4.27 \times 10^5 \pm 1.90 \times 10^5$ vs. $3.83 \times 10^5 \pm 1.91 \times 10^5$, $p = 0.047$) (Figure 7). The proportion of HLA-DR$^+$ moDCs in total moDCs in the pomalidomide group was significantly higher than that in the control group (97.65% ± 3.87% vs. 92.4% ± 5.31%, $p < 0.001$), and the MFI of HLA-DR expressed on moDCs in pomalidomide group was also significantly higher than that in the control group ($7.23 \times 10^5 \pm 3.06 \times 10^5$ vs. $5.64 \times 10^5 \pm 2.75 \times 10^5$, $p = 0.006$) (Figure 7). Overall, pomalidomide

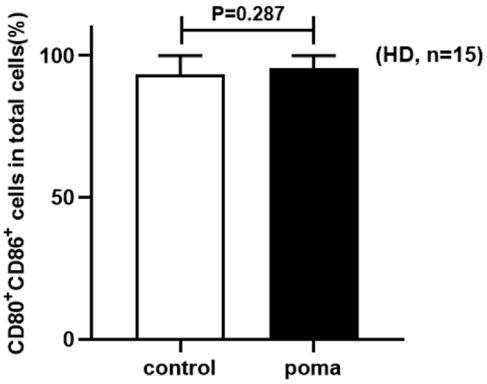

FIGURE 4
The comparison of the proportion of CD80+ CD86+ cells in total cells between the pomalidomide group and the control group in HDs.

significantly increases the expression of CD40 and HLA-DR on MM patient-moDCs. CD40 and HLA-DR are DC maturation-related surface markers. The results suggest pomalidomide significantly enhances the maturation of moDCs derived from MM patients.

Effect of pomalidomide on cytokines produced by HD-moDCs and MM patient-moDCs

MoDCs were treated with 10 μM pomalidomide or without pomalidomide, and supernatant from the incubation system was

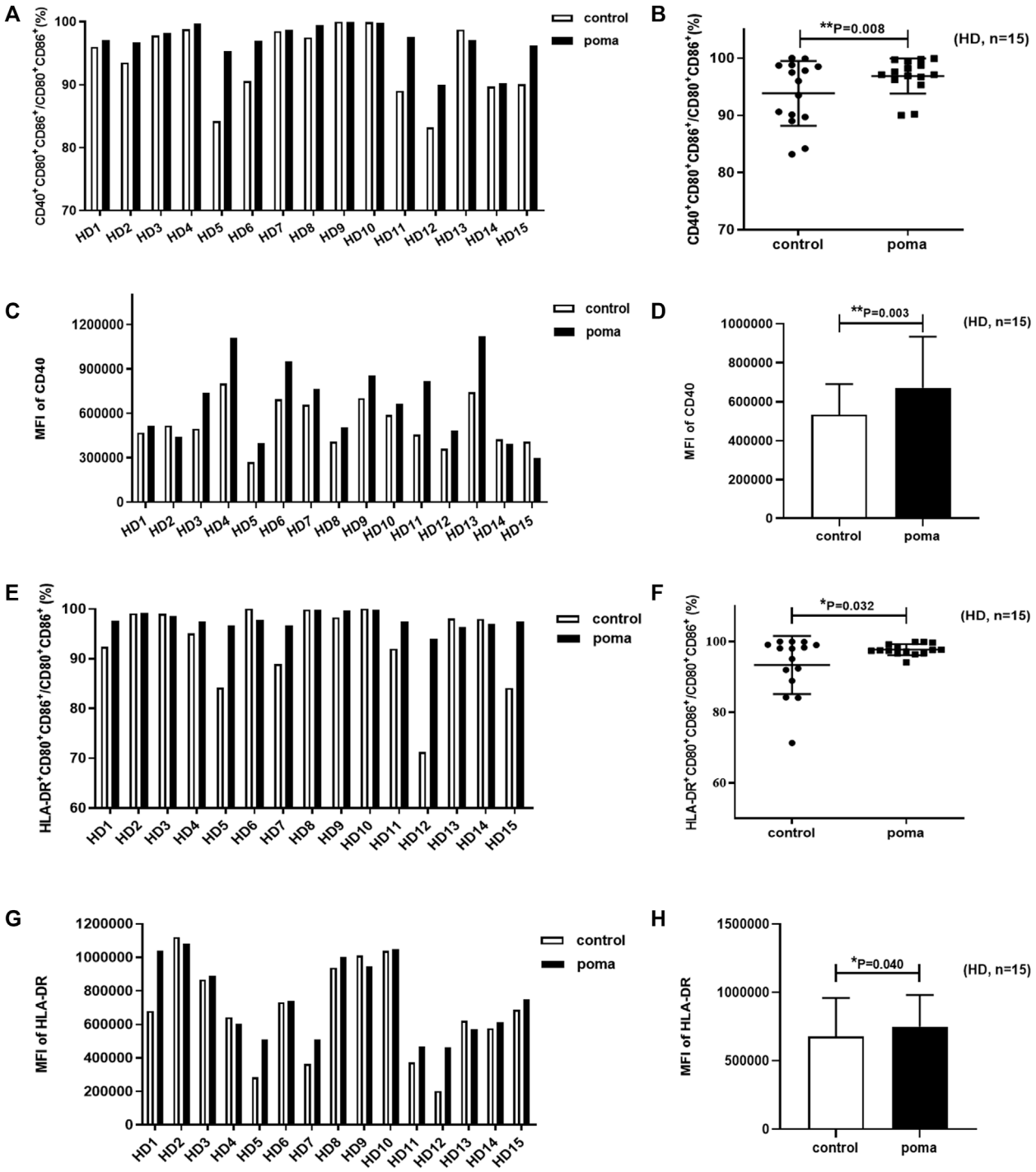

FIGURE 5
The effect of pomalidomide on the expression of maturation-related surface markers of HD-moDCs (n = 15). The proportion of $CD40^+$ moDCs in total moDCs was shown in **(A,B)** while the MFI of CD40 expression on moDCs was shown in **(C,D)**. The proportion of $HLA\text{-}DR^+$ moDCs in total moDCs was shown in **(E,F)** while the MFI of CD40 expression on moDCs was shown in **(G,H)**.

collected on the eighth day. The expression of IL-12, TNF-α, and MIP-1α was analyzed by ELISA. Pomalidomide treated HD-moDCs (n = 8) produced 192% IL-12 (9.42 ± 4.31 vs. 4.90 ± 1.61 pg/ml, p = 0.020), 110% TNF-α (4.54 ± 0.28 vs. 4.11 ± 0.20 pg/ml, p = 0.006) and 112% MIP-1α (14.21 ± 2.54 vs. 12.68 ± 1.53 pg/ml, p = 0.055) of untreated moDCs. However, when

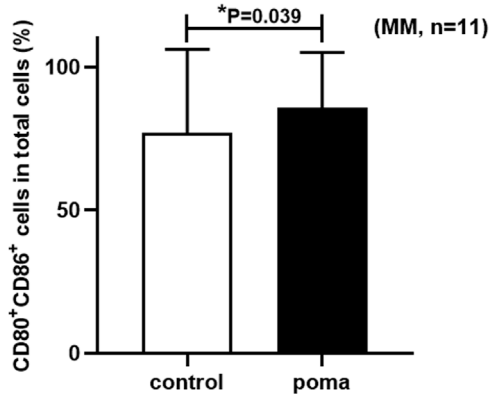

FIGURE 6
The comparison of the proportion of CD80$^+$ CD86$^+$ cells in total cells between the pomalidomide group and the control group in MM patients.

analyzing MM patient-moDCs (n = 10), the expression of IL-12 (6.34 ± 5.51 vs. 8.27 ± 6.88 pg/ml, p = 0.458), TNF-α (4.42 ± 0.21 vs. 4.32 ± 0.32 pg/ml, p = 0.377) and MIP-1α (14.53 ± 2.76 vs. 13.76 ± 2.48 pg/ml, p = 0.248) from moDCs showed no significant difference between pomalidomide group and the control group (Figure 8).

Discussion

It is well known that not only the cancer cells but also the cancer microenvironment plays an essential role in the oncogenesis, progression, and relapse of cancer diseases (Kawano et al., 2017). The immunosuppressive mechanisms during cancer progression mainly include 1) Expansion of regulatory immune cells such as regulatory T cells, 2) Inhibition of immune effector cells such as effector T cells and NK cells, and 3) Dysfunction of APCs (Pinzon-Charry et al., 2005; Andersen, 2014; Vinay et al., 2015). It is well established that MM patients show significant immune deficiency. Importantly, the DCs in MM patients are dysfunctional (Shinde et al., 2018; Li and Wang, 2019; Tamura et al., 2019). Therefore, it is urgent to search for strategies which can improve the function of DCs in MM patients. In this study, we demonstrated that pomalidomide significantly increases the expression of DC maturation-related surface markers CD40 and HLA-DR on MM-patient moDCs. As pomalidomide significantly enhances the maturation of MM patient-moDCs, pomalidomide is an effective and potential strategy to reverse the DC dysfunction of MM patients.

In our study, we firstly compared the HD-moDCs and MM patient-moDCs. The proportion of CD80$^+$ CD86$^+$ cells in total harvested cells in the MM group was lower than that in the HD group, indicating that fewer moDCs can be generated from MM patients than from HDs *in vitro*. Notably, when analyzing moDCs from MM patients, we further found that pomalidomide significantly enhanced the proportion of moDCs in total harvested cells. This result suggested that pomalidomide can increase the number of MM patient-moDCs cultured *in vitro*, which lays the foundation for applying DC-based immunotherapy strategies to MM patients. In addition, the CD40 expression on HD-moDCs was significantly higher than that on MM patient-moDCs, but the expression of HLA-DR as well as the secretion of IL-12, TNF-α and MIP-1α don't show differences between the MM patient group and the HD group (data is not shown). The MM patient donors enrolled in this study all achieved a favorable remission of PR or CR. It is possible that the immune status of these patients has improved with the remission. Thus, further investigations on moDCs from MM patients with different disease stages, such as newly diagnosed MM patients or relapsed MM patients, should be conducted for a comprehensive understanding of the differences between HD-moDCs and MM patient-moDCs.

We then analyzed whether common surface markers of DC maturation were affected by pomalidomide. Pomalidomide induced the significant increases in CD40 and HLA-DR expression on the HD-moDCs and MM patient-moDCs, suggesting pomalidomide can significantly enhance the maturation of moDCs derived from both HDs and MM patients.

Next, we also examined the effect of pomalidomide on the cytokine secretion from DCs to analyze the effect of pomalidomide on the activity/maturation of moDCs. Cytokines secreted by DCs such as interleukin-10 (IL-10), IL-12, interleukin-6 (IL-6), IFN-γ, TNF-α, monocyte chemotactic protein-1 (MCP-1), and MIP-1α can reflect the activity/maturation of DCs (Dudek et al., 2013; Henry et al., 2013; Choi et al., 2018; Gierlich et al., 2020). Among them, the cytokines IL-12, TNF-α, and MIP-1α are most commonly used in many studies, which were detected in this study. HD-moDCs with pomalidomide administration secrete significantly enhanced levels of IL-12 and TNF-α, which indicates that pomalidomide is able to enhance the maturation/activity of HD-moDCs. For those healthy people with high risk of cancer diseases, our results suggest that pomalidomide is potential to enhance the DC maturation/activity of these people, so as to prevent the occurrence of disease or the pre-clinical abnormalities from progression into disease. Moreover, MM patient-derived moDCs with pomalidomide administration secrete enhanced levels of TNF-α and MIP-1α, however, the difference is not statistically significant. This may result from the limited sample size of MM patients. In the future, further research should be conducted with an enlarged sample size of MM patients to demonstrate the effect of pomalidomide on the cytokines secreted by MM patient-moDCs.

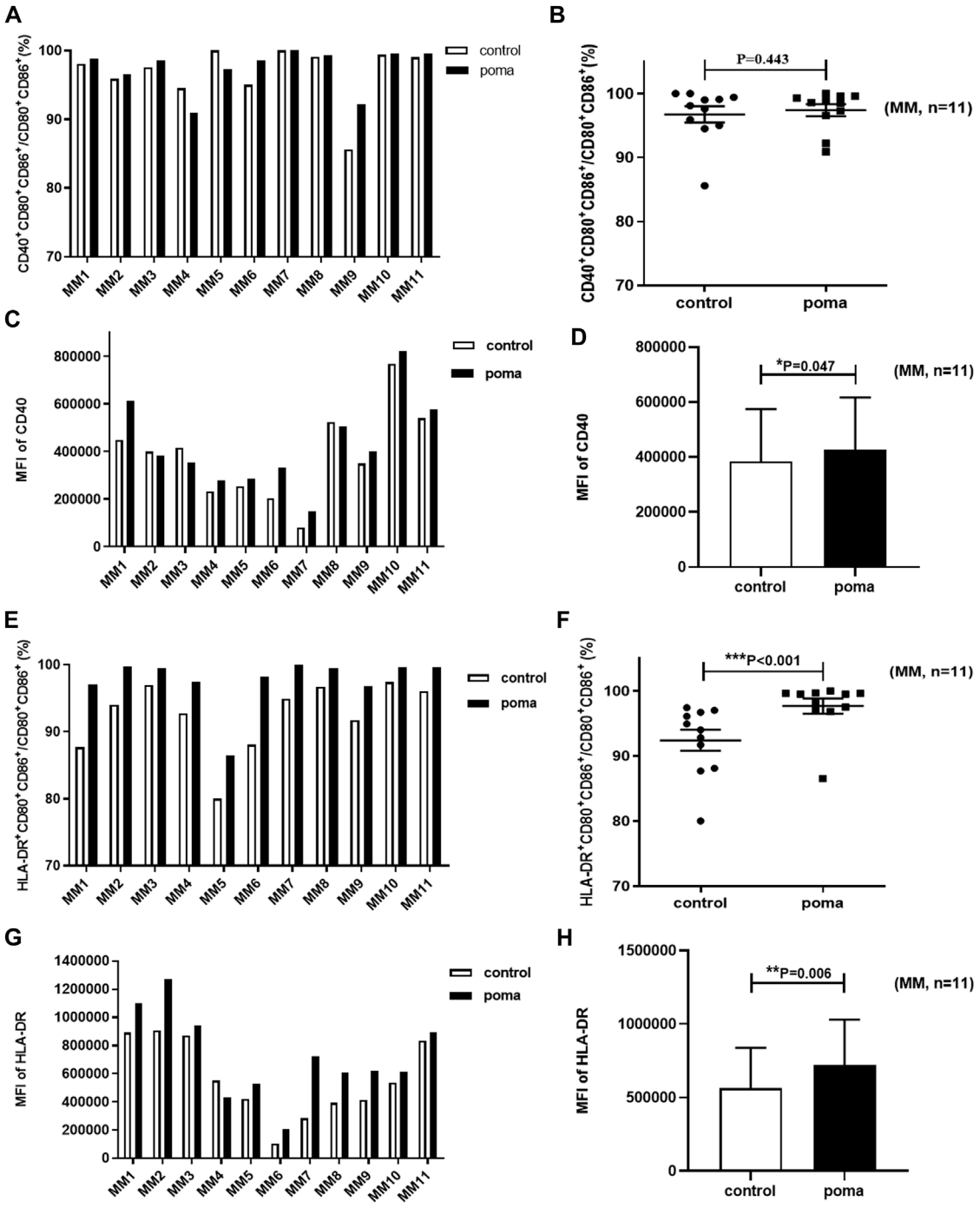

FIGURE 7
The effect of pomalidomide on the expression of maturation-related surface markers of MM patient-moDCs (n = 11). The proportion of $CD40^+$ moDCs in total moDCs was shown in **(A,B)** while the MFI of CD40 expression on moDCs was shown in **(C,D)**. The proportion of $HLA\text{-}DR^+$ moDCs in total moDCs was shown in **(E,F)** while the MFI of HLA-DR expression on moDCs was shown in **(G,H)**.

In conclusion, our study indicates that pomalidomide enhances the maturation of HD-moDCs and MM patient-moDCs. This mechanism possibly contributes to the total therapeutic efficacy of pomalidomide in MM patients. In addition, pomalidomide shows the potential as a DC adjuvant for application in DC-based therapeutic strategies, such as DC vaccine and DC cell therapy.

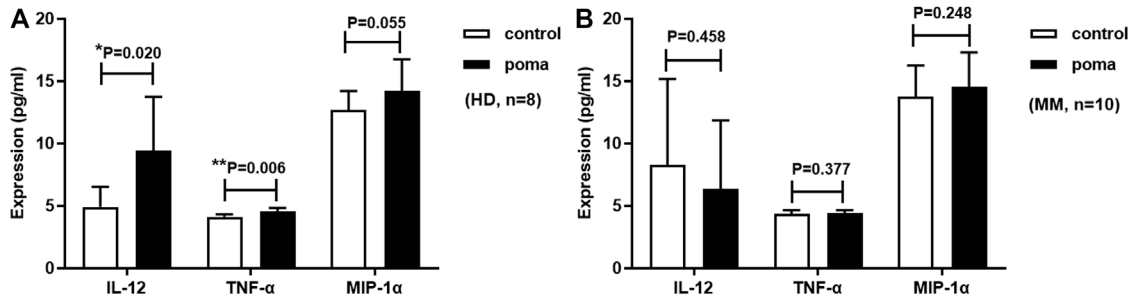

FIGURE 8
Pomalidomide affects moDC cytokine expression. **(A)** shows that the expression of IL-12 and TNF-α produced by pomalidomide treated HD-moDCs was significantly higher than untreated HD-moDCs (n = 8). **(B)** shows that the expression of IL-12, TNF-α, and MIP-1α from MM patient-moDCs showed no significant difference between the pomalidomide group and the control group (n = 10).

Data availability statement

The original contributions presented in the study are included in the article/supplementary material, further inquiries can be directed to the corresponding author.

Ethics statement

The studies involving human participants were reviewed and approved by the Ethics Committee of the Sichuan Provincial People's Hospital. The patients/participants provided their written informed consent to participate in this study.

Author contributions

Conception and design of the experiments: LH, RX, XW, and JD; collection, analysis, and interpretation of the data: JD, XW, JX, ZY, XH, and WC; writing—original draft: XW and JD; writing—review and editing: LH and RX.

Funding

Youth Program of the National Natural Science Foundation of China (Grant Number. 82003767), the Sichuan Academy of Medical Sciences and the Sichuan Provincial People's Hospital clinical study and translational fund (Grant Number. 2020LZ01), Sichuan Provincial Cadre Health Care Project (Grant Number. 2018-244).

Conflict of interest

The authors declare that the research was conducted in the absence of any commercial or financial relationships that could be construed as a potential conflict of interest.

Publisher's Note

All claims expressed in this article are solely those of the authors and do not necessarily represent those of their affiliated organizations, or those of the publisher, the editors and the reviewers. Any product that may be evaluated in this article, or claim that may be made by its manufacturer, is not guaranteed or endorsed by the publisher.

References

Andersen, M. H. (2014). The targeting of immunosuppressive mechanisms in hematological malignancies. *Leukemia* 28, 1784–1792. doi:10.1038/leu.2014.108

Bila, J., Katodritou, E., Guenova, M., Basic-Kinda, S., Coriu, D., Dapcevic, M., et al. (2021). Bone marrow microenvironment interplay and current clinical practice in multiple myeloma: A review of the balkan myeloma study group. *J. Clin. Med.* 10, 3940. doi:10.3390/jcm10173940

Büll, C., Collado-Camps, E., Kers-Rebel, E. D., Heise, T., Søndergaard, J. N., den Brok, M. H., et al. (2017). Metabolic sialic acid blockade lowers the activation threshold of moDCs for TLR stimulation. *Immunol. Cell Biol.* 95, 408–415. doi:10.1038/icb.2016.105

Choi, S., Choi, H. G., Lee, J., Shin, K. W., and Kim, H. J. (2018). Mycobacterium tuberculosis protein Rv2220 induces maturation and activation of dendritic cells. *Cell. Immunol.* 328, 70–78. doi:10.1016/j.cellimm.2018.03.012

Dudek, A. M., Martin, S., Garg, A. D., and Agostinis, P. (2013). Immature, semi-mature, and fully mature dendritic cells: Toward a DC-cancer cells interface that augments anticancer immunity. *Front. Immunol.* 4, 438. doi:10.3389/fimmu.2013.00438

Escoubet-Lozach, L., Lin, I. L., Jensen-Pergakes, K., Brady, H. A., Gandhi, A. K., Schafer, P. H., et al. (2009). Pomalidomide and lenalidomide induce p21 WAF-1 expression in both lymphoma and multiple myeloma through a LSD1-mediated epigenetic mechanism. *Cancer Res.* 69, 7347–7356. doi:10.1158/0008-5472.CAN-08-4898

Galustian, C., Meyer, B., Labarthe, M. C., Dredge, K., Klaschka, D., Henry, J., et al. (2009). The anti-cancer agents lenalidomide and pomalidomide inhibit the proliferation and function of T regulatory cells. Cancer immunology, immunotherapy: CII. *Cancer Immunol. Immunother.* 58, 1033–1045. doi:10.1007/s00262-008-0620-4

Gierlich, P., Lex, V., Technau, A., Keupp, A., Morper, L., Glunz, A., et al. (2020). Prostaglandin E2 in a TLR3- and 7/8-agonist-based DC maturation cocktail generates mature, cytokine-producing, migratory DCs but impairs antigen cross-presentation to CD8+ T cells. Cancer immunology, immunotherapy: CII. *Cancer Immunol. Immunother.* 69, 1029–1042. doi:10.1007/s00262-019-02470-1

Henry, J. Y., Labarthe, M. C., Meyer, B., Dasgupta, P., Dalgleish, A. G., and Galustian, C. (2013). Enhanced cross-priming of naive CD8+ T cells by dendritic cells treated by the IMiDs® immunomodulatory compounds lenalidomide and pomalidomide. *Immunology* 139, 377–385. doi:10.1111/imm.12087

Kawano, Y., Roccaro, A. M., Ghobrial, I. M., and Azzi, J. (2017). Multiple myeloma and the immune microenvironment. *Curr. Cancer Drug Targets* 17, 806–818. doi:10.2174/1568009617666170214102301

Li, L., and Wang, L. (2019). Multiple myeloma: What do we do about immunodeficiency? *J. Cancer* 10, 1675–1684. doi:10.7150/jca.29993

Li, S., Pal, R., Monaghan, S. A., Schafer, P., Ouyang, H., Mapara, M., et al. (2011). IMiD immunomodulatory compounds block C/EBP{beta} translation through eIF4E down-regulation resulting in inhibition of MM. *Blood* 117, 5157–5165. doi:10.1182/blood-2010-10-314278

Liu, K., He, K., Xue, T., Liu, P., and Xu, L. X. (2018). The cryo-thermal therapy-induced IL-6-rich acute pro-inflammatory response promoted DCs phenotypic maturation as the prerequisite to CD4+ T cell differentiation. *Int. J. Hyperth.* 34, 261–272. doi:10.1080/02656736.2017.1332394

Mitsiades, N., Mitsiades, C. S., Poulaki, V., Chauhan, D., Richardson, P. G., Hideshima, T., et al. (2002). Apoptotic signaling induced by immunomodulatory thalidomide analogs in human multiple myeloma cells: Therapeutic implications. *Blood* 99, 4525–4530. doi:10.1182/blood.v99.12.4525

Pinto, V., Bergantim, R., Caires, H. R., Seca, H., Guimarães, J. E., and Vasconcelos, M. H. (2020). Multiple myeloma: Available therapies and causes of drug resistance. *Cancers* 12, 407. doi:10.3390/cancers12020407

Pinzon-Charry, A., Maxwell, T., and López, J. A. (2005). Dendritic cell dysfunction in cancer: A mechanism for immunosuppression. *Immunol. Cell Biol.* 83, 451–461. doi:10.1111/j.1440-1711.2005.01371.x

Rajkumar, S. V., and Kumar, S. (2016). Multiple myeloma: Diagnosis and treatment. *Mayo Clin. Proc.* 91, 101–119. doi:10.1016/j.mayocp.2015.11.007

Sehgal, K., Das, R., Zhang, L., Verma, R., Deng, Y., Kocoglu, M., et al. (2015). Clinical and pharmacodynamic analysis of pomalidomide dosing strategies in myeloma: Impact of immune activation and cereblon targets. *Blood* 125, 4042–4051. doi:10.1182/blood-2014-11-611426

Shinde, P., Fernandes, S., Melinkeri, S., Kale, V., and Limaye, L. (2018). Compromised functionality of monocyte-derived dendritic cells in multiple myeloma patients may limit their use in cancer immunotherapy. *Sci. Rep.* 8, 5705. doi:10.1038/s41598-018-23943-w

Sung, S. J. (2019). Monocyte-derived dendritic cells as antigen-presenting cells in T-cell proliferation and cytokine production. *Methods Mol. Biol.* 2020, 131–141. doi:10.1007/978-1-4939-9591-2_9

Tamura, H., Ishibashi, M., Sunakawa, M., and Inokuchi, K. (2019). Immunotherapy for multiple myeloma. *Cancers* 11, 2009. doi:10.3390/cancers11122009

Vinay, D. S., Ryan, E. P., Pawelec, G., Talib, W. H., Stagg, J., Elkord, E., et al. (2015). Immune evasion in cancer: Mechanistic basis and therapeutic strategies. *Semin. Cancer Biol.* 35, S185–S198. doi:10.1016/j.semcancer.2015.03.004

Walker, B. A., Mavrommatis, K., Wardell, C. P., Ashby, T. C., Bauer, M., Davies, F. E., et al. (2018). Identification of novel mutational drivers reveals oncogene dependencies in multiple myeloma. *Blood* 132, 587–597. doi:10.1182/blood-2018-03-840132

Wang, H., Wu, S., Huang, S., Yin, S., Zou, G., Huang, K., et al. (2016). Follistatin-like protein 1 contributes to dendritic cell and T-lymphocyte activation in nasopharyngeal carcinoma patients by altering nuclear factor κb and jun N-terminal kinase expression. *Cell biochem. Funct.* 34, 554–562. doi:10.1002/cbf.3227

Xue, T., Liu, P., Zhou, Y., Liu, K., Yang, L., Moritz, R. L., et al. (2016). Interleukin-6 induced "acute" phenotypic microenvironment promotes Th1 anti-tumor immunity in cryo-thermal therapy revealed by shotgun and parallel reaction monitoring proteomics. *Theranostics* 6, 773–794. doi:10.7150/thno.14394

frontiers | Frontiers in Oncology

TYPE Mini Review
PUBLISHED 20 December 2022
DOI 10.3389/fonc.2022.1091782

OPEN ACCESS

EDITED BY
Lili Feng,
Harbin Engineering University, China

REVIEWED BY
Pooya Farhangnia,
Iran University of Medical Sciences, Iran

*CORRESPONDENCE
Jin Zhang
Jeanzhang@zju.edu.cn

SPECIALTY SECTION
This article was submitted to Pharmacology of Anti-Cancer Drugs, a section of the journal Frontiers in Oncology

RECEIVED 07 November 2022
ACCEPTED 06 December 2022
PUBLISHED 20 December 2022

CITATION
Jin S, Zhang Y, Zhou F, Chen X, Sheng J and Zhang J (2022) TIGIT: A promising target to overcome the barrier of immunotherapy in hematological malignancies. *Front. Oncol.* 12:1091782. doi: 10.3389/fonc.2022.1091782

TIGIT: A promising target to overcome the barrier of immunotherapy in hematological malignancies

Shenhe Jin[1], Ye Zhang[1], Fengping Zhou[1], Xiaochang Chen[1], Jianpeng Sheng[2] and Jin Zhang[1*]

[1]Department of Hematology, Sir Run Run Shaw Hospital, College of Medicine, Zhejiang University, Hangzhou, China, [2]School of Biological Sciences, Nanyang Technological University, Singapore, Singapore

Immune evasion through up-regulating checkpoint inhibitory receptors on T cells plays an essential role in tumor initiation and progression. Therefore, immunotherapy, including immune checkpoint inhibitor targeting programmed cell death protein 1 (PD-1) and chimeric antigen receptor T cell (CAR-T) therapy, has become a promising strategy for hematological malignancies. T cell immunoreceptor with immunoglobulin and ITIM domain (TIGIT) is a novel checkpoint inhibitory receptor expressed on immune cells, including cytotoxic T cells, regulatory T cells, and NK cells. TIGIT participates in immune regulation *via* binding to its ligand CD155. Blockage of TIGIT has provided evidence of considerable efficacy in solid tumors in preclinical research and clinical trials, especially when combined with PD-1 inhibition. However, the mechanism and function of TIGIT in hematological malignancies have not been comprehensively studied. In this review, we focus on the role of TIGIT in hematological malignancies and discuss therapeutic strategies targeting TIGIT, which may provide a promising immunotherapy target for hematological malignancies.

KEYWORDS

TIGIT, immunotherapy, hematological malignancy, lymphoma, multiple myeloma, leukemia

Introduction

Hematological malignancy is a group of clonal malignant diseases of the hemopoietic system with highly invasive potential and heterogeneity. Despite those treatments, including chemotherapy and stem cell transplantation, improving survival, some patients still experience disease relapse without long-term survival, partly due to tumor evasion from immune recognition and killing by effector cells (1–3). In recent

years, immune checkpoint blockade (ICB) therapy targeting cytotoxic T lymphocyte-associated protein 4 (CTLA-4) or programmed cell death protein 1 (PD-1), and chimeric antigen receptor T cell (CAR-T) therapy utilizing genetic engineering to alter T cells to produce transmembrane proteins on the cell surface with an extracellular antibody fragment domain that recognizes tumor antigen, brings a new direction for cancer immunotherapy (4–6). Although anti-PD-1 monoclonal antibodies (mAbs) and CAR-T therapies have been actively applied in relapsed and refractory lymphoma, multiple myeloma (MM), and leukemia, which also achieved remarkable success in some cases, a part of patients still have no response to these therapies (7–10). Therefore, in-depth research on immune checkpoint molecules' interaction mechanisms and the discovery of novel target to overcome the barrier of immunotherapy are necessary. In addition, immune checkpoint inhibitor-related toxicity is another challenge. For example, Quagliariello reported that nivolumab and pembrolizumab would induce cardiotoxicity by increasing the inflammation of cardiomyocytes (11, 12). T cell immunoglobulin and ITIM domain (TIGIT), another inhibitory immune checkpoint molecule, has emerged as a potential target in cancer immunotherapy (13, 14). In this review, we focus on the immunomodulatory role and mechanism of TIGIT, discuss its potential as an immune target in hematological malignancies.

TIGIT structure and its ligands

TIGIT, also named as V-set and immunoglobulin domain-containing protein 9 (VSIG9), V-set and transmembrane do-maincontaining protein 3 (VSTM3) and Washington University cell adhesion molecule (WUCAM), is a co-inhibitory molecule belonging to the immunoglobulin superfamily that was first discovered in 2009 (15–17). It consists of an extracellular immunoglobulin variable (IgV) domain, a type I transmembrane domain and an intracellular domain with an immunoreceptor tyrosine-based inhibitory motif (ITIM) and an immunoglobulin tail tyrosine (ITT)-like motif (18). TIGIT is exclusively expressed on natural killer (NK) cells and T cells, including CD8+ T cells, CD4+ T cells, and regulatory T cells (Tregs) (19, 20).

The relationship between TIGIT, its ligands, and competitive receptors is complex. On the one hand, the immunoglobulin variable domain of TIGIT shares sequence homology with members of the polio virus receptors (PVR) family, including CD155 (also named as Necl-5 or PVR), CD112 (also named as Nectin-2 or PVRL2), CD113 (also named as Nectin-3 or PVRL3), and Nectin-4 (PVRL4) (21, 22). CD155 is a member of the immunoglobulin superfamily, mainly expressed on dendritic cells (DCs), macrophages, and lymphocytes. CD112 belongs to single-pass type-I membrane glycoproteins, which is expressed on DCs and monocytes. Interestingly, CD155 and CD112 are over-expressed on different cancer cells as reported recently (23–26). In addition, CD155 has a higher affinity than CD112 to TIGIT, which became the primary ligand for TIGIT (27). By interacting with its ligands, TIGIT participates in the regulation of cellular immune function. On the other hand, TIGIT shares these ligands with other receptors, including CD226 (DNAM-1) and CD96 (TACTILE). As the costimulatory receptor, CD226 competes with TIGIT for binding to CD155 in spite of its lower affinity (27). Furthermore, CD226 also competes with TIGIT and CD112R (PVRIG) for binding to CD112 (28, 29). Therefore, CD226 also plays an essential role in immune regulation (Figure 1).

Function and mechanism of TIGIT in immune regulation

Through complex interaction with ligands, TIGIT family receptors transfer inhibitory signals to immune cells, contributing to innate and adaptive immunity regulation (30–32). On the one hand, TIGIT inhibits the activity of T cells intrinsically. Firstly, TIGIT binds to CD155 and transmits intracellular inhibitory signals, directly suppressing T cell receptor (TCR) expression and signaling. Engagement of TIGIT induces down-regulation of the TCRα chain and molecules that comprise the TCR complex, as well as reduction of TCR-induced p-ERK signaling and interferon-γ (IFNγ) production in CD8+ T cells (33, 34). Secondly, TIGIT possesses a higher affinity of CD155 when competing with its costimulatory counterpart CD226, which impaires T cell function by either directly disrupting homodimerization of CD226 or decreasing expression of T-bet and production of IFNγ (35, 36).

Abbreviations: ICB, immune checkpoint blockade; CTLA-4, cytotoxic T lymphocyte-associated protein 4; PD-1, programmed cell death protein 1; CAR-T, chimeric antigen receptor T cell; mAbs, monoclonal antibodies; MM, multiple myeloma; TIGIT, T cell immunoglobulin and ITIM domain; VSIG9, V-set and immunoglobulin domain-containing protein 9; VSTM3, V-set and transmembrane do-maincontaining protein 3; WUCAM, Washington University cell adhesion molecule; IgV, immunoglobulin variable; ITIM, immunoreceptor tyrosine-based inhibitory motif; ITT, immunoglobulin tail tyrosine; NK, natural killer; Tregs, regulatory T cells; PVR, polio virus receptors; DCs, dendritic cells; TCR, T cell receptor; IFNγ, interferon-γ; IL-10, interleukin-10; Fgl2, fibrinogen-like protein 2; Th1, T helper 1 cells; ERK, extracellular signal-regulated kinase; TNFα, tumor necrosis factor α; TILs, tumor infiltrating lymphocytes; FL, follicular lymphoma; CLL, chronic lymphocytic leukemia; IgHv, immunoglobulin heavy chain variable region; cHL, classic hodgkin lymphoma; AML, acute myeloid leukemia; allo-SCT, allogeneic stem cell transplantation; irAEs, immune-related adverse events; LAG-3, lymphocyte activation gene 3; TIM-3, T-cell immunoglobulin-3; HIF-1α, hypoxia-inducible factor 1-alpha.

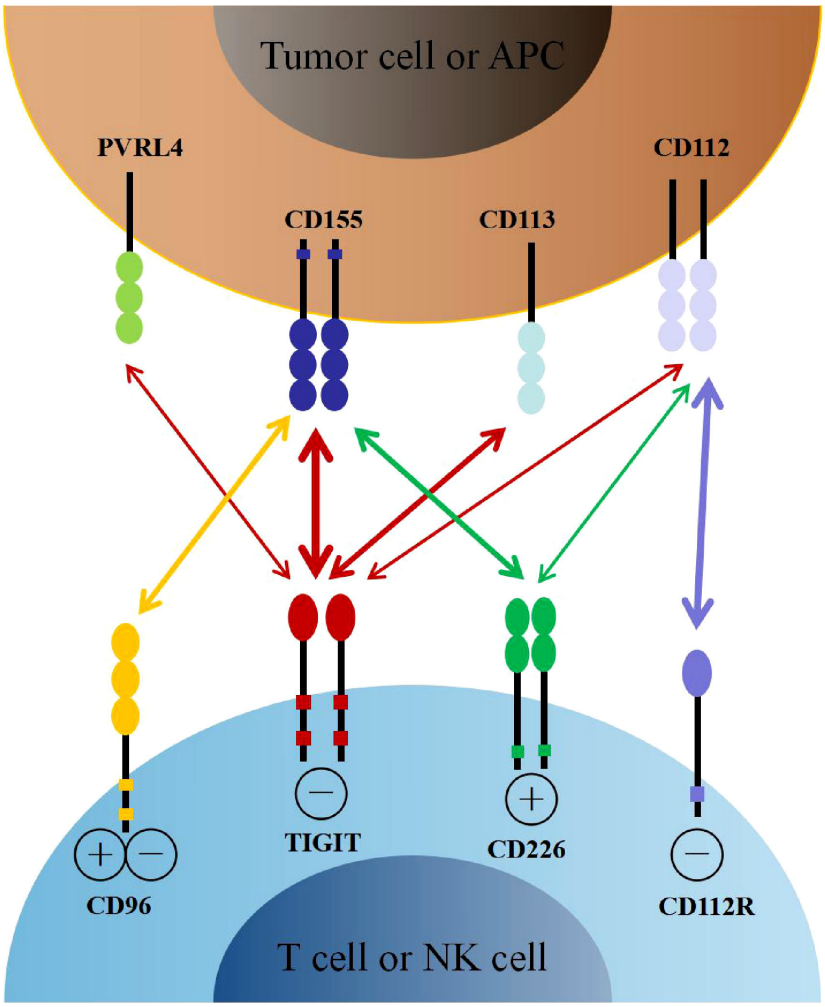

FIGURE 1
The interaction of TIGIT family receptors and ligands. TIGIT, CD226, CD96 and CD112R are expressed on T cells and NK cells. The ligands CD155, CD113, CD112 and PVRL4 are expressed on tumor cells or APCs. TIGIT delivers inhibitory signals by binding to CD155, CD113, CD112 and PVRL4, with highest affinity for CD155. CD226 and CD96 compete with TIGIT for binding to CD155, but with lower affinity than TIGIT. CD226 delivers activating signals. However, whether CD96 triggers inhibitory or activating signals remains to be determined. CD112R and CD226 also competitively binding to CD112, with higher affinity with CD112R. APCs, antigen presenting cells.

On the other hand, TIGIT can exogenously enhance the immunosuppressive functions of Treg cells. TIGIT is enriched in Treg cells, which is associated with the suppressive capacity of effector T cells. Conversely, CD226 inhibits the expansion of Treg cells and promotes the secretion of IFNγ and other effector cytokines (37, 38). TIGIT expression on Treg cells also suppresses the proliferation of effector T cells *via* increased production of interleukin-10 (IL-10) and fibrinogen-like protein 2 (Fgl2), as well as the response of pro-inflammatory T helper 1 (Th1) and Th17 cells, but not Th2 cells (39). Besides, TIGIT can suppress T cell activation through DCs and macrophage-mediated cytokines disturbance. TIGIT interacts with CD155 expressed on DCs, and induces phosphorylation of CD155 through extracellular signal-regulated kinase (ERK) signaling, consequently increasing the production of anti-inflammatory cytokine IL-10 and decreasing pro-inflammatory cytokine IL-12, which inhibits T cell function (40). TIGIT also enhances the secretion of IL-10 and reduces the secretion of IFNγ and tumor necrosis factor α (TNFα) *via* c-Maf nuclear translocation, which switches macrophages from M1 to anti-inflammatory M2 phenotype (41). In addition, TIGIT also directly induces exhaustion of tumor-infiltrating NK cells with lower expression of IFNγ and TNF or indirectly contributes to exhaustion of CD8+ T cells, impairing anti-tumor immune response (42) (Figure 2).

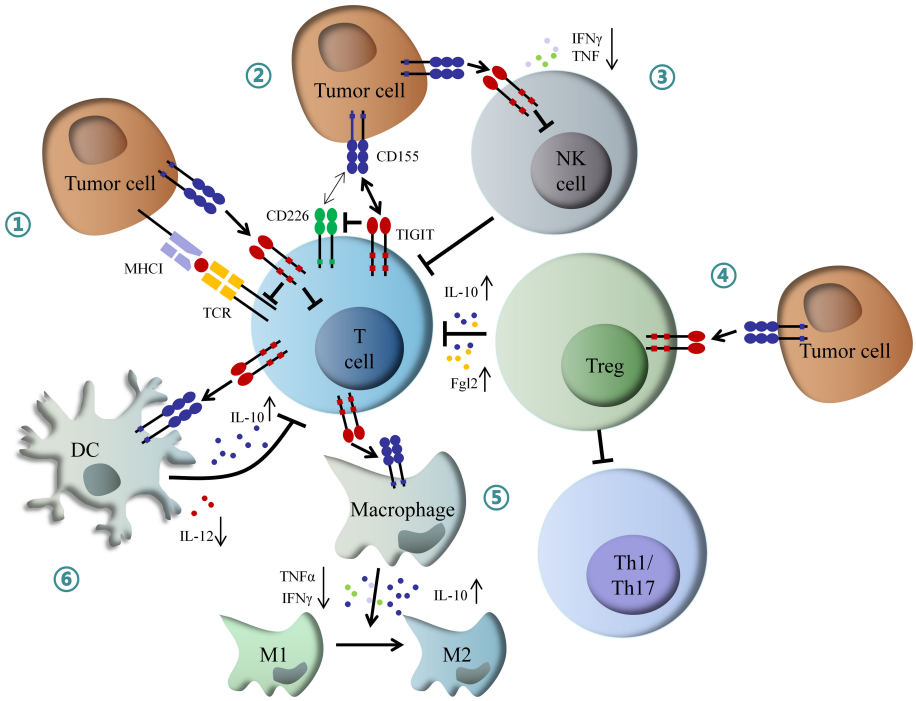

FIGURE 2
Mechanism of inhibitory role of TIGIT in immunoregulation. (1) Interaction of TIGIT with CD155 transmits intracellular inhibitory signals, which directly suppressed TCR signal and effector T cell function. (2) TIGIT inhibits CD226-induced T cell activation by disrupting CD226 homodimerization and decreasing IFNγ production. (3) TIGIT directly induces NK cell exhaustion, contributing to inactivation of CD8+ T cell. (4) TIGIT enhances Tregs mediated dysfunction of effector T cell by increased IL-10 and Fgl2, as well as inhibition of Th1 and Th17 cells. (5) TIGIT promotes macrophage switching from pro-inflammatory M1 to anti-inflammatory M2 phenotype through increased IL-10 and decreased IFNγ and TNFα. (6) TIGIT inhibits T cell function by DCs-mediated abnormal secretion of cytokines. IFNγ, interferon-γ; IL-10, interleukin-10; Fgl2, fibrinogen-like protein 2; Th1, T helper 1 cell; Th17, T helper 17 cell; TNFα, tumor necrosis factor α; DCs, dendritic cells; NK, natural killer.

TIGIT expression and prognostic role in hematological malignancies

Increasing evidence has demonstrated that TIGIT was highly expressed on tumor-infiltrating lymphocytes (TILs) in different hematological malignancies, resulting in tumor progression and poor outcomes. Josefsson reported that TIGHT expression was significantly higher in T cells of follicular lymphoma (FL) than in healthy controls. Besides, up-regulation of TIGIT was associated with the advanced disease stage (34, 43). Yang also reported that TIGIT expression was increased on TILs in FL, and TIGIT+ T cells predicted worse treatment response and inferior survival (44). Likewise, CD4+ TIGIT+ T cells were increased in chronic lymphocytic leukemia (CLL) patients, which was also correlated with unmutated immunoglobulin heavy chain variable region (IgHv) and advanced stage (45).

Furthermore, TIGIT was similarly up-regulated in classic Hodgkin lymphoma (cHL) and Sezary syndrome (46, 47). In acute myeloid leukemia (AML) patients, elevated TIGIT expression on CD8+ T cells was observed. High TIGIT expression was associated with primary refractory disease and relapse after allogeneic stem cell transplantation (allo-SCT) with poorer survival (48, 49). TIGIT was also reported to be increased on γδ T cells and NK cells, which became an independent risk factor for prognosis (50–52). In addition, increasing frequency of TIGIT on CD8+ T cells was reported in mice models of newly diagnosed and relapsed multiple myeloma, which positively correlated with tumor burden (53, 54). These studies indicated a negative role of TIGIT in anti-tumor immunity. Therefore, targeting TIGIT may be an effective approach for ICB therapy in hematological malignancies.

Immunotherapy targeting TIGIT in hematological malignancies

To date, immunotherapy targeting TIGIT has shown significant anti-tumor effects in several pieces of research. Catakovic reported that blockage of TIGIT by recombinant TIGIT-Fc would reduce CLL viability *in vitro* due to

decreasing production of pro-survival cytokines IL-10 (45). In AML, TIGIT expression inhibited cytokine production and induced apoptosis of CD8+ T cells. Knockdown of TIGIT by siRNA could restore T cell function *via* decreasing susceptibility to apoptosis, simultaneously increasing production of TNFα and IFNγ. Besides, blockage of TIGIT significantly increased IFNγ production and NK cell degranulation, contributing to NK cells mediated anti-leukemia effects (52, 55).

Similarly, high TIGIT expression promoted T cells exhaustion, leading to myeloma progression. Conversely, the anti-TIGIT treatment prevented T cells exhaustion, decreased growth rate of tumor cells, and prolonged survival of MM mice (53). Guillerey also reported that either TIGIT deficiency or blockage by mAbs restored the immune function of anti-MM CD8+ T cells and improved survival *in vivo* (54).

In addition, dual blockade of TIGIT and PD-1 showed potential synergistic immune killing effects. On the one hand, Wang observed a higher frequency of TIGIT and PD-1 dual expression in AML patients, which was associated with a higher frequency of FLT3-ITD mutation and a lower remission rate (56). Studies showed that 68-84% of T cells had co-expression of TIGIT and PD-1 in hodgkin lymphoma (HL) (46, 57). A high frequency of TIGIT and PD-1 dual expression was also observed in CLL and FL (34, 58). On the other hand, Zhang reported that blockage of TIGIT alone only up-regulated TNFα in TIGIT+ CD4+ T cells and IFNγ, TNFα in TIGIT+ CD8+ T cells. However, combined inhibition of TIGIT, PD-1, and Tim-3 significantly up-regulated IL-2, IFNγ, and TNFα in both CD4+ and CD8+ T cells, which may enhance anti-leukemia immune responses (59). Based on the remarkable efficacy of anti-TIGIT mAbs in solid tumors and potential immune-killing effects mentioned above in preclinical research, human anti-TIGIT mAbs are being tested in phase 1/2 clinical trials either as a monotherapy or, in most studies, in combination with anti-PD-1/PD-L1 antibodies or chemotherapies for the treatment of malignant lymphoma and multiple myeloma (Table 1). In summary, these researches supported the progress of immunotherapy targeting the TIGIT axis in hematological malignancies.

Toxicities of TIGIT blockage

Even though therapeutic strategy targeting TIGIT has provided evidence of encouraging efficacy in hematological malignancies, the immune-related adverse events (irAEs) mediated by over-activated T cells may result in multiple organ dysfunction and poor prognosis. Phase 1 study of the anti-TIGIT antibody vibostolimab reported that two patients suffered irAEs, including one adrenal insufficiency and one

TABLE 1 Ongoing clinical trials targeting TIGIT in hematological malignancies.

NCT number	Agent	Treatment	Tumor type	Phase
NCT05315713	Tiragolumab	Combined with mosunetuzumab ± atezolizumab (anti-PD-L1 mAb)	r/r-DLBCL r/r-FL	Phase 1/2
NCT04045028	Tiragolumab	Monotherapy Combined with rituximab Combined with daratumumab ± atezolizumab	r/r-B-NHL r/r-MM	Phase 1
NCT05267054	Ociperlimab (BGB A1217)	Combined with rituximab Combined with tislelizumab (anti-PD-1 mAb)	r/r-DLBCL	Phase 1/2
NCT04150965	BMS-986207	Combined with pomalidomide and dexamethasone	r/r-MM	Phase 1/2
NCT05005442	Vibostolimab (MK7684A)	Combined with pembrolizumab (anti-PD-1 mAb)	r/r-HL r/r-B-NHL r/r-MM	Phase 2
NCT04354246	COM902	Monotherapy Combined with COM701 (anti-PVRIG mAb)	MM	Phase 1
NCT04254107	SEA-TGT	Monotherapy Combined with sasanlimab (anti-PD-1 mAb)	cHL DLBCL PTCL-NOS	Phase 1
NCT04772989	AB308	Combined with zimberelimab (anti-PD-1 mAb)	DLBCL MM	Phase 1
NCT05289492	EOS-448	Monotherapy Combined with iberdomide ± dexamethasone	r/r-MM	Phase 1/2

r/r-DLBCL, relapsed or refractory diffuse large B cell lymphoma; r/r-FL, relapsed or refractory follicular lymphoma; r/r-B-NHL, relapsed or refractory B cell non-hodgkin's lymphoma; r/r-MM, relapsed or refractory multiple myeloma; r/r-HL, relapsed or refractory hodgkin's lymphoma; PTC-NOS, peripheral T-cell lymphoma, not otherwise specified; cHL, classical hodgkin's lymphoma.

severe skin reaction (60). Another phase 1 study of anti-TIGIT antibody ociperlimab in combination with anti-PD-1 antibody tislelizumab in advanced solid tumors showed that 15 of 26 patients suffered irAEs, including three severe irAEs (grade≥3) (61). CITYSCAPE trial also reported that 69% of patients experienced irAEs after treated with anti-TIGIT antibody tiragolumab and anti-PD-L1 antibody atezolizumab, in which skin rash was the most common, followed by pancreatitis, hypothyroidism, colitis and diabetes mellitus (62). Therefore, clinicians should pay more attention to the immune toxicity of anti-TIGIT therapy.

Conclusion

The immune checkpoint molecule TIGIT plays an inhibitory role in anti-tumor immunity by inactivating immune effector cells. Up-regulation of TIGIT has been reported in various hematological malignancies, which predicts poor outcomes. Preclinical research has demonstrated that blocking TIGIT alone or combined with PD-1 improves anti-tumor immune responses. The clinical evidence of its efficacy in ongoing clinical trials, especially synergized with other immune checkpoint inhibitors, for example PD-1, lymphocyte activation gene 3 (LAG-3) and T-cell immunoglobulin-3 (TIM-3), is eagerly awaited. Furthermore, simultanously blockade of TIGIT and hypoxia-inducible factor 1-alpha (HIF-1α) may also become a potential treatment strategy (63). In the future, a comprehensive understanding of the intricate immunoregulatory network among TIGIT family members and other immune checkpoint molecules may provide more effective options for patients with hematological malignancies.

Author contributions

JZ contributed to the conception of this review, SJ and YZ were responsible for screening literatures and drafting the manuscript, FZ, XC, and JS edited tables and figures. All authors revised the manuscript and JZ gave the final approval of the manuscript.

Funding

This study was supported by Zhejiang Provincial Natural Science Foundation of China (LQ21H160036).

Conflict of interest

The authors declare that the research was conducted in the absence of any commercial or financial relationships that could be construed as a potential conflict of interest.

Publisher's note

References

1. Auberger P, Tamburini-Bonnefoy J, Puissant A. Drug resistance in hematological malignancies. *Int J Mol Sci* (2020) 21(17):6091. doi: 10.3390/ijms21176091

2. Shimada A. Hematological malignancies and molecular targeting therapy. *Eur J Pharmacol* (2019) 862:172641. doi: 10.1016/j.ejphar.2019.172641

3. Farnault L, Sanchez C, Baier C, Le Treut T, Costello RT. Hematological malignancies escape from NK cell innate immune surveillance: mechanisms and therapeutic implications. *Clin Dev Immunol* (2012) 2012:421702. doi: 10.1155/2012/421702

4. Salik B, Smyth MJ, Nakamura K. Targeting immune checkpoints in hematological malignancies. *J Hematol Oncol* (2020) 13(1):111. doi: 10.1186/s13045-020-00947-6

5. Haslauer T, Greil R, Zaborsky N, Geisberger R. CAR T-cell therapy in hematological malignancies. *Int J Mol Sci* (2021) 22(16):8996. doi: 10.3390/ijms22168996

6. Ok CY, Young KH. Checkpoint inhibitors in hematological malignancies. *J Hematol Oncol* (2017) 10(1):103. doi: 10.1186/s13045-017-0474-3

7. Annibali O, Crescenzi A, Tomarchio V, Pagano A, Bianchi A, Grifoni A, et al. PD-1 /PD-L1 checkpoint in hematological malignancies. *Leuk Res* (2018) 67:45–55. doi: 10.1016/j.leukres.2018.01.014

8. Song W, Zhang M. Use of CAR-T cell therapy, PD-1 blockade, and their combination for the treatment of hematological malignancies. *Clin Immunol* (2020) 214:108382. doi: 10.1016/j.clim.2020.108382

9. Hou JZ, Ye JC, Pu JJ, Liu H, Ding W, Zheng H, et al. Novel agents and regimens for hematological malignancies: recent updates from 2020 ASH annual meeting. *J Hematol Oncol* (2021) 14(1):66. doi: 10.1186/s13045-021-01077-3

10. Armand P, Lesokhin A, Borrello I, Timmerman J, Gutierrez M, Zhu L, et al. A phase 1b study of dual PD-1 and CTLA-4 or KIR blockade in patients with relapsed/refractory lymphoid malignancies. *Leukemia.* (2021) 35(3):777–86. doi: 10.1038/s41375-020-0939-1

11. Quagliariello V, Passariello M, Rea D, Barbieri A, Iovine M, Bonelli A, et al. Evidences of CTLA-4 and PD-1 blocking agents-induced cardiotoxicity in cellular and preclinical models. *J Pers Med* (2020) 10(4):179. doi: 10.3390/jpm10040179

12. Quagliariello V, Passariello M, Coppola C, Rea D, Barbieri A, Scherillo M, et al. Cardiotoxicity and pro-inflammatory effects of the immune checkpoint inhibitor pembrolizumab associated to trastuzumab. *Int J Cardiol* (2019) 292:171–9. doi: 10.1016/j.ijcard.2019.05.028

13. Chauvin JM, Zarour HM. TIGIT in cancer immunotherapy. *J Immunother Cancer* (2020) 8(2):e000957. doi: 10.1136/jitc-2020-000957

14. Liu L, You X, Han S, Sun Y, Zhang J, Zhang Y. CD155/TIGIT, a novel immune checkpoint in human cancers (Review). *Oncol Rep* (2021) 45(3):835–45. doi: 10.3892/or.2021.7943

15. Qiu D, Liu X, Wang W, Jiang X, Wu X, Zheng J, et al. TIGIT axis: novel immune checkpoints in anti–leukemia immunity. *Clin Exp Med* (2022). doi: s00262-018-2246-5/s10238-022-00817-0

16. Boles KS, Vermi W, Facchetti F, Fuchs A, Wilson TJ, Diacovo TG, et al. A novel molecular interaction for the adhesion of follicular CD4 T cells to follicular dendritic cells. *Eur J Immunol* (2009) 39(3):695–703. doi: 10.1002/eji.200839116

17. Levin SD, Taft DW, Brandt CS, Bucher C, Howard ED, Chadwick EM, et al. Vstm3 is a member of the CD28 family and an important modulator of T cell function. *Eur J Immunol* (2011) 41(4):902–15. doi: 10.1002/eji.201041136

18. Harjunpää H, Guillerey C. TIGIT as an emerging immune checkpoint. *Clin Exp Immunol* (2020) 200(2):108–19. doi: 10.1111/cei.13407

19. Ge Z, Peppelenbosch MP, Sprengers D, Kwekkeboom J. TIGIT, the next step towards successful combination immune checkpoint therapy in cancer. *Front Immunol* (2021) 12:699895. doi: 10.3389/fimmu.2021.699895

20. Stanietsky N, Simic H, Arapovic J, Toporik A, Levy O, Novik A, et al. The interaction of TIGIT with PVR and PVRL2 inhibits human NK cell cytotoxicity. *Proc Natl Acad Sci U S A*. (2009) 106(42):17858–63. doi: 10.1073/pnas.0903474106

21. Rotte A, Sahasranaman S, Budha N. Targeting TIGIT for immunotherapy of cancer: Update on clinical development. *Biomedicines*. (2021) 9(9):1277. doi: 10.3390/biomedicines9091277

22. Reches A, Ophir Y, Stein N, Kol I, Isaacson B, Charpak Amikam Y, et al. Nectin4 is a novel TIGIT ligand which combines checkpoint inhibition and tumor specificity. *J Immunother Cancer* (2020) 8(1):e000266. doi: 10.1136/jitc-2019-000266

23. Yeo J, Ko M, Lee DH, Park Y, Jin HS. TIGIT/CD226 axis regulates anti-tumor immunity. *Pharm (Basel)* (2021) 14(3):200. doi: 10.3390/ph14030200

24. Masson D, Jarry A, Baury B, Blanchardie P, Laboisse C, Lustenberger P, et al. Overexpression of the CD155 gene in human colorectal carcinoma. *Gut*. (2001) 49 (2):236–40. doi: 10.1136/gut.49.2.236

25. Oshima T, Sato S, Kato J, Ito Y, Watanabe T, Tsuji I, et al. Nectin-2 is a potential target for antibody therapy of breast and ovarian cancers. *Mol Cancer* (2013) 12:60. doi: 10.1186/1476-4598-12-60

26. Lupo KB, Matosevic S. CD155 immunoregulation as a target for natural killer cell immunotherapy in glioblastoma. *J Hematol Oncol* (2020) 13(1):76. doi: 10.1186/s13045-020-00913-2

27. Solomon BL, Garrido-Laguna I. TIGIT: a novel immunotherapy target moving from bench to bedside. *Cancer Immunol Immunother* (2018) 67(11):1659–67. doi: s00262-018-2246-5/s00262-018-2246-5

28. Zhu Y, Paniccia A, Schulick AC, Chen W, Koenig MR, Byers JT, et al. Identification of CD112R as a novel checkpoint for human T cells. *J Exp Med* (2016) 213(2):167–76. doi: 10.1084/jem.20150785

29. Bottino C, Castriconi R, Pende D, Rivera P, Nanni M, Carnemolla B, et al. Identification of PVR (CD155) and nectin-2 (CD112) as cell surface ligands for the human DNAM-1 (CD226) activating molecule. *J Exp Med* (2003) 198(4):557–67. doi: 10.1084/jem.20030788

30. Jin HS, Park Y. Hitting the complexity of the TIGIT-CD96-CD112R-CD226 axis for next-generation cancer immunotherapy. *BMB Rep* (2021) 54(1):2–11. doi: 10.5483/BMBRep.2021.54.1.229

31. Blake SJ, Dougall WC, Miles JJ, Teng MW, Smyth MJ. Molecular pathways: Targeting CD96 and TIGIT for cancer immunotherapy. *Clin Cancer Res* (2016) 22 (21):5183–8. doi: 10.1158/1078-0432.CCR-16-0933

32. Dougall WC, Kurtulus S, Smyth MJ, Anderson AC. TIGIT and CD96: new checkpoint receptor targets for cancer immunotherapy. *Immunol Rev* (2017) 276 (1):112–20. doi: 10.1111/imr.12518

33. Joller N, Hafler JP, Brynedal B, Kassam N, Spoerl S, Levin SD, et al. Cutting edge: TIGIT has T cell-intrinsic inhibitory functions. *J Immunol* (2011) 3):1338–42. doi: 10.4049/jimmunol.1003081

34. Josefsson SE, Huse K, Kolstad A, Beiske K, Pende D, Steen CB, et al. T Cells expressing checkpoint receptor TIGIT are enriched in follicular lymphoma tumors and characterized by reversible suppression of T-cell receptor signaling. *Clin Cancer Res* (2018) 24(4):870–81. doi: 10.1158/1078-0432.CCR-17-2337

35. Johnston RJ, Comps-Agrar L, Hackney J, Yu X, Huseni M, Yang Y, et al. The immunoreceptor TIGIT regulates antitumor and antiviral CD8(+) T cell effector function. *Cancer Cell* (2014) 26(6):923–37. doi: 10.1016/j.ccell.2014.10.018

36. Lozano E, Dominguez-Villar M, Kuchroo V, Hafler DA. The TIGIT/CD226 axis regulates human T cell function. *J Immunol* (2012) 188(8):3869–75. doi: 10.4049/jimmunol.1103627

37. Fuhrman CA, Yeh WI, Seay HR, Saikumar Lakshmi P, Chopra G, Zhang L, et al. Divergent phenotypes of human regulatory T cells expressing the receptors TIGIT and CD226. *J Immunol* (2015) 195(1):145–55. doi: 10.4049/jimmunol.1402381

38. Fourcade J, Sun Z, Chauvin JM, Ka M, Davar D, Pagliano O, et al. CD226 opposes TIGIT to disrupt tregs in melanoma. *JCI Insight* (2018) 3(14):e121157. doi: 10.1172/jci.insight.121157

39. Joller N, Lozano E, Burkett PR, Patel B, Xiao S, Zhu C, et al. Treg cells expressing the coinhibitory molecule TIGIT selectively inhibit pro-inflammatory Th1 and Th17 cell responses. *Immunity*. (2014) 40(4):569–81. doi: 10.1016/j.immuni.2014.02.012

40. Yu X, Harden K, Gonzalez LC, Francesco M, Chiang E, Irving B, et al. The surface protein TIGIT suppresses T cell activation by promoting the generation of mature immunoregulatory dendritic cells. *Nat Immunol* (2009) 10(1):48–57. doi: 10.1038/ni.1674

41. Chen X, Lu PH, Liu L, Fang ZM, Duan W, Liu ZL, et al. TIGIT negatively regulates inflammation by altering macrophage phenotype. *Immunobiology*. (2016) 221(1):48–55. doi: 10.1016/j.imbio.2015.08.003

42. Zhang Q, Bi J, Zheng X, Chen Y, Wang H, Wu W, et al. Blockade of the checkpoint receptor TIGIT prevents NK cell exhaustion and elicits potent anti-tumor immunity. *Nat Immunol* (2018) 19(7):723–32. doi: 10.1038/s41590-018-0132-0

43. Josefsson SE, Beiske K, Blaker YN, Førsund MS, Holte H, Østenstad B, et al. TIGIT and PD-1 mark intratumoral T cells with reduced effector function in b-cell non-Hodgkin lymphoma. *Cancer Immunol Res* (2019) 7(3):355–62. doi: 10.1158/2326-6066.CIR-18-0351

44. Yang ZZ, Kim HJ, Wu H, Jalali S, Tang X, Krull JE, et al. TIGIT expression is associated with T-cell suppression and exhaustion and predicts clinical outcome and anti– PD-1 response in follicular lymphoma. *Clin Cancer Res* (2020) 26 (19):5217–31. doi: 10.1158/1078-0432.CCR-20-0558

45. Catakovic K, Gassner FJ, Ratswohl C, Zaborsky N, Rebhandl S, Schubert M, et al. TIGIT expressing CD4+T cells represent a tumor-supportive T cell subset in chronic lymphocytic leukemia. *Oncoimmunology*. (2017) 7(1):e1371399. doi: 10.1080/2162402X.2017.1371399

46. Annibali O, Bianchi A, Grifoni A, Tomarchio V, Tafuri M, Verri M, et al. A novel scoring system for TIGIT expression in classic Hodgkin lymphoma. *Sci Rep* (2021) 11(1):7059. doi: 10.1038/s41598-021-86655-8

47. Anzengruber F, Ignatova D, Schlaepfer T, Chang YT, French LE, Pascolo S, et al. Divergent LAG-3 versus BTLA, TIGIT, and FCRL3 expression in sézary syndrome. *Leuk Lymphoma* (2019) 60(8):1899–907. doi: 10.1080/10428194.2018.1564827

48. Kong Y, Zhu L, Schell TD, Zhang J, Claxton DF, Ehmann WC, et al. T-Cell immunoglobulin and ITIM domain (TIGIT) associates with CD8+ T-cell exhaustion and poor clinical outcome in AML patients. *Clin Cancer Res* (2016) 22(12):3057–66. doi: 10.1158/1078-0432.CCR-15-2626

49. Hattori N, Kawaguchi Y, Sasaki Y, Shimada S, Murai S, Abe M, et al. Monitoring TIGIT/DNAM-1 and PVR/PVRL2 immune checkpoint expression levels in allogeneic stem cell transplantation for acute myeloid leukemia. *Biol Blood Marrow Transplant* (2019) 25(5):861–7. doi: 10.1016/j.bbmt.2019.01.013

50. Jin Z, Ye W, Lan T, Zhao Y, Liu X, Chen J, et al. Characteristic of TIGIT and DNAM-1 expression on Foxp3+ γδ T cells in AML patients. *BioMed Res Int* (2020) 2020:4612952. doi: 10.1155/2020/4612952

51. Jin Z, Lan T, Zhao Y, Du J, Chen J, Lai J, et al. Higher TIGIT+CD226- γδ T cells in patients with acute myeloid leukemia. *Immunol Invest* (2022) 51(1):40–50. doi: 10.1080/08820139.2020.1806868

52. Liu G, Zhang Q, Yang J, Li X, Xian L, Li W, et al. Increased TIGIT expressing NK cells with dysfunctional phenotype in AML patients correlated with poor prognosis. *Cancer Immunol Immunother* (2022) 71(2):277–87. doi: 10.1007/s00262-021-02978-5

53. Minnie SA, Kuns RD, Gartlan KH, Zhang P, Wilkinson AN, Samson L, et al. Myeloma escape after stem cell transplantation is a consequence of T-cell exhaustion and is prevented by TIGIT blockade. *Blood*. (2018) 132(16):1675–88. doi: 10.1182/blood-2018-01-825240

54. Guillerey C, Harjunpää H, Carrié N, Kassem S, Teo T, Miles K, et al. TIGIT immune checkpoint blockade restores CD8+ T cell immunity against multiple myeloma. *Blood*. (2018) 132(16):1689–94. doi: 10.1182/blood-2018-01-825265

55. Brauneck F, Seubert E, Wellbrock J, Schulze Zur Wiesch J, Duan Y, Magnus T. Combined blockade of TIGIT and CD39 or A2AR enhances NK-92 cell-mediated cytotoxicity in AML. *Int J Mol Sci* (2021) 22(23):12919. doi: 10.3390/ijms222312919

56. Wang M, Bu J, Zhou M, Sido J, Lin Y, Liu G, et al. CD8+T cells expressing both PD-1 and TIGIT but not CD226 are dysfunctional in acute myeloid leukemia (AML) patients. *Clin Immunol* (2018) 190:64–73. doi: 10.1016/j.clim.2017.08.021

57. Li W, Blessin NC, Simon R, Kluth M, Fischer K, Hube-Magg C, et al. Expression of the immune checkpoint receptor TIGIT in hodgkin's lymphoma. *BMC Cancer* (2018) 18(1):1209. doi: 10.1186/s12885-018-5111-1

58. Hajiasghar-Sharbaf R, Asgarian-Omran H, Valadan R, Hossein-Nattaj H, Shekarriz R, Zaboli E, et al. CD8+ T-cells Co-expressing PD-1 and TIGIT are highly frequent in chronic lymphocytic leukemia. *Iran J Allergy Asthma Immunol* (2021) 20(6):751–63. doi: 10.18502/ijaai.v20i6.8027

59. Zhang X, Zhang H, Chen L, Feng Z, Gao L, Li Q. TIGIT expression is upregulated in T cells and causes T cell dysfunction independent of PD-1 and Tim-3 in adult b lineage acute lymphoblastic leukemia. *Cell Immunol* (2019) 344:103958. doi: 10.1016/j.cellimm.2019.103958

60. Niu J, Maurice-Dror C, Lee DH, Kim DW, Nagrial A, Voskoboynik M, et al. First-in-human phase 1 study of the anti-TIGIT antibody vibostolimab as monotherapy or with pembrolizumab for advanced solid tumors, including non-small-cell lung cancer. *Ann Oncol* (2022) 33(2):169–80. doi: 10.1016/j.annonc.2021.11.002

61. Frentzas S, Meniawy T, Kao S, Wang RH, Zheng H, Budha N, et al. ADVANTIG-105: Phase 1 dose-escalation study of anti-TIGIT monoclonal antibody ociperlimab (BGB-A1217) in combination with tislelizumab in patients with advanced solid tumors. *J Clin Oncol* (2021). doi: 10.1200/JCO.2021.39.15_suppl.2583

62. Rodriguez-Abreu D, Johnson ML, Hussein MA, Cobo M, Patel AJ, Secen NM, et al. Primary analysis of a randomized, double-blind, phase II study of the anti-TIGIT antibody tiragolumab (Tira) plus atezolizumab (Atezo) versus placebo plus atezo as first-line (1L) treatment in patients with PD-L1-Selected NSCLC (CITYSCAPE). *J Clin Oncol* (2020) 38(15_suppl):9503. doi: 10.1200/JCO.2020.38.15_suppl.9503

63. Fathi M, Bahmanpour S, Barshidi A, Rasouli H, Karoon Kiani F, Mahmoud Salehi Khesht A, et al. Simultaneous blockade of TIGIT and HIF-1α induces synergistic anti-tumor effect and decreases the growth and development of cancer cells. *Int Immunopharmacol* (2021) 101(Pt A):108288. doi: 10.1016/j.intimp.2021.108288

frontiers | Frontiers in Pharmacology

TYPE Original Research
PUBLISHED 13 January 2023
DOI 10.3389/fphar.2022.1059930

OPEN ACCESS

EDITED BY
Qin Wang,
Southwest Jiaotong University, China

REVIEWED BY
Xi Zhang,
Xinqiao Hospital, China
Ming Jiang,
The First Affiliated Hospital of Xinjiang Medical University, China
Sanbin Wang,
The 920th Hospital of Joint Logistics Support Force, China
Guangxun Gao,
Fourth Military Medical University, China

*CORRESPONDENCE
Huang Xiaobing,
huangxiaobing@med.uestc.edu.cn

†These authors have contributed equally to this work

SPECIALTY SECTION
This article was submitted to Pharmacology of Anti-Cancer Drugs, a section of the journal Frontiers in Pharmacology

RECEIVED 02 October 2022
ACCEPTED 22 December 2022
PUBLISHED 13 January 2023

CITATION
Xi Y, Chenglong L, Rong Z, Wen W, Yu W, Jiao C, Juan H, Feifei C, Rong X, Tao J, Hui L and Xiaobing H (2023), Chidamide-based 3-drug combination regimen reverses molecular relapse post transplantation in AML1-ETO–positive acute myeloid leukemia.
Front. Pharmacol. 13:1059930.
doi: 10.3389/fphar.2022.1059930

Chidamide-based 3-drug combination regimen reverses molecular relapse post transplantation in AML1-ETO–positive acute myeloid leukemia

Yang Xi[1†], Li Chenglong[1†], Zhang Rong[1], Wang Wen[1], Wang Yu[2], Chen Jiao[1], Huang Juan[1], Che Feifei[1], Xiao Rong[1], Jiang Tao[1], Li Hui[1] and Huang Xiaobing[1*]

[1]Sichuan Provincial People's Hospital, Affliated Hospital of University of Electronic Science and Technology of China, Chengdu, China, [2]Sichuan Provincial People's Hospital (Medical Group), Dongli Hospital, Chengdu, China

Objective: We aimed to explore a new method to reverse early relapse in patients with AML1-ETO–positive acute myeloid cell transplantation.

Methods: A chidamide-based 3-drug combination regimen was used in our center to treat patients with AML1-ETO–positive AML post transplantation but negative flow cytometry results. A retrospective analysis was performed of the survival rate and possible influencing factors of patients with relapse treated with this regimen in our center from January 2018 to January 2022.

Results: The overall response rate was 95.8% (23/24), and the median number of treatment courses was 4 (range, 3–12 courses). The total molecular complete response (MCR) was 79.1% (19/24) after all treatments, and the molecular complete response was 37.5% (9/24) after one cycle of treatment but reached 58.3% (14/24) after four cycles; overall, the proportion of MCR increased gradually with the increase in treatment cycles. The projected 5-year overall survival rate was 73.9%. The projected 5-year leukemia-free survival rate was 64.8%, and the projected 1-year cumulative relapse rate was 35.5%. The incidence of grade II–IV graft-versus-host diseases (GVHD) was 29.2% (7/24), and that of grade III–IV GVHD was 20.8% (5/24), which could be effectively controlled by glucocorticoid therapy combined with calcineurin inhibitors The total incidence of chronic GVHD was 29.2% (7/24), and all cases were localized chronic GVHD. The total infection rate was 33.3% (8/24), mainly involving bacterial and fungal infections, and the incidence of life-threatening infections was 4.17% (1/24). The treatment-related mortality rate was 0%; and the total mortality rate was 20.8% (5/24). Nausea and vomiting, thrombocytopenia, and neutropenia were common adverse reactions, all of which were Common Terminology Criteria for Adverse Events grade 2–3 events and reversible after drug withdrawal. In terms of immunity, Th1 cell counts gradually increased, Th17 cell counts gradually decreased, and the Th1/Th17 ratio gradually increased after treatment. The $CD8^+$ T lymphocyte count increased gradually, while the $CD4^+$ T lymphocyte count did not change significantly.

Conclusion: Our chidamide-based 3-drug combination regimen led to a high remission rate and tolerable adverse reactions in patients with AML1-

ETO–positive post-transplant relapse, and most patients can achieve long-term survival with this regimen.

KEYWORDS

chidamide, 3-drug combination, AML1-ETO, post-transplantation, relapse

1 Introduction

AML1-ETO is determined by t (8; 21) (q22; Q22) chromosomal translocation of tumor proteins, which are seen in 1%–5% of patients with acute myeloid leukemia, most often in younger patients. According to ELN stratification, t (8; 21) (q22; Q22) cases may be classified into the good prognosis group. Studies in China have shown that the HAA regimen can increase the rate of early remission in induction therapy among AML1-ETO–positive AML patients, but about 40% of patients relapse within 2 years (Zhu et al., 2016). A number of real-world studies in China have confirmed that patients with continuous positive AML1-ETO have a poor prognosis and low long-term survival rate, and only allogeneic hematopoietic stem cell transplantation (allo-HSCT) can improve the long-term survival of these patients (Zhang et al., 2014; Ren et al., 2019; Hu et al., 2020). However, in clinical practice, post-transplant relapse is still the main factor affecting the long-term survival of patients, and the survival rate after relapse decreases significantly (Yoshimoto et al., 2021). At present, there is no targeted treatment for post-transplant relapse for this group of patients, but common post-transplant relapse treatment strategies are still being adopted, such as donor lymphocyte infusion (DLI), traditional chemotherapy, targeted drug therapy and secondary transplantation. In recent years, immunotherapy for acute lymphoblastic leukemia has made rapid progress and achieved remarkable efficacy, but it is still difficult to obtain satisfactory treatment efficacy in AML patients. Although secondary transplantation has a better response rate, it also has more complications and its long-term survival benefit is insignificant.

Multiple studies have confirmed that, for these patients, the time when the AML1-ETO status becomes positive again post transplantation is the best time for pre-emptive treatment, which can improve the long-term survival of patients (Elmaagacli et al., 1997; Wang et al., 2014; Qin et al., 2017). To improve patient tolerance of treatment, possible adverse reactions must be reduced. Our center uses a 3-drug combination regimen based on chidamide (chidamide, decitabine and interferon (IFN)-α2b) for AML1-ETO patients with early post-transplant relapse. In this study, we sought to explore the safety and efficacy of the combined regimen for AML1-ETO patients with molecular relapse post transplantation.

2 Methods

2.1 Population

In this single-center, single-arm, non-randomized retrospective study, a total of 24 patients with AML1-ETO–positive AML were enrolled, including 10 men and 14 women; of these, three patients had a consistently positive AML1-ETO status before transplantation. All patients received a modified conditioning regimen containing Flu/BU/CY/ATG-F and underwent bone marrow and peripheral blood or peripheral HSCT at our center between January 2018 and January 2022, followed by a routine graft-versus-host disease (GVHD) prophylaxis regimen (cyclosporine (CSA) and mycophenolate mofetil (MMF)). The median follow-up time was 25 (6–60) months. The basic information about the enrolled patients is shown in Table 1.

2.2 Transplantation

See our previous article for details (Xi et al., 2021).

2.3 Regimen

All patients received induction therapy with a 3-drug combination regimen based on chidamide, as follows: 1) 10 mg/d of oral chidamide once daily (Monday to Saturday); 2) 10 mg of subcutaneously injected decitabine twice weekly (Monday and Tuesday); and 3) 20 μg of

TABLE 1 Patients'clinical characteristics.

Characteristic	Number	Percent
Gender		
Female	14	58.3
Male	10	41.7
Type of disease		
AML	20	83.3
Secondary AML	2	8.3
MDS transfer to AML	2	8.3
Molecular genetic changes		
KIT	6	25.0
FLT3-ITD	3	12.5
TET2	2	8.33
RUNX1	2	8.33
ASXL1	2	8.33
Without changes	10	41.7
Status before transplantation		
CR1	20	83.3
CR2	4	16.7
MRD-positive	3	12.5
Type of transplantation		
Sibling-matched	6	25.0
Haploidentical	16	66.7
Unrelated	2	8.33
Achieved MCR or not after treatment?		
Yes	19	79.2
No	5	20.8

subcutaneously administered IFN-α2b every other day (Tuesday, Thursday, and Saturday). The treatment cycle was 4 weeks, and the treatment plans contained at least three cycles. The detection of measurable residual disease (MRD) including molecular and flow cytometry results was performed after treatment. Subjects whose MRD result was complete remission (CR) or partial remission (PR) entered the consolidation treatment period and continued to complete two treatment cycles for consolidation; subjects who experienced disease progression could choose whether to continue to complete the study.

2.4 Clinical definition

Efficacy evaluation was conducted for each treatment cycle, including bone marrow cell morphology, bone marrow cell MRD (flow cytometry) result, and bone marrow cell molecular MRD (quantitative polymerase chain reaction, qPCR) result (including AML1-ETO gene and other molecular genetic abnormalities). All experiments were performed by Kangsheng Global Medical Laboratory in accordance with international standard testing procedures.

The efficacy evaluation criteria were as follows: 1) the MRD result turned negative within three treatment cycles, indicating complete remission (MCR); 2) after three treatment cycles, the MRD result improved compared to before treatment but did not turn negative, indicating partial remission (MPR); 3) there was no change in MRD between before treatment and after three cycles of treatment, suggesting the disease was stable (MSD); and 4) the MRD result worsened or even progressed to hematological relapse after the completion of three treatment cycles, indicating disease progression (MPD), which required withdrawal from this clinical study.

2.5 Ethics approval

This protocol was re-registered in the Chinese Clinical Research Registry (registration no. ChiCTR2000032330). This study was approved by the Ethics Committee of Sichuan Provincial People's Hospital, Affiliated Hospital of UESTC (ethics batch no. 2015 Kelun (Vaissiere et al., 2008)). All patients or their guardians signed written informed consent forms to participate in the study in accordance with the Declaration of Helsinki.

2.5 Detection of immune cells by flow cytometry

This study focused on changes in immune indexes in patients between before and after treatment. Protocol immunophenotypic analysis was performed for all relapsed patients at baseline time points of 0, 1, 2, and 3 months after the start of the protocol and 3 months after discontinuation. CTL cells were defined as $CD3^+CD4^-CD8^+$ cells, natural killer (NK) cells were defined aas $CD3^-CD56^+$ cells, T helper (Th) cells were defined as $CD3^+CD4^+CD8^-$ cells, B-cells were defined as $CD3^-CD19^+$ cells, Th1 cells were defined as $CD3^+CD4^+CD8^-INF\gamma^+$ cells, Th2 cells were defined as $CD3^+CD4^+CD8^-IL4^+$, Th17 cells were defined as $CD3^+CD4^+CD8^-IL17^+$ cells, and Treg cells were defined as $CD3^+CD4^+CD25^+Foxp3^+$ cells.

2.6 Data analysis and statistics

GraphPad Prism version 5.0 (GraphPad Software, San Diego, CA, United States) was used for survival analysis and mapping. A *t*-test was used for statistical analysis of measurement data between the two groups, and the chi-squared test was used for statistical analysis of classification data. The cumulative incidence of relapse (CIR), leukemia-free survival (LFS), and overall survival (OS) were measured from the time of relapse post-transplantation by the Kaplan-Meier method and Greenwood's formula. The log-rank test was used for group comparison. SPSS 13.0 (IBM Corporation, Armonk, NY, United States) was used for these data. $p < 0.05$ was considered to be statistically significant.

3 Results

3.1 Basic information of patients

A total of 24 patients were enrolled from January 2018 to January 2022. There were 24 AML1-ETO–positive AML patients, including 10 men and 14 women, and three of these patients were in a persistent positive AML1-ETO state before transplantation.

Only AML1-ETO gene were detected in 10 patients, and AML1-ETO accompanied by other molecular genetic abnormalities were detected in 14 patients. The median age of patients in this cohort was 29 years (range, 6–59 years). See Table 1 for details.

3.2 Clinical efficacy

In terms of efficacy, AML1-ETO decreased or turned negative in 23 of 24 patients after treatment. The overall response rate was 95.8% (23/24), and the median number of treatment courses was 4 (range, 3–12 courses). The total molecular complete response (MCR) was 79.1% (19/24); more specifically, it was 37.5% (9/24) after one course of treatment but reached 58.3% (14/24) after four courses, suggesting that the proportion of MCR gradually increases with the increase in treatment courses (see Figure 1A and Table 2). The projected 5-year overall survival rate was 73.9% (see Figure 1B). Patients with hematologic relapse died within 6 months, but those with molecular relapse could be managed with continuous treatment. The estimated 5-year leukemia-free survival rate was 64.8% (see Figure 1C), and the estimated 1-year cumulative relapse rate was 35.5% (see Figure 1D).

3.3 Adverse reactions

Among the 24 patients, seven developed varying degrees of GVHD (see Figure 2A), mainly presenting as skin rejection and liver rejection. The overall incidence of GVHD was 29.2% (7/24), among which the incidence of grade III–IV GVHD was 20.8% (5/24), and cases could be effectively controlled by glucocorticoid therapy combined with calcination inhibitors. The total incidence of chronic GVHD was 29.2% (7/24), and all cases were localized chronic GVHD. The projected 5-year GRFS is 40.4% (see Figure 2B).

Eight patients developed different degrees of pulmonary infection, with an infection rate of 33.3% (8/24). The main pathogens were

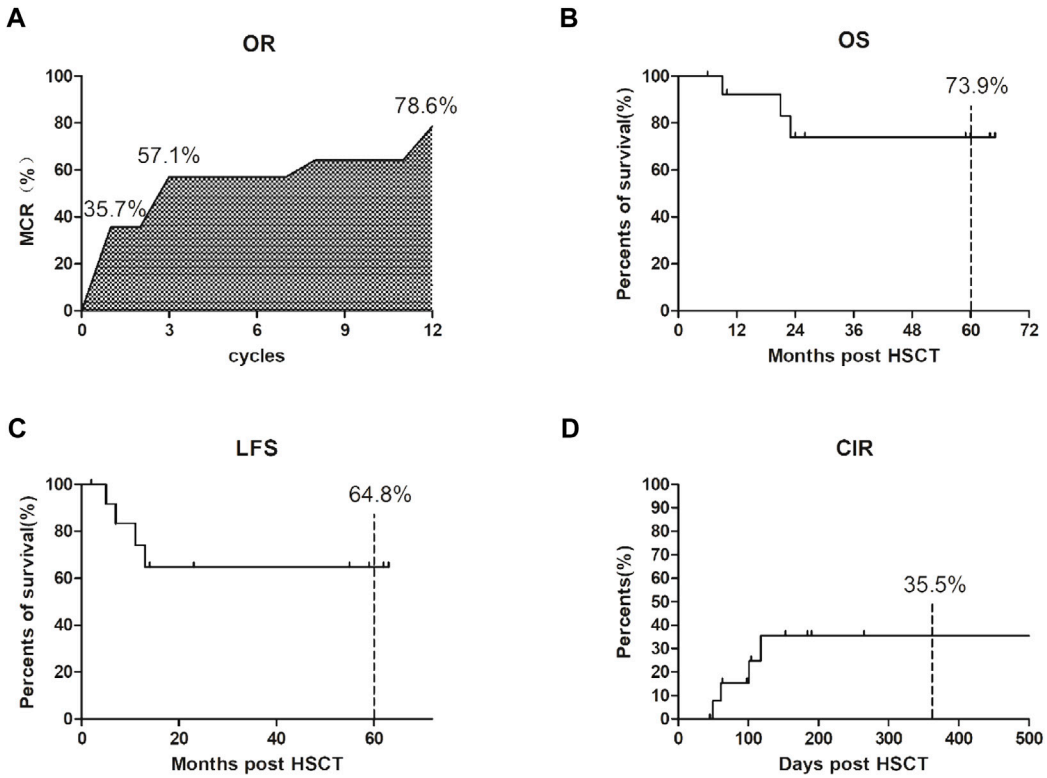

FIGURE 1
Clinical efficacy after our 3-drug combination regimen based on chidamide. **(A)** The overall response rate (OR) was 95.8% (23/24); The total molecular complete response (MCR) was 79.1% (19/24); the proportion of MCR gradually increases with the increase in treatment courses. **(B)** The projected 5-year overall survival (OS) rate was 73.9%; **(C)** The estimated 5-year leukemia-free survival (LFS) rate was 64.8%; **(D)** The estimated 1-year cumulative relapse rate (CIR) was 35.5%.

TABLE 2 Dynamics of AM LI-ETO transcripts post therapy in AML with molecular relapse post transplantation.

Months post this regimen	Number of patients evaluated (%)	Median AML1-ETO transcri • levels (range)	Patients with negative AML1-ET0 (%)
1	24 (100)	0.42% (0%–5.81%)	9 (37.5)
2	24 (100)	0.11% (0%–2.8%)	9 (37.5)
3	24 (100)	0.031% (0%–3.1%)	9 (37.5)
4	24 (100)	0% (0%–8.1%)	14 (58.3)
5	24 (100)	0% (0–3.1%)	14 (58.3)
6	24 (100)	0% (0%–11.2%)	14 (58.3)
7	22 (92.6)	0% (0%–39.3%)	14 (63.6)
8	22 (92.6)	0% (0%–1.1%)	15 (68.2)
9	22 (92.6)	0% (0%–0.25%)	15 (68.2)
10	22 (92.6)	0% (0%–4.3%)	15 (68.2)
11	22 (92.6)	0% (0%–8.9%)	15 (68.2)
12	20 (83.3)	0% (0%–65.3%)	19 (95.0)
18	20 (83.3)	0% (0%–54.6%)	19 (95.0)
24	19 (83.3)	0% (0.0%)	19 (100)
30	19 (83.3)	0% (0%–0%)	19 (100)
36	19 (83.3)	0% (0%–0%)	19 (100)

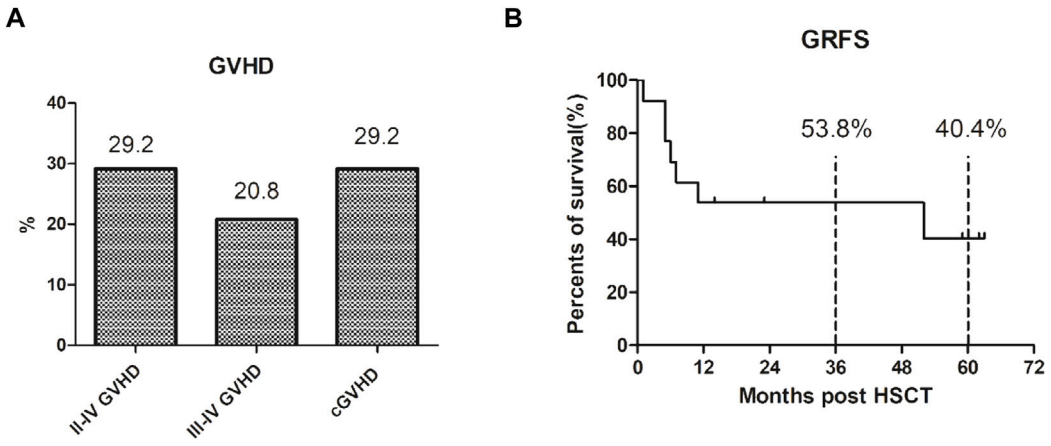

FIGURE 2
The GVHD and GRFS after our 3-drug combination regimen based on chidamide. **(A)** The overall incidence of III–IV GVHD was 29.2% (7/24), III–IV GVHD was 20.8% (5/24), and the total incidence of chronic GVHD was 29.2% (7/24), which were localized chronic GVHD. **(B)** The projected 3-year GRFS is 53.8% and 5-year GRFS is 40.4%.

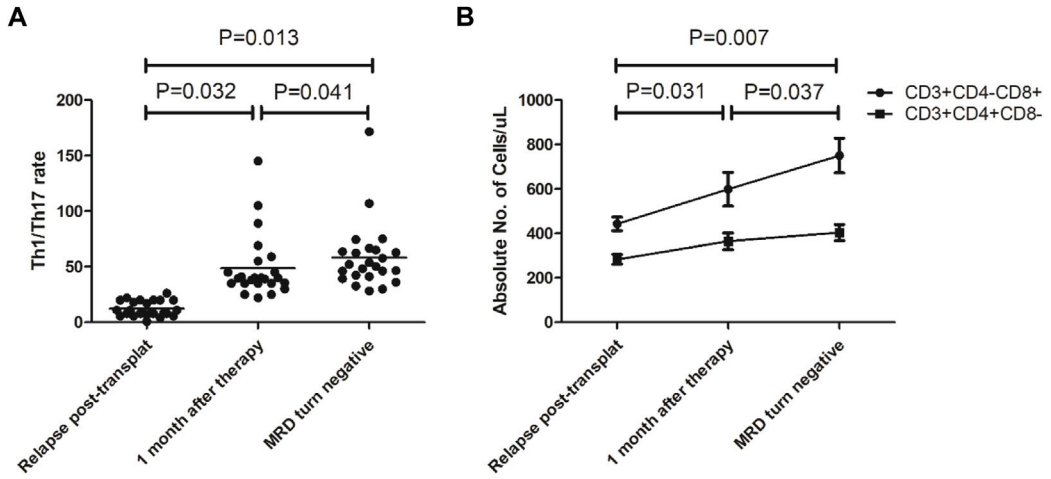

FIGURE 3
Changes in immune constituents after our 3-drug combination regimen based on chidamide. **(A)** Th1/Th17 ratio gradually increased compared to that before treatment; **(B)** The $CD8^+$ T lymphocyte count increased gradually, while the $CD4^+$ T lymphocyte count did not change significantly.

bacteria and fungi. One patient developed a serious life-threatening pneumocystis *pneumoniae* infection (4.17%, 1/24), which improved after active treatment and respiratory support. There were no treatment-related deaths in the 24 patients, and the treatment-related mortality rate was 0%. The overall mortality rate was 20.8% (5/24). Nausea and vomiting, elevated aminotransferase levels, thrombocytopenia, and neutropenia are common adverse reactions, all of which were Common Terminology Criteria for Adverse Events grade 2–3 and could be reversed after drug withdrawal or combined hepatoprotective therapy.

3.4 Changes in immune constituents

The cellular immune constituents of patients were dynamically monitored before and after treatment. The results showed Th1 cell counts gradually increased, Th17 cell counts gradually decreased, and the Th1/Th17 ratio gradually increased compared to that before treatment (see Figure 3A). The $CD8^+$ T lymphocyte count increased gradually, while the $CD4^+$ T lymphocyte count did not change significantly (see Figure 3B).

4 Discussion

Currently, the commonly used treatment options for post-transplant relapse include secondary allo-HSCT (Choi et al., 2021; Yalniz et al., 2021), donor lymphocyte infusion (Zhao et al., 2022), traditional chemotherapy or targeted drug therapy (Yoshimoto et al., 2021), and chimeric antigen receptor T-cell (CAR-T) and cellular immunotherapy (Cui et al., 2021). There is still no safe and effective treatment for post-transplant relapse in AML1-ETO patients, and

secondary transplantation has been reported to have the highest remission rate. Choi et al. (2021) reported that 80 patients with acute leukemia who had relapsed post allo-HSCT (HSCT1) were treated again with allo-HSCT (HSCT2). Patients with genetic testing results included 54 AML patients, including 44 patients at low or moderate risk (the number of patients with AML1-ETO was not given). The results showed that the median overall survival and event-free survival were 10.3 and 6.1 months after HSCT2, respectively, and acute GVHD cases numbered as high as 28 (35.0%), while grade 3–4 acute GVHD cases totaled as high as 11 (13.8%). While chronic GVHD was found in 27 patients, generalized chronic GVHD was found in 17 patients. Moreover, severe liver veno-occlusive disease (VOD) was found in seven patients (8.8%). At the same time, studies have shown that patients who relapsed less than 6 months after HSCT1 or who failed to achieve a CR/CR with incomplete CR (CRi) result after HSCT2 could not benefit from HSCT2. Acute and chronic GVHD cases associated with HSCT2 increase significantly, especially for patients with relapse of HSCT1 among 6 months. This data suggests it is difficult to benefit from HSCT2, whereas HSCT2 will greatly increase the economic burden of patients. Zhao et al. (2022) enrolled 26 patients with relapsed AML after allo-HSCT, including 18 patients in the medium-risk group, who were treated with venetoclax, azacytidine, and DLI. CR/CRi and PR rates were 26.9% and 34.6% post treatment, respectively. The median event-free survival and overall survival were 120 days and 284.5 days, respectively; however, six patients (23.1%) developed severe GVHD. With the progress of medical science, new treatments are also emerging, such as CD38-targeted CAR-T therapy (Cui et al., 2021). Although this new immunotherapy strategy achieved a high response rate early in treatment, its cumulative relapse rate at 6 months was up to 50%, and its median overall survival and leukemia-free survival times were 7.9 and 6.4 months, with a higher risk of cytokine release synthesis (CRS). In addition, this study was a small sample study with selection bias in enrolled patients, so it is still worth exploring whether this approach can be used as the optimal treatment strategy for patients with post-transplant relapse. In conclusion, for AML1-ETO positive AML patients post transplantion, the existing treatments have poor efficacy and many adverse reactions, including especially III-IV GVHD. It is extremely urgent to explore a safe and effective regimen for these post-transplant relapse patients.

Epigenetic modifications, such as DNA methylation and histone and non-histone acetylation, are important regulators of all aspects of T-cell life and are involved in T-cell development, differentiation, and activation. In recent years, studies have found that epigenetic regulation disorders are closely related to the pathogenesis of AML, in that > 70% of AML patients have DNA methylation–related gene mutations or histone modification mutations, and demethylation drugs can effectively reverse such abnormal changes (Mehdipour et al., 2015). Reduced histone acetylation mediated by histone deacetylase (HDAC) is another common epigenetic anomaly, and targeted inhibition of HDAC reverses dysacetylation. In patients with AML1-ETO, ETO replaces the c-terminal regulatory regions of activation and inhibition of wild-type AML1 in its encoded protein. ETO binds to co-inhibitory factors and recruits HDAC1, 2, and three to form co-inhibitory complexes, thus silencing target genes and preventing hematopoietic differentiation and transformation. It also interacts with secondary mutations, including C-KIT, FLT3, and RAS, ultimately leading to the occurrence or progression of AML1-ETO–positive leukemia (Zhang et al., 2021). The chidamide-based 3-drug combination regimen adopted in this study is based on the theory of correcting epigenetic disorders. As a commonly used HDAC inhibitor (HDACi), chidamide can selectively inhibit HDAC1, 2, 3, and 10, and it is widely used in T-cell lymphoma, advanced breast cancer, and other diseases. Decitabine is a commonly used clinical demethylation drug, which is widely used in myelodysplastic syndrome, acute myeloid leukemia, and refractory immune thrombocytopenia. Basic studies have shown that HDACis interact with DNA methylation, and HDACis help remove methyl-CPG–binding proteins (MePC2) from methylated cytosine. HDACi therapy also allows histone acetyltransferases to re-acetylate histones at gene promoters, and highly acetylated histones can recruit DNA demethylases to further protect DNA from methylation (Vaissiere et al., 2008). For AML1-ETO, HDACi degrades this fusion protein by upregulating E2 ubiquitin binding enzyme and E3 ubiquitin ligase (Buchwald et al., 2009). In *in vitro* studies, chidamide inhibited the proliferation of AML1-ETO–positive AML cells, induced cell cycle arrest, and stimulated apoptosis. At the same time, histone three acetylation and ERK1/2 phosphorylation of AML1-ETO–positive AML cells were inhibited, and the ERK1/2 pathway was regulated to inhibit the proliferation of AML1-ETO–positive AML cells and c-kit expression was reduced (Liu et al., 2020). Of note, immune escape is another mechanism of poor outcome in patients with AML1-ETO–positive leukemia. Elias et al. (2014) found the AML1-ETO gene downregulated the expression of CD48 on the surfaces of leukocytes, thereby reducing the killing effect of natural killer cells, while HDACi can promote the re-expression of CD48 and restore the sensitivity of leukemia cells to natural killer cells. Demethylation drugs also have a similar effect on promoting immune cell recognition (Ganetsky, 2012). Therefore, double-epigenetic treatment has a synergistic effect; on the one hand, it directly exerts anti-leukemia effects, while on the other, it promotes the immune system to better recognize tumor cells and enhance the ability to eliminate leukemia cells. This anti-leukemia mechanism is especially suitable for patients post-HSCT, which gives full play to amplify the graft *versus* leukemia (GVL) effct.

IFN-α, as a type I IFN, is approved by the United States. Food and Drug Administration for the treatment of various malignant blood tumors and solid tumors. In this study, the addition of IFN-α to the epigenetic therapy strategy is an important improvement of the previous epigenetic regulation therapy. Over the past few decades, increasing evidence showed that IFN-α can promote type-I anti-tumor effects (Th1-mediated), playing a key role in anti-tumor immune responses. Medrano R. et al. (Medrano et al., 2017) found that 69 of 100 patients with recurrent acute leukemia post allo-HSCT in a single center (AML72, ALL28) received chemotherapy/supportive therapy, with an average survival time of 51 days. Eleven patients were treated with DLI, and the mean survival time was 84 days. Thirteen patients underwent secondary transplantation, with an average survival time of 303 days; seven patients were treated with IFN-α2b combined with GM-CSF, and the mean survival time was 442 days. The efficacy of this group was significantly better than that in other treatment groups. In mechanism studies, several reports have explored the role of IFN-

α in the treatment of relapsed AML post transplantation (Mo et al., 2018; Molica et al., 2019; Magenau et al., 2021). First, IFN-α was found to have direct anti-tumor effects on AML cells: it 1) inhibited the secretion of growth promoting factors; 2) stimulated apoptosis, 3) inhibited the proliferation of tumor cells, and 4) increased the immunogenicity of AML cells. Second, IFN-α was found to have indirect anti-tumor effects on AML cells through the 1) activation of natural killer cells and T-cells; 2) by enhancing the antigen-presentation of dendritic cells, and 3) showing a similar effect to that of interleukin-15, which can induce dendritic (DC) cells to become natural killer (NK) cells, thus directly producing cytotoxic effect on AML cells. These experimental results support the multiple roles of IFN-α in anti-AML. Thus, presumably, in our 3-drug combination, the effect of IFN-α was multifaceted, which may synergy with chidamide and decitabine. The mechanism has yet to further define by experiment researches.

4 Conclusion

There are limited treatment options for patients with relapse post allo-HSCT. Rapid and sustained reversion of AML1-ETO leukemia relapse post transplantation is the key to improving the long-term survival. Chidamide, as a common HDACi, combining with decitabine and IFN-α2b, is an effective regimen to reverse the molecular biological relapse of AML1-ETO leukemia post transplantation, with a high remission rate and significantly lower adverse reactions than current strategies for post-transplantation relapse. It is worth further extending clinical researches to evaluate the efficacy of this regimen.

Data availability statement

The raw data supporting the conclusions of this article will be made available by the authors, without undue reservation.

Ethics statement

The studies involving human participants were reviewed and approved by. This protocol was re-registered in the Chinese Clinical Research Registry (registration no. ChiCTR2000032330). Written informed consent to participate in this study was provided by the participants legal guardian/next of kin.

Author contributions

All authors listed have made a substantial, direct, and intellectual contribution to the work and approved it for publication.

Funding

This research was funded by Science and Technology Program of Sichuan Province (No.23ZDYF1859 and No.2020YFS0434) and Sichuan Provincial People's Hospital Program (2020LY08).

Conflict of Interest

The authors declare that the research was conducted in the absence of any commercial or financial relationships that could be construed as a potential conflict of interest.

Publisher's note

References

Buchwald, M., Kramer, O. H., and Heinzel, T. (2009). HDACi--targets beyond chromatin. *Cancer Lett.* 280 (2), 160–167. doi:10.1016/j.canlet.2009.02.028

Choi, Y., Choi, E. J., Lee, J. H., Lee, K. H., Jo, J. C., Park, H. S., et al. (2021). Second allogeneic hematopoietic stem cell transplantation in patients with acute leukemia relapsed after allogeneic hematopoietic stem cell transplantation. *Clin. Transpl.* 35 (3), e14199. doi:10.1111/ctr.14199

Cui, Q., Qian, C., Xu, N., Kang, L., Dai, H., Cui, W., et al. (2021). CD38-directed CAR-T cell therapy: A novel immunotherapy strategy for relapsed acute myeloid leukemia after allogeneic hematopoietic stem cell transplantation. *J. Hematol. Oncol.* 14 (1), 82. doi:10.1186/s13045-021-01092-4

Elias, S., Yamin, R., Golomb, L., Tsukerman, P., Stanietsky-Kaynan, N., Ben-Yehuda, D., et al. (2014). Immune evasion by oncogenic proteins of acute myeloid leukemia. *Blood* 123 (10), 1535–1543. doi:10.1182/blood-2013-09-526590

Elmaagacli, A. H., Beelen, D. W., Stockova, J., TrzenSky, S., KrollM. Schaefer, U. W., et al. (1997). Detection of AML1/ETO fusion transcripts in patients with t(8;21) acute myeloid leukemia after allogeneic bone marrow transplantation or peripheral blood progenitor cell transplantation. *Blood* 90 (8), 3230–3231. doi:10.1182/blood.v90.8.3230

Ganetsky, A. (2012). The role of decitabine for the treatment of acute myeloid leukemia. *Ann. Pharmacother.* 46 (11), 1511–1517. doi:10.1345/aph.1R151

Hu, G. H., Cheng, Y. F., Lu, A. D., Wang, Y., Zuo, Y. X., Yan, C. H., et al. (2020). Allogeneic hematopoietic stem cell transplantation can improve the prognosis of high-risk pediatric t(8;21) acute myeloid leukemia in first remission based on MRD-guided treatment. *BMC Cancer* 20 (1), 553. doi:10.1186/s12885-020-07043-5

Liu, J., Lv, N., Zhou, L., Li, Y., and Yu, L. (2020). Chidamide inhibits t(8;21) AML cell proliferation and AMK1/ETO and C-KIT expression by inhibiting ERK1/2 signaling pathway. *Transl. Cancer Res.* 9 (2), 827–839. doi:10.21037/tcr.2019.12.07

Magenau, J. M., Peltier, D., Riwes, M., Pawarode, A., Parkin, B., Braun, T., et al. (2021). Type 1 interferon to prevent leukemia relapse after allogeneic transplantation. *Blood Adv.* 5 (23), 5047–5056. doi:10.1182/bloodadvances.2021004908

Medrano, R., Hunger, A., Mendonca, S. A., Barbuto, J. A. M., and Strauss, B. E. (2017). Immunomodulatory and antitumor effects of type I interferons and their application in cancer therapy. *Oncotarget* 8 (41), 71249–71284. doi:10.18632/oncotarget.19531

Mehdipour, P., Santoro, F., and Minucci, S. (2015). Epigenetic alterations in acute myeloid leukemias. *FEBS J.* 282, 1786–1800. doi:10.1111/febs.13142

Mo, X. D., Wang, Y., Zhang, X. H., Xu, L. P., Yan, C. H., Chen, H., et al. (2018). Interferon-α is effective for treatment of minimal residual disease in patients with t(8;21) acute myeloid leukemia after allogeneic hematopoietic stem cell transplantation: Results of a prospective Registry study. *Oncologist* 23 (11), 1349–1357. doi:10.1634/theoncologist.2017-0692

Molica, M., Breccia, M., Foa, R., Jabbour, E., and Kadia, T. M. (2019). Maintenance therapy in AML: The past, the present and the future. *Am. J. Hematol.* 94 (11), 1254–1265. doi:10.1002/ajh.25620

Qin, Y. Z., Wang, Y., Xu, L. P., Zhang, X. H., Chen, H., Han, W., et al. (2017). The dynamics of RUNX1-RUNX1T1 transcript levels after allogeneic hematopoietic stem cell transplantation predict relapse in patients with t(8;21) acute myeloid leukemia. *J. Hematol. Oncol.* 10 (1), 44. doi:10.1186/s13045-017-0414-2

Ren, J. R., Zhu, X. Y., Tang, B. L., Wan, X., Tong, J., Zhang, L., et al. (2019). Efficacy analysis of unrelated cord blood transplantation for high-risk refractory AML1-ETO positive myeloid leukemia. *Zhongguo Shi Yan Xue Ye Xue Za Zhi* 27 (4), 1246–1252. doi:10.19746/j.cnki.issn.1009-2137.2019.04.042

Vaissiere, T., Sawan, C., and Herceg, Z. (2008). Epigenetic interplay between histone modifications and DNA methylation in gene silencing. *Mutat. Research/Reviews Mutat. Res.* 659 (1-2), 40–48. doi:10.1016/j.mrrev.2008.02.004

Wang, Y., Wu, D. P., Liu, Q. F., Qin, Y. Z., Wang, J. B., Xu, L. P., et al. (2014). In adults with t(8;21)AML, posttransplant RUNX1/RUNX1T1-based MRD monitoring, rather than c-KIT mutations, allows further risk stratification. *Blood* 124 (12), 1880–1886. doi:10.1182/blood-2014-03-563403

Xi, Y., Jingying, D., Chenglong, L., Hong, Z., Rong, Z., Xiaodong, W., et al. (2021). Epigenetic therapy promotes the ratio of Th1/Th17 lineage to reverse immune evasion and treat leukemia relapse post-allogeneic stem cell transplantation in non-apl aml patients. *Front. Mol. Biosci.* 7, 595395. doi:10.3389/fmolb.2020.595395

Yalniz, F. F., Saliba, R. M., Greenbaum, U., Ramdial, J., Popat, U., Oran, B., et al. (2021). Outcomes of second allogeneic hematopoietic cell transplantation for patients with acute myeloid leukemia. *Transplant. Cell. Ther.* 27 (8), 689–695. doi:10.1016/j.jtct.2021.05.007

Yoshimoto, G., Mori, Y., Kato, K., Odawara, J., Kuriyama, T., Ueno, T., et al. (2021). Azacitidine for the treatment of patients with relapsed acute myeloid leukemia after allogeneic stem cell transplantation. *Leukemia lymphoma* 62 (12), 2939–2948. doi:10.1080/10428194.2021.1941937

Zhang, J., Gao, X., and Yu, L. (2021). Roles of histone deacetylases in acute myeloid leukemia with fusion proteins. *Front. Oncol.* 11, 741746. doi:10.3389/fonc.2021.741746

Zhang, Q. Y., Huang, W. R., Dou, L. P., Deng, A. L., Fu, L., Xu, X. H., et al. (2014). Effect of autologous peripheral blood stem cell transplantation in 13 patients with AML1/ETO (+) acute myeloid leukemia. *Zhongguo Shi Yan Xue Ye Xue Za Zhi* 22 (2), 447–452. doi:10.7534/j.issn.1009-2137.2014.02.033

Zhao, P., Ni, M., Ma, D., Fang, Q., Zhang, Y., Li, Y., et al. (2022). Venetoclax plus azacitidine and donor lymphocyte infusion in treating acute myeloid leukemia patients who relapse after allogeneic hematopoietic stem cell transplantation. *Ann. Hematol.* 101 (1), 119–130. doi:10.1007/s00277-021-04674-x

Zhu, H., Jiang, H., Jiang, Q., Jia, J. S., Qin, Y. Z., and Huang, X. J. (2016). Homoharringtonine, aclarubicin and cytarabine (HAA) regimen as the first course of induction therapy is highly effective for acute myeloid leukemia with t (8;21). *Leukemia Res.* 44, 40–44. doi:10.1016/j.leukres.2016.02.012

frontiers | Frontiers in Pharmacology

TYPE Original Research
PUBLISHED 23 January 2023
DOI 10.3389/fphar.2023.1104403

OPEN ACCESS

EDITED BY
Qin Wang,
Southwest Jiaotong University, China

REVIEWED BY
Xu Funeng,
Sichuan Agricultural University, China
Lei Wang,
Heidelberg University Hospital, Germany

*CORRESPONDENCE
Jingying Dai,
741107213@qq.com
Yizhun Zhu,
yzzhu@must.edu.mo

†These authors have contributed equally to this work

SPECIALTY SECTION
This article was submitted to Pharmacology of Anti-Cancer Drugs, a section of the journal Frontiers in Pharmacology

RECEIVED 21 November 2022
ACCEPTED 09 January 2023
PUBLISHED 23 January 2023

CITATION
Chen C, He L, Wang X, Xiao R, Chen S, Ye Z, Wang X, Wang Y, Zhu Y and Dai J (2023), Leonurine promotes the maturation of healthy donors and multiple myeloma patients derived-dendritic cells *via* the regulation on arachidonic acid metabolism.
Front. Pharmacol. 14:1104403.
doi: 10.3389/fphar.2023.1104403

Leonurine promotes the maturation of healthy donors and multiple myeloma patients derived-dendritic cells *via* the regulation on arachidonic acid metabolism

Cheng Chen[1†], Lin He[1†], Xi Wang[1], Rong Xiao[1], Shu Chen[2], Zichen Ye[1], Xuemei Wang[3], Yu Wang[3], Yizhun Zhu[4*†] and Jingying Dai[1*†]

[1]Sichuan Provincial People's Hospital, Sichuan Academy of Medical Sciences, School of Medicine of University of Electronic Science and Technology of China, Chengdu, Sichuan, China, [2]School of Pharmacy, North Sichuan Medical College, Nanchong, Sichuan, China, [3]Sichuan Provincial People's Hospital (Medical Group), Dongli Hospital, Sichuan Academy of Medical Sciences and Sichuan Provincial People's Hospital, Chengdu, Sichuan, China, [4]State Key Laboratory of Quality Research in Chinese Medicine, School of Pharmacy, Macau University of Science and Technology, Taipa, Macau, China

Objective: Leonurine is a bioactive alkaloid compound extracted from Leonurus japonicus Houtt, which potentially has immunomodulatory effects. The immunomodulatory effect and mechanism of leonurine on monocyte derived dendritic cells (moDCs) from healthy donors (HDs) and multiple myeloma (MM) patients were investigated for the first time.

Methods: Peripheral blood from HDs and MM patients was isolated for peripheral blood mononuclear cells (PBMCs). The generation of moDCs was conducted by the incubation of monocytes from PBMCs in the medium consisting of RPMI 1640 medium, 2 mmol/L L-glutamine, 5% human serum, 800 U/mL GM-CSF, 500 U/mL IL-4, 100 U/mL penicillin and 0.1 mg/mL streptomycin. During the incubation of 7 days, the cells were administrated with 1 μM leonurine or 1 × PBS as the control group. On the 8th day, cells were harvested. The expression of maturation associated surface markers CD40, CD83, and HLA-DR on moDCs was analyzed by flow cytometry. Moreover, moDCs with or without 1 μM leonurine administration were evaluated by LC-MS/MS for metabolomics which was further analyzed for the potential mechanism of leonurine on moDCs.

Results: The proportion of moDCs in the harvested cells was significantly higher in the HD group (n = 14) than in the MM patient group (n = 11) (p = 0.000). Leonurine significantly enhanced the median fluorescence intensity of CD83, HLA-DR and CD40 expression on HD-moDCs (n = 14; p = 0.042, p = 0.013, p = 0.084) as well as MM paitent-moDCs (n = 11; p = 0.020, p = 0.006, p = 0.025). The metabolomics data showed that in moDCs (HD, n = 15), 18 metabolites in the pathway of arachidonic acid metabolism showed significant differences between the leonurine group and the control group (VIP all >1 and P all <0.05). To be specific, 6-Keto-PGE1, 8,9-DHET, 11 (R)-HETE, 12-Keto-LTB4, 12-OxoETE, 15 (S)-HETE, 15-Deoxy-Delta12,14-PGJ2, 15-Keto-PGF2a, 20-COOH-LTB4, Lecithin, PGA2, PGB2, PGE2, PGF2a, PGG2, Prostacyclin were significantly upregulated in the leonurine group than in the

control group, while Arachidonic Acid and TXB2 were significantly downregulated in the leonurine group than in the control group.

Conclusion: Leonurine significantly promotes the maturation of moDCs derived from HDs and MM patients, the mechanism of which is related to arachidonic acid metabolism.

KEYWORDS

leonurine, multiple myeloma, monocyte derived dendritic cells, maturation, metabolomics

1 Introduction

Multiple myeloma (MM) is a hematological malignancy originating from the malignant transformation of plasma cells, the incidence of which is the second highest in hematological malignancies (Pinto et al., 2020). MM patients show significant immunodeficiency. The immunodeficiency of dendritic cells (DCs) is one of the key reasons for the inability to efficiently elicit anticancer specific immune responses. Moreover, cancer can also suppress the normal function of DCs for immune escape. DC is the most important antigen-presenting cell in the immune system, which presents antigen peptides to specific T cell and provides costimulatory signals for T cell activation. Thus, DC plays the important role in initiating anticancer specific immune responses (Tan et al., 2012). However, adverse conditions in the cancer microenvironment can inhibit the activity of DCs by modulating metabolic programs in DCs (Giovanelli et al., 2019). Therefore, enhancing the DC activity in MM patients to effectively elicit the anticancer specific immune response is one of the main directions for cancer immunotherapy today.

Some studies have shown that the maturation and activity of DCs is closely related to the cellular metabolism, including the glucose metabolism and the fatty acid metabolism. When glycogen phosphorylase is inhibited, the activation of DCs and the immune response mediated by DCs can be significantly inhibited (Curtis et al., 2020). Intracellular glycogen metabolism supports the early function of activated DCs, while inhibition of glycogen degradation significantly impedes DC maturation and impairs their ability to initiate lymphocyte activation (Thwe et al., 2019). Inhibitors of fatty acid synthesis or oxidation can significantly inhibit the activation of DCs, which indicates that fatty acid metabolism plays an important role in the activation of DCs (Qiu et al., 2019). Based on the above background,

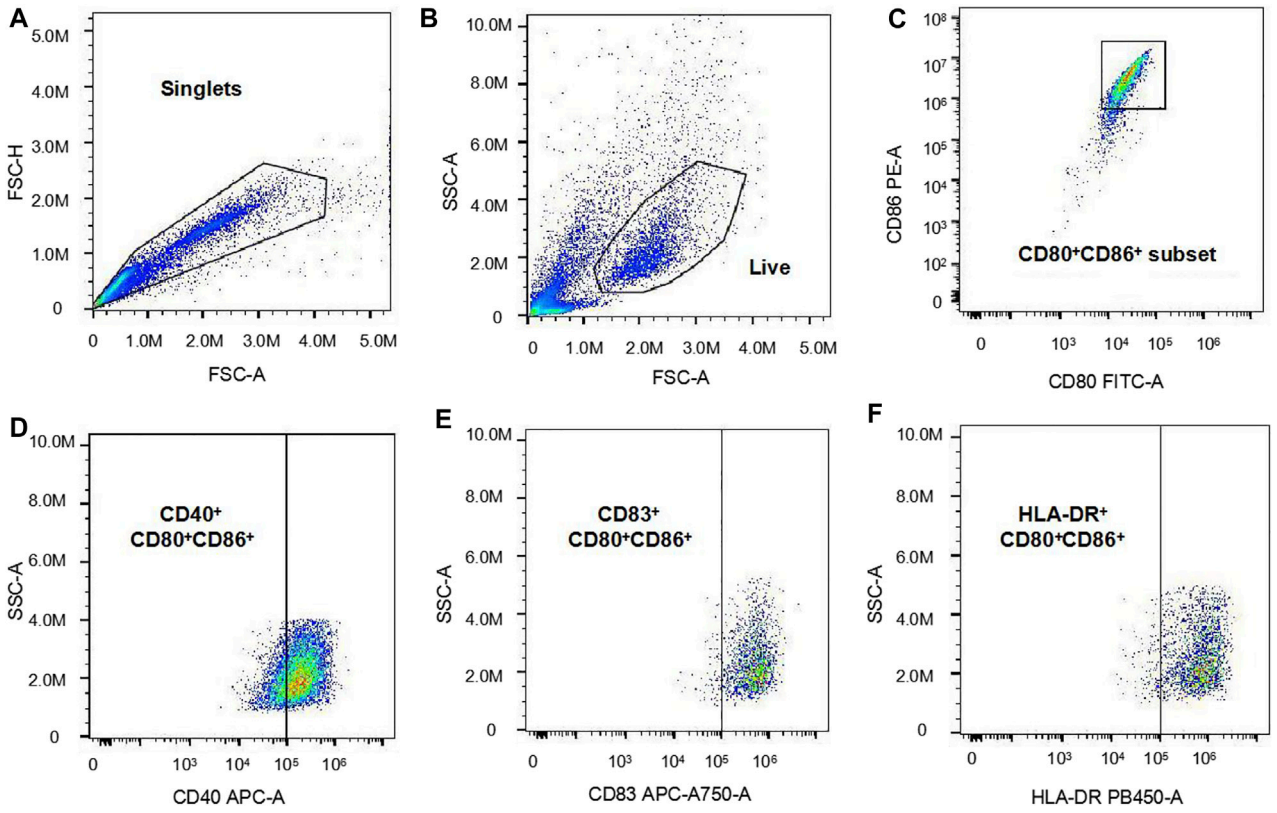

FIGURE 1
The analysis of the flow cytometry data. **(A)**: The forward scatter area (FSC-A) and the forward scatter height (FSC-H) were used for the selection of single cells. **(B)**: The FSC-A and the side scatter area (SSC-A) were used for the selection of live cells. **(C)**: $CD80^+CD86^+$ cells were selected from the live cells and defined as moDCs **(D–F)**: The MFI of CD40, CD83 and HLA-DR expression on moDCs were analyzed respectively.

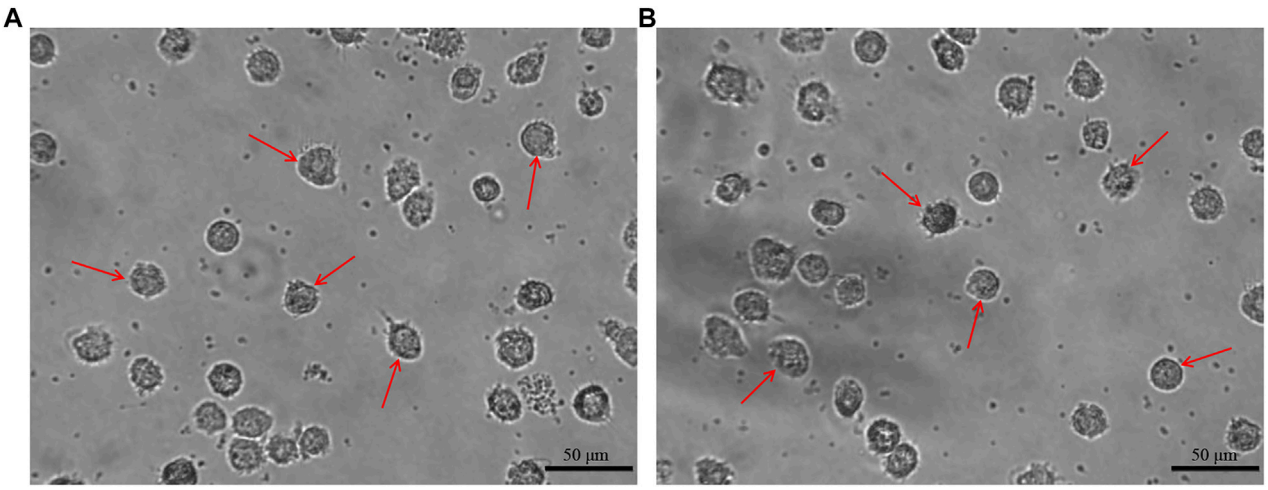

FIGURE 2
The morphology of moDCs. The moDCs derived from a HD and a MM patient are shown in figure **(A, B)** respectively, which are large, irregular in shape with obvious dendritic protrusions.

searching for adjuvants (Ho et al., 2018), which can enhance the maturation and activity of DCs by modulating glucose metabolism and fatty acid metabolism is a promising method to efficiently activate anticancer specific immune responses for an improved clinical efficacy.

Leonurine is a bioactive alkaloid compound extracted from Leonurus japonicus Houtt. Recent researches have proven that leonurine can modulate glucose metabolism and fatty acid metabolism, thus performing significantly protective effects in atherosclerotic disease, diabetes, etc. Huang et al. reported that leonurine modulates glucose metabolism *via* the inhibition of advanced glycation end product (AGE) formation, which exhibits potential to prevent diabetes and its complications (Huang et al., 2015). Jiang et al. reported that leonurine can regulate lipid metabolism *via* the promotion of cholesterol efflux and the reduction of cellular lipid accumulation. This results in the effect of leonurine to prevent atherosclerosis (Jiang et al., 2017). Zhu et al. reported that in the db/db mice model, leonurine (200 mg/kg) administered for 3 weeks significantly reduces the fasting blood glucose level and increases the plasma insulin level. Furthermore, leonurine reduces the plasma triacylglycerol concentration and increases the plasma (high-density lipoprotein)-cholesterol concentration (Huang et al., 2012). Therefore, we hypothesis that leonurine is potential to modulate the glucose metabolism and the fatty acid metabolism of DCs so as to increase the maturation and activity of DCs. Thus, in the current study, we investigated for the first time the effect and mechanism of leonurine on DCs derived from healthy donors (HDs) and MM patients.

2 Materials and methods

2.1 The storage and administration of leonurine

Leonurine was provided by Prof. Yizhun Zhu from School of Pharmacy, Macau University of Science and Technology, China. Leonurine was firstly dissolved in DMSO (Solarbio, China), which was then stored in aliquots at −20°C. The stored leonurine was diluted with 1 × PBS (Solarbio, China), which was then administrated to the cells at the final concentration of 1 μM in the incubation medium.

2.2 Donors

Peripheral blood of 14 HDs and 11 MM patients was used for the investigation on moDC maturation by flow cytometry. The 14 HDs included 7 males and 7 females with the age ranging from 24–37 years old. The 11 MM patients included 6 males and 5 females with the age ranging from 47–77 years old. The MM patients all achieved partial remission (PR) with VRD (bortezomib + lenalidomide + dexamethasone) therapeutic regimen. Peripheral blood of 15 HDs was used for the investigation on the metabolomics of moDC. The 15 HDs included 7 males and 8 females with the age ranging from 22–40 years old. The study has been approved by the Ethics Committee of the Sichuan Provincial People's Hospital. All donors signed the informed consents.

2.3 Generating moDCs *in vitro*

20–30 mL peripheral blood from each donor was isolated for peripheral blood mononuclear cells (PBMCs) by density gradient centrifugation. Firstly, peripheral blood was diluted with the equal volume of 1 × PBS. Then, the diluted blood was pipetted over Human Lymphocyte separation medium Ficoll-Paque (GE Lifesciences, United State) with a volume ratio of 4: 3, which was then centrifuged at 400 × g, acceleration 1, deceleration 0 for 30 min. Thereafter, PBMCs were collected as the buffy coat in the tube. PBMCs were divided evenly into 2 groups. Then, PBMCs were incubated for adhesion in the medium consisting of RPMI 1640 medium (Gibco, United State.), 2 mmol/L L-glutamine (Gibco, United State.), 5% human serum (Sigma, United State), 100 U/mL penicillin (Hyclone, China) and 0.1 mg/mL streptomycin (Hyclone, China) for 24 h. Then non-adherent cells were removed while adherent cells were kept for further incubation. The generation of moDCs was conducted by the incubation of monocytes from adherent cells in the medium consisting of RPMI 1640 medium, 2 mmol/L L-glutamine, 5% human serum, 100 U/

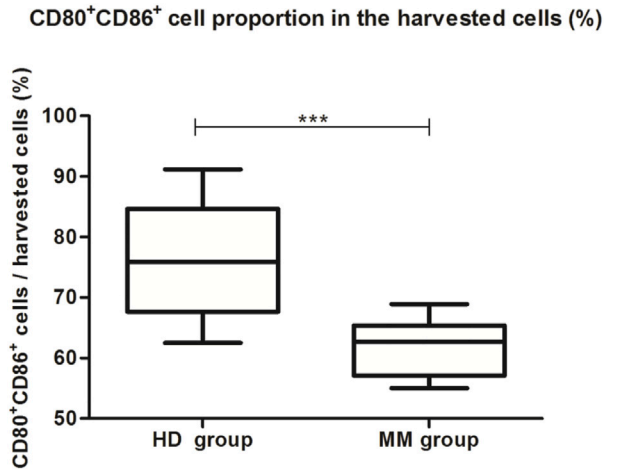

FIGURE 3
The proportion of moDCs in the harvested cells between the HD group and the MM group. The boxplot shows that the proportion of moDCs in the harvested cells in the HD group was significantly higher than in the MM group (75.55% ± 9.69% vs. 61.39% ± 4.86%, p = 0.000, independent-sample t-test).

mL penicillin, 0.1 mg/mL streptomycin, 800 U/mL GM-CSF (Novoprotein, China) and 500 U/mL IL-4 (Novoprotein, China) for 7 days. On the 1st day of incubation, the 2 groups of cells were administrated with or without 1 μM leonurine. On the 8th day, cells were harvested, which were then evaluated by flow cytometry and LC-MS/MS. The morphology of the moDCs was observed and recorded by the inverted microscope (OLYMPUS, Japan).

2.4 The expression of surface markers on moDCs by flow cytometry analysis

1×10^5–1×10^6 of the harvested cells were suspended in 100 ul 1 × PBS and stained with APC anti-human CD40 mAb, FITC anti-human CD80 mAb, APC/Cyanine 7 anti-human CD83 mAb, PE anti-human CD86 mAb and Pacific Blue anti-human HLA-DR mAb (all mAbs are from BioLegend, United State). After the cells were incubated with mAbs for 25–30 min at 4°C in darkness, the stained cells were washed for 2 times by 1 × PBS. Then the cells were suspended in 1×PBS for flow cytometry analysis. FlowJo software was used to analyze the data.

In this study, the technique for generating moDCs *in vitro* is a usually used and efficient technique, which can effectively generate moDCs from PBMCs (Chometon et al., 2020). DC expresses high levels of the surface markers CD80 and CD86, which can serve as the definition of DC (Yonggang et al., 2012). Therefore, in our study, the $CD80^+CD86^+$ cell population in the total harvested cells was defined as moDCs. Then, the median fluorescence intensity (MFI) of surface markers CD40, CD83, and HLA-DR expression on moDCs were analyzed respectively. In our study, we used the Cytoflex flow cytometer (Beckman, United State) to analyze the harvested cells. The analysis of the flow cytometry data is displayed as Figure 1. Firstly, the forward scatter area (FSC-A) and the forward scatter height (FSC-H) were used for the selection of single cells from the total cells. Subsequently, the FSC-A and the side scatter area (SSC-A) were used for the selection of live cells from single cells. Then, $CD80^+CD86^+$ cells were selected from the live cells and defined as moDCs. Finally, the MFI of CD40, CD83 and HLA-DR expression on moDCs were analyzed respectively.

2.5 Evaluation and analysis of metabolomics

HD-moDCs (n = 15) were evaluated for metabolomics. 1×10^6 harvested cells were mixed with 200 μL ultrapure water and vortexed for 30 s. Subsequently, the samples were quickly frozen with liquid nitrogen and then quickly thawed for 3 times. Then, the samples were sonicated for 10 min in ice-water bath. 50 μL of the obtained homogenate was used for the detection of protein concentration. The rest 150 μL homogenate was added with 450 μL methanol (CNW Technologies, Germany) and vortexed for 30 s. The samples were kept at −40°C for 1 h and then centrifuged at 13800 × g for 15 min at 4°C. 550 μL supernatant was transferred into an EP tube and dried in a vacuum concentrator. Then the diluted methanol (methanol: water = 3: 1) with isotopically-labelled internal standard mixture was added into the EP tube and vortexed for 30 s. The samples were sonicated for 10 min in ice-water

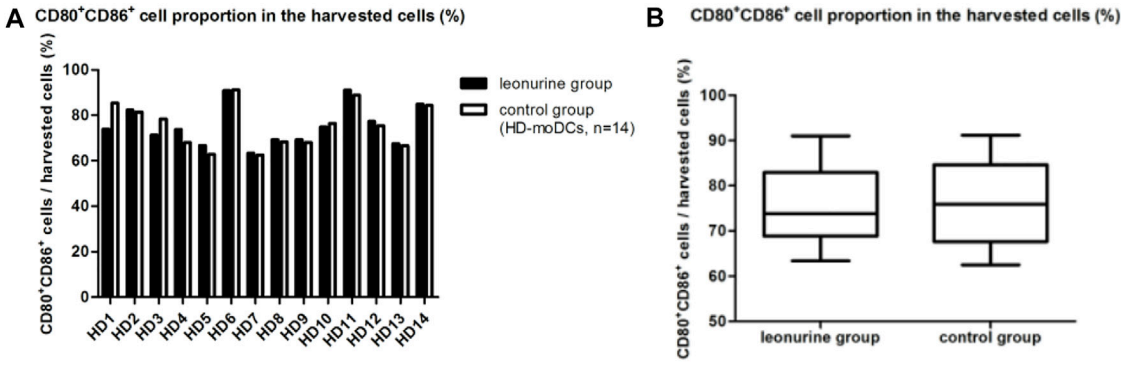

FIGURE 4
The proportion of moDCs ($CD80^+CD86^+$ cells) in the harvested cells between the leonurine group and the control group (HD-moDCs, n = 14). **(A)** The graph shows the proportion of moDCs in the harvested cells between the leonurine group and the control group for each HD. **(B)** The boxplot shows that when moDCs derived from all 14 HDs were analyzed together, there was no statistical difference in the proportion of moDCs in the harvested cells between the leonurine group and the control group (75.45% ± 8.79% vs. 75.55% ± 9.69%, p = 0.300, paired-sample Wilcoxon signed-rank test).

TABLE 1 The proportion of moDCs in the harvested cells (%) in the HD group (*n* = 14) and the MM group (*n* = 11).

Group	1	2	3	4	5	6	7	8	9	10	11	12	13	14
HD	85.4	81.4	78.4	68	62.8	91.2	62.5	68.3	68	76.4	88.9	75.4	66.6	84.4
MM	64.1	68.9	65.4	55.1	58.1	63.2	67.2	55	58.5	62.7	57.1			

TABLE 2 The proportion of moDCs in the harvested cells (%) (HD-moDCs, *n* = 14).

Group	HD1	HD2	HD3	HD4	HD5	HD6	HD7	HD8	HD9	HD10	HD11	HD12	HD13	HD14
Leon	73.9	82.3	71.3	73.7	66.7	90.9	63.4	69.3	69.3	74.8	91	77.3	67.5	84.9
Control	85.4	81.4	78.4	68	62.8	91.2	62.5	68.3	68	76.4	88.9	75.4	66.6	84.4

TABLE 3 The MFI of CD40 expression on moDCs (×105) (HD-moDCs, n = 14).

Group	HD1	HD2	HD3	HD4	HD5	HD6	HD7	HD8	HD9	HD10	HD11	HD12	HD13	HD14
Leon	1.11	1.80	1.60	1.40	1.11	1.27	3.35	3.00	3.67	2.70	1.52	3.02	2.73	1.24
Control	1.08	1.91	1.81	1.42	1.07	1.55	2.24	2.54	3.49	1.66	1.52	1.70	2.60	0.73

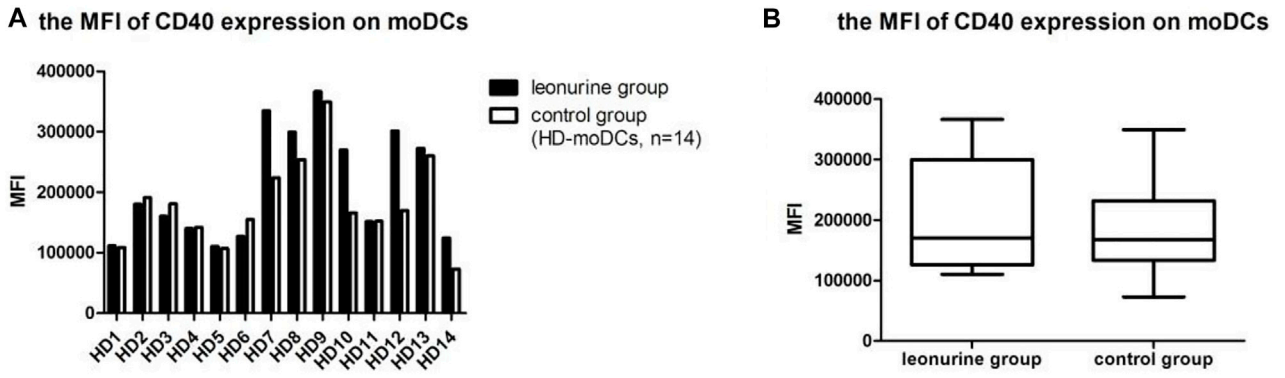

FIGURE 5
The MFI of CD40 expression on moDCs between the leonurine group and the control group (HD-moDCs, *n* = 14). **(A)** The graph shows the MFI of CD40 expression on moDCs between the leonurine group and the control group for each HD. **(B)** The boxplot shows that when moDCs derived from all 14 HDs were analyzed together, the MFI of CD40 expression on moDCs was significantly higher in the leonurine group than in the control group ($2.11 \times 10^5 \pm 0.92 \times 10^5$ vs. $1.81 \times 10^5 \pm 0.72 \times 10^5$, $p = 0.084$, paired-sample Wilcoxon signed-rank test).

bath and then centrifuged at 13800 × g for 15 min at 4°C. The obtained supernatant was transferred into a fresh glass vial for analysis.

Liquid chromatography-tandem mass spectrometry (LC-MS/MS) analysis was performed by an UHPLC system (Thermo Fisher Scientific, United State) with a UPLC HSS T3 column (2.1 × 100 mm, 1.8 μm) coupled to Orbitrap Exploris 120 mass spectrometer (Thermo Fisher Scientific, United State). The mobile phase A consisted of 5 mmol/L ammonium acetate (Sigma, United State) and 5 mmol/L acetic acid (Fisher Chemical, United State) in water (pH = 9.75)while the mobile phase B consisted of acetonitrile (CNW Technologies, Germany). The auto-sampler was set at 4°C with the injection volume of 2 μL. The Orbitrap Exploris 120 mass spectrometer was used to acquire MS/MS spectra on information-dependent acquisition (IDA) mode under the control of the acquisition software. In this mode, the acquisition software continuously evaluated the full scan MS spectrum. The ESI source conditions were set as the following: Sheath gas flow rate as 50 Arb, Aux gas flow rate as 15 Arb, Capillary temperature as 320°C, Full MS resolution as 60000, MS/MS resolution as 15000, Collision energy as 10/30/60 in NCE mode, Spray voltage as 3.8 kV (positive) or −3.4 kV (negative), respectively.

The MS raw data was transformed into the mzXML format by ProteoWizard, which was then processed with R package based on XCMS for peak recognition, peak extraction, peak alignment and integration. Then MS2 database (BiotreeDB) was applied in metabolite annotation. The final dataset containing the information of peak number, sample name and normalized peak area was imported into SIMCA16.0.2 software for multivariate analysis to obtain the variable importance in the projection (VIP) values. Further, the differentially expressed metabolites were screened *via* the criteria of VIP >1 and $p < 0.05$. In addition, the Kyoto Encyclopedia of Genes and Genomes (KEGG) database (http://www.genome.jp/kegg/) was used for pathway analysis.

TABLE 4 The MFI of CD83 expression on moDCs (×105) (HD-moDCs, *n* = 14).

Group	HD1	HD2	HD3	HD4	HD5	HD6	HD7	HD8	HD9	HD10	HD11	HD12	HD13	HD14
Leon	0.82	0.78	1.19	0.70	0.80	0.64	4.44	5.74	7.17	1.89	1.60	1.82	2.99	3.11
Control	0.97	0.81	1.07	0.69	0.69	0.63	4.04	5.18	5.64	1.51	1.61	1.49	3.16	2.39

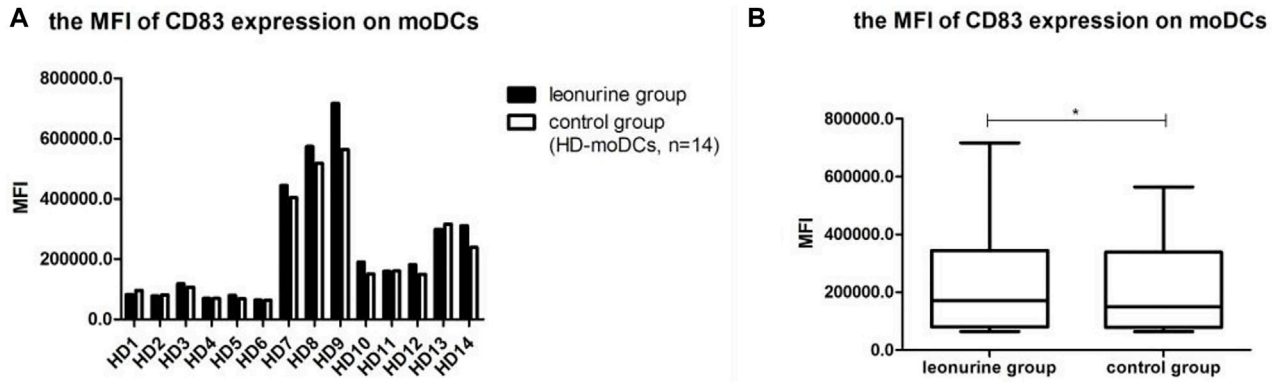

FIGURE 6
The MFI of CD83 expression on moDCs between the leonurine group and the control group (HD-moDCs, *n* = 14). **(A)** The graph shows the MFI of CD83 expression on moDCs between the leonurine group and the control group for each HD. **(B)** The boxplot shows that when moDCs derived from all 14 HDs were analyzed together, the MFI of CD83 expression on moDCs was significantly higher in the leonurine group than in the control group ($2.41 \times 10^5 \pm 2.06 \times 10^5$ vs. $2.14 \times 10^5 \pm 1.71 \times 10^5$, $p = 0.042$, paired-sample *t*-test).

TABLE 5 The MFI of HLA-DR expression on moDCs (× 105) (HD-moDCs, *n* = 14).

Group	HD1	HD2	HD3	HD4	HD5	HD6	HD7	HD8	HD9	HD10	HD11	HD12	HD13	HD14
Leon	6.82	6.06	9.53	16.2	14.3	10.8	7.85	16.0	20.1	11.5	15.7	15.8	11.3	8.98
Control	5.76	6.58	9.22	15.7	14.4	11.8	6.43	13.7	18.5	10.2	15.2	11.4	8.22	8.45

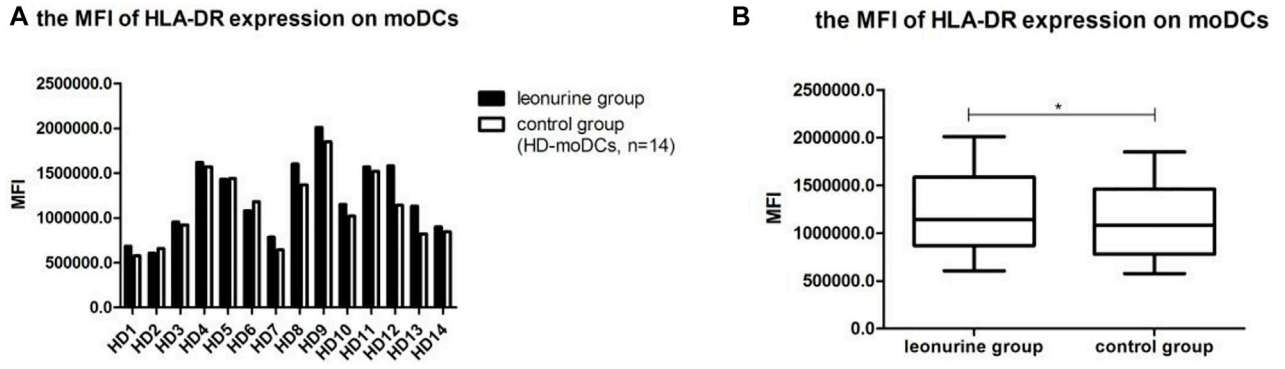

FIGURE 7
The MFI of HLA-DR expression on moDCs between the leonurine group and the control group (HD-moDCs, *n* = 14). **(A)** The graph shows the MFI of HLA-DR expression on moDCs between the leonurine group and the control group for each HD. **(B)** The boxplot shows that when moDCs derived from all 14 HDs were analyzed together, the MFI of HLA-DR expression on moDCs was significantly higher in the leonurine group than in the control group ($12.21 \times 10^5 \pm 4.20 \times 10^5$ vs. $11.11 \times 10^5 \pm 3.94 \times 10^5$, $p = 0.013$, paired-sample *t*-test).

TABLE 6 The proportion of moDCs in the harvested cells (%) (MM patient-moDCs, *n* = 11).

Group	MM1	MM2	MM3	MM4	MM5	MM6	MM7	MM8	MM9	MM10	MM11
Leon	60.7	75.1	61.4	61.5	65.2	67	67.7	58.2	68.1	70.6	58
Control	64.1	68.9	65.4	55.1	58.1	63.2	67.2	55	58.5	62.7	57.1

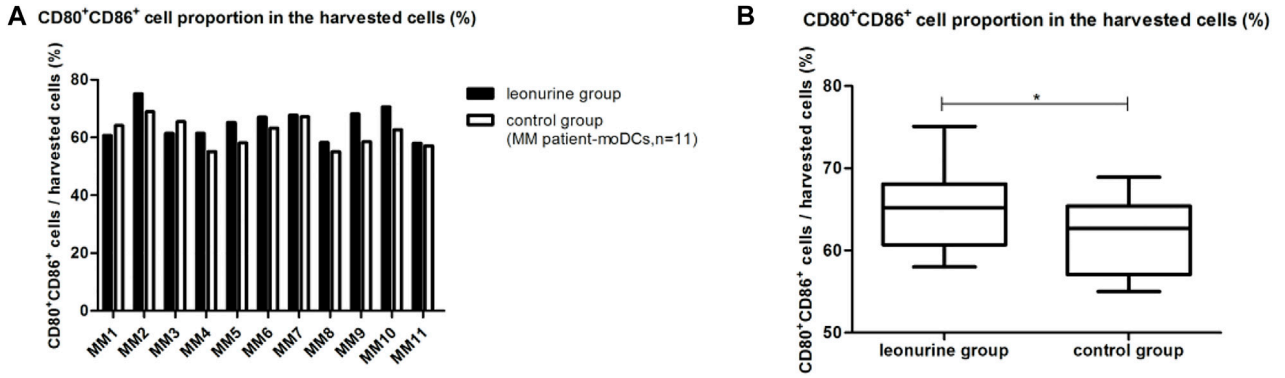

FIGURE 8
The proportion of moDCs in the harvested cells between the leonurine group and the control group (MM patient-moDCs, *n* = 11). **(A)** The graph shows the proportion of moDCs in the harvested cells between the leonurine group and the control group for each MM patient. **(B)** The boxplot shows that when moDCs derived from all 11 MM patients were analyzed together, the proportion of moDCs in the harvested cells was significantly higher in the leonurine group than in the control group (64.86% ± 5.41% vs. 61.39% ± 4.86%, $p = 0.029$, paired-sample *t*-test).

TABLE 7 The MFI of CD40 expression on moDCs (× 10^5) (MM patient-moDCs, *n* = 11).

Group	MM1	MM2	MM3	MM4	MM5	MM6	MM7	MM8	MM9	MM10	MM11
Leon	3.77	1.58	2.70	1.61	0.85	1.81	1.36	3.20	1.22	2.87	0.94
Control	3.18	1.61	2.02	1.45	0.81	1.99	1.07	2.90	1.13	1.91	0.84

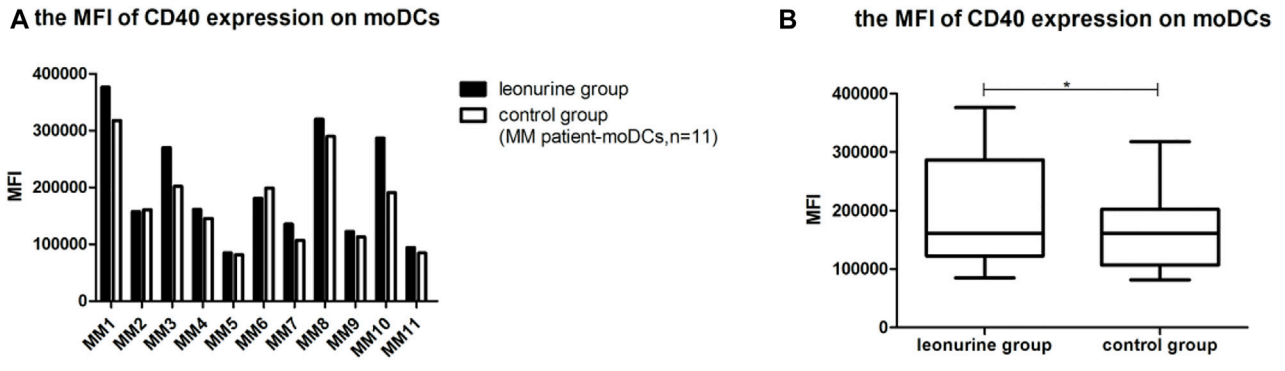

FIGURE 9
The MFI of CD40 expression on moDCs between the leonurine group and the control group (MM patient-moDCs, *n* = 11). **(A)** The graph shows the MFI of CD40 expression on moDCs between the leonurine group and the control group for each MM patient. **(B)** The boxplot shows that when moDCs derived from all 11 MM patients were analyzed together, the MFI of CD40 expression on moDCs was significantly higher in the leonurine group than in the control group ($1.99 \times 10^5 \pm 0.98 \times 10^5$ vs. $1.72 \times 10^5 \pm 0.78 \times 10^5$, $p = 0.025$, paired-sample *t*-test).

TABLE 8 The MFI of CD83 expression on moDCs (× 10^5) (MM patient-moDCs, *n* = 11).

Group	MM1	MM2	MM3	MM4	MM5	MM6	MM7	MM8	MM9	MM10	MM11
Leon	0.62	0.52	0.06	0.26	0.14	0.29	0.22	0.47	0.22	0.40	0.15
Control	0.56	0.47	0.05	0.23	0.14	0.31	0.18	0.43	0.20	0.26	0.14

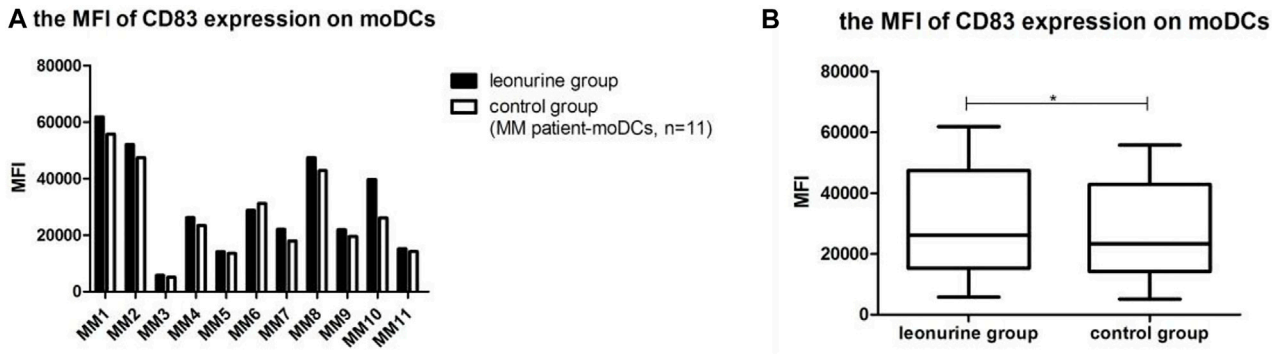

FIGURE 10
The MFI of CD83 expression on moDCs between the leonurine group and the control group (MM patient-moDCs, *n* = 11). **(A)** The graph shows the MFI of CD83 expression on moDCs between the leonurine group and the control group for each MM patient. **(B)** The boxplot shows that when moDCs derived from all 11 MM patients were analyzed together, the MFI of CD83 expression on moDCs was significantly higher in the leonurine group than in the control group ($0.30{\times}10^5 \pm 0.18 \times 10^5$ vs. $0.27 \times 10^5 \pm 0.16 \times 10^5$, $p = 0.020$, paired-sample *t*-test).

TABLE 9 The MFI of HLA-DR expression on moDCs (× 10^5) (MM patient-moDCs, *n* = 11).

Group	MM1	MM2	MM3	MM4	MM5	MM6	MM7	MM8	MM9	MM10	MM11
Leon	11.1	6.30	9.81	7.10	7.73	4.23	6.95	11.5	8.61	5.10	3.97
Control	10.0	6.73	8.55	6.49	7.66	4.27	5.80	9.86	7.31	4.94	3.20

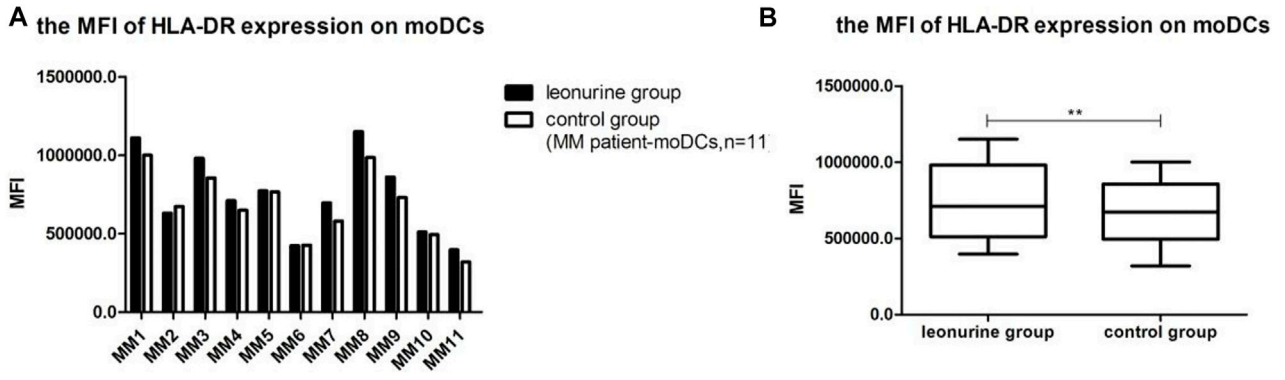

FIGURE 11
The MFI of HLA-DR expression on moDCs between the leonurine group and the control group (MM patient-moDCs, *n* = 11). **(A)** The graph shows the MFI of HLA-DR expression on moDCs between the leonurine group and the control group for each MM patient. **(B)** The boxplot shows that when moDCs derived from all 11 MM patients were analyzed together, the MFI of HLA-DR expression on moDCs was significantly higher in the leonurine group than in the control group ($7.49 \times 10^5 \pm 2.58 \times 10^5$ vs. $6.80 \times 10^5 \pm 2.18 \times 10^5$, $p = 0.006$, paired-sample *t*-test).

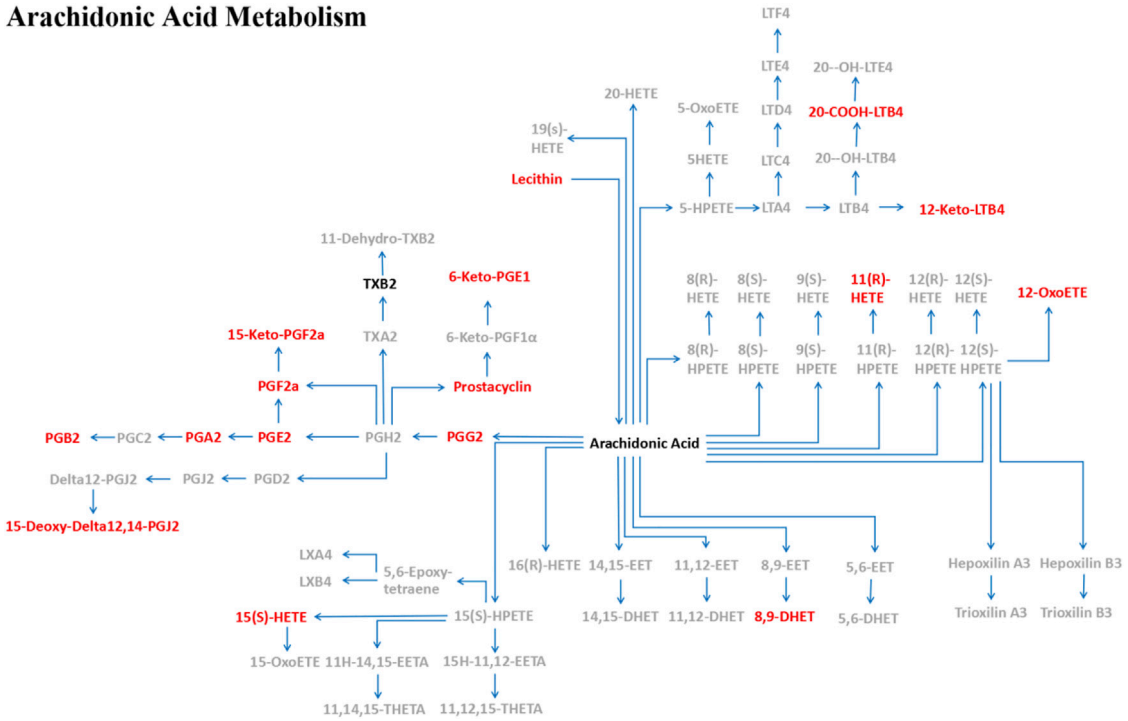

FIGURE 12
The pathway of arachidonic acid metabolism in moDCs with leonurine administration. After moDCs were administrated with leonurine, 16 metabolites (red) were significantly upregulated while 2 metabolites (black) were significantly downregulated in the pathway of arachidonic acid metabolism. 6-Keto-PGE1: 6-Ketoprostaglandin E1; 8,9-DHET: 8,9-DiHETrE; 12-Keto-LTB4: 12-Keto-leukotriene B4; 12-OxoETE: 12-KETE; 15-Deoxy-Delta12,14-PGJ2: 15-Deoxy-d-12,14-PGJ2; 15-Keto-PGF2a: 15-Keto-prostaglandin F2a; 20-COOH-LTB4: 20-Carboxy-leukotriene B4; Lecithin: PC(22:5 (7Z,10Z,13Z,16Z,19Z)/22:4 (7Z,10Z,13Z,16Z)); PGA2: Prostaglandin A2; PGB2: Prostaglandin B2; PGE2: Prostaglandin E2; PGF2a: Prostaglandin F2a; PGG2: Prostaglandin G2; Prostacyclin: Prostaglandin I2; TXB2: Thromboxane B2.

2.6 Statistical analysis

All data was expressed as Mean ± Standard Deviation (SD). All p values were two-sided and p values < 0.05 ($^{*}p < 0.05$, $^{**}p < 0.01$ and $^{***}p < 0.001$) were defined to be statistically significant. All data was subjected to normality test. The statistical analysis of data was performed by SPSS Statistics25.0 software. The graph and boxplot were produced with GraphPad Prism5.0 software. Independent-sample t-test was used for comparing the differences between the HD group and the MM patient group. When the difference between the leonurine group and the control group was analyzed, data which was normally distributed was analyzed with paired-sample t-test while data which was not normally distributed was analyzed with paired-sample Wilcoxon signed-rank test.

3 Results

To prime T cell activation, DCs present antigen-bound MHC molecules to naïve T cell meanwhile provide naïve T cell with costimulatory molecules including CD40, CD80, and CD86, etc. CD40 upregulates CD80, CD83, CD86, and HLA-DR, which promote DC maturation (Levin et al., 2017). Typical costimulatory molecules CD80 and CD86 are highly expressed on the surface of DCs. The expression level of costimulatory molecules CD40, CD80, and CD86 can reflect the maturation and activity of DCs (Hua et al., 2012). HLA-DR belongs to the MHC II molecular family, which usually binds to exogenous antigens and is recognized by $CD4^{+}$ T lymphocytes. DCs with the higher level of maturation express a higher level of HLA-DR molecule (Saito et al., 2008). CD83 provides the signals of the T cell differentiation, which is a maturation marker for DCs (Cao et al., 2005; Pinho et al., 2014). Consequently, we chose these five surface markers as DC maturation markers in order to clarify the possible immunomodulatory effects of leonurine on DCs. During the incubation procedure, cells were administrated with 1 μM leonurine or 1 × PBS as the control group. Then cells were harvested and observed for the morphology of moDCs. Afterwards, cells were analyzed for the expression of CD40, CD80, CD83, CD86, and HLA-DR by flow cytometry. Furthermore, moDCs with or without 1 μM leonurine administration were evaluated by LC-MS/MS for metabolomics which was further analyzed for the potential mechanism of leonurine on moDCs.

3.1 The morphology of moDCs

After incubation of 7 days, the moDCs were obtained. The morphology of the moDCs was observed and recorded by inverted microscope. The moDCs derived from a HD and a MM patient are shown in Figures 2A, B respectively as the examples. Both Figures 2A, B show that the moDCs are large, irregular in shape with obvious dendritic protrusions on the cell surface.

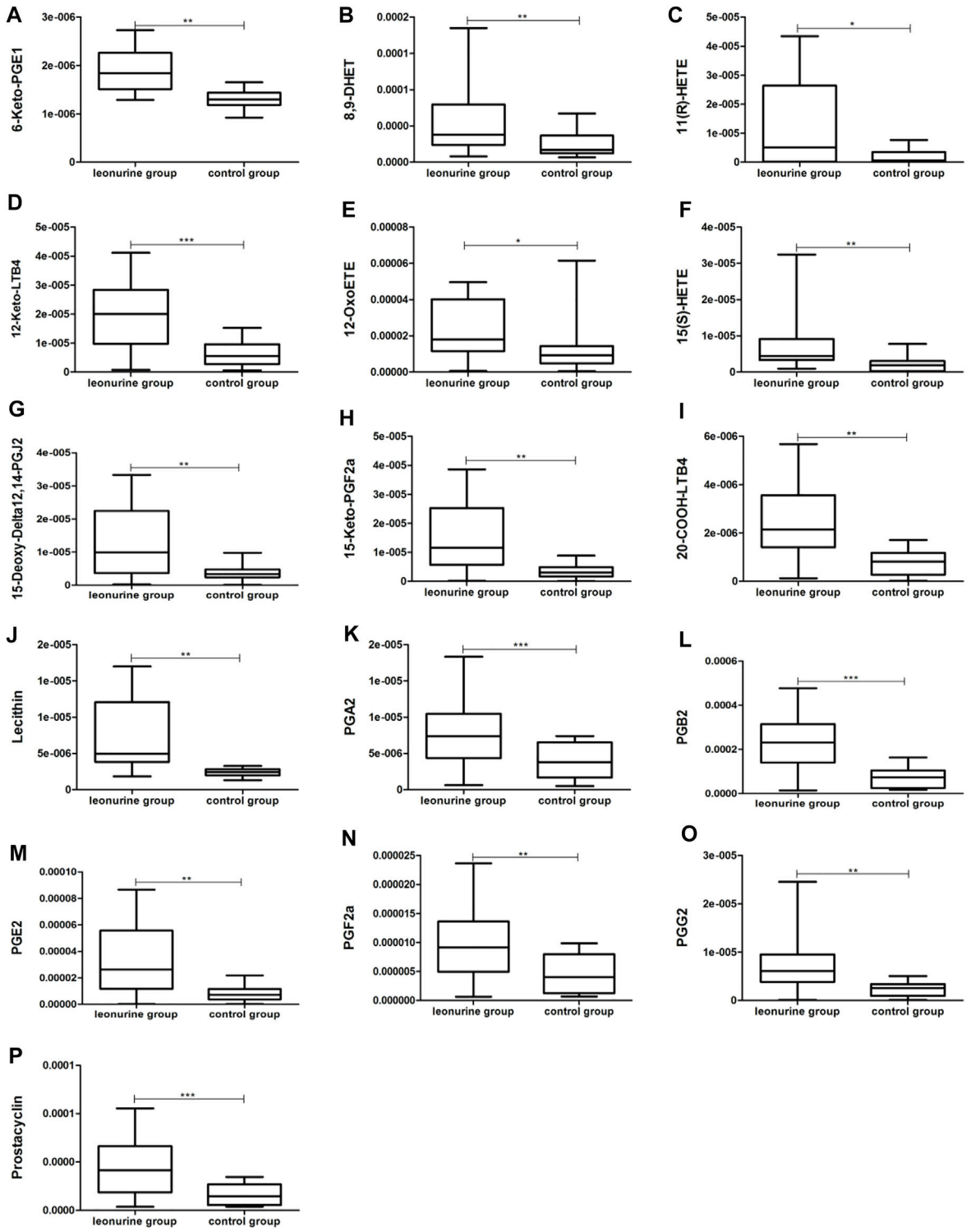

FIGURE 13
The significantly up-regulated metabolites in moDCs with leonurine administration (HD-moDCs, n = 15). 16 metabolites as shown in the above boxplots **(A–P)** were significantly up-regulated in the leonurine group than in the control group.

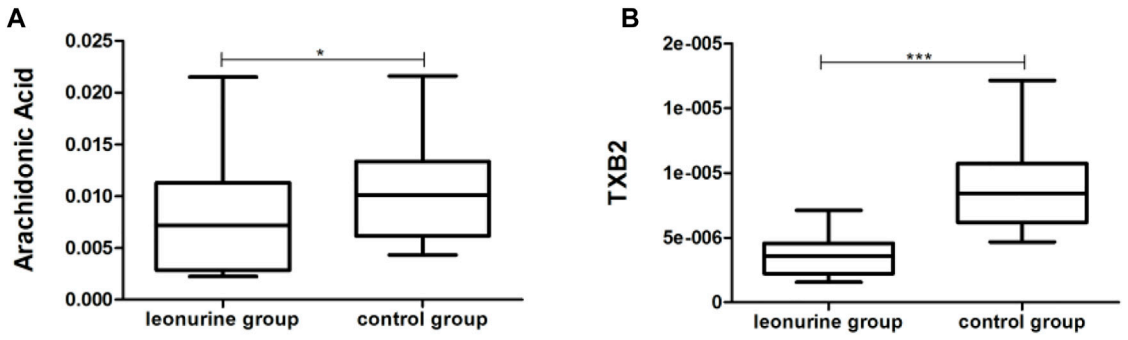

FIGURE 14
The significantly down-regulated metabolites in moDCs with leonurine administration (HD-moDCs, n = 15). 2 metabolites as shown in the above boxplots **(A,B)** were significantly down-regulated in the leonurine group than in the control group.

3.2 The comparison between the HD group and the MM group

Firstly, we compared the proportion of moDCs ($CD80^+CD86^+$ cells) in the total harvested cells between the HD group and the MM group. The proportion of moDCs in the harvested cells in the HD group was significantly higher than in the MM group (75.55% ± 9.69% vs. 61.39% ± 4.86%, p = 0.000, independent-sample t-test) (Table 1; Figure 3).

4 The effects of leonurine on the moDCs derived from HDs

4.1 The effect of leonurine on the proportion of moDCs in the total harvested cells (%)

When moDCs ($CD80^+$ $CD86^+$ cells) derived from all 14 HDs were analyzed together, there was no statistical difference in the proportion of moDCs in the harvested cells between the leonurine group and the control group (75.45% ± 8.79% vs. 75.55% ± 9.69%, p = 0.300, paired-sample Wilcoxon signed-rank test) (Table 2; Figure 4).

4.2 The effect of leonurine on CD40 expression of moDCs

When moDCs derived from all 14 HDs were analyzed together, the MFI (mean fluorescence intensity) of CD40 expression on moDCs was significantly higher in the leonurine group than in the control group ($2.11 \times 10^5 \pm 0.92 \times 10^5$ vs. $1.81 \times 10^5 \pm 0.72 \times 10^5$, p = 0.084, paired-sample Wilcoxon signed-rank test) (Table 3; Figure 5).

4.3 The effect of leonurine on CD83 expression of moDCs

When moDCs derived from all 14 HDs were analyzed together, the MFI of CD83 expression on moDCs was significantly higher in the leonurine group than in the control group ($2.41 \times 10^5 \pm 2.06 \times 10^5$ vs. $2.14 \times 10^5 \pm 1.71 \times 10^5$, p = 0.042, paired-sample t-test) (Table 4; Figure 6).

4.4 The effect of leonurine on HLA-DR expression of moDCs

When moDCs derived from all 14 HDs were analyzed together, the MFI of HLA-DR expression on moDCs was significantly higher in the leonurine group than in the control group ($12.21 \times 10^5 \pm 4.20 \times 10^5$ vs. $11.11 \times 10^5 \pm 3.94 \times 10^5$, p = 0.013, paired-sample t-test) (Table 5; Figure 7).

5 The effects of leonurine on the moDCs derived from MM patients

5.1 The effect of leonurine on the proportion of moDCs in the total harvested cells (%)

When moDCs derived from all 11 MM patients were analyzed together, the proportion of moDCs in the harvested cells was significantly higher in the leonurine group than in the control group (64.86% ± 5.41% vs. 61.39% ± 4.86%, p = 0.029, paired-sample t-test) (Table 6; Figure 8).

5.2 The effect of leonurine on CD40 expression of moDCs

When moDCs derived from all 11 MM patients were analyzed together, the MFI of CD40 expression on moDCs was significantly higher in the leonurine group than in the control group ($1.99 \times 10^5 \pm 0.98 \times 10^5$ vs. $1.72 \times 10^5 \pm 0.78 \times 10^5$, p = 0.025, paired-sample t-test) (Table 7; Figure 9).

5.3 The effect of leonurine on CD83 expression of moDCs

When moDCs derived from all 11 MM patients were analyzed together, the MFI of CD83 expression on moDCs in the leonurine group was significantly higher than in the control group ($0.30 \times 10^5 \pm 0.18 \times 10^5$ vs. $0.27 \times 10^5 \pm 0.16 \times 10^5$, p = 0.020, paired-sample t-test) (Table 8;Figure 10).

5.4 The effect of leonurine on HLA-DR expression of moDCs

When moDCs derived from all 11 MM patients were analyzed together, the MFI of HLA-DR expression on moDCs was significantly higher in the leonurine group than in the control group ($7.49 \times 10^5 \pm 2.58 \times 10^5$ vs. $6.80 \times 10^5 \pm 2.18 \times 10^5$, $p = 0.006$, paired-sample *t*-test) (Table 9;Figure 11).

6 Leonurine regulates on the metabolism of moDCs

MoDCs with or without 1 μM leonurine administration (HD-moDCs, n = 15) were evaluated by LC-MS/MS for metabolomics. The metabolomics data showed that in moDCs, 18 metabolites in the pathway of arachidonic acid metabolism were significantly different between the leonurine group and the control group (VIP all >1 and *P* all <0.05; Figure 12). To be specific, 16 metabolites including 6-Keto-PGE1 (Figure 13A), 8,9-DHET (Figure 13B), 11(R)-HETE (Figure 13C), 12-Keto-LTB4 (Figure 13D), 12-OxoETE (Figure 13E), 15(S)-HETE (Figure 13F), 15-Deoxy-Delta12,14-PGJ2 (Figure 13G), 15-Keto-PGF2a (Figure 13H), 20-COOH-LTB4 (Figure 13I), Lecithin (Figure 13J), PGA2 (Figure 13K), PGB2 (Figure 13L), PGE2 (Figure 13M), PGF2a (Figure 13N), PGG2 (Figure 13O) and Prostacyclin (Figure 13P) were significantly up-regulated in the leonurine group than in the control group (Figure 13), while 2 metabolites including Arachidonic Acid (Figure 14A) and TXB2 (Figure 14B) were significantly down-regulated in the leonurine group than in the control group (Figure 14).

7 Discussion

MM is a hematological malignancy originating from the malignant transformation of plasma cells, which is still incurable up to date with the second highest incidence in hematological malignancies. MM patients show significant immunodeficiency. Especially, the immunodeficiency of DCs results in the inability of DCs to efficiently elicit anticancer specific immune responses, which leads to the development and recurrence of the disease. Therefore, it is an important therapeutic direction to reverse the immunodeficiency of DCs in MM patients, in order to efficiently activate anticancer specific immune responses and prevent disease progression. In the current study, we for the first time found that leonurine can significantly enhance the maturation and activity of moDCs both in HDs and MM patients. It is shown that leonurine significantly enhances the MFI of CD40, CD83 and HLA-DR expression on HD-moDCs as well as MM patient-moDCs, which indicates that leonurine can promote the maturation and activity of both HD-moDCs and MM patient-moDCs. Moreover, the proportion of moDCs in the total harvested cells is significantly higher in the HD group than in the MM patient group, which also indicates the immunodeficiency of MM patients compared with HDs (Shinde et al., 2018). Therefore, our results show the potential of leonurine as a DC adjuvant to promote the maturation and activity of DCs of MM patients. Leonurine is promising to be applied in DC-based anticancer therapy strategies such as DC vaccine and DC cell-therapy in MM.

As leonurine has been shown in several studies to modulate the glucose metabolism and the fatty acid metabolism, we hypothesis that leonurine is potential to regulate the metabolism of DCs. In the current study, we further confirm that leonurine significantly regulates on the pathway of the arachidonic acid metabolism. The metabolomics data showed that in the pathway of arachidonic acid metabolism, 16 metabolites were significantly upregulated while 2 metabolites were significantly downregulated in moDCs administrated with leonurine. Liu et al. also reported that leonurine can regulate the arachidonic acid metabolism pathway of macrophages by the inhibition of Cyclooxygenase-2, 5-lipoxygenase and microsomal prostaglandin E synthase-1 (Liu et al., 2018). Thus, the mechanism of leonurine is closely related to arachidonic acid metabolism pathway. On the other hand, since the maturation and activity of moDCs is closely related to the cellular metabolism of moDCs including the fatty acid metabolism (Williams and O'Neill, 2018), our study shows the consistent results that arachidonic acid metabolism of moDCs is significantly increased, while the maturation of moDCs is significantly enhanced.

In conclusion, this study indicates for the first time that leonurine significantly promotes the maturation of moDCs derived from both HDs and MM patients, the mechanism of which is related to the regulation on the arachidonic acid metabolism pathway. Leonurine is potential to be applied as a DC adjuvant in DC-based therapeutic strategies for MM patients such as DC vaccine and DC cell therapy.

Data availability statement

The original contributions presented in the study are included in the article/Supplementary Material, further inquiries can be directed to the corresponding authors.

Ethics statement

The studies involving human participants were reviewed and approved by The Ethics Committee of the Sichuan Provincial People's Hospital. The patients/participants provided their written informed consent to participate in this study.

Author contributions

All authors listed have made a substantial and direct contribution to the work and approved it for publication. CC and LH prepared the first draft of the manuscript. The study was conceptualized by JD who also supervised the work and reviewed the entire manuscript. YZ provided leonurine for this study, who took part in the design and discussion of this study. XW, SC and ZY collected samples of healthy donors. RX, YW, and XW collected samples of MM patients. All authors read and approved the final version of the manuscript.

Funding

This study was supported by Youth Program of National Natural Science Foundation of China (G0582003767), Sichuan Academy of Medical Sciences and Sichuan Provincial People's Hospital clinical study and translational fund (2020LZ01) and Sichuan Science and Technology Program (2023YFS0159).

Acknowledgments

Thanks to Shanghai Biotree Biotechnology which provides help on the analysis of the metabolomics data in this study.

Conflict of interest

The authors declare that the research was conducted in the absence of any commercial or financial relationships that could be construed as a potential conflict of interest.

Publisher's note

All claims expressed in this article are solely those of the authors and do not necessarily represent those of their affiliated organizations, or those of the publisher, the editors and the reviewers. Any product that may be evaluated in this article, or claim that may be made by its manufacturer, is not guaranteed or endorsed by the publisher.

References

Cao, W., Lee, S. H., and Lu, J. (2005). CD83 is preformed inside monocytes, macrophages and dendritic cells, but it is only stably expressed on activated dendritic cells. *Biochem. J.* 385, 85–93. doi:10.1042/BJ20040741

Chometon, T. Q., Siqueira, M. D. S., Sant Anna, J. C., Almeida, M. R., Gandini, M., Martins de Almeida Nogueira, A. C., et al. (2020). A protocol for rapid monocyte isolation and generation of singular human monocyte-derived dendritic cells. *PLoS One* 15 (4), e0231132. doi:10.1371/journal.pone.0231132

Curtis, K. D., Smith, P. R., Despres, H. W., Snyder, J. P., Hogan, T. C., Rodriguez, P. D., et al. (2020). Glycogen metabolism supports early glycolytic reprogramming and activation in dendritic cells in response to both TLR and syk-dependent CLR agonists. *Cells* 9 (3), 715. doi:10.3390/cells9030715

Giovanelli, P., Sandoval, T. A., and Cubillos-Ruiz, J. R. (2019). Dendritic cell metabolism and function in tumors. *Trends Immunol.* 40 (8), 699–718. doi:10.1016/j.it.2019.06.004

Ho, N. I., Huis, L. G. M., 't VeldRaaijmakers, T. K., and Adema, G. J. (2018). Adjuvants enhancing cross-presentation by dendritic cells: The key to more effective vaccines? *Front. Immunol.* 9, 2874. doi:10.3389/fimmu.2018.02874

Hua, H., Liang, Z., Li, W., Meng, Y., Li, X., Zhang, Z., et al. (2012). Phenotypic and functional maturation of murine dendritic cells (DCs) induced by purified Glycyrrhizin (GL). *Int. Immunopharmacol.* 12 (3), 518–525. doi:10.1016/j.intimp.2012.01.006

Huang, H., Xin, H., Liu, X., Xu, Y., Wen, D., Zhang, Y., et al. (2012). Novel anti-diabetic effect of SCM-198 via inhibiting the hepatic NF-κB pathway in db/db mice. *Biosci. Rep.* 32 (2), 185–195. doi:10.1042/BSR20110017

Huang, L., Yang, X., Peng, A., Wang, H., Lei, X., Zheng, L., et al. (2015). Inhibitory effect of leonurine on the formation of advanced glycation end products. *Food Funct.* 6 (2), 584–589. doi:10.1039/c4fo00960f

Jiang, T., Ren, K., Chen, Q., Li, H., Yao, R., Hu, H., et al. (2017). Leonurine prevents atherosclerosis via promoting the expression of ABCA1 and ABCG1 in a ppary/lxrα signaling pathway-dependent manner. *Cell Physiol. Biochem.* 43 (4), 1703–1717. doi:10.1159/000484031

Levin, N., Pato, A., Cafri, G., Eisenberg, G., Peretz, T., Margalit, A., et al. (2017). Spontaneous activation of antigen-presenting cells by Genes encoding truncated homo-oligomerizing derivatives of CD40. *J. Immunother.* 40 (2), 39–50. doi:10.1097/CJI.0000000000000150

Liu, Y., Duan, C., Chen, H., Wang, C., Liu, X., Qiu, M., et al. (2018). Inhibition of COX-2/mPGES-1 and 5-LOX in macrophages by leonurine ameliorates monosodium urate crystal-induced inflammation. *Toxicol. Appl. Pharmacol.* 351, 1–11. doi:10.1016/j.taap.2018.05.010

Pinho, M. P., Migliori, I. K., Flatow, E. A., and Barbuto, J. A. (2014). Dendritic cell membrane CD83 enhances immune responses by boosting intracellular calcium release in T lymphocytes. *J. Leukoc. Biol.* 95 (5), 755–762. doi:10.1189/jlb.0413239

Pinto, V., Bergantim, R., Caires, H. R., Seca, H., Guimaraes, J. E., and Vasconcelos, M. H. (2020). Multiple myeloma: Available therapies and causes of drug resistance. *Cancers (Basel)* 12 (2), 407. doi:10.3390/cancers12020407

Qiu, C. C., Atencio, A. E., and Gallucci, S. (2019). Inhibition of fatty acid metabolism by etomoxir or TOFA suppresses murine dendritic cell activation without affecting viability. *Immunopharmacol. Immunotoxicol.* 41 (3), 361–369. doi:10.1080/08923973.2019.1616754

Saito, K., Ait-Goughoulte, M., Truscott, S. M., Meyer, K., Blazevic, A., Abate, G., et al. (2008). Hepatitis C virus inhibits cell surface expression of HLA-DR, prevents dendritic cell maturation, and induces interleukin-10 production. *J. Virol.* 82 (7), 3320–3328. doi:10.1128/JVI.02547-07

Shinde, P., Fernandes, S., Melinkeri, S., Kale, V., and Limaye, L. (2018). Compromised functionality of monocyte-derived dendritic cells in multiple myeloma patients may limit their use in cancer immunotherapy. *Sci. Rep.* 8 (1), 5705. doi:10.1038/s41598-018-23943-w

Tan, Y., Meng, Y., Wang, Z., Shan, F., Wang, Q., and Zhang, N. (2012). Maturation of morphology, phenotype and functions of murine bone marrow-derived dendritic cells (DCs) induced by polysaccharide Kureha (PSK). *Hum. Vaccin Immunother.* 8 (12), 1808–1816. doi:10.4161/hv.21993

Thwe, P. M., Pelgrom, L. R., Cooper, R., Beauchamp, S., Reisz, J. A., D'Alessandro, A., et al. (2019). Cell-intrinsic glycogen metabolism supports early glycolytic reprogramming required for dendritic cell immune responses. *Cell Metab.* 30 (1), 225. doi:10.1016/j.cmet.2019.05.017

Williams, N. C., and O'Neill, L. A. J. (2018). A role for the krebs cycle intermediate citrate in metabolic reprogramming in innate immunity and inflammation. *Front. Immunol.* 9, 141. doi:10.3389/fimmu.2018.00141

Yonggang, T., Yiming, M., Heying, Z., Cheng, S., Qiushi, W., Xianghong, Y., et al. (2012). Maturation and upregulation of functions of murine dendritic cells (DCs) under the influence of purified aromatic-turmerone (AR). *Hum. Vaccin Immunother.* 8 (10), 1416–1424. doi:10.4161/hv.21526

frontiers | Frontiers in Oncology

TYPE Review
PUBLISHED 23 February 2023
DOI 10.3389/fonc.2023.1141610

OPEN ACCESS

EDITED BY
Lili Feng,
Harbin Engineering University, China

REVIEWED BY
Ernestina Saulle,
National Institute of Health (ISS), Italy
Nicolas Chatain,
University Hospital RWTH Aachen, Germany

*CORRESPONDENCE
Nunzio Vicario
nunziovicario@unict.it
Giuseppe Musumeci
g.musumeci@unict.it

†These authors have contributed equally to this work and share first authorship

‡These authors have contributed equally to this work and share last authorship

SPECIALTY SECTION
This article was submitted to Pharmacology of Anti-Cancer Drugs, a section of the journal Frontiers in Oncology

RECEIVED 10 January 2023
ACCEPTED 13 February 2023
PUBLISHED 23 February 2023

CITATION
La Spina E, Giallongo S, Giallongo C, Vicario N, Duminuco A, Parenti R, Giuffrida R, Longhitano L, Li Volti G, Cambria D, Di Raimondo F, Musumeci G, Romano A, Palumbo GA and Tibullo D (2023) Mesenchymal stromal cells in tumor microenvironment remodeling of BCR-ABL negative myeloproliferative diseases. *Front. Oncol.* 13:1141610. doi: 10.3389/fonc.2023.1141610

Mesenchymal stromal cells in tumor microenvironment remodeling of BCR-ABL negative myeloproliferative diseases

Enrico La Spina[1†], Sebastiano Giallongo[1†], Cesarina Giallongo[2†], Nunzio Vicario[1*‡], Andrea Duminuco[3], Rosalba Parenti[1], Rosario Giuffrida[1], Lucia Longhitano[1], Giovanni Li Volti[1], Daniela Cambria[3], Francesco Di Raimondo[3], Giuseppe Musumeci[1*‡], Alessandra Romano[3], Giuseppe Alberto Palumbo[2‡] and Daniele Tibullo[1‡]

[1]Department of Biomedical and Biotechnological Sciences, University of Catania, Catania, Italy, [2]Department of Medical-Surgical Science and Advanced Technologies "Ingrassia", University of Catania, Catania, Italy, [3]Department of General Surgery and Medical-Surgical Specialties, A.O.U. "Policlinico-Vittorio Emanuele", University of Catania, Catania, Italy

Chronic myeloproliferative neoplasms encompass the BCR-ABL1-negative neoplasms polycythemia vera (PV), essential thrombocythemia (ET), and primary myelofibrosis (PMF). These are characterized by calreticulin (CALR), myeloproliferative leukemia virus proto-oncogene (MPL) and the tyrosine kinase Janus kinase 2 (JAK2) mutations, eventually establishing a hyperinflammatory tumor microenvironment (TME). Several reports have come to describe how constitutive activation of JAK-STAT and NFκB signaling pathways lead to uncontrolled myeloproliferation and pro-inflammatory cytokines secretion. In such a highly oxidative TME, the balance between Hematopoietic Stem Cells (HSCs) and Mesenchymal Stromal Cells (MSCs) has a crucial role in MPN development. For this reason, we sought to review the current literature concerning the interplay between HSCs and MSCs. The latter have been reported to play an outstanding role in establishing of the typical bone marrow (BM) fibrotic TME as a consequence of the upregulation of different fibrosis-associated genes including PDGF- β upon their exposure to the hyperoxidative TME characterizing MPNs. Therefore, MSCs might turn to be valuable candidates for niche-targeted targeting the synthesis of cytokines and oxidative stress in association with drugs eradicating the hematopoietic clone.

KEYWORDS

oxidative stress, mesenchymal stromal cells, tumor microenvironment, myeloproliferative cancer, JAK - STAT signaling pathway

1 Introduction

Chronic myeloproliferative neoplasms (MPNs) might be defined as clonal hematopoietic stem cell (HSC) disorders characterized by an aberrant proliferation of myeloid lineages (1). Furthermore, according to the 2008 World Health Organization Classification Scheme, MPNs are classified by as BCR-ABL1-negative neoplasms (2–5). MPNs encompass a spectrum of clonal hematological disorders, including three main clinical entities: polycythemia vera (PV), essential thrombocythemia (ET), and primary myelofibrosis (PMF) (6). These myeloid malignancies arise due to acquired somatic stem cell lesions affecting calreticulin (CALR), myeloproliferative leukemia virus proto-oncogene (MPL), and the tyrosine kinase Janus kinase 2 (JAK2), usually displaying a valine-to-phenylalanine mutation at 617 (JAK2V617F) (7). This turns to be the most prevalent mutation associated with 95% of PV, 60% of ET and PMF, while CALR and MPL mutations are mainly associated with ET and MF (about the 50% of patients) (8–11). Even though the 10% of MPNs patients are triple negative for these mutations, ET and MF patients may harbor a noncanonical mutations in JAK2 or MPL with its subsequent clonal evolution (12). CALR plays an essential role in programmed cell death induced by oxidative stress (13–16). It is an endoplasmic reticulum chaperone acting in the regulation of protein folding and Ca^{2+} homeostasis (17) by controlling cellular stress responses (18–20). Increased CALR levels enhance cell sensitivity to hydrogen peroxide (H_2O_2)-mediated cytotoxicity (21). Although the mechanism of action triggered by mutated CALR has not been elucidated yet, its role in inflammation has been associated with its oncogenic action, since it works as an autocrine growth factor in synergy with MPL. Corroborating this scenario, several studies showed that CALR mutations drive oncogenic transformation in a MPL-dependent manner, eventually stimulating JAK-STAT signaling (22–25). For these reasons, CALR, MPL and JAK2V617F, despite they are usually mutually exclusive, have been defined as “driving mutations”. “Founding mutation”, on the other hand, are still unknown (26). Several studies reported MPNs propensity to progress through different disease stages starting from PV or ET towards an aggressive secondary myelofibrosis (MF), finally leading to fibrosis, osteosclerosis, and extramedullary hematopoiesis (27–29). Besides any classification, accumulating evidence suggests that MPNs may be considered as a valid “human inflammation model” for cancer development due to JAK-STAT and NFκB hyperactivation, eventually leading to uncontrolled myeloproliferation and pro-inflammatory cytokines secretion. The most abundant pro-inflammatory cytokines involved in the alteration of hematopoietic TME include platelets-derived growth factor (PDGF), interleukin-1 (IL-1), lipocalin and fibrogenic transforming growth factor-beta (TGF-β). The latter plays a multitude of roles in osteosclerosis and myeloproliferation, promoting Bone Marrow (BM) fibrosis, microvessel density and suppressing physiological blood cell development (30–32). The JAK2V617F mutation has been correlated with a prominent redox alteration since the huge amount of reactive oxygen species (ROS) levels, resulting from an unbalanced H_2O_2 ratio following misbalanced catalase concentration (33). The genesis of a steady inflammatory stream ultimately induces a chronic oxidative stress state with elevated ROS levels in the BM niche (34). In such highly oxidative environment, cellular and extra-cellular components need to form a continuum to maintain the balance between biological processes involving HSCs and Mesenchymal Stromal Cells (MSCs). While BM-HSCs are mostly kept in a quiescent state, MSCs differentiate into several cell subpopulation of mesodermal origin, such as adipocytes, chondroblasts, and osteoblasts (OBs) (35, 36). Anatomically, MSCs may be found in various structures, including BM, adipose tissue, and umbilical cord. Inside BM-TME, MSCs are mainly involved in intercellular crosstalk and proliferation (37). As precursors of BM stromal cells, they are thought to play a pivotal role in the pathophysiology of hematological diseases including MPNs. Within this pathological condition, a significant difference between patient-derived and donor-derived MSCs has been described (38). The interplay between MSCs and HSCs in conditioning each other also concerns HSCs-MSCs-lineage (39). Thus, during ROS accumulation, the balance between the two populations is impaired, and it eventually sets the stage for HSCs to evolve

perpetuating vicious circle generates ROS, in turn establishing a prooxidative and inflammatory microenvironment. To escape from these non-permissive conditions, the Suppressors of Cytokine Signaling (SOCS) is activated and binds JAKs and ensures an arrest of the whole inflammatory process (40–42). Another intriguing survival pathway in MPNs has been described by Forte and coworkers, suggesting the contribution of $Nestin^+$ BM-MSCs in acute myeloid leukemia (AML) development and chemoresistance *in vivo* (43). In particular, it has been found that GSH-dependent antioxidant pathways hold as key role in the BM-MSCs crosstalk and represents a potential target for adjuvant therapies in MPNs. It has been also found that Nestin+ niches are reduced in humans or mice with MPNs (43). Despite the existence of different pharmacological strategies against MPNs, including interferon-alpha2 hydroxyurea and statins, patients have higher probability to experience autoimmune issues or the risk of Acute Myeloid Leukemia transformation (44). With the introduction of JAK1/2 inhibitors, such as Ruxolitinib, immune system is potently suppressed, constitutional symptoms are decreased together with pro-inflammatory cytokines burden in BM-TME (45). Nowadays, the main issue with JAK-STAT inhibition is related to the poor Ruxolitinib antioxidant capacity (46). Bjørn et al., evaluated the effect of Ruxolitinib in producing superoxide radicals and H_2O_2 by HSCs-derived monocytes in blood samples from patients with MF together with DNA damage. The production of superoxide was significantly decreased during treatment, but no influence on the generation of H_2O_2 or the global level of oxidatively altered DNA was found. As the pro-inflammatory cytokine TGF-β plays a central role in MF genesis, and the effect of TGF-β on ROS concentrations has been evaluated in recent studies (47, 48). Results demonstrated that TGF-β administration increases expression levels of a specific miRNA, decreasing SOD2 action, and eventually promoting ROS increase. The recent employment of galunisertib, a small molecule antagonist of the TGF-β receptor type 1 (TGF-βR1) with possible antineoplastic action decreased miRNA expression and ROS increase while resulting in re-established SOD2 activity decreasing the altered oxidative stress state (49). Considering the vicious cycle between chronic inflammation and ROS overproduction, we herein

will discuss the role of ROS in MPNs pathogenesis, together with the role of JAK2V617F+ neighboring BM healthy MSCs, as tumor own ability to adapt to BM-TME to manage chronic oxidative stress.

2 Role of MSCs in fibrosis

The plethora of stromal cells in a normal BM niche suggests that distinct stromal subtypes have specific roles, not only in normal hematopoiesis but also in fibrosis (50, 51). MF was thought to be a reactive phenomenon caused by the interaction between malignant hematopoiesis and BM-TME mediated by profibrotic cytokines (52). In this context a breakthrough work has been recently published by Schneider's group. Here, the authors performed a spatial RNA-seq analysis to depict a scenario in which two distinct MSC populations (MSC-1 and MSC-2) are the main drivers of BM fibrosis. The progression towards this phenotype was marked by overexpression of the alarmin complex S100A8/S100A9, which once targeted by a specific inhibitor improved the overall MPN and fibrosis status (53). By the abovementioned genetic fate tracing experiments, together with single-cell RNA-Seq data of the BM niche cell populations, it was possible to identify five major fibrosis-driving MSCs populations: i) GLI1+ myofibroblasts; ii) Leptin receptor (LepR)-; iii) platelet-derived growth factor receptor α (PDGFR-α)-; iv) vascular cellular adhesion molecule 1 (VCAM1)- and v) Nestin-expressing MSCs. Besides their role in fibrosis, these populations also downregulated the expression of key HSC-supporting factors while they upregulated fibrosis-related genes (54). GLI1$^+$ myofibroblasts together with activated cancer-associated fibroblasts (CAFs), play an important role in BM fibrosis genesis (55) and are assumed to be the major sources of new matrix components as well as to reorganize the extracellular matrix (Figure 1) (56). This population is characterized by the expression of cell surface antigens typical of the hematopoietic lineage, such as CD45 and CD11b, and also matrix proteins as type I-III collagen and fibronectin. in this context, recent evidence depicted the involvement of IGFBP6/sonic hedgehog (SHH)/Toll-like receptor 4 (TLR4) axis in the TME alterations (57). This cascade has been reported to promote MSCs CAF transition upon IGFBP-6 signaling stimulation (58). Despite high levels of collagen expressed by activated fibrocytes, the extracellular space in their immediate proximity contains few collagen particles and no collagen fibers, thus suggesting that collagen fibers in MF are not polymerized by megakaryocytes' LOX2 (59). To further investigate possible player within this context, several mice model have been established, which however usually lack in mirroring patients' condition (32). ASXL mutations, for instance, accelerate BM fibrosis by reprograming the fibrosis-driving potential of hematopoietic cells to fibrocytes, and further confirm that neoplastic fibrocytes are the major contributors to BM fibrosis. Regarding BM fibrosis, GLI1$^+$ myofibroblasts are

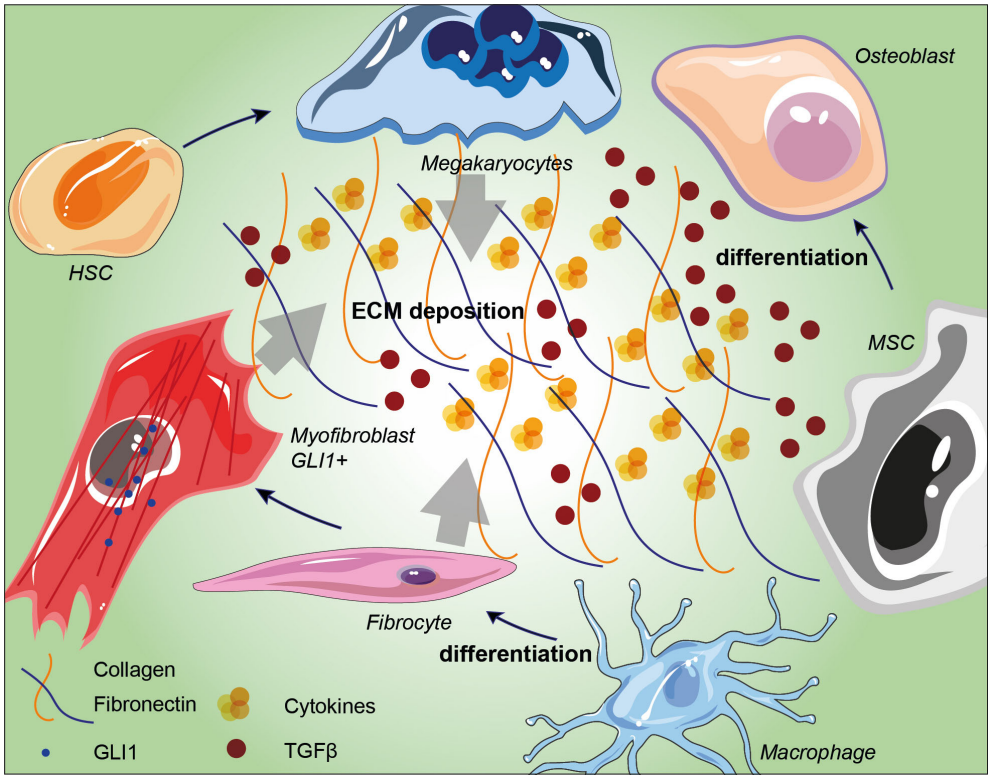

FIGURE 1
Schematic representation of BM niche fibrosis-driving cell populations and their involvement in extracellular matrix deposition. Arrows indicate the influence of megakaryocytes, fibrocytes and GLI1$^+$ myofibroblasts in conditioning ECM in BM niches. TGF-β accumulation induces MSC differentiation into osteoblast and its overall accumulation within the ECM induces ROS production and bone remodeling. HSC: hematopoietic stem cell; MSC: mesenchymal stromal cell; ECM: extracellular matrix; TGF-β: transforming growth factor-beta.

highly active and contractile cells, characterized by dense rough ER, collagen secretion granules, and α-smooth muscle actin (α-SMA) expression (60). Differential gene expression analysis demonstrated that megakaryocyte-associated genes were significantly up-regulated by these cells. Interestingly, among them CXCL4, cytokine-cytokine receptor interaction pathway, has been depicted as crucial in establishing a fibrotic state (61) and in regulating HSCs (60). Approximatively half of all myofibroblasts derive from the GLI1 migrate into the hematopoietic marrow and differentiate into matrix-producing cells (60). Data indicate that targeting GLI proteins inhibits GLI1+ cell proliferation and myofibroblast differentiation, which results in reduced fibrosis and improved organ function (62). Intriguingly, GLI1+ and LepR+ cells are CD45– non-hematopoietic cells, which indicates that their differentiation into myofibroblasts is a distinct process and is independent of monocyte-derived fibrocytes (55). Arranz et al., showed that BM Nestin+ MSCs, which are innervated by sympathetic nerve fibers, regulate normal HSCs and that abrogation of this regulatory circuit is essential for MPN pathogenesis. It has been demonstrated in MPN and also in other tumors, that MSCs expressing the marker Nestin directly support cell survival and chemoresistance by increasing oxidative phosphorylation (OXPHOS) and simultaneously provide with key antioxidant tools necessary to balance ROS levels during chemotherapy (63–65).

3 The role of MSCs in osteosclerosis

In addition to BM fibrosis, up to 70% of MF patients develop osteosclerosis, a well-established indicator of poor prognosis. Recently, Avanzini and colleagues reported genetic and functional aberrations of BM-MSCs in MPNs and showed that MSCs exhibit decreased proliferative abilities as well as decreased osteogenic capacities also confirmed through *in vitro* ed *in vivo* experiments (32). The direct effect of these alterations is a shift in the balance between osteoblastogenesis and osteoclastogenesis, creating an osteosclerotic state (66). Bone modifications are hallmark of PMF since they represent one of the direct results of BM disruption. Osteosclerosis remains the most common bone change, which represents a pathological event characterized by increased bone density and abnormal hardening (66), and its pathogenesis is still largely unknown. In recent years, an increasing number of studies point towards an important involvement of the MSCs niche in osteosclerosis. Firstly, osteosclerotic regions are produced by the irregular thickening of bone trabeculae, new bone shaping and consequent bone volume growth, secondly, increased BM activity in some regions, such as the vertebral column, pelvis or proximal segments of long bones, remain the most affected by such alterations (67). The physiological bone morphology and functionality are strictly dependent on the accurate setting of the marrow osteoblastic niche as well as the balance between mature bone tissue, endosteum and central BM (68). As part of the BM niche, MSCs support hematopoiesis and restore the differentiated compartment of OBs during tissue growth and turnover (69–71). Tumoral hematopoietic cells stimulate MSCs to proliferate and to adopt an abnormal differentiation program that results in the overproduction of functionally altered OBs lineage cells, which accumulate in the BM cavity as inflammatory myelofibrotic cells (Figure 2) (72). Park et al. (73), showed that a subset of Nestin+ MSCs found *in vivo* are able to replace short-lived mature OBs to maintain homeostasis and respond to bone injury. MF osteosclerosis is thought to be induced by overstimulated MSC-derived OBs or impaired bone resorption. While OBs differentiation is also due to TGF-β1 release, in turn inducing the expression of bone morphogenetic protein (BMP), osteoclasts (OCs) are increased and they show an impaired osteolytic activity, eventually distorting bone remodeling and contributing to the induction of osteosclerosis (74). The development of OCs is highly skewed towards proliferation in both primary and secondary MPN-associated MF. Veletic and coworkers demonstrated that neoplastic monocytic progenitors retain their aberrant genetic constitution, even after full differentiation into mature OCs (74). However, fusion of such progenitors seems to be profoundly impaired, and MF OCs are unable to fully acquire the phenotypical features associated with efficient bone resorption, particularly multinucleation and the development of actin-rich structures. At least to a certain extent, this process happens independently of the non-malignant MSCs, although it seems to be impacting the OBs as well. Evidence demonstrates that even though MF OCs are hyperproliferative, their function is intrinsically suppressed due to the inherited neoplastic burden, which in turn contributes to the osteosclerotic dysplasia of the MPN-affected BM (74). Schepers and coworkers showed that OBCs derived from multipotent stromal cells, expand in the presence of malignant hematopoietic cells, which results in matrix production and trabecular thickening (75). Under osteogenic differentiation conditions, MSCs from PMF patients showed an increased capacity to mineralize extracellular bone matrix *in vitro* and to form new bone *in vivo* in immunodeficient mice (32). Furthermore, novel pharmacological approaches are on their way to improve the current strategies in fighting MPNs progression. In this context it has been reported that targeting IL-1β by using a specific antibody might decrease reticulin fibrosis and osteosclerosis in a preclinical JAK2-V617F MPN mouse model. For this reason, a combination therapy with JAK1/2 inhibitor might represent a future direction for MPN therapeutic approach [86].

4 The role of oxidative stress in MPN-MSCs

As described above, the perpetual generation of an inflammatory stressing state, leads to the establishment of an optimal environment for mutations accumulation, including MSCs. Allegra et al. reported that by stimulating p38–MAPK, AKT/mTOR and JAK/STAT in progenitors and leukocytes it causes a condition of chronic oxidative stress with increased concentrations of ROS in the BM, eventually triggering germline mutations (40). Such not permissive condition has been correlated with MPN onset. Supporting this data, increased ROS levels produced by TME components the stem cell clone itself

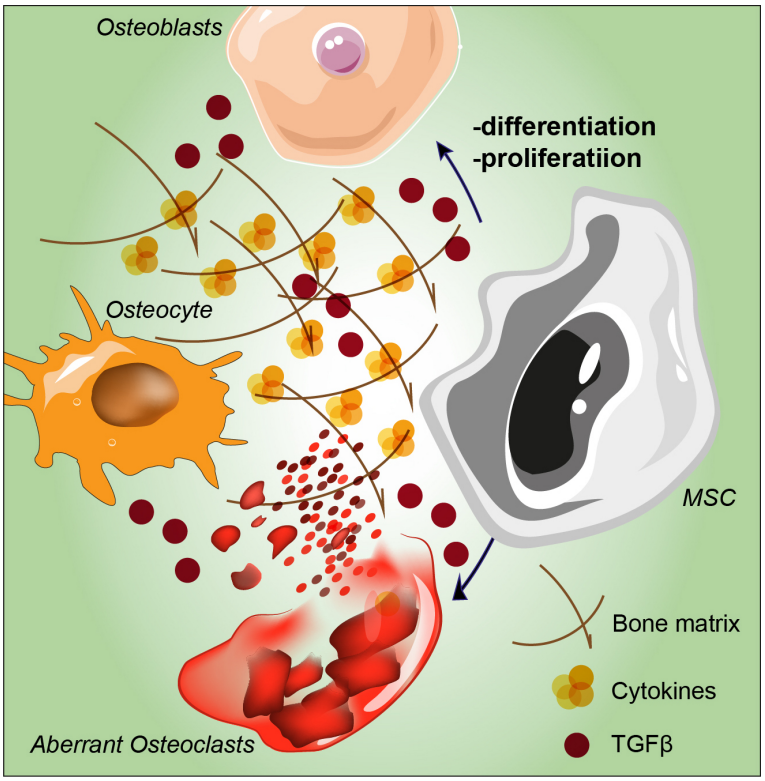

FIGURE 2
Schematic representation of MSC proliferation and differentiation abnormalities stimulated by tumoral hematopoietic cells. Aberrant osteolytic activity mediated by osteoclasts leads to bone remodeling and to altered osteocytes, overall contributing to the induction of osteosclerosis. MSC: mesenchymal stromal cell; TGF-β: transforming growth factor-beta.

constantly produces inflammatory components in the BM. These elements further increase clonal expansion, thus leading to a positive feedback loop (40). In order to characterize the role of altered BM-MSCs during inflammation, Desterke et al. collected information from PubMed and gene databases and crossed these with the gene expression profile of BM-MSCs performed in PMF patients (76). Several altered pathways were identified including oncostatin M and TGF-β signaling triggering misregulated DNA damage, senescence, and autophagy. This has been also confirmed in PV and ET where chronic inflammation in BM-TME induces a hypersensibility of MSCs to inflammatory molecules participating in creating the previous mentioned vicious circle (77). Since TGF-β1 and the subsequent oxidative stress are key regulators for DNA methylation in cancer (78), it has been reported that PDGF-β gene is hypomethylated, thus correlating with a poor prognosis, eventually harboring a significant fibrosis grade (76). Halogenated cytosine residues are indeed one of the most common DNA damage signature mediated by inflammation (79–81). These inflammation damage products have been detected in human leukocytes where the methyl-binding proteins are not able to distinguish methylated and halogenated DNA; thus, DNA methyltransferase (DNMT) 1 could be deceived and they lead to the accumulation of these analogues within the genome (82–86). An initial halogenation, triggered by inflammation, could direct methylation of the complementary DNA strand, eventually resulting in heritable alterations in genome methylation pattern.

5 Conclusions and future directions

Herein, we reviewed the regulatory properties of MSCs in immune-mediated or inflammatory conditions, shed light on the fact that MPNs are diseases sensitive to ROS overload together with the central role of the innate immune system in the modulatory effects of MSCs. The pro-inflammatory status induced by oxidative stress increases the risk of malignant transformation. Many aspects concerning the relationship between chronic myeloproliferative diseases, genetic alterations, and inflammation were recently clarified. MPNs are characterized by increased generation of one or more forms of myeloid cells, together with the impairment of neighboring healthy MSCs (40). The excessive ROS accumulation give rise to overstimulated fibrocytes and OCs leading to the onset and progression of disease (87). Inflammatory cytokines are also capable of influencing disease onset as well as its evolution and prognosis. This altered state is also sustained by platelets and megakaryocytes which participate in inflammation and immunity (88). The employment of antioxidants could be advantageous in the treatment of MPNs, since Ruxolitinib has little antioxidative capacity. Furthermore, MPNs patients usually undergoes blood transfusion. The iron overload resulting upon this step might also enhance ROS accumulation (65, 89). For this reason, in the latest research lines has been reported that the usage of N-adenyl-cysteine (NAC) decreases bone marrow fibrosis in patients with MPN and could potentially aid with HSCT engraftment (90). This work might

potentially open the path towards the inclusion of antioxidant drugs in the fight against MPN progression. Recognizing the genetic and external elements that participate in the myelofibrotic evolution of MPNs is of crucial importance for early detection as well as to initiate therapies inhibiting or reversing disease development in MPN patients. The fact that genetic ablation of GLI1+ cells abolish BM fibrosis and restores hematopoiesis indicates that GLI1+ MSCs are a promising therapeutic target (53, 60). Considering the cross-influence between the BM extracellular matrix composition and the proliferation/differentiation capability of HSCs, the stimulating issue concerning the impact of stromal cell alterations on hematopoiesis needs to be elucidated. By being "bad stromal cells", MSCs take entirely part in the "bad seed in bad soil" concept and strengthen the importance of stromal cells in the development of a neoplasia. Therefore, MSCs from patients are good candidates for niche-targeted therapies that, in association with drugs eradicating the hematopoietic clone, would improve patient treatment. In this scenario, novel therapeutic targets are stepping in front. It has been recently reported that MF patients overexpress the cyclin dependent kinase 6 (CDK6) which might turn to be a novel target. Corroborating this idea, the authors show an enhancement of the Ruxolitinib effect in synergy with CDK6 inhibitor Palbociclib, significantly reducing leukocytosis, splenomegaly, and bone marrow fibrosis in Jak2V617F and MPLW515L murine models. However, the improvement of MF-related animal model is nowadays a crucial step to dissect the effect of novel approaches on immune cells and the mesenchymal counterpart in the BM *milieu*. To develop animal models that appropriately address the complex interplay among HSCs, MSCs and immune system in TME where these cells execute their regulatory function, becomes extremely important. In particular, it may be helpful to dissect the molecular pathway involved in the generation of anti-inflammatory cells, *in vitro* and that result may help to design relevant immunocompetent animal models in order to enhance the antioxidant capability of MSCs to positively counterbalance the negative effect of the oxidative damage. From the MSCs point of view it could be possible to manage the mechanisms through which MSCs may promote or suppress tumor progression and the possible tumor-promoting activity of MSCs may be useful in choosing the right mesenchymal population based on the specific cancer type with a successful application in patients. As the main goal to be achieved is to operate on the pathways that control the synthesis of cytokines, oxidative stress and genome instability as well, it may be suggested that acting on the inflammatory state as a therapeutic approach in MPNs could be effective in reducing the possibility of leukemic progression and onset of complications. Nevertheless, this promising property of MSCs, independently on their HSC-supporting capacity and the immunomodulatory effect, warrants extensive and deeper studies.

Author contributions

Conceptualization, EL, SG, CG, NV, and DT. Writing—original draft preparation, EL, SG, CG, NV, GM, and LL. Writing—review and editing, CG, NV, RP, RG, DC, GL, FD, AR, GM, AD, GP, LL, and DT. Supervision, CG, NV, RP, RG, GM, GL, FD, AR, GP, and DT. Project administration, EL, DT, and NV. All authors contributed to the article and approved the submitted version.

Funding

CG was supported by the PON AIM: R&I 2014–2020-E68D19001340001. NV was supported by the PON AIM: R&I 2014-2020-E66C18001240007. This work was funded by the University Research Project Grant (PIACERI Found – 2020-2022), Department of Biomedical and Biotechnological Sciences (BIOMETEC), University of Catania, Italy.

Conflict of interest

The authors declare that the research was conducted in the absence of any commercial or financial relationships that could be construed as a potential conflict of interest.

Publisher's note

All claims expressed in this article are solely those of the authors and do not necessarily represent those of their affiliated organizations, or those of the publisher, the editors and the reviewers. Any product that may be evaluated in this article, or claim that may be made by its manufacturer, is not guaranteed or endorsed by the publisher.

References

1. Paule R, Ponsoye M, Gueutin V, Deray G, Izzedine H. Myeloproliferative neoplasms related glomerulopathy. *Rev Med Interne* (2013) 34(6):369–72. doi: 10.1016/j.revmed.2012.12.013

2. Tefferi A, Thiele J, Vardiman JW. The 2008 world health organization classification system for myeloproliferative neoplasms: order out of chaos. *Cancer* (2009) 115(17):3842–7. doi: 10.1002/cncr.24440

3. Tefferi A, Vardiman JW. Classification and diagnosis of myeloproliferative neoplasms: the 2008 world health organization criteria and point-of-care diagnostic algorithms. *Leukemia* (2008) 22(1):14–22. doi: 10.1038/sj.leu.2404955

4. Smith CA, Fan G. The saga of JAK2 mutations and translocations in hematologic disorders: pathogenesis, diagnostic and therapeutic prospects, and revised world health organization diagnostic criteria for myeloproliferative neoplasms. *Hum Pathol* (2008) 39(6):795–810. doi: 10.1016/j.humpath.2008.02.004

5. Orazi A, Germing U. The myelodysplastic/myeloproliferative neoplasms: myeloproliferative diseases with dysplastic features. *Leukemia* (2008) 22(7):1308–19. doi: 10.1038/leu.2008.119

6. Hoffman R, Prchal JT, Samuelson S, Ciurea SO, Rondelli D. Philadelphia Chromosome-negative myeloproliferative disorders: biology and treatment. *Biol Blood Marrow Transplant* (2007) 13(1 Suppl 1):64–72. doi: 10.1016/j.bbmt.2006.11.003

7. Grinfeld J, Nangalia J, Green AR. Molecular determinants of pathogenesis and clinical phenotype in myeloproliferative neoplasms. *Haematologica* (2017) 102(1):7–17. doi: 10.3324/haematol.2014.113845

8. Constantinescu SN, Vainchenker W, Levy G, Papadopoulos N. Functional consequences of mutations in myeloproliferative neoplasms. *Hemasphere* (2021) 5 (6):e578. doi: 10.1097/HS9.0000000000000578

9. Levine RL, Wadleigh M, Cools J, Ebert BL, Wernig G, Huntly BJ, et al. Activating mutation in the tyrosine kinase JAK2 in polycythemia vera, essential thrombocythemia, and myeloid metaplasia with myelofibrosis. *Cancer Cell* (2005) 7(4):387–97. doi: 10.1016/j.ccr.2005.03.023

10. Kralovics R, Passamonti F, Buser AS, Teo SS, Tiedt R, Passweg JR, et al. A gain-of-function mutation of JAK2 in myeloproliferative disorders. *N Engl J Med* (2005) 352 (17):1779–90. doi: 10.1056/NEJMoa051113

11. James C, Ugo V, Le Couedic JP, Staerk J, Delhommeau F, Lacout C, et al. A unique clonal JAK2 mutation leading to constitutive signalling causes polycythaemia vera. *Nature* (2005) 434(7037):1144–8. doi: 10.1038/nature03546

12. Larsen TS, Christensen JH, Hasselbalch HC, Pallisgaard N. The JAK2 V617F mutation involves b- and T-lymphocyte lineages in a subgroup of patients with Philadelphia-chromosome negative chronic myeloproliferative disorders. *Br J Haematol* (2007) 136(5):745–51. doi: 10.1111/j.1365-2141.2007.06497.x

13. Zhang Y, Liu L, Jin L, Yi X, Dang E, Yang Y, et al. Oxidative stress-induced calreticulin expression and translocation: new insights into the destruction of melanocytes. *J Invest Dermatol* (2014) 134(1):183–91. doi: 10.1038/jid.2013.268

14. Yu B, Choi B, Li W, Kim DH. Magnetic field boosted ferroptosis-like cell death and responsive MRI using hybrid vesicles for cancer immunotherapy. *Nat Commun* (2020) 11(1):3637. doi: 10.1038/s41467-020-17380-5

15. Song S, Lee JY, Ermolenko L, Mazumder A, Ji S, Ryu H, et al. Tetrahydrobenzimidazole TMQ0153 triggers apoptosis, autophagy and necroptosis crosstalk in chronic myeloid leukemia. *Cell Death Dis* (2020) 11(2):109. doi: 10.1038/s41419-020-2304-8

16. Ikezaki M, Minakata S, Nishitsuji K, Tabata S, Lee Matsui IS, Takatani M, et al. Calreticulin protects insulin against reductive stress in vitro and in MIN6 cells. *Biochimie* (2020) 171-172:1–11. doi: 10.1016/j.biochi.2020.01.011

17. Michalak M, Corbett EF, Mesaeli N, Nakamura K, Opas M. Calreticulin: one protein, one gene, many functions. *Biochem J* (1999) 344(Pt 2):281–92. doi: 10.1042/bj3440281

18. Wang WA, Groenendyk J, Michalak M. Calreticulin signaling in health and disease. *Int J Biochem Cell Biol* (2012) 44(6):842–6. doi: 10.1016/j.biocel.2012.02.009

19. Houen G, Hojrup P, Ciplys E, Gaboriaud C, Slibinskas R. Structural analysis of calreticulin, an endoplasmic reticulum-resident molecular chaperone. *Prog Mol Subcell Biol* (2021) 59:13–25. doi: 10.1007/978-3-030-67696-4_2

20. Danilczyk UG, Cohen-Doyle MF, Williams DB. Functional relationship between calreticulin, calnexin, and the endoplasmic reticulum luminal domain of calnexin. *J Biol Chem* (2000) 275(17):13089–97. doi: 10.1074/jbc.275.17.13089

21. Ihara Y, Urata Y, Goto S, Kondo T. Role of calreticulin in the sensitivity of myocardiac H9c2 cells to oxidative stress caused by hydrogen peroxide. *Am J Physiol Cell Physiol* (2006) 290(1):C208–21. doi: 10.1152/ajpcell.00075.2005

22. Merlinsky TR, Levine RL, Pronier E. Unfolding the role of calreticulin in myeloproliferative neoplasm pathogenesis. *Clin Cancer Res* (2019) 25(10):2956–62. doi: 10.1158/1078-0432.CCR-18-3777

23. How J, Hobbs GS, Mullally A. Mutant calreticulin in myeloproliferative neoplasms. *Blood* (2019) 134(25):2242–8. doi: 10.1182/blood.2019000622

24. Prins D, Gonzalez Arias C, Klampfl T, Grinfeld J, Green AR. Mutant calreticulin in the myeloproliferative neoplasms. *Hemasphere* (2020) 4(1):e333. doi: 10.1097/HS9.0000000000000333

25. How J, Garcia JS, Mullally A. Biology and therapeutic targeting of molecular mechanisms in MPN. *Blood* (2022) 19:blood.2022017416. doi: 10.1182/blood.2022017416

26. Cazzola M, Kralovics R. From janus kinase 2 to calreticulin: the clinically relevant genomic landscape of myeloproliferative neoplasms. *Blood* (2014) 123 (24):3714–9. doi: 10.1182/blood-2014-03-530865

27. Khalid F, Damlaj M, AlZahrani M, Abuelgasim KA, Gmati GE. Reactivation of tuberculosis following ruxolitinib therapy for primary myelofibrosis: Case series and literature review. *Hematol Oncol Stem Cell Ther* (2021) 14(3):252–6. doi: 10.1016/j.hemonc.2020.02.003

28. Pietra D, Rumi E, Ferretti VV, Di Buduo CA, Milanesi C, Cavalloni C, et al. Differential clinical effects of different mutation subtypes in CALR-mutant myeloproliferative neoplasms. *Leukemia* (2016) 30(2):431–8. doi: 10.1038/leu.2015.277

29. Mesa RA, Li CY, Ketterling RP, Schroeder GS, Knudson RA, Tefferi A. Leukemic transformation in myelofibrosis with myeloid metaplasia: a single-institution experience with 91 cases. *Blood* (2005) 105(3):973–7. doi: 10.1182/blood-2004-07-2864

30. Scherer A, Graff JM. Calmodulin differentially modulates Smad1 and Smad2 signaling. *J Biol Chem* (2000) 275(52):41430–8. doi: 10.1074/jbc.M005727200

31. Lu M, Xia L, Liu YC, Hochman T, Bizzari L, Aruch D, et al. Lipocalin produced by myelofibrosis cells affects the fate of both hematopoietic and marrow microenvironmental cells. *Blood* (2015) 126(8):972–82. doi: 10.1182/blood-2014-12-618595

32. Martinaud C, Desterke C, Konopacki J, Pieri L, Torossian F, Golub R, et al. Osteogenic potential of mesenchymal stromal cells contributes to primary myelofibrosis. *Cancer Res* (2015) 75(22):4753–65. doi: 10.1158/0008-5472.CAN-14-3696

33. Heck DE, Shakarjian M, Kim HD, Laskin JD, Vetrano AM. Mechanisms of oxidant generation by catalase. *Ann N Y Acad Sci* (2010) 1203:120–5. doi: 10.1111/j.1749-6632.2010.05603.x

34. Hasselbalch HC. Chronic inflammation as a promotor of mutagenesis in essential thrombocythemia, polycythemia vera and myelofibrosis. a human inflammation model for cancer development? *Leuk Res* (2013) 37(2):214–20. doi: 10.1016/j.leukres.2012.10.020

35. Mannino G, Vicario N, Parenti R, Giuffrida R, Lo Furno D. Connexin expression decreases during adipogenic differentiation of human adipose-derived mesenchymal stem cells. *Mol Biol Rep* (2020) 47(12):9951–8. doi: 10.1007/s11033-020-05950-1

36. Musumeci G, Lo Furno D, Loreto C, Giuffrida R, Caggia S, Leonardi R, et al. Mesenchymal stem cells from adipose tissue which have been differentiated into chondrocytes in three-dimensional culture express lubricin. *Exp Biol Med (Maywood)* (2011) 236(11):1333–41. doi: 10.1258/ebm.2011.011183

37. Lo Furno D, Mannino G, Giuffrida R. Functional role of mesenchymal stem cells in the treatment of chronic neurodegenerative diseases. *J Cell Physiol* (2018) 233 (5):3982–99. doi: 10.1002/jcp.26192

38. Giallongo C, Tibullo D, Camiolo G, Parrinello NL, Romano A, Puglisi F, et al. TLR4 signaling drives mesenchymal stromal cells commitment to promote tumor microenvironment transformation in multiple myeloma. *Cell Death Dis* (2019) 10 (10):704. doi: 10.1038/s41419-019-1959-5

39. Goloviznina NA, Verghese SC, Yoon YM, Taratula O, Marks DL, Kurre P. Mesenchymal stromal cell-derived extracellular vesicles promote myeloid-biased multipotent hematopoietic progenitor expansion *via* toll-like receptor engagement. *J Biol Chem* (2016) 291(47):24607–17. doi: 10.1074/jbc.M116.745653

40. Allegra A, Pioggia G, Tonacci A, Casciaro M, Musolino C, Gangemi S. Synergic crosstalk between inflammation, oxidative stress, and genomic alterations in BCR-ABL-Negative myeloproliferative neoplasm. *Antioxidants (Basel)* (2020) 9(11):1037. doi: 10.3390/antiox9111037

41. Kile BT, Alexander WS. The suppressors of cytokine signalling (SOCS). *Cell Mol Life Sci* (2001) 58(11):1627–35. doi: 10.1007/PL00000801

42. Palmer DC, Restifo NP. Suppressors of cytokine signaling (SOCS) in T cell differentiation, maturation, and function. *Trends Immunol* (2009) 30(12):592–602. doi: 10.1016/j.it.2009.09.009

43. Forte D, Garcia-Fernandez M, Sanchez-Aguilera A, Stavropoulou V, Fielding C, Martin-Perez D, et al. Bone marrow mesenchymal stem cells support acute myeloid leukemia bioenergetics and enhance antioxidant defense and escape from chemotherapy. *Cell Metab* (2020) 32(5):829–43.e9. doi: 10.1016/j.cmet.2020.09.001

44. Quattrone F, Dini V, Barbanera S, Zerbinati N, Romanelli M. Cutaneous ulcers associated with hydroxyurea therapy. *J Tissue Viability* (2013) 22(4):112–21. doi: 10.1016/j.jtv.2013.08.002

45. Ostojic A, Vrhovac R, Verstovsek S. Ruxolitinib for the treatment of myelofibrosis: its clinical potential. *Ther Clin Risk Manag* (2012) 8:95–103. doi: 10.2147/TCRM.S23277

46. Bjorn ME, Brimnes MK, Gudbrandsdottir S, Andersen CL, Poulsen HE, Henriksen T, et al. Ruxolitinib treatment reduces monocytic superoxide radical formation without affecting hydrogen peroxide formation or systemic oxidative nucleoside damage in myelofibrosis. *Leuk Lymphoma* (2019) 60(10):2549–57. doi: 10.1080/10428194.2019.1579323

47. Yao JC, Oetjen KA, Wang T, Xu H, Abou-Ezzi G, Krambs JR, et al. TGF-beta signaling in myeloproliferative neoplasms contributes to myelofibrosis without disrupting the hematopoietic niche. *J Clin Invest* (2022) 132(11):e154092. doi: 10.1172/JCI154092

48. Teodorescu P, Pasca S, Jurj A, Gafencu G, Joelsson JP, Selicean S, et al. Transforming growth factor beta-mediated micromechanics modulates disease progression in primary myelofibrosis. *J Cell Mol Med* (2020) 24(19):11100–10. doi: 10.1111/jcmm.15526

49. Rossi C, Zini R, Rontauroli S, Ruberti S, Prudente Z, Barbieri G, et al. Role of TGF-beta1/miR-382-5p/SOD2 axis in the induction of oxidative stress in CD34+ cells from primary myelofibrosis. *Mol Oncol* (2018) 12(12):2102–23. doi: 10.1002/1878-0261.12387

50. Baryawno N, Przybylski D, Kowalczyk MS, Kfoury Y, Severe N, Gustafsson K, et al. A cellular taxonomy of the bone marrow stroma in homeostasis and leukemia. *Cell* (2019) 177(7):1915–32.e16. doi: 10.1016/j.cell.2019.04.040

51. Tikhonova AN, Dolgalev I, Hu H, Sivaraj KK, Hoxha E, Cuesta-Dominguez A, et al. The bone marrow microenvironment at single-cell resolution. *Nature* (2019) 569 (7755):222–8. doi: 10.1038/s41586-019-1104-8

52. Malara A, Abbonante V, Zingariello M, Migliaccio A, Balduini A. Megakaryocyte contribution to bone marrow fibrosis: many arrows in the quiver. *Mediterr J Hematol Infect Dis* (2018) 10(1):e2018068. doi: 10.4084/mjhid.2018.068

53. Leimkuhler NB, Gleitz HFE, Ronghui L, Snoeren IAM, Fuchs SNR, Nagai JS, et al. Heterogeneous bone-marrow stromal progenitors drive myelofibrosis *via* a druggable alarmin axis. *Cell Stem Cell* (2021) 28(4):637–52.e8. doi: 10.1016/j.stem.2020.11.004

54. Decker M, Martinez-Morentin L, Wang G, Lee Y, Liu Q, Leslie J, et al. Leptin-receptor-expressing bone marrow stromal cells are myofibroblasts in primary myelofibrosis. *Nat Cell Biol* (2017) 19(6):677–88. doi: 10.1038/ncb3530

55. Reinhardt JW, Breuer CK. Fibrocytes: A critical review and practical guide. *Front Immunol* (2021) 12:784401. doi: 10.3389/fimmu.2021.784401

56. Sapudom J, Muller CD, Nguyen KT, Martin S, Anderegg U, Pompe T. Matrix remodeling and hyaluronan production by myofibroblasts and cancer-associated fibroblasts in 3D collagen matrices. *Gels* (2020) 6(4):33. doi: 10.3390/gels6040033

57. Tibullo D, Longo A, Vicario N, Romano A, Barbato A, Di Rosa M, et al. Ixazomib improves bone remodeling and counteracts sonic hedgehog signaling inhibition mediated by myeloma cells. *Cancers (Basel)* (2020) 12(2):323. doi: 10.3390/cancers12020323

58. Longhitano L, Tibullo D, Vicario N, Giallongo C, La Spina E, Romano A, et al. IGFBP-6/sonic hedgehog/TLR4 signalling axis drives bone marrow fibrotic transformation in primary myelofibrosis. *Aging (Albany NY)* (2021) 13(23):25055–71. doi: 10.18632/aging.203779

59. Zahr AA, Salama ME, Carreau N, Tremblay D, Verstovsek S, Mesa R, et al. Bone marrow fibrosis in myelofibrosis: pathogenesis, prognosis and targeted strategies. *Haematologica* (2016) 101(6):660–71. doi: 10.3324/haematol.2015.141283

60. Schneider RK, Mullally A, Dugourd A, Peisker F, Hoogenboezem R, Van Strien PMH, et al. Gli1(+) mesenchymal stromal cells are a key driver of bone marrow fibrosis and an important cellular therapeutic target. *Cell Stem Cell* (2017) 20(6):785–800.e8. doi: 10.1016/j.stem.2017.03.008

61. van Bon L, Affandi AJ, Broen J, Christmann RB, Marijnissen RJ, Stawski L, et al. Proteome-wide analysis and CXCL4 as a biomarker in systemic sclerosis. *N Engl J Med* (2014) 370(5):433–43. doi: 10.1056/NEJMoa1114576

62. Kramann R, Schneider RK. The identification of fibrosis-driving myofibroblast precursors reveals new therapeutic avenues in myelofibrosis. *Blood* (2018) 131 (19):2111–9. doi: 10.1182/blood-2018-02-834820

63. Arranz L, Sanchez-Aguilera A, Martin-Perez D, Isern J, Langa X, Tzankov A, et al. Neuropathy of haematopoietic stem cell niche is essential for myeloproliferative neoplasms. *Nature* (2014) 512(7512):78–81. doi: 10.1038/nature13383

64. Torrisi F, Alberghina C, D'Aprile S, Pavone AM, Longhitano L, Giallongo S, et al. The hallmarks of glioblastoma: Heterogeneity, intercellular crosstalk and molecular signature of invasiveness and progression. *Biomedicines* (2022) 10(4):806. doi: 10.3390/biomedicines10040806

65. Camiolo G, Barbato A, Giallongo C, Vicario N, Romano A, Parrinello NL, et al. Iron regulates myeloma cell/macrophage interaction and drives resistance to bortezomib. *Redox Biol* (2020) 36:101611. doi: 10.1016/j.redox.2020.101611

66. Spampinato M, Giallongo C, Romano A, Longhitano L, La Spina E, Avola R, et al. Focus on osteosclerotic progression in primary myelofibrosis. *Biomolecules* (2021) 11(1):122. doi: 10.3390/biom11010122

67. Osterhoff G, Morgan EF, Shefelbine SJ, Karim L, McNamara LM, Augat P. Bone mechanical properties and changes with osteoporosis. *Injury* (2016) 47 Suppl 2(Suppl 2):S11–20. doi: 10.1016/S0020-1383(16)47003-8

68. Morrison SJ, Scadden DT. The bone marrow niche for haematopoietic stem cells. *Nature* (2014) 505(7483):327–34. doi: 10.1038/nature12984

69. Sacchetti B, Funari A, Michienzi S, Di Cesare S, Piersanti S, Saggio I, et al. Self-renewing osteoprogenitors in bone marrow sinusoids can organize a hematopoietic microenvironment. *Cell* (2007) 131(2):324–36. doi: 10.1016/j.cell.2007.08.025

70. Mannino G, Russo C, Maugeri G, Musumeci G, Vicario N, Tibullo D, et al. Adult stem cell niches for tissue homeostasis. *J Cell Physiol* (2022) 237(1):239–57. doi: 10.1002/jcp.30562

71. Musumeci G, Mobasheri A, Trovato FM, Szychlinska MA, Graziano AC, Lo Furno D, et al. Biosynthesis of collagen I, II, RUNX2 and lubricin at different time points of chondrogenic differentiation in a 3D *in vitro* model of human mesenchymal stem cells derived from adipose tissue. *Acta Histochem* (2014) 116(8):1407–17. doi: 10.1016/j.acthis.2014.09.008

72. Glenn JD, Whartenby KA. Mesenchymal stem cells: Emerging mechanisms of immunomodulation and therapy. *World J Stem Cells* (2014) 6(5):526–39. doi: 10.4252/wjsc.v6.i5.526

73. Park D, Spencer JA, Koh BI, Kobayashi T, Fujisaki J, Clemens TL, et al. Endogenous bone marrow MSCs are dynamic, fate-restricted participants in bone maintenance and regeneration. *Cell Stem Cell* (2012) 10(3):259–72. doi: 10.1016/j.stem.2012.02.003

74. Veletic I, Manshouri T, Multani AS, Yin CC, Chen L, Verstovsek S, et al. Myelofibrosis osteoclasts are clonal and functionally impaired. *Blood* (2019) 133 (21):2320–4. doi: 10.1182/blood-2018-10-878926

75. Schepers K, Pietras EM, Reynaud D, Flach J, Binnewies M, Garg T, et al. Myeloproliferative neoplasia remodels the endosteal bone marrow niche into a self-reinforcing leukemic niche. *Cell Stem Cell* (2013) 13(3):285–99. doi: 10.1016/j.stem.2013.06.009

76. Desterke C, Martinaud C, Ruzehaji N, Le Bousse-Kerdiles MC. Inflammation as a keystone of bone marrow stroma alterations in primary myelofibrosis. *Mediators Inflammation* (2015) 2015:415024. doi: 10.1155/2015/415024

77. Fisher DAC, Fowles JS, Zhou A, Oh ST. Inflammatory pathophysiology as a contributor to myeloproliferative neoplasms. *Front Immunol* (2021) 12:683401. doi: 10.3389/fimmu.2021.683401

78. Ramundo V, Giribaldi G, Aldieri E. Transforming growth factor-beta and oxidative stress in cancer: A crosstalk in driving tumor transformation. *Cancers (Basel)* (2021) 13(12):3093. doi: 10.3390/cancers13123093

79. Fedeles BI, Freudenthal BD, Yau E, Singh V, Chang SC, Li D, et al. Intrinsic mutagenic properties of 5-chlorocytosine: A mechanistic connection between chronic inflammation and cancer. *Proc Natl Acad Sci U.S.A.* (2015) 112(33):E4571–80. doi: 10.1073/pnas.1507709112

80. Knutson CG, Mangerich A, Zeng Y, Raczynski AR, Liberman RG, Kang P, et al. Chemical and cytokine features of innate immunity characterize serum and tissue profiles in inflammatory bowel disease. *Proc Natl Acad Sci U.S.A.* (2013) 110(26): E2332–41. doi: 10.1073/pnas.1222669110

81. Mangerich A, Knutson CG, Parry NM, Muthupalani S, Ye W, Prestwich E, et al. Infection-induced colitis in mice causes dynamic and tissue-specific changes in stress response and DNA damage leading to colon cancer. *Proc Natl Acad Sci U S A* (2012) 109(27):E1820–9. doi: 10.1073/pnas.1207829109

82. Jin B, Robertson KD. DNA Methyltransferases, DNA damage repair, and cancer. *Adv Exp Med Biol* (2013) 754:3–29. doi: 10.1007/978-1-4419-9967-2_1

83. Giallongo S, Lo Re O, Lochmanova G, Parca L, Petrizzelli F, Zdrahal Z, et al. Phosphorylation within intrinsic disordered region discriminates histone variant macroH2A1 splicing isoforms-macroH2A1.1 and macroH2A1.2. *Biol (Basel)* (2021) 10(7):659. doi: 10.3390/biology10070659

84. Giallongo S, Longhitano L, Denaro S, D'Aprile S, Torrisi F, La Spina E, et al. The role of epigenetics in neuroinflammatory-driven diseases. *Int J Mol Sci* (2022) 23 (23):15218. doi: 10.3390/ijms232315218

85. Van den Worm E, Beukelman CJ, Van den Berg AJ, Kroes BH, Labadie RP, Van Dijk H. Effects of methoxylation of apocynin and analogs on the inhibition of reactive oxygen species production by stimulated human neutrophils. *Eur J Pharmacol* (2001) 433(2-3):225–30. doi: 10.1016/S0014-2999(01)01516-3

86. Valinluck V, Liu P, Kang JIJr., Burdzy A, Sowers LC. 5-halogenated pyrimidine lesions within a CpG sequence context mimic 5-methylcytosine by enhancing the binding of the methyl-CpG-binding domain of methyl-CpG-binding protein 2 (MeCP2). *Nucleic Acids Res* (2005) 33(9):3057–64. doi: 10.1093/nar/gki612

87. Checa J, Aran JM. Reactive oxygen species: Drivers of physiological and pathological processes. *J Inflammation Res* (2020) 13:1057–73. doi: 10.2147/JIR.S275595

88. Haas S, Hansson J, Klimmeck D, Loeffler D, Velten L, Uckelmann H, et al. Inflammation-induced emergency megakaryopoiesis driven by hematopoietic stem cell-like megakaryocyte progenitors. *Cell Stem Cell* (2015) 17(4):422–34. doi: 10.1016/j.stem.2015.07.007

89. Di Veroli A, Campagna A, De Muro M, Maurillo L, Trawinska MM, LeonettiCrescenzi S, et al. Deferasirox in the treatment of iron overload during myeloproliferative neoplasms in fibrotic phase: does ferritin decrement matter? *Leuk Res* (2019) 76:65–9. doi: 10.1016/j.leukres.2018.11.012

90. Mendez Luque LF, Blackmon AL, Ramanathan G, Fleischman AG. Key role of inflammation in myeloproliferative neoplasms: Instigator of disease initiation, progression. and symptoms. *Curr Hematol Malig Rep* (2019) 14(3):145–53. doi: 10.1007/s11899-019-00508-w

frontiers | Frontiers in Pharmacology

TYPE Original Research
PUBLISHED 28 February 2023
DOI 10.3389/fphar.2023.1126602

OPEN ACCESS

EDITED BY
Qin Wang,
Southwest Jiaotong University, China

REVIEWED BY
Michael Super,
Harvard University, United States
Peter Kristensen,
Aalborg University, Denmark
Bo Zhang,
Sichuan University, China
Qiu Hua,
Anhui Medical University, China

*CORRESPONDENCE
Xiaoqi Liu,
liuxiaoqi76@163.com
Jiang Chen,
283876533@qq.com
Xin Liu,
zxkglx@126.com

†These authors have contributed equally to this work

SPECIALTY SECTION
This article was submitted to Pharmacology of Anti-Cancer Drugs, a section of the journal Frontiers in Pharmacology

RECEIVED 18 December 2022
ACCEPTED 08 February 2023
PUBLISHED 28 February 2023

CITATION
Deng H, Liu X, Chen J, He Y, Lin L, Liu X, Chen J and Liu X (2023), Photo-functionalized TiO_2 film for facile immobilization of EpCAM antibodies and efficient enrichment of circulating tumor cells.
Front. Pharmacol. 14:1126602.
doi: 10.3389/fphar.2023.1126602

Photo-functionalized TiO_2 film for facile immobilization of EpCAM antibodies and efficient enrichment of circulating tumor cells

Huan Deng[1†], Xiangqin Liu[2†], Jie Chen[3†], Yi He[4], Lanke Lin[1], Xin Liu[2*], Jiang Chen[5*] and Xiaoqi Liu[6,7*]

[1]College of Medical Technology, Chengdu University of Traditional Chinese Medicine, Chengdu, China, [2]Department of Laboratory Medicine and Sichuan Provincial Key Laboratory for Human Disease Gene Study, Sichuan Provincial People's Hospital, University of Electronic Science and Technology of China, Chengdu, China, [3]Department of Core laboratory, Sichuan Provincial People's Hospital, University of Electronic Science and Technology of China, Chengdu, China, [4]Department of Blood Transfusion, Sichuan Academy of Medical Sciences & Sichuan Provincial People's Hospital, Chengdu, China, [5]The Department of Ophthalmology, Sichuan Provincial People's Hospital, University of Electronic Science and Technology of China, Chengdu, China, [6]Sichuan Provincial Key Laboratory for Human Disease Gene Study, Center for Medical Genetics, Sichuan Academy of Medical Sciences & Sichuan Provincial People's Hospital, University of Electronic Science and Technology of China, Chengdu, China, [7]Research Unit for Blindness Prevention of Chinese Academy of Medical Sciences (2019RU026), Sichuan Academy of Medical Sciences & Sichuan Provincial People's Hospital, Chengdu, Sichuan, China

The highly efficient capture of circulating tumor cells (CTCs) in the blood is essential for the screening, treatment, and assessment of the risk of metastasis or recurrence of cancer. Immobilizing specific antibodies, such as EpCAM antibodies, on the material's surface is currently the primary method for efficiently capturing CTCs. However, the strategies for immobilizing antibodies usually have the disadvantages of requiring multiple chemical reagents and a complex pre-treatment process. Herein we developed a simple strategy for the immobilization of EpCAM antibodies without additional chemical reagents. By utilizing the positive charge property of the photo-functionalized titanium dioxide (TiO_2), the negatively charged carboxyl terminal of EpCAM antibodies was immobilized by electrostatic interaction, allowing the antibodies to expose the antigen binding site fully. The experimental results showed that the photo-functionalized TiO_2 surface had a marked positive charge and super-hydrophilic properties that could immobilize large amounts of EpCAM antibodies and keep excellent activity. CTCs capture experiments *in vitro* showed that the EpCAM antibodies-modified photo-functionalized TiO_2 could efficiently capture CTCs. The results of blood circulation experiments in rabbits showed that the EpCAM antibodies-modified photo-functionalized TiO_2 could accurately capture CTCs from the whole body's blood. It was foreseen that the strategy of simple immobilization of EpCAM antibodies based on photo-functionalized TiO_2 is expected to serve in the efficient capture of CTCs in the future.

KEYWORDS

photo-functionalized TiO_2, EpCAM antibodies, circulating tumor cells (CTCs), capture, tumor screening

1 Introduction

Cancer is a significant public health threat, inducing more than 10 million deaths in 2020 worldwide (Sung et al., 2021). Circulating tumor cells (CTCs) are cancer cells that are shed from the primary lesion of a solid tumor, enter the circulation and/or lymphatic system, and translocate to distant tissues to form a secondary tumor (Plaks et al., 2013; Castro-Giner and Aceto, 2020). Increased CTCs in the blood are associated with tumor metastasis and the short interval between tumor recurrences (Chaffer and Weinberg, 2011). Therefore, as a new target for "liquid biopsy," CTCs are of great clinical significance in assessing patients for postoperative monitoring, postoperative adjuvant therapy, and guiding the development of targeted treatment plans (Lin et al., 2018).

Currently, the enrichment methods for CTCs can be divided into *in vitro* and *in vivo* enrichment methods. The common *in vitro* CTCs enrichment methods include microfluidic devices (Su et al., 2019; Shi et al., 2021; Abdulla et al., 2022; Liu et al., 2022), photoelectrochemical platforms (Parker et al., 2018; Xu et al., 2021), immunomagnetic beads (Mohamadi et al., 2015; Wang et al., 2019; Li et al., 2020; Liang et al., 2020; Zhou et al., 2022), and new patterns (Jahangiri et al., 2020; Kang et al., 2021; Zhang et al., 2021; Wang et al., 2022b; Wang et al., 2022c) et al. False negative test results are the main problem that plagues these *in vitro* methods, because CTCs are very scarce in peripheral blood. There are only a few CTCs in 1 mL of blood, but there are millions of blood cells (Paterlini-Brechot and Benali, 2007). Therefore, materials that can efficiently enrich CTCs from a few mL of collected blood are crucial to improving the sensitivity and accuracy of CTCs detection. Compared to the *in vitro* methods, the *in vivo* enrichment methods, such as vein indwelling needles (Zhang et al., 2015), flexible electronic catheters (Wang et al., 2022a), plasmon resonance fiber probes (Zhu et al., 2022), and black phosphorus-modified intravenous catheters (Wang et al., 2020), are expected to enrich more CTCs from whole body blood, thus reducing the number of false negative results. However, these methods need to implant the CTC-enrich materials into the body, which may lead to various host reactions such as coagulation and inflammation. Therefore, beyond the ability to efficiently enrich CTCs, the *in vivo* enrichment method places additional requirements on the materials, namely, excellent biocompatibility.

Furthermore, a common problem faced by both *in vivo* and *in vitro* enrichment methods is that the strategy for the immobilization of CTC-capture antibodies on the surface of the material needs to be further simplified. For example, in the immobilization of EpCAM antibodies (the most used CTCs capture antibody), Parker et al. (2018) used oligo oxide molecules to attach antibodies on the silicon surface *via* an N, N-disuccinimidyl carbonate activating group. Wang et al. (2020) used the carbodiimide crosslinking agent 1-(3-dimethylaminopropyl)-3-ethyl carbodiimide hydrochloride to conjugate EpCAM antibodies *via* amido linkage on the surface of the intravenous catheter. Stott et al. (2010) used coupling agents attached to avidin and then coupled them to biotinylated EpCAM antibodies to functionalize the microfluidic device. All of these methods required using complex tools and toxic chemical reagents. Therefore, it is of great significance to develop a strategy to fix EpCAM antibodies more simply.

Titanium dioxide (TiO_2) is a ceramic material popular in orthopedics and blood contact materials for its excellent biocompatibility. Therefore, TiO_2 meets the stringent bio-safety and biocompatibility required by CTCs *in vivo* capture materials. Chen et al. have shown that TiO_2 irradiated by ultraviolet light (UV) has better anticoagulation compared with unirradiated TiO_2 (Chen et al., 2014; Chen et al., 2015). When TiO_2 was irradiated by UV, the electrons in the valence band transitioned, and the positive holes were generated at simultaneously, forming the electron-hole pairs (Wang et al., 1997; Zubkov et al., 2005; Hori et al., 2010a). Among them, photogenerated electrons have a strong oxidation capacity, while photogenerated holes have a reducing capacity (Hori et al., 2010a; Pelaez et al., 2012), resulting in the transformation of TiO_2 from biologically inert to biologically active and causing a self-cleaning effect (Hori et al., 2010b; Ueno et al., 2010), which desorbs many inert hydrocarbons adsorbed on the surface, exposing a more positive charged surface of TiO_2, and increasing the hydrophilicity of the surface (that is, increasing the surface energy) (Takeuchi et al., 2005; Zhang et al., 2008; Hori et al., 2010a; Iwasa et al., 2010). Therefore, the Photo-functionalized TiO_2 could improve the adsorption of the proteins through electrostatic adsorption and thermodynamics.

EpCAM antibodies are composed of multiple amino acids. The negatively charged carboxyl terminal is the constant region of the antibody, and the positively charged amino terminal is the variable region of the antibody, which is also the binding site for the CTCs surface antigen. At physiological pH (7.0), the surfaces of TiO_2 are known to be negatively charged (Ellingsen, 1991; Hori et al., 2010a). Therefore, we hypothesized that the photo-functionalized TiO_2 surface could bind to the negatively charged carboxyl terminal of the antibody through an electrostatic mechanism to immobilize the EpCAM antibodies and expose the binding site of the EpCAM antibodies to the antigens, thereby achieving highly sensitive capture CTCs (Figure 1). Compared with the traditional method of chemically grafting antibodies, photo-functionalized TiO_2 as a substrate to bind EpCAM antibodies has the characteristics of simplicity and no need to use toxic chemical reagents. As mentioned above, TiO_2 has excellent biocompatibility. In addition, TiO_2 can also be used on the surface of various inorganic materials by the physical vapor deposition method. Therefore, the method may be suitable for constructing various devices for capturing CTCs *in vitro* (such as magnetic beads and silicon-based photoelectrochemical platforms) and *in vivo* (stainless steel indwelling needles).

In this study, we characterized the surface physicochemical properties of photo-functionalized TiO_2 by X-ray photoelectron spectroscopy, water contact angle measurement meter, and potentiometric analysis. Then we immobilized the EpCAM antibodies on the photo-functionalized TiO_2. After that, we comprehensively studied the CTCs-capture efficiency of the EpCAM antibodies-modified photo-functionalized TiO_2 *in vitro* and *in vivo* dynamic environments to evaluate the application potential of the strategy in various typical CTCs capture scenes.

2 Materials and methods

2.1 Materials

Human breast cancer cells (MCF-7) were purchased from Chuan Qiu Biotechnology Company Limited (Shanghai). EpCAM

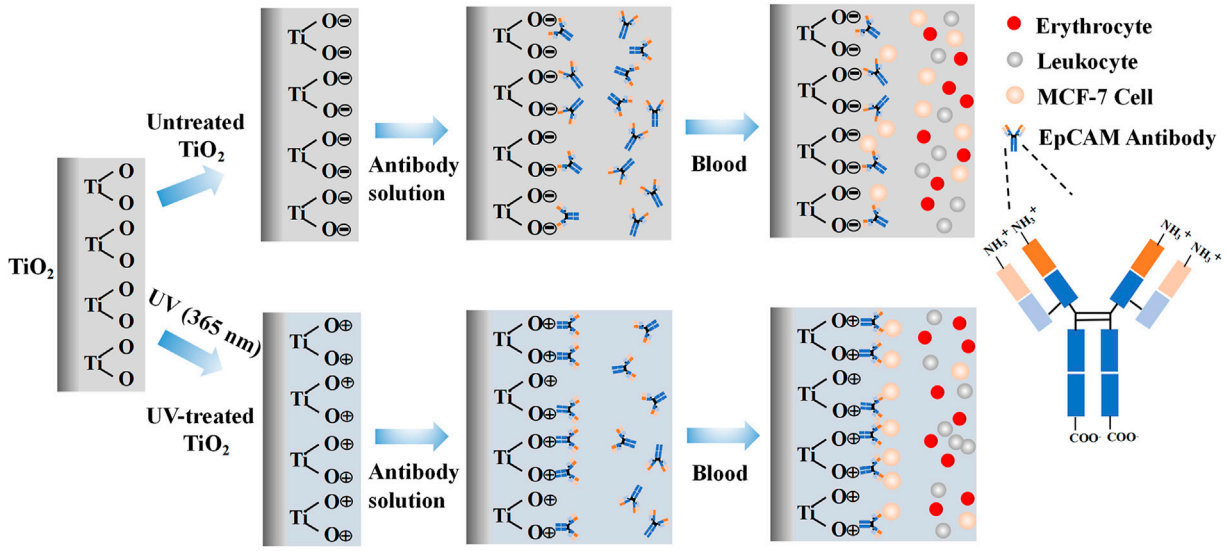

FIGURE 1
Hypothetical mechanism of electrostatic interaction between EpCAM antibodies and photo-functionalized TiO_2 surface, and schematic diagram of cells capture.

monoclonal antibody was purchased from Proteintech Group, Inc., (Wuhan). Rhodamine stain solution was purchased from Sigma-Aldrich (United States). The CFDA SE Cell Proliferation Assay and Tracking Kit were purchased from Beyotime Biotechnology Company Limited (Shanghai). TiO_2 nanoparticles were purchased from Sigma-Aldrich (United States).

2.2 Construction of CTCs capture materials

Anatase TiO_2 films were prepared on the Si substrate by an unbalanced magnetron sputtering equipment (UBMS450, Southwest Jiaotong University), according to the deposition parameters of Cui et al. (2021) The TiO_2 films were cut into 0.7 cm × 0.7 cm pieces and placed in a dark environment for 1 month to stabilize the chemical properties of the surface of the samples. The TiO_2 films were then irradiated for 1 h at 365 nm UV intensity using a model URE-2000/25-T9 lithography machine (Institute of Optics and Electronics, Chinese Academy of Sciences, China) with a UV intensity of 10 mW/cm^2. UV-irradiated TiO_2 films (UV-TiO_2) and unirradiated TiO_2 films (UNT-TiO_2) were separately placed in 24-well plates. The EpCAM antibody solution was diluted with phosphate buffer saline (PBS) to make antibody dilutions at concentrations of 0, 0.001, 0.01, and 0.1 mg/mL, which were prepared and ready to use. The UV-TiO_2 groups and UNT-TiO_2 groups were then incubated with different concentrations of antibody solutions for 5 min at room temperature. After the incubation, the samples were washed 3 times with PBS to remove the antibodies that did not adhere firmly. Finally, the samples were stored at 4°C. These prepared samples are respectively represented as UV-TiO_2-0, UV-TiO_2-0.001, UV-TiO_2-0.01, UV-TiO_2-0.1, and UNT-TiO_2-0, UNT-TiO_2-0.001, UNT-TiO_2-0.01, UNT-TiO_2-0.1.

2.3 Characterization of TiO_2 film

Atomic Force Microscope (AFM; Nano Navi E-Sweep, Hitachi, Japan) was used to observe the surface morphologies of the samples. X-ray photoelectron spectroscopy (XPS; XSAM800, Kratos Ltd., United Kingdom) was performed to detect the changes in the surface chemical state of the samples before and after antibody adsorption. The hydrophilicity of the samples was detected by a water contact angle measurement meter (WCA; JY-82, Kruss, Germany). A Zeta electric potential analyzer (ZEN3600, Malvern Nano ZS, United Kingdom) was employed to detect the change in the surface charge of the samples (Due to the requirements of the detection equipment, the TiO_2 films were replaced with TiO_2 nanoparticles. All other processing factors were the same as above).

2.4 *In vitro* capture of CTCs

Each prepared sample was placed in a 24-well plate, and MCF-7 cells were diluted to 10^5 cells/mL in the DMEM medium. Then 500 μL of cell suspension was added to each sample and placed on a shaker for 40 min. After 40 min, they were washed 3 times with PBS to remove uncaptured cells, followed by 2.5% (v/v) glutaraldehyde for fixation. Finally, cells captured on the surface of different samples were stained with rhodamine stain and observed under a fluorescent microscope (IX51, Olympus, Japan).

2.5 Dynamic capture of CTCs *in vitro*

Foldable Ti foils (0.7 cm × 1 cm) covered with TiO_2 films were used to test the capture efficiency of CTCs in the blood flow state.

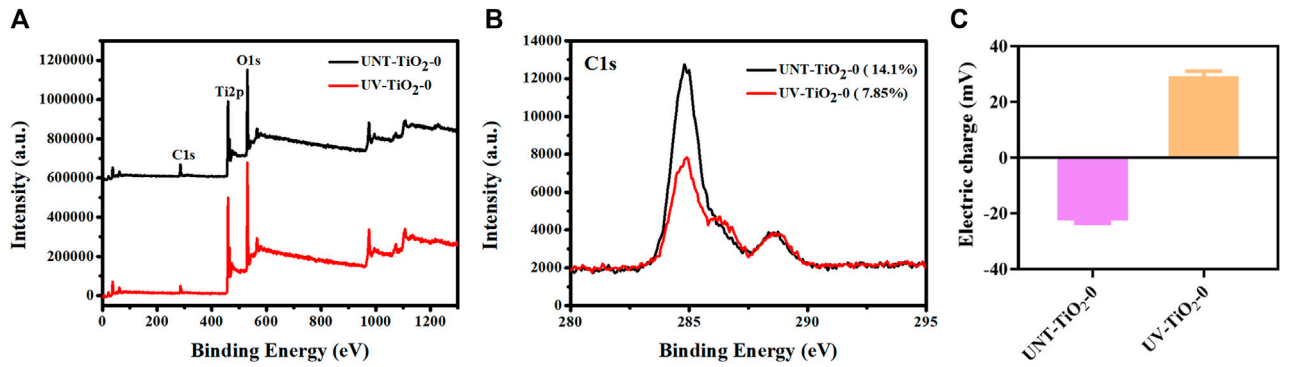

FIGURE 2
(A) XPS full spectrum of elements on TiO_2 surface before and after UV irradiation. **(B)** XPS high-resolution spectra of C1s on TiO_2 surfaces before and after UV irradiation. **(C)** Charge changes on the TiO_2 surface before and after UV irradiation.

A chandler loop system (CJ23, Sichuan Academy of Medical Sciences—Sichuan Provincial People's Hospital) was used to simulate blood flow to capture CTCs. The chandler loop system can better simulate extracorporeal blood circulation and rotate at a certain speed in a temperature-controlled environment to simulate blood flow conditions. The medical catheters containing fresh whole blood (collected in an ethically approved manner from healthy people at the Sichuan Provincial People's Hospital) with MCF-7 cells (labelled in advance using the CFDA SE fluorescent stain) were connected to the chandler loop system to form a closed circulatory system (Figure 5A). The TiO_2 foils from the UV-TiO_2-0, UV-TiO_2-0.1, and UNT-TiO_2-0, UNT-TiO_2-0.1 groups were rolled into separate medical catheters, with each TiO_2 foil tightly attached to the inner wall of the catheter, and based on the catheter diameter of the chandler loop system and the flow rate of a human arm vein, the liquid flow of the chandler loop system was set to 50 mL/min, the temperature was set to 37°C and cycled for 40 min. Afterward, the samples were gently removed, washed 3 times in PBS, and immediately observed under a fluorescent microscope.

2.6 *In vivo* capture of CTCs

All animal experiments were performed in accordance with Chinese regulations on laboratory animal management. New Zealand White rabbits weighing 4.0–4.5 Kg were used. The UV-TiO_2-0.1 and UNT-TiO_2-0.1 were selected for the test, and UV-TiO_2-0 and UNT-TiO_2-0 were used as controls. The samples were rolled into separate medical catheters, with each sample tightly attached to the inner wall of the catheter. One side of the catheter was connected to the carotid artery of the rabbit and the other to the jugular vein, forming a closed circulatory system (Figure 6A). After successful connection, 1 mL of MCF-7 cells (labelled in advance using the CFDA SE fluorescent stain) were injected from the rabbit's ear vein. After 40 min of cycling, the samples were gently removed, washed 3 times in PBS, and immediately observed under a fluorescent microscope.

2.7 Statistical analysis

One-way ANOVA of SPSS 26.0 software was performed to assess statistical differences between the sample groups. $^*p < 0.05$ indicated significance. Three independent samples were used for each experimental sample group if not otherwise indicated.

3 Results and discussion

3.1 Characterization of TiO_2 film

Figures 2A, B showed the XPS spectra of C1s of the TiO_2 surface before and after the UV irradiation. The content of the carbon (C) element on the unirradiated TiO_2 surface was 14.1%, while after UV irradiation, the content of the C element decreased to 7.85%. This might be due to the self-clean effect, which decomposed the hydrocarbons adsorbed on the TiO_2 surface (Takeuchi et al., 2005; Zhang et al., 2008). The decrease of the C element indicated the exposure of the clean TiO_2 surface, which might bind more of the antibodies.

As shown in Figure 2C, the changes in charge of the TiO_2 surface before and after UV irradiation were examined. The TiO_2 surface was negatively charged before UV irradiation, while the surface showed a positive charge after UV irradiation. This positively charged surface could facilitate the carboxyl terminal of the antibody to conjugate with the TiO_2 surface through electrostatic interaction, thus fully exposing the antibody's antigen-binding site. However, there was also a problem that there are usually many amino and carboxyl groups in the side chain of an antibody, which would affect the adhesion mode of antibodies and TiO_2. That is, in addition to the binding method shown in Figure 1, antibodies might also be combined with TiO_2 through carboxyl groups on the side chain, in the form of lying on the side, which would affect the exposure of the antigen-binding site of the antibody and hence the effectiveness of cell capture.

As the EpCAM antibodies contain the characteristic element nitrogen (N), XPS was used to detect the atomic percentage of N on the surface of the sample to semi-quantitatively calculate the number of antibodies bound on the sample surface. Figure 3A

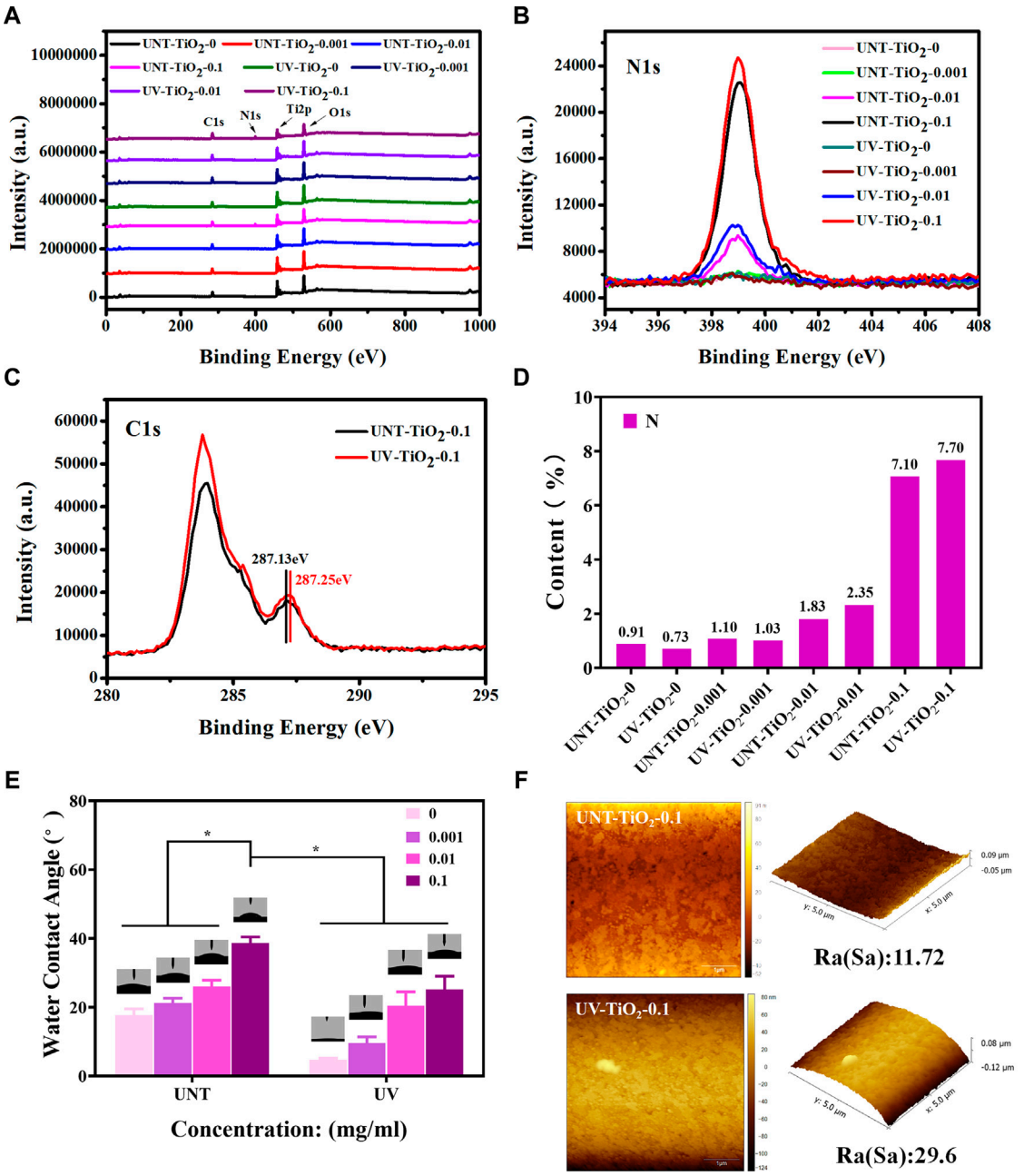

FIGURE 3
(A) XPS full spectrum of TiO_2 surface modified with EpCAM antibodies. **(B)** XPS high-resolution spectra of N1s on TiO_2 surface modified with EpCAM antibodies. **(C)** XPS high-resolution spectra of C1s on TiO_2 surface modified with EpCAM antibodies. **(D)** The statistical plot of the N element content of the TiO_2 surface modified with EpCAM antibodies. **(E)** The water contact angle of TiO_2 surface modified with EpCAM antibodies. **(F)** AFM image of TiO_2 surface modified with EpCAM antibodies. Data were expressed as mean ± standard deviation (n = 3) and analyzed using a one-way ANOVA, $*p < 0.05$.

showed the XPS full spectrum, Figure 3B showed the high-resolution spectra of N1s, and Figure 3D showed the N element content statistics. The results revealed that the N element content of the TiO_2 surface modified with EpCAM antibodies showed the following order: UV-TiO_2-0.1 > UNT-TiO_2-0.1 > UV-TiO_2-0.01 > UNT-TiO_2-0.01, indicating that UV-TiO_2 was able to adsorb more antibodies compared to the UNT-TiO_2 when immersed in the same concentration of antibody solution. Meanwhile, the N element content of UNT-TiO_2-0.001 and UV-TiO_2-0.001 was similar to that of UNT-TiO_2-0 and UV-TiO_2-0. This might be due to the adsorbed antibodies in the TiO_2-0.001 groups being below the XPS device's detection limit; Figure 3C showed that the peak of UV-TiO_2-0.1 was higher than the UNT-TiO_2-0.1, further proving that there were more antibodies adsorbed to UV-TiO_2-0.1. And they both had a small spike at about 287 eV binding energy, which was attributed to the presence of oxygen-containing

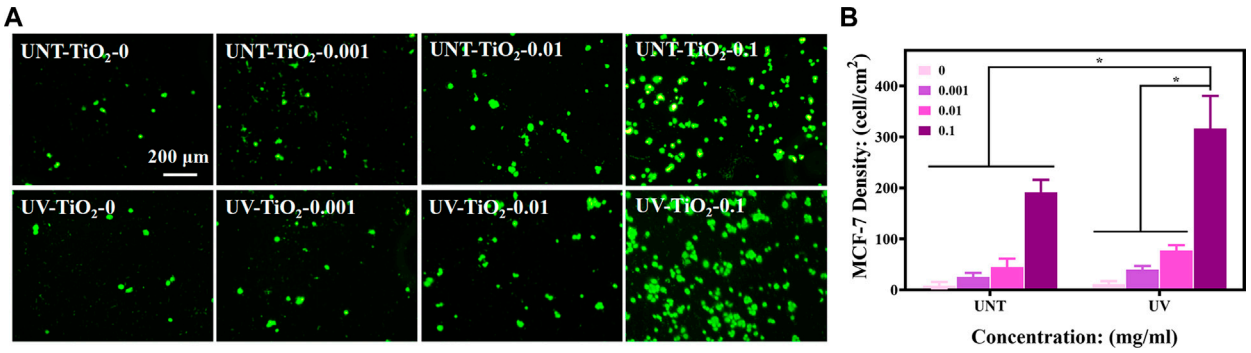

FIGURE 4
(A) Fluorescent images of different sample groups after capturing MCF-7 cells. **(B)** Plots of statistical analysis of the number of MCF-7 cells for **(A)**. Data were expressed as mean ± standard deviation (n = 3) and analyzed using one-way ANOVA, *$p < 0.05$.

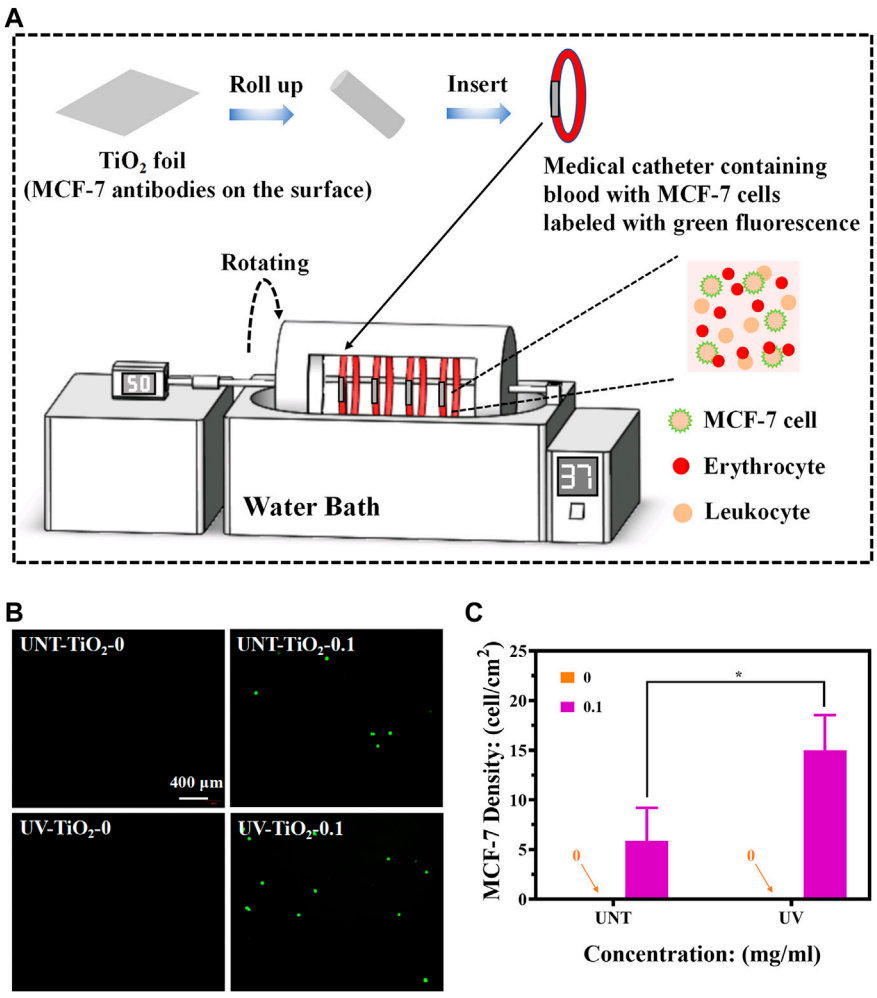

FIGURE 5
(A) Schematic diagram of capturing MCF-7 cells using the chandler loop system device (MCF-7 cells labelled with green fluorescence). **(B)** Fluorescence images of different sample groups after capturing MCF-7 cells. **(C)** Plot of statistical analysis of the number of MCF-7 cells for **(B)**. Data were expressed as mean ± standard deviation (n = 3) and analyzed using one-way ANOVA, *$p < 0.05$.

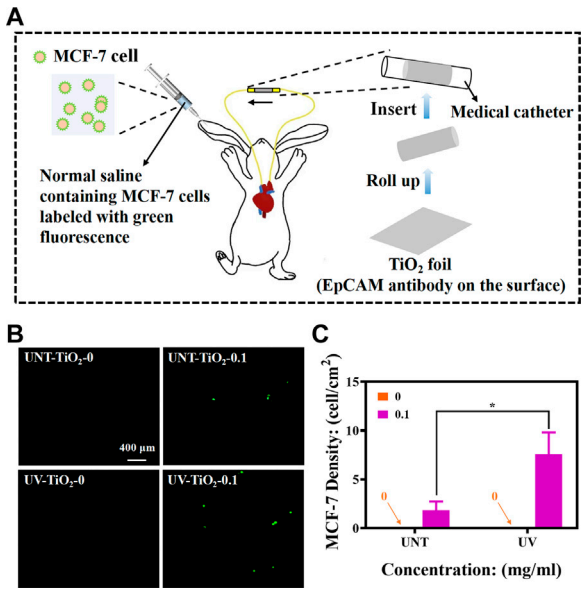

FIGURE 6
(A) Schematic diagram of *in vivo* MCF-7 cell capture using New Zealand white rabbits (MCF-7 cells labelled with green fluorescence). **(B)** Fluorescence images of different sample groups after capturing MCF-7 cells. **(C)** Plot of statistical analysis of the number of MCF-7 cells for **(B)**. Data were expressed as mean ± standard deviation (n = 3) and analyzed using one-way ANOVA, $*p < 0.05$.

hydrocarbons and could be assigned to the -COOH group (Aita et al., 2009; Att et al., 2009). Compared with the small peak of UNT-TiO_2-0.1 (287.13 eV), the small peak of UV-TiO_2-0.1 (287.25 eV) was shifted to the right, indicating that the -COOH group lost hydrogen and might be absorbed on the TiO_2 surface in a bidentate binding structure. UV irradiation can lead to various physicochemical changes in the TiO_2 surface, including photo-induced superhydrophilicity (Wang et al., 1997; Takeuchi et al., 2005). As shown in Figure 3E, the results showed that the water contact angle of the unirradiated TiO_2 surface (UNT-TiO_2-0) was approximately 17.93° ± 1.59°. In comparison, the water contact angle of the UV-irradiated TiO_2 surface (UV-TiO_2-0) was approximately 4.9° ± 0.3°, because of the fact that the UV irradiation causes the TiO_2 surface to become superhydrophilic. The hydrophilic surface is conducive to keeping its activity (Giacomelli et al., 1999). The water contact angles on all the TiO_2 surfaces increased after the addition of EpCAM antibodies and were positively correlated with the antibody concentration. At the same antibody concentration, the water contact angle of the UV-TiO_2 groups was lower than that of the UNT-TiO_2 groups, indicating that the antibodies adhered to the UV-TiO_2 groups, compared to the UNT-TiO_2 groups, exposed to fewer hydrophobic terminal.

As shown in Figure 3F, the AFM results showed that the surface roughness of UNT-TiO_2-0.1 and UV-TiO_2-0.1 was 11.72 nm and 29.6 nm, respectively. UV-TiO_2-0.1 had a higher roughness than UNT-TiO_2-0.1, indicating that the UV-treated TiO_2 could promote antibodies' binding to the TiO_2 surface.

3.2 *In vitro* capture of CTCs

As epithelial cell adhesion molecule (EpCAM) is highly expressed in breast cancer cells (Cimino et al., 2010; Chen et al., 2018), MCF-7 cells were used for capture experiments in the study. As shown in Figures 4A ,B, the number of captured cells increased with the increase of antibody concentration in both the UNT-TiO_2 and UV-TiO_2 groups. Among all the samples, UV-TiO_2-0.1 captured the most cells. This result indicated that as the antibody concentration increased, the more EpCAM antibodies adsorbed on the TiO_2 surface, the more cells were captured. The cells in UV-TiO_2-0 groups and UNT-TiO_2-0 groups were probably caused by the natural settling of the cells and occasional contact. Moreover, at the same concentration, the UV-TiO_2 groups could capture about 1.5 times more MCF-7 cells than the UNT-TiO_2 groups. The result indicated that the photo-functionalized TiO_2 surface modified with EpCAM antibodies could efficiently capture CTCs from the environment *in vitro*.

3.3 Dynamic capture of CTCs *in vitro*

To explore the capture efficiency of MCF-7 cells by EpCAM antibodies-modified TiO_2 in the blood flow state and eliminate the influence of complex components in blood on the capture of MCF-7 cells, this experiment would use the chandler loop system to simulate blood circulation.

As shown in Figures 5B, C, the TiO_2-0 groups could not capture MCF-7 cells in flowing blood conditions. The EpCAM antibodies-modified TiO_2, either UV-TiO_2-0.1 or UNT-TiO_2-0.1 group, could successfully capture MCF-7 cells. Notably, in the above *in vitro* capture results, the UV-TiO_2-0.1 groups captured only approximately 165% more MCF-7 cells than the UNT-TiO_2-0.1 groups, but in the fluid conditions, the UV-TiO_2-0.1 groups captured approximately 252% more MCF-7 cells than the UNT-TiO_2-0.1 groups. The reason for the difference could be that some of the antibodies on the unirradiated TiO_2 surface were easily washed away due to physical adsorption under fluid conditions. In contrast, antibodies adsorbed on the Photo-functionalized TiO_2 surface had a strong binding force that resisted fluid washout and captured the cells in the fluid. However, the number of MCF-7 cells captured by UV-TiO_2-0.1 and UNT-TiO_2-0.1 groups in this experiment was far less than that of MCF-7 cells captured *in vitro* mentioned above. The possible reason was that in the complex whole blood condition, blood cells in the blood obstructed the contact of MCF-7 cells with antibodies on the TiO_2, resulting in insufficient contact of MCF-7 cells with TiO_2. In conclusion, the above results demonstrated that photo-functionalized TiO_2 surfaces modified with EpCAM antibodies could efficiently capture CTCs from the environment *in vitro*.

3.4 *In vivo* capture of CTCs

Furthermore, we constructed a rabbit model to simulate human blood circulation to determine whether TiO_2 modified with EpCAM antibodies could capture MCF-7 cells *in vivo*.

As shown in Figure 6A, a medical catheter containing TiO_2 modified with EpCAM antibodies was used to connect the rabbit's

carotid artery and jugular vein to construct a closed circulatory system. MCF-7 cells labelled with CFDA SE stain (emitting green fluorescence) were then injected into the body from the rabbit's ear vein, and the MCF-7 cells were captured as the blood flowed through the TiO_2 modified with EpCAM antibodies. As shown in Figures 6B, C, the TiO_2-0 groups could not capture MCF-7 cells *in vivo*. In contrast, after the immobilization of EpCAM antibodies, TiO_2 could effectively capture MCF-7 cells, and UV-TiO_2-0.1 captured about 4 times more MCF-7 cells than UNT-TiO_2-0.1. However, the number of cells captured by both was less than that of cells captured *in vitro*, probably because the rabbit's immune system rejected the foreign bodies and cleared some MCF-7 cells. These results indicated that photo-functionalized TiO_2 with EpCAM antibodies could capture CTCs from the dynamic environment *in vivo*.

4 Conclusion

In summary, we have constructed a new platform that significantly increased the capture efficiency of CTCs by bonding EpCAM antibodies with electrostatic mechanisms based on the charge change on the TiO_2 surface caused by UV irradiation, which exposed more binding sites for antibodies bound to the TiO_2 surface. Our experimental results also showed that the photo-functionalized TiO_2 modified with EpCAM antibodies could efficiently capture CTCs from environments *in vitro* and *in vivo*. Since TiO_2 can be deposited on the surface of various inorganic materials by physical vapor deposition and has excellent biocompatibility. Therefore, the method may be suitable for the construction of a variety of various materials for the capture of CTCs *in vitro* (such as magnetic beads and silicon-based photoelectrochemical platforms) and *in vivo* (stainless steel indwelling needles).

Data availability statement

The original contributions presented in the study are included in the article/Supplementary Material, further inquiries can be directed to the corresponding authors.

Ethics statement

The animal study was reviewed and approved by the Medical Ethics Committee of the Sichuan Provincial People's Hospital.

Author contributions

HD and XQL: Experiment, data curation, writing-original draft preparation. JC and YH: Supervision and language polishment. LKL: Writing-Reviewing. XL, JC, and XQL: Conceptualization and manuscript revision.

Funding

This work was supported by the National Natural Science Foundation of China (Nos. 82070930, 82171026), the Sichuan Science and Technology Program (2022YFS0022, 2023YFS0043, 2023YFS0308 and 2022NSFSC0385), the Foundation of Technology and Science and Technology Bureau of Chengdu (2021-YF05-02398-SN), Medico-Engineering Cooperation Funds from University of Electronic Science and Technology of China (ZYGX2021YGLH020).

Conflict of interest

The authors declare that the research was conducted in the absence of any commercial or financial relationships that could be construed as a potential conflict of interest.

Publisher's note

All claims expressed in this article are solely those of the authors and do not necessarily represent those of their affiliated organizations, or those of the publisher, the editors and the reviewers. Any product that may be evaluated in this article, or claim that may be made by its manufacturer, is not guaranteed or endorsed by the publisher.

References

Abdulla, A., Zhang, T., Li, S., Guo, W., Warden, A. R., Xin, Y., et al. (2022). Integrated microfluidic single-cell immunoblotting chip enables high-throughput isolation, enrichment and direct protein analysis of circulating tumor cells. *Microsyst. Nanoeng.* 8, 13. doi:10.1038/s41378-021-00342-2

Aita, H., Att, W., Ueno, T., Yamada, M., Hori, N., Iwasa, F., et al. (2009). Ultraviolet light-mediated photofunctionalization of titanium to promote human mesenchymal stem cell migration, attachment, proliferation and differentiation. *Acta Biomater.* 5 (8), 3247–3257. doi:10.1016/j.actbio.2009.04.022

Att, W., Hori, N., Takeuchi, M., Ouyang, J., Yang, Y., Anpo, M., et al. (2009). Time-dependent degradation of titanium osteoconductivity: An implication of biological aging of implant materials. *Biomaterials* 30 (29), 5352–5363. doi:10.1016/j.biomaterials.2009.06.040

Castro-Giner, F., and Aceto, N. (2020). Tracking cancer progression: From circulating tumor cells to metastasis. *Genome Med.* 12 (1), 31. doi:10.1186/s13073-020-00728-3

Chaffer, C. L., and Weinberg, R. A. (2011). A perspective on cancer cell metastasis. *Science* 331 (6024), 1559–1564. doi:10.1126/science.1203543

Chen, J., Yang, P., Liao, Y., Wang, J., Chen, H., Sun, H., et al. (2015). Effect of the duration of UV irradiation on the anticoagulant properties of titanium dioxide films. *ACS Appl. Mater Interfaces* 7 (7), 4423–4432. doi:10.1021/am509006y

Chen, J., Zhao, A., Chen, H., Liao, Y., Yang, P., Sun, H., et al. (2014). The effect of full/partial UV-irradiation of TiO_2 films on altering the behavior of fibrinogen and platelets. *Colloids Surf. B Biointerfaces* 122, 709–718. doi:10.1016/j.colsurfb.2014.08.004

Chen, L., Peng, M., Li, N., Song, Q., Yao, Y., Xu, B., et al. (2018). Combined use of EpCAM and FRalpha enables the high-efficiency capture of circulating tumor cells in non-small cell lung cancer. *Sci. Rep.* 8 (1), 1188. doi:10.1038/s41598-018-19391-1

Cimino, A., Halushka, M., Illei, P., Wu, X., Sukumar, S., and Argani, P. (2010). Epithelial cell adhesion molecule (EpCAM) is overexpressed in breast cancer metastases. *Breast Cancer Res. Treat.* 123 (3), 701–708. doi:10.1007/s10549-009-0671-z

Cui, J. W., He, S., Dai, S., Liu, L. Y., Zhao, A. S., Lu, L., et al. (2021). Stepwise assembly of functional proteins on Photo-activated TiO_2 surfaces confers anti-oxidative stress ability and stealth effect to vascular stents. *Chem. Eng. J.* 424, 130392. doi:10.1016/j.cej.2021.130392

Ellingsen, J. E. (1991). A study on the mechanism of protein adsorption to TiO_2. *Biomaterials* 12 (6), 593–596. doi:10.1016/0142-9612(91)90057-h

Giacomelli, C. E., Bremer, M. G., and Norde, W. (1999). ATR-FTIR study of IgG adsorbed on different silica surfaces. *J. Colloid Interface Sci.* 220 (1), 13–23. doi:10.1006/jcis.1999.6479

Hori, N., Ueno, T., Minamikawa, H., Iwasa, F., Yoshino, F., Kimoto, K., et al. (2010a). Electrostatic control of protein adsorption on UV-photofunctionalized titanium. *Acta Biomater.* 6 (10), 4175–4180. doi:10.1016/j.actbio.2010.05.006

Hori, N., Ueno, T., Suzuki, T., Yamada, M., Att, W., Okada, S., et al. (2010b). Ultraviolet light treatment for the restoration of age-related degradation of titanium bioactivity. *Int. J. Oral Maxillofac. Implants* 25 (1), 49–62.

Iwasa, F., Hori, N., Ueno, T., Minamikawa, H., Yamada, M., and Ogawa, T. (2010). Enhancement of osteoblast adhesion to UV-photofunctionalized titanium via an electrostatic mechanism. *Biomaterials* 31 (10), 2717–2727. doi:10.1016/j.biomaterials.2009.12.024

Jahangiri, M., Ranjbar-Torkamani, M., Abadijoo, H., Ghaderinia, M., Ghafari, H., Mamdouh, A., et al. (2020). Low frequency stimulation induces polarization-based capturing of normal, cancerous and white blood cells: A new separation method for circulating tumor cell enrichment or phenotypic cell sorting. *Analyst* 145 (23), 7636–7645. doi:10.1039/d0an01033b

Kang, K., Zhou, X., Zhang, Y., Zhu, N., Li, G., Yi, Q., et al. (2021). Cell-released magnetic vesicles capturing metabolic labeled rare circulating tumor cells based on bioorthogonal chemistry. *Small* 17 (18), e2007796. doi:10.1002/smll.202007796

Li, F., Wang, M., Cai, H., He, Y., Xu, H., Liu, Y., et al. (2020). Nondestructive capture, release, and detection of circulating tumor cells with cystamine-mediated folic acid decorated magnetic nanospheres. *J. Mater Chem. B* 8 (43), 9971–9979. doi:10.1039/d0tb01091j

Liang, N., Liu, L., Li, P., Xu, Y., Hou, Y., Peng, J., et al. (2020). Efficient isolation and quantification of circulating tumor cells in non-small cell lung cancer patients using peptide-functionalized magnetic nanoparticles. *J. Thorac. Dis.* 12 (8), 4262–4273. doi:10.21037/jtd-20-1026A

Lin, E., Cao, T., Nagrath, S., and King, M. R. (2018). Circulating tumor cells: Diagnostic and therapeutic applications. *Annu. Rev. Biomed. Eng.* 20, 329–352. doi:10.1146/annurev-bioeng-062117-120947

Liu, J., Enloe, C., Li-Oakey, K. D., and Oakey, J. (2022). Optimizing immunofunctionalization and cell capture on micromolded hydrogels via controlled oxygen-inhibited photopolymerization. *ACS Appl. Bio Mater* 2022, 776. doi:10.1021/acsabm.2c00776

Mohamadi, R. M., Ivanov, I., Stojcic, J., Nam, R. K., Sargent, E. H., and Kelley, S. O. (2015). Sample-to-Answer isolation and mRNA profiling of circulating tumor cells. *Anal. Chem.* 87 (12), 6258–6264. doi:10.1021/acs.analchem.5b01019

Parker, S. G., Yang, Y., Ciampi, S., Gupta, B., Kimpton, K., Mansfeld, F. M., et al. (2018). A photoelectrochemical platform for the capture and release of rare single cells. *Nat. Commun.* 9 (1), 2288. doi:10.1038/s41467-018-04701-y

Paterlini-Brechot, P., and Benali, N. L. (2007). Circulating tumor cells (CTC) detection: Clinical impact and future directions. *Cancer Lett.* 253 (2), 180–204. doi:10.1016/j.canlet.2006.12.014

Pelaez, M., Nolan, N. T., Pillai, S. C., Seery, M. K., Falaras, P., Kontos, A. G., et al. (2012). A review on the visible light active titanium dioxide photocatalysts for environmental applications. *Appl. Catal. B Environ.* 125, 331-349. doi:10.1016/j.apcatb.2012.05.036

Plaks, V., Koopman, C. D., and Werb, Z. (2013). Cancer. Circulating tumor cells. *Science* 341 (6151), 1186–1188. doi:10.1126/science.1235226

Shi, F., Jia, F., Wei, Z., Ma, Y., Fang, Z., Zhang, W., et al. (2021). A microfluidic chip for efficient circulating tumor cells enrichment, screening, and single-cell RNA sequencing. *Proteomics* 21 (3-4), e2000060. doi:10.1002/pmic.202000060

Stott, S. L., Hsu, C. H., Tsukrov, D. I., Yu, M., Miyamoto, D. T., Waltman, B. A., et al. (2010). Isolation of circulating tumor cells using a microvortex-generating herringbone-chip. *Proc. Natl. Acad. Sci. U. S. A.* 107 (43), 18392–18397. doi:10.1073/pnas.1012539107

Su, W., Yu, H., Jiang, L., Chen, W., Li, H., and Qin, J. (2019). Integrated microfluidic device for enrichment and identification of circulating tumor cells from the blood of patients with colorectal cancer. *Dis. Markers* 2019, 8945974. doi:10.1155/2019/8945974

Sung, H., Ferlay, J., Siegel, R. L., Laversanne, M., Soerjomataram, I., Jemal, A., et al. (2021). Global cancer statistics 2020: GLOBOCAN estimates of incidence and mortality worldwide for 36 cancers in 185 countries. *CA Cancer J. Clin.* 71 (3), 209–249. doi:10.3322/caac.21660

Takeuchi, M., Sakamoto, K., Martra, G., Coluccia, S., and Anpo, M. (2005). Mechanism of photoinduced superhydrophilicity on the TiO_2 photocatalyst surface. *J. Phys. Chem. B* 109 (32), 15422–15428. doi:10.1021/jp058075i

Ueno, T., Yamada, M., Suzuki, T., Minamikawa, H., Sato, N., Hori, N., et al. (2010). Enhancement of bone-titanium integration profile with UV-photofunctionalized titanium in a gap healing model. *Biomaterials* 31 (7), 1546–1557. doi:10.1016/j.biomaterials.2009.11.018

Wang, D., Dong, R., Wang, X., and Jiang, X. (2022a). Flexible electronic catheter based on nanofibers for the *in vivo* elimination of circulating tumor cells. *ACS Nano* 16 (4), 5274–5283. doi:10.1021/acsnano.1c09807

Wang, D., Ge, C., Liang, W., Yang, Q., Liu, Q., Ma, W., et al. (2020). *In vivo* enrichment and elimination of circulating tumor cells by using a black phosphorus and antibody functionalized intravenous catheter. *Adv. Sci. (Weinh)* 7 (17), 2000940. doi:10.1002/advs.202000940

Wang, D., Huo, T., Du, Y., Qian, M., Lin, C., Nie, H., et al. (2022c). Sensitive CTC analysis and dual-mode MRI/FL diagnosis based on a magnetic core-shell aptasensor. *Biosens. Bioelectron.* 215, 114530. doi:10.1016/j.bios.2022.114530

Wang, D., Wang, J., Wang, Y. X., Ma, J. Y., Liu, B., Tang, A. N., et al. (2022b). A CRISPR/Cas12a-responsive dual-aptamer DNA network for specific capture and controllable release of circulating tumor cells. *Chem. Sci.* 13 (35), 10395–10405. doi:10.1039/d2sc03374g

Wang, R., Hashimoto, K., Fujishima, A., Chikuni, M., Kojima, E., Kitamura, A., et al. (1997). Light-induced amphiphilic surfaces. *Nature* 388 (6641), 431–432. doi:10.1038/41233

Wang, Z., Sun, N., Liu, H., Chen, C., Ding, P., Yue, X., et al. (2019). High-efficiency isolation and rapid identification of heterogeneous circulating tumor cells (CTCs) using dual-antibody-modified fluorescent-magnetic nanoparticles. *ACS Appl. Mater Interfaces* 11 (43), 39586–39593. doi:10.1021/acsami.9b14051

Xu, J., Zhao, C., Niu, K., Gao, Z., and Song, Y. Y. (2021). Renewable photoelectrochemical cytosensing platform for rapid capture and detection of circulating tumor cells. *Anal. Chim. Acta* 1142, 1–9. doi:10.1016/j.aca.2020.10.049

Zhang, H., Jia, Z., Wu, C., Zang, L., Yang, G., Chen, Z., et al. (2015). *In vivo* capture of circulating tumor cells based on transfusion with a vein indwelling needle. *ACS Appl. Mater Interfaces* 7 (36), 20477–20484. doi:10.1021/acsami.5b06874

Zhang, L., Li, P., Gong, Z., and Li, X. (2008). Photocatalytic degradation of polycyclic aromatic hydrocarbons on soil surfaces using TiO(2) under UV light. *J. Hazard Mater* 158 (2-3), 478–484. doi:10.1016/j.jhazmat.2008.01.119

Zhang, T., Peng, W., Jiang, W., Gao, K., and Liu, W. (2021). Ultradense erythrocyte bionic layer used to capture circulating tumor cells and plasma-assisted high-purity release. *ACS Appl. Mater Interfaces* 13 (21), 24543–24552. doi:10.1021/acsami.1c05806

Zhou, X., Zhang, Y., Kang, K., Mao, Y., Yu, Y., Yi, Q., et al. (2022). Controllable environment protein corona-disguised immunomagnetic beads for high-performance circulating tumor cell enrichment. *Anal. Chem.* 94 (11), 4650–4657. doi:10.1021/acs.analchem.1c04587

Zhu, S., Xie, Z., Chen, Y., Liu, S., Kwan, Y. W., Zeng, S., et al. (2022). Real-time detection of circulating tumor cells in bloodstream using plasmonic fiber sensors. *Biosens. (Basel)* 12 (11). doi:10.3390/bios12110968

Zubkov, T., Stahl, D., Thompson, T. L., Panayotov, D., Diwald, O., and Yates, J. T., Jr. (2005). Ultraviolet light-induced hydrophilicity effect on TiO_2(110)(1 x 1)Dominant role of the photooxidation of adsorbed hydrocarbons causing wetting by water droplets. *J. Phys. Chem. B* 109 (32), 15454–15462. doi:10.1021/jp058101c

frontiers | Frontiers in Pharmacology

TYPE Original Research
PUBLISHED 01 March 2023
DOI 10.3389/fphar.2023.1134895

OPEN ACCESS

EDITED BY
Qin Wang,
Southwest Jiaotong University, China

REVIEWED BY
Xiaolei Wei,
Southern Medical University, China
Xingli Zou,
North Sichuan Medical College, China
Fang-Yi Fan,
General Hospital of the Chinese People's Liberation Army Western Theater, China

*CORRESPONDENCE
Xiaoqi Liu,
liuxiaoqi76@163.com
Tao Jiang,
suyeku@126.com
Chunle Zhang,
xiwang5297@163.com

†These authors contributed equally to this work

SPECIALTY SECTION
This article was submitted to Pharmacology of Anti-Cancer Drugs, a section of the journal Frontiers in Pharmacology

RECEIVED 31 December 2022
ACCEPTED 14 February 2023
PUBLISHED 01 March 2023

CITATION
Lin L, Liu X, Yu H, Deng H, Peng K, Chen J, Zhang C, Jiang T and Liu X (2023), Inhibitory effect and related mechanism of decitabine combined with gemcitabine on proliferation of NK/T cell lymphoma cells.
Front. Pharmacol. 14:1134895.
doi: 10.3389/fphar.2023.1134895

Inhibitory effect and related mechanism of decitabine combined with gemcitabine on proliferation of NK/T cell lymphoma cells

Lanke Lin[1†], Xiangqin Liu[2†], Hui Yu[3†], Huan Deng[1], Kun Peng[4], Jiang Chen[5], Chunle Zhang[6*], Tao Jiang[7*] and Xiaoqi Liu[8,9*]

[1]College of Medical Technology, Chengdu University of Traditional Chinese Medicine, Chengdu, China, [2]Department of Laboratory Medicine and Sichuan Provincial Key Laboratory for Human Disease Gene Study, Sichuan Provincial People's Hospital, University of Electronic Science and Technology of China, Chengdu, China, [3]Department of Laboratory Medicine, The People's Hospital of Leshan, Leshan, China, [4]Health Management Center, Sichuan Provincial People's Hospital, University of Electronic Science and Technology of China, Chengdu, China, [5]The Department of Ophthalmology, Sichuan Provincial People's Hospital, University of Electronic Science and Technology of China, Chengdu, China, [6]Division of Nephrology, Kidney Research Institute, West China Hospital of Sichuan University, Chengdu, China, [7]Department of Hematology, Sichuan Academy of Medical Sciences & Sichuan Provincial People's Hospital, Chengdu, China, [8]Sichuan Provincial Key Laboratory for Human Disease Gene Study, Center for Medical Genetics, Sichuan Academy of Medical Sciences & Sichuan Provincial People's Hospital, University of Electronic Science and Technology of China, Chengdu, China, [9]Research Unit for Blindness Prevention of Chinese Academy of Medical Sciences (2019RU026), Sichuan Academy of Medical Sciences & Sichuan Provincial People's Hospital,, Chengdu, Sichuan, China

Background: EBV-associated lymphoma is a neoplasm with a poor prognosis, highly aggressive, and progressive rapidly. There is no standard clinical treatment protocol. Decitabine and gemcitabine are known to have anticancer properties against cells of various cancer, respectively. However, the effect of the combination medication on NK/T cell lymphoma cells and potential mechanisms have not been thoroughly investigated.

Methods: Human NK/T cell lymphoma cells NK92MI were treated with decitabine and gemcitabine alone or in combination. Experiments, including the Cell Counting Kit-8 and flow cytometry, were performed to investigate how the combination of decitabine and gemcitabine affects the biological behavior of NK92MI cells *in vitro*. mRNA sequencing, RT-PCR, and western blotting were used to detect changes in the related signal pathway, mRNA, and protein expressions.

Results: Decitabine and gemcitabine significantly inhibited the viability and proliferation of NK92MI cells in a dose-dependent manner. The combination index was less than 1 after treating with two drugs, which was a significant synergistic effect. The decitabine concentration with the best synergistic effect was 4.046 μM, and the gemcitabine concentration was 0.005 μM. Flow cytometry showed that combining two drugs could significantly promote apoptosis and arrest the cell cycle at the S phase. In the combined DAC and GEM group, caspase3 protein levels were higher than in either group alone or the control group. The transcriptome sequence, KEGG, and PPI analysis showed that the differential genes after combined treatment were mainly enriched in signal pathways related to cell proliferation, adhesion, and migration compared with using alone and control groups. Based on the sequencing results, we further

investigated the role of DAC and GEM in ferroptosis-related signaling molecules using RT-PCR and Western blot techniques. RT-PCR and western blotting showed that the expression levels of HMOX1 and EBV cleavage gene BRLF1 were higher in the group with combined DAC and GEM than in the group alone and the control group, while the protein and mRNA expression levels of SLC7A11 were lower than the others. In addition, the GPX4 protein expression level in the combination group was lower than in the drug-alone and control groups. In addition, the combination treatment increased the ROS level of NK92MI cells.

Conclusion: Our current findings suggested that decitabine had an inhibitory effect on the proliferation of NK92MI cells when co-treated with gemcitabine. This combination may increase the expression of ferroptosis-related signaling molecules, thus inhibiting the proliferation of NK92MI cells. It also promoted apoptosis in NK/T cell lymphoma. For patients with NK/T cell lymphoma, this novel combination may provide clinical benefits.

KEYWORDS

NK/T cell lymphoma, decitabine, gemcitabine, ferroptosis, apoptosis, drug combination

1 Introduction

Since Epstein-Barr virus (EBV) has been detected in Burkitt's lymphoma (BL) in Africa, its oncogenicity was confirmed as it could transform resting B cells into long-living cells *in vitro* (Pope et al., 1968). The virus is associated with proliferative lesions and malignant lymphomas of B, T, and NK cell origin in lymphoid tissue (Shannon-Lowe et al., 2017). Patients with EBV-positive lymphoma have a more dismal outcome and are usually treated in the same manner as EBV-negative lymphomas (Oyama et al., 2007). Patients with NK/T cell lymphoma (NKTCL) are ineffective to anthracycline-based chemotherapy due to high expression of multidrug-resistant P-glycoprotein (Yamaguchi et al., 1995). It is usually treated with a combination of radiotherapy and chemotherapy. Patients with stage I and II NKTCL are usually treated with radiotherapy, but the systemic recurrence rate is surprisingly high (Tse and Kwong, 2015). Asparaginase has a good survival rate for limited-stage NKTCL, with ORR and CR exceeding 75%, but not for advanced-stage NKTCL. Combination chemotherapy regimens including GELOX (pegaspargase, gemcitabine, oxaliplatin) (Wang et al., 2013), p-GEMOX (pegaspargase, gemcitabine, oxaliplatin) (Xia et al., 2021), MESA (methotrexate, etoposide, dexamethasone, and pegaspargase) (Xu et al., 2017), SMILE (dexamethasone, methotrexate, ifosfamide, L-asparaginase, and etoposide) (Kwong et al., 2012), DICE-L-sp (pegaspargase, gemcitabine, oxaliplatin) (Dong et al., 2016), LVP(pegaspargase, gemcitabine, oxaliplatin) (Jiang et al., 2012) all showed good clinical performance with 5-year PFS ranging from 64% to 83%. In contrast, L-asparaginase exhibits high immunogenicity and is less widely used, and its substitute, pegaspargase, is also associated with hyperlipidemia and fatal pancreatitis. Some novel targeted drugs have been investigated to overcome conventional therapies' limitations. Anti-PD-1 monoclonal antibodies activate depleted T cells and promote immune effects for anti-tumor purposes. Among the other agents being tested in clinical trials is lenalidomide, which can stimulate angiogenesis and immunomodulate the immune system (Jones et al., 2016; Kishimoto et al., 2019). In addition, infusion of cytotoxic T lymphoma with specific antigenic specificity can re-establish immunity to EBV, thus targeting malignant cells or already infected cells (Heslop et al., 2010). However, limitations such as high cost of targeted drugs, lack of prospective studies, safety issue of biological therapies, and complexity of preparing biological materials hamper clinical applications of these methods. Hence, a combination of old medications seems to be cost-effective and practical.

Decitabine (5-Aza-2′-deoxycytidine, DAC) is a natural adenosine analog of 2′-deoxycytidine, which inhibits tumor cell proliferation by inhibiting DNA methyltransferase and reducing DNA methylation. DAC activates hypermethylated silenced genes at low doses and exerts cytotoxic effects at high doses. DAC is available for various hematologic tumors (Seelan et al., 2018; Gao et al., 2020; Patel et al., 2021; Wu et al., 2021). Furthermore, DAC has been shown to be highly effective in treating malignant lymphomas (Dalton et al., 2020; Liu et al., 2021; Zhang et al., 2021). Low-dose DAC has been shown to initiate LMP1 demethylation in EBV-positive Burkitt lymphoma. (Dalton et al., 2020). In conjunction with adoptive T-cell therapy, DAC has improved the prognosis for patients with EBV-positive Hodgkin lymphoma (Cruz et al., 2011).

Gemcitabine ((2′,2′-difluoro 2′-deoxycytidine, GEM) is a pyrimidine analog named after its structure. GEM has shown apparent efficacy in various malignancies (Mini et al., 2006; Gesto et al., 2012; Abdel-Rahman et al., 2018). Studies have shown that when combined with other cytotoxic drugs, GEM has good efficacy and is less toxic in treating EBV-associated lymphomas (Xia et al., 2021; Xie et al., 2021; Zhang et al., 2022). Additionally, GEM induces lytic EBV in nasopharyngeal carcinoma tumor cells, enabling them to be treated with antiviral therapy.

In this study, EBV-positive lymphoma-derived NK92MI cells were used to assess the synergistic effects and mechanisms of the DAC combination of the GEM.

2 Materials and methods

2.1 Cell line

NK-92MI cells were obtained from Procell Life Science&Technology Co, Ltd. They were cultures in αMEM(Gibco, Cat#41061029) medium supported with 12.5% heat-inactivated FBS(Hyclone, Cat#SH30088.03HI), 12.5% heat-inactivated horse

serum (Gibco, Cat#26050088), 0.2 mM inositol (Solarbio, Cat#I8050), 0.1 mM 2-mercaptoethanol (Solarbio, Cat#M8210), and 0.02 mM folic acids (Solarbio, Cat#P1400). All media were supplemented with 100 U/mL penicillin and 100 mg/mL streptomycin (Solarbio, Cat#P1400). Cells were cultivated at 37 °C in a humidified atmosphere of 5% CO_2 in the air.

2.2 Cell proliferation assay

For the growth inhibition assay, NK92MI cells were grown in 96-well plates at a density of 4×10^5/mL. After the cell growth was stabilized, treated with different doses of decitabine (DAC) or gemcitabine (GEM) for 48 h, then Cell Counting Kit-8 (CCK-8, Dojindo, Tokyo, Japan) was added to each well and was incubated at 37 °C in a humidified atmosphere of 5% CO_2 in the air for 4 h to assess the cell viability. An enzyme-labeled instrument measured absorbance at a wavelength of 450 nm. IC10, IC20, and IC30 values for two drugs were calculated using Prism six software. In order to investigate the synergistic Effect of two drugs, NK92MI cells were treated with IC10, IC20, and IC30 of DAC and IC10, IC20, and IC30 of GEM alone and in cross-pairing, respectively. The proportion of live cells was measured by CCK-8 regent. The effects of combinations were estimated using the Compusyn software, which was developed based on the median-effect method created by Chou and Talalay.

2.3 Apoptosis assay

For this assay, the cells were seeded in 6-well plates at a density of 4×10^5/mL, which were treated with the best effective combinations. After 48 h of treatment, cells were collected and washed with PBS. Then, the cells were stained with AnnexinV Alexa Fluor488/PI(Solarbio, Cat#CA1020) according to the manufacturer's protocol. Next, the stained cells were analyzed using a FACS Canto II flow cytometer (BD Bioscience, United States), and the data were analyzed using FlowJo version software (FlowJo LLC, United States).

2.4 Cell cycle assay

The cells were plated in 6-well plates at a density of 4×10^5/mL. They were treated with the best effective combinations to analyze the cell cycle, which was analyzed by measuring DNA content using a flow cytometer (FACS Canto, BD Bioscience, CA). In the following step, the cells were collected and washed with PBS, and then they were fixed overnight in ice-cold 70% ethanol at −20°C. Next, the cells were resuspended in PBS, incubated with 100 μL RNase at 37 °C for 30 min, and stained with 400 μL PI(Solarbio, Cat#CA1510) at 4 °C for 30 min in the dark prior before flow cytometer analysis.

2.5 RNA-seq

After drug treatments, the Total RNA of each group was extracted by TRIzol reagent. Then, RNA sequencing was performed, and its data was analyzed by the Annaroad Gene Technology (Shanghai, China) Co., Ltd.

2.6 RT PCR

The total RNA of the cells was extracted using TRIzol, and RNA was eluted with RNase-free water and quantified at an absorbance of 260/280 nm. Then cDNA was synthesized by using HiFiScript gDNA Removal cDNA Synthesis Kit (Cwbio, Cat#CW 2020). Real-time PCR was performed in an optional 96-well plate with ABI7500 system and a commercial MagicSYBR mixture kit (Cwbio, Cat#CW3008M), according to the manufacturer's instructions. GAPDH was used as an endogenous control.

2.7 Western blot

The cells were collected and lysed on ice by RIPA (Solarbio, Cat#R0010) lysis buffer containing 1% PMSF. Protein concentration was determined by BCA protein assay kit (Beyotime, Cat#ST2222). 30 μg of total lysate protein sample was separated by SDS-PAGE (Shanghai Epizyme Biomedical Technology Co., Ltd, Cat#PG114) and transferred onto the NC membrane (Merck, Cat#HATF02500). Then membranes were incubated overnight at 4 °C with primary antibodies. Membranes were washed with Western washing buffer triplicates at room temperature and then incubated with secondary antibody for 1 h at room temperature. Membranes were rewashed with Western washing buffer triplicates at room temperature, and results were acquired using the Gel Logic 1,500 imaging system. *GAPDH* was used as the loading control.

2.8 Reactive oxygen species assay

The collected cell suspension was centrifuged at 250 g for 5 min and washed twice with PBS. Dilute DCFH-DA with serum-free culture medium at 1:1,000 to a final concentration of 10 μmol/L, add 1 mL of DCFH-DA (Beyotime, Cat#S0033M) dilution to each tube, and incubate in a 37°C cell culture incubator for 20 min. Next, the cells were washed three times with a serum-free cell culture medium to remove DCFH-DA that did not enter the cells fully. After loading the probes in the positive control group, dilute ROS-up with the serum-free medium at a ratio of 1:1,000 to make ROS-up dilution, add 1 mL of ROS-up dilution to the positive control, and incubate in a cell culture box at 37°C for 30 min. Cells were washed three times with serum cell culture medium. After washing once with pre-cooled PBS, the cell pellet was resuspended with 1 mL of PBS and immediately detected using a FACSCanto II flow cytometer according to the manufacturer's instructions. Flow cytometry results were analyzed with the software FlowJo.

2.9 Statistical analysis

Numerical data were expressed as mean ± SD, and statistical analyses were performed using unpaired *t*-test by SPSS 26.0 software. $P < 0.05$ was considered to be statistically significant.

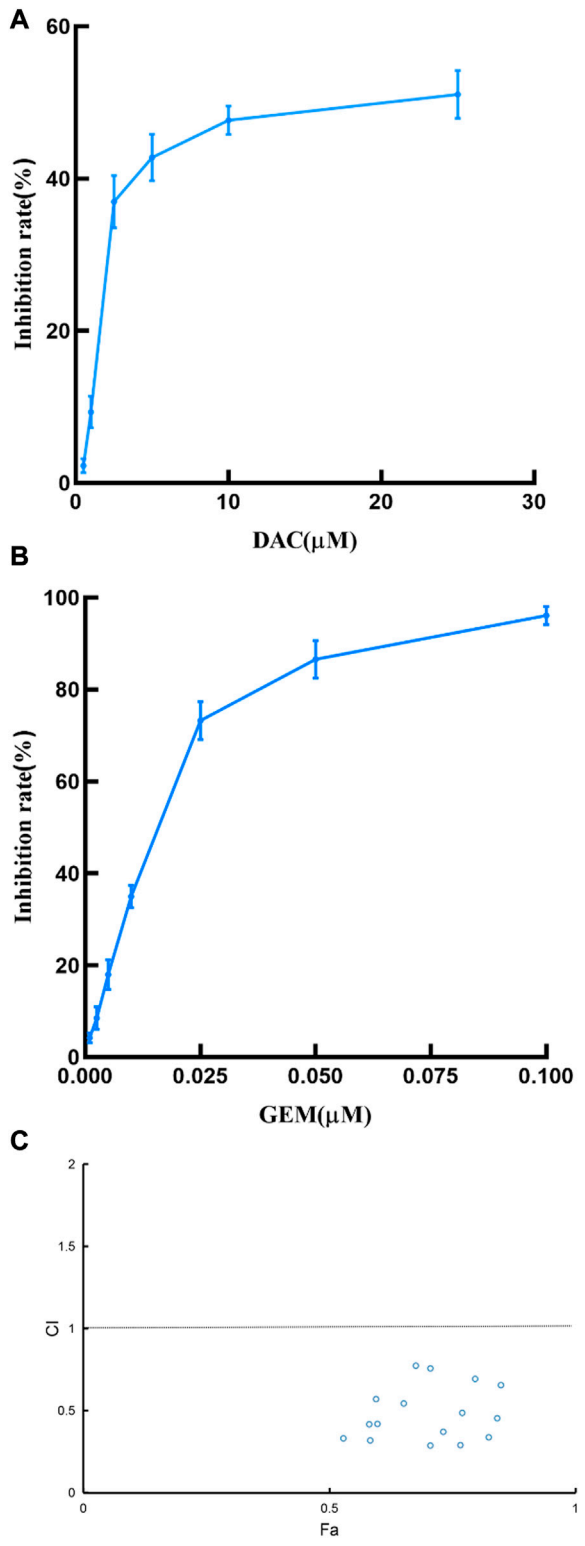

FIGURE 1
Effects of DAC and GEM on NK92MI cell viability and confirmation of the best combination of DAC and GEM. **(A)** Effects of DAC on cell growth in NK92MI cell lines. **(B)** Effects of GEM on cell growth in NK92MI cell lines. **(C)** CI plots of DAC and GEM combinations in NK92MI cells. The combination index was estimated using Compusyn software. CI < 1 indicates synergy; CI = 1 indicates an additive effect; CI > 1 indicates antagonism.

TABLE 1 IC10, 1C20, and IC30 of DAC and GEM in NK92MI cells.

Inhibition rate	DAC (μM)	GEM (μM)
IC10	1.603	0.005
IC20	2.100	0.007
IC30	4.046	0.010

3 Results

3.1 The combination of DAC and GEM showed synergistic inhibition of cell viability on NK92MI cells

We first determined the inhibition of cell viability of DAC and GEM on the EBV-positive lymphoma cell line NK92MI cells separately. NK92MI cells were treated with DAC and GEM gradient concentrations for 48 h. Both DAC and GEM exhibited dose-dependent proliferation inhibitory effects on NK92MI cells (Figures 1A, B). Next, the IC10, IC20, and IC30 values were calculated for DAC and GEM (Table 1). We performed a 48-h cross-combination of DAC and GEM in NK92MI cells with IC10, IC20, and IC30. The combination index (CI) values were under one in all groups (Table 2; Figure 1C). As expected, the combination caused a significant reduction in cell growth compared to drugs alone. For further experiments, we selected the pairing with the lowest CI value, representing the highest synergistic efficiency (Section 3.5).

3.2 The combination of DAC and GEM significantly promotes apoptosis in NK92MI cells

We performed a flow cytometric analysis on the intervened cells to confirm whether DAC and GEM promote apoptosis. We incubated the cells for 48 h under the following conditions: 4.046 μM DAC, 0.005 μM GEM, 4.046 μM DAC+ 0.005 μM GEM. The apoptosis rate of the control group was 6.76% ± 1.54%, the DAC group was 8.74% ± 1.53%, the GEM group was 7.72% ± 0.28%, and the combined was 24.57% ± 0.42%. The apoptosis rate was increased in the group DAC + GEM than DAC group ($p < 0.05$) or GEM group ($p < 0.05$) (Figures 2A, B). In addition, the western blot demonstrated that caspase3, an apoptosis-associated marker, was increased by DAC, GEM, and DAC-GEM. A significant increase in expression was observed in the combined group (Figure 2C). These results show that DAC can synergistically induce apoptosis in EBV-positive lymphoma NK92MI cells with GEM.

3.3 The combination of DAC and GEM induces arrest in the S phase of EBV-positive lymphoma cells

We treated NK92MI cells in the same group as before for 48 h and then measured the cell cycle by flow cytometry. We found that

TABLE 2 Proliferation inhibition rate or combination index of NK92MI cells treated with different concentrations of DAC and GEM.

DAC (μM)	GEM(μM)	Inhibition rate (%)	Combination index
1.603	0.005	54.33 ± 1.06	0.379 ± 0.039
1.603	0.007	57.16 ± 2.44	0.474 ± 0.041
1.603	0.010	58.80 ± 2.12	0.631 ± 0.045
2.100	0.005	60.07 ± 1.53	0.361 ± 0.039
2.100	0.007	61.13 ± 3.19	0.457 ± 0.033
2.100	0.010	64.90 ± 1.20	0.592 ± 0.036
4.046	0.005	72.09 ± 1.43	0.322 ± 0.030
4.046	0.007	74.74 ± 2.76	0.389 ± 0.033
4.046	0.010	76.99 ± 1.92	0.510 ± 0.046

the proportion of cells in the S phase in the combined DAC and GEM group (72.82 + 3.09)% was significantly higher than that in the DAC (40.35 + 2.93)% and GEM (36.86 + 0.84%) alone groups. Compared with the control group (31.40 + 1.48%), the proportion of S phase cells increased regardless of whether the drug was used alone or in combination (Figures 3A, B). The results showed that DAC plus GEM could block the cell cycle progression of EBV-positive lymphoma cells NK92MI in the S phase and reduce the cells in the proliferative phase.

3.4 Combination of DAC and GEM induced transcriptome level changes

To assess gene expression changes mediated by different treatments, we performed transcriptome sequencing on the control group, the DAC group, the GEM group, and DAC plus GEM groups using RNA-seq technology. Compared with the control group, NK92MI cells treated with DAC and GEM showed 2,382 gene expression changes, of which 2,142 were upregulated and 240 were downregulated. There were 235 gene expression changes between the DAC group and the combination group, of which 149 genes were upregulated and 86 genes were down-regulated. A total of 2,204 genes were induced by DAC plus GEM compared with the GEM group, with 2,056 genes being upregulated and 148 genes being downregulated. The results indicate that DAC was the primary mediator of the changes in gene expression profiles caused by the use of both drugs (Figure 4).

As a next step, we utilized Venn diagrams to visualize the number of differentially expressed genes (DEGs) in the combined group compared with the single and control groups. Based on the analysis results, 186 differentially expressed genes were significantly altered when the DAC and GEM were connected (Figure 5A). Then we performed pathway enrichment analyses comparing DEGs between DAC, GEM, and DAC plus GEM treated cells using the well-annotated reactome and Kyoto Encyclopedia of Genes and Genomes (KEGG) databases. Compared to the other three groups, the DEGs were primarily enriched in signaling pathways related to cell proliferation, adhesion, and migration in the combination treatment (Figure 5B). Such as Focal adhesion, PI3K Akt signaling pathway, and Rap1 signaling pathway. Using PPI network analysis, we investigated the interaction between DEGs by analyzing their interactions. The networks formed by DEGs mainly regulate metabolic pathways and cell proliferation and migration pathways (Figure 5C). For further investigation, we selected molecules with high node expression and high relative expressions in 186 DEGs for validation, such as HMOX1 and SLC7A11.

3.5 The possible mechanism of the combined application of DAC and GEM to inhibit cell viability

We also chose *BRLF1* as an additional observation in order to judge whether the EBV lytic state should be activated. After treatment with the indicated dose of DAC and GEM alone or in combination, *BRLF1* mRNA expression was by RT-PCR in NK92MI cells. The combination of DAC and GEM induced the expression of *BRLF1*. This combination may break the viral latency (Figure 6A).

RT-PCR and Western Blot experiments were performed on HMOX1 and SLC7A11 to study the mechanism of action of DAC and GEM combined to inhibit cell proliferation. The results showed that the combined treatment of DAC and GEM with NK92MI cells induced the expression of HMOX1 at the mRNA level ($p < 0.05$) and protein level and inhibited the expression of SLC7A11 at the mRNA level ($p < 0.05$) and protein level (Figures 6B, C, E). Based on these results, it is possible that DAC + GEM may influence the changes in ferroptosis-related molecules. GPX4 is crucial in regulating ferroptosis, and SLC7A11 serves as its upstream mediator. To explore whether the proliferation inhibition induced by the combined application of DAC and GEM is associated with ferroptosis-related genes in NK92MI cells, we further investigated the protein and mRNA levels of GPX4. There was no significant difference in GPX4 mRNA levels between the single and control groups (Figure 6D); however, the protein expression of GPX4 was decreased (Figure 6E). The primers used in the study are listed in Table 3.

TABLE 3 Primer sequences used for RT-PCR detection.

Primer name	Sequence (5′–3′)
GAPDH-F	TGACAACTTTGGTATCGTGGAAGGAC
GAPDH-R	GTGTCGCTGTTGAAGTCAGAGGAG
BRLF-F	GAGTCCATGACAGAGGATTTGA
BRLF-R	GCAGCAGACATTCATCATTTAGA
HMOX1-F	AAGACTGCGTTCCTGCTCAAC
HMOX1-R	AAAGCCCTACAGCAACTGTCG
SLC7A11-F	ACCTTTTCTGAGCGGCTACT
SLC7A11-R	CCCTCTCGAGACGCAACATA
GPX4-F	ATACGCTGAGTGTGGTTTGC
GPX4-R	CTTCATCCACTTCCACAGCG

3.6 The combined application of DAC and GEM increases the ROS level of NK92MI cells

As a result of an increase in reactive oxygen species (ROS) related to iron, lipid peroxidation occurs, which impairs cellular function and ultimately results in ferroptosis. Therefore, we examined ROS levels in four groups using flow cytometry. The mean fluorescence intensities of each group were: the control group was 7.9×10^6, the DAC group was 10.7×10^6, the GEM group was 12.7×10^6, and the combination group was 14.1×10^6 (Figures 6F, G). The results showed that ROS levels in NK92MI cells were significantly elevated after the combined treatment of DAC and GEM($p < 0.05$).

4 Discussion

EBV is a "kiss virus" that spreads mainly through the respiratory tract in humans. About 95% of the population have been infected in childhood and carried it in a latent state for life. In immunocompromised patients, EBV activates B cells and leads to the malignant proliferation of B cells to trigger monoclonal or polyclonal lymphoproliferative disorders or EBV-related malignancies. Studies have shown that LMP1 and LMP2 can be detected in 30%–45% of human lymphoma cells (Ramos et al., 2016). Previous clinical trials found that lymphoma patients with EBV usually have a high probability of extranodal involvement, advanced stage, older age, and higher risk (Beltran et al., 2011; Ok et al., 2014; Witte et al., 2020).

NK/T-cell lymphoma is a non-Hodgkin's lymphoma with prominent geographical characteristics. It is more common in Asians and Latin Americans to develop NK/T-cell lymphoma, especially in patients with EBV positivity. The disease is characterized by a high degree of malignancy, extreme aggressiveness, rapid progression, and high recurrence rates. At present, there is no standard treatment for NK/T cell lymphoma, and asparaginase and gemcitabine are usually used as primary chemotherapy agents. However, the prognosis of this disease is inferior due to the emergence of drug resistance in many patients. Therefore therapeutic regimens targeting both the EBV virus and lymphoma cells are needed.

DAC is a highly efficient inhibitor of DNA methyltransferase. DAC can induce self-renewal of normal hematopoietic stem cells, which has excellent potential for treating hematological diseases (Pinto et al., 1984; Hu et al., 2010). Zhang et al. reported a phase 1/2 and biomarker study on the Effect of DAC combination with R-CHOP in patients with diffuse large B cell lymphoma; 76.6% of patients achieved complete remission, and 12.2% of patients achieved partial remission (Zhang et al., 2021). GEM is an antimetabolite drug targeting specific stages of the cell cycle. It promotes the death of tumor cells with cytotoxicity and is widely used in clinical practice. Chen et al. (2021) demonstrated that Gem and thymosin alpha one combined suppressed NNKTL progression *in vivo* and *in vitro*. A therapeutic strategy for NNKTL could potentially be used in clinical practice due to their study. According to research reports, GEM combined with cisplatin and dexamethasone has a good effect in treating refractory non-Hodgkin lymphoma, with an overall response rate of 56.4% and an overall response rate of 72.8% in the treatment of refractory Hodgkin lymphoma (Mi et al., 2020). The above studies show that GEM can safely and effectively improve anti-tumor efficiency when combined with other drugs. In addition, GEM can induce EBV from a latent state to a lytic state, improving tumor cells' sensitivity to antiviral therapy (Feng et al., 2004; Wildeman et al., 2012; Chen et al., 2021).

Few studies have combined low doses of DAC and GEM. Clouser et al. found that low doses potently inhibited HIV-1 replication *in vitro* and can inhibit the progression of the disease *in vivo* (Clouser et al., 2012). Valdez et al. designed a safe and effective pretreatment protocol for hematopoietic stem cell transplantation. Combining busulfan, melphalan, GEM and DAC inhibited lymphoma cell growth. Additionally, a recent study demonstrated that the combination of DAC and GEM inhibited osteosarcoma cell proliferation and retarded tumor growth (Gutierrez et al., 2022). We studied DAC and GEM's *in vitro* antiproliferative effects on NK92MI. We demonstrated that DAC and GEM single-drugs are effective against the growth of NK92MI cells in dose-dependent manners. The combined drug effect was better than the single. In tumor cells, ROS accumulation is a double-edged sword; a slight increase in ROS promotes tumor cell proliferation, while an excessive increase can lead to cancer cell death. It is important to note that apoptosis is one of the most common methods of cell death. Apoptosis is divided into intrinsic, extrinsic, and perforin/granzyme pathways (Romero et al., 2015). Induced by intracellular stress, apoptosis is primarily initiated *via* the intrinsic pathway. The mitochondrial outer membrane is altered by ROS accumulation, releasing cytochrome C and activating caspase-9 in the apoptotic body. This causes caspase-3 to be activated, which is the ultimate executor of apoptosis (Ashkenazi and Dixit, 1998). Our study first demonstrated that the combination of DAC and GEM could effectively inhibit the proliferation of NK92MI cells, increase ROS accumulation, increase caspase3 protein level, promote cell apoptosis, and induce an S phase arrest. These results showed that the apoptotic process induced the combination by upregulating caspase3. However, the effects of DAC plus GEM on anti-proliferation may not only depend on apoptosis.

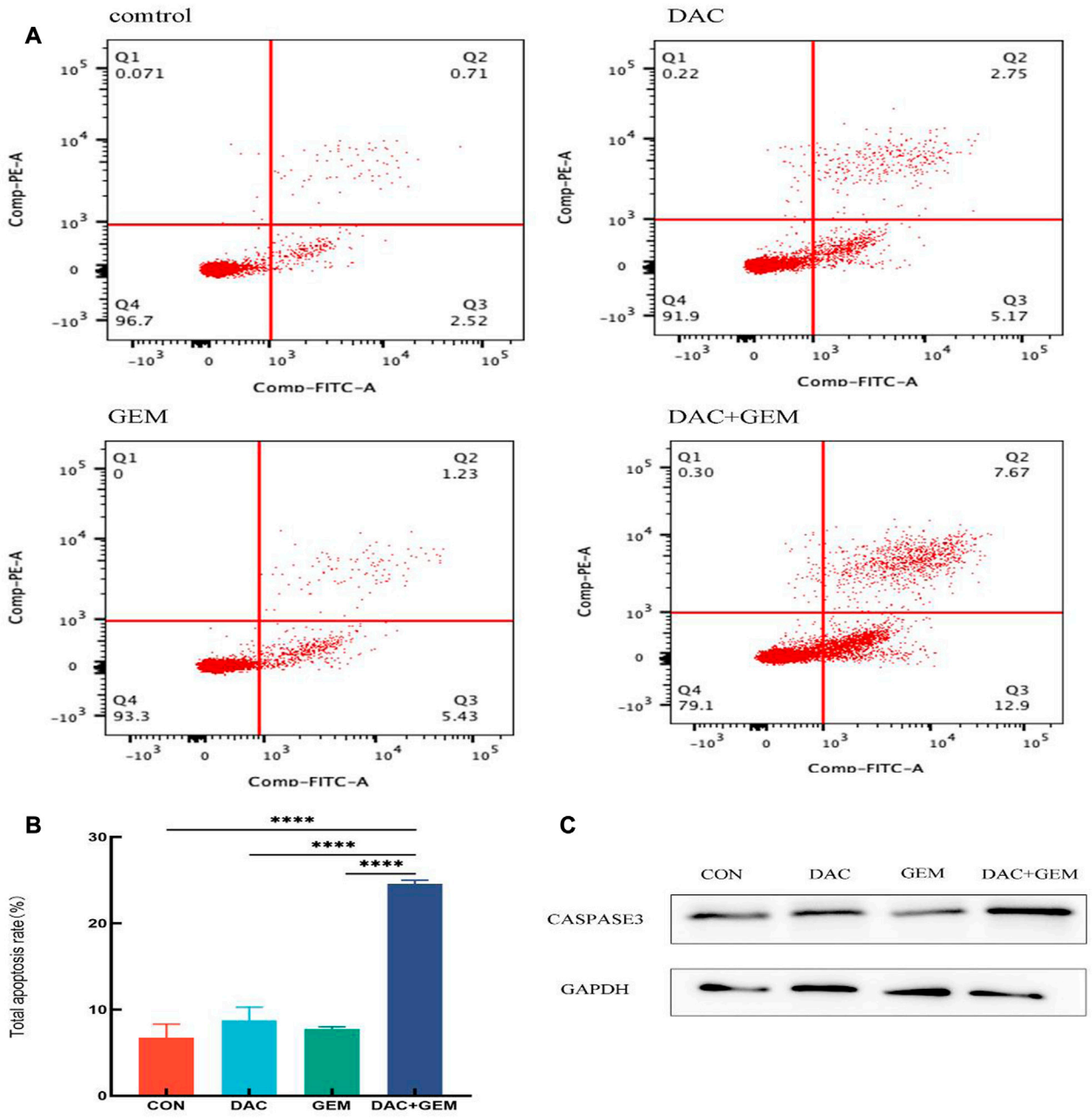

FIGURE 2
The combination of DAC with 4.046 μM and GEM with 0.005 μM significantly promotes apoptosis in NK92MI cells. **(A, B)** Cell apoptosis assay in NK92MI cells treated with the indicated dose of DAC and GEM alone or in combination. **(C)** After treating with the indicated dose of DAC and GEM alone or in combination, Caspase-3 protein expression was immunoblotted in NK92MI cells. *$p < 0.05$, **$p < 0.01$, ***$p < 0.001$ versus control group and alone group.

After initial infection, the virus establishes latency predominantly in B cells and cannot be cleared up. A persistent state of latent infection is closely associated with malignancies of human epithelial cell origin and lymphocytic origin. However, the viral latency is disrupted if external stimuli infect cells. And then, the virus enters a lytic state (Munz, 2019; Rosemarie and Sugden, 2020; Munz, 2021). Our study found that the combination group increased *BRLF1* expression in NK92MI cells compared to the single group. As is well known, EBV lytic activation is closely correlated with the expression of two EBV immediate early genes *BRLF1*, and *BZLF1*. Based on the study's results, it appears that the combination of DAC and GEM may induce replicative lysis of EBV in the NK92MI cell line.

Following this, we investigated other mechanisms of DAC and GEM's antiproliferative effects on NK92MI. In this experiment, we investigated the gene expression levels between the single and

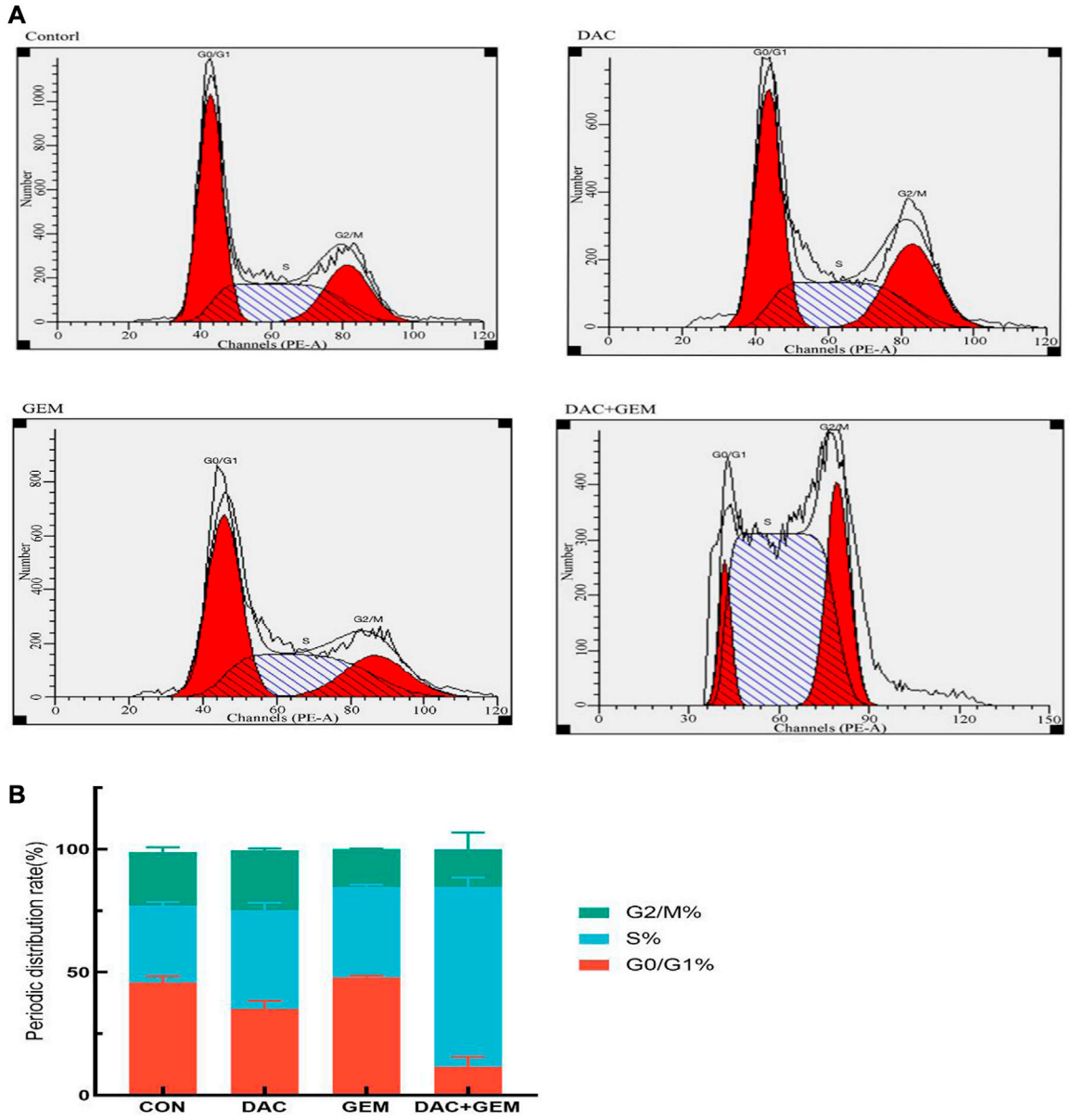

FIGURE 3
The cell cycle distribution of NK92MI cells after 48-h exposure to DAC and GEM. **(A, B)** The proportion of NK92MI cells in the S phase in the combination of DAC with 4.046 μM and GEM with 0.005 μM was significantly higher.

combination groups after 48 h of nk92mi cell treatment using whole gene transcriptome sequencing. A total of 186 differential genes were screened when the combined group was compared with the single and control groups. HMOX1 and SLC7A11 were found to be responsive to the combinations of DAC and GEM by KEGG enrichment analysis and PPI network analysis. Compared to the single and control groups, the combination group increased the expression of HMOX1 and decreased the expression of SLC7A11 at mRNA and protein levels. HMOX1 is a rate-limiting enzyme in the metabolism of the iron porphyrin compound heme catabolism, which breaks down heme to carbon monoxide, biliverdin, and Fe^{2+}. HMOX1 expression is mainly induced by its heam, iron, oxidative stress, and inflammation (Chang et al., 2015). HMOX1 is vital in maintaining iron homeostasis and protecting cells from oxidative damage. It has been shown that adequate levels of HMOX1 can act as antioxidants and prevent cell oxidative damage (Kim et al., 2012). Chang et al. (2015) indicated that treatment with DNA methylation transferase inhibitors significantly increased the expression of HMOX1 mRNA (Sung et al., 2016). In the present study, we observed an increased expression of HMOX1 in the DAC-alone group compared to the control group. The expression of HMOX1 was significantly increased in the combined DAC and GEM group compared with the control group and the drug-alone group. This phenomenon may

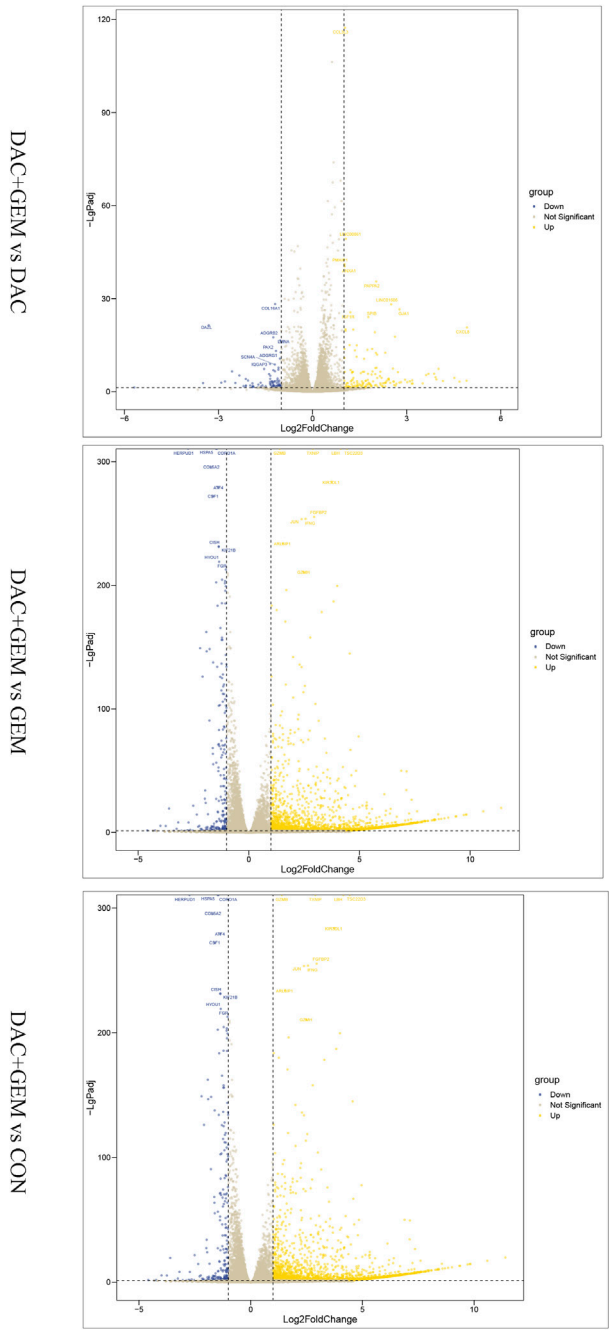

FIGURE 4
Combination of DAC and GEM induced transcriptome level changes. After treatment with the indicated dose of DAC and GEM alone or in combination, a volcano plot of differentially expressed genes in the combination group was compared with each single drug group or control group in NK92MI cells.

be caused by DAC's inhibitory effect on methylation, which was amplified by the combination with GEM. However, overexpression of HMOX1 and Fe^{2+} accumulation and ROS accumulation exert a role in inducing cellular ferroptosis. In ferroptosis, there is an imbalance of intracellular iron and depletion of glutathione, resulting in the accumulation of ROS and lipid peroxidation.

Although ROS is not a specific indicator of ferroptosis, ROS plays an important role in ferroptosis. Kong et al. (2019) observed an increase in Fe and an increase in ROS after the artesunate treatment of hepatic stellate cells in a study of liver fibrosis in mice treated with artesunate. In a study on paraquat + maneb-induced dopaminergic neurodegeneration, NADPH oxidase was found to be involved in ferroptosis. When NOX was inhibited with NADPH oxidase, cellular GSH and GPX4 levels were restored, and ferroptosis was reduced (Hou et al., 2019). DAC caused ROS accumulation in leukemia cells but not in solid tumor cells, thereby promoting leukemic cell death (Fandy et al., 2014; Jain et al., 2017). Our study also showed that the combination induced an increase in ROS levels. It is well known that SLC7A11 and GPX4 are critical molecules in ferroptosis. GPX4 is the core enzyme regulating the glutathione system of the endogenous antioxidant system, and inhibition of GPX4 activity leads to ROS overload, disrupting cell membranes and thus inducing ferroptosis (Dixon et al., 2012). The efficiency of cysteine transport directly affects glutathione synthesis, and its main depends mainly on the cystine/glutamate reverse transporter protein in the cell membrane. SLC7A11, an essential part of the cystine/glutamate reverse transporter protein, is a negative ferroptosis regulator. SLC7A11 downregulation affects glutathione synthesis's inhibition, leading to GPX4 downregulation, cellular ROS accumulation, and ultimately oxidative damage and ferroptosis.

Interestingly, this study's protein level of GPX4 was down-regulated, but the mRNA level did not change significantly. The combination caused the downregulation of GPX4 and SLC7A11, leading to an overload of ROS, which induced the expression of HMOX1. The recent discovery that early transformed stages of EBV and Burkitt's lymphoma cells trigger ferroptosis suggests that ferroptosis may be therapeutically beneficial in treating EBV-positive lymphomas (Burton et al., 2022). This may be another reason why this combination inhibited cell growth proliferation.

In conclusion, the combination of DAC and GEM has synergistic effects for cell viability inhibition in NK92MI cells through apoptosis and ferroptosis. Although the combination of DAC and GEM has mediated many forms of anti-proliferation, more research is needed to determine which form is critical. Our study has some limitations. First of all, our study mainly discussed the inhibitory effect of DAC + GEM on the proliferation of NK92MI cells *in vitro* and did not observe the effect *in vivo*. The construction of a xenograft mouse model is of great significance for exploring the inhibition of tumor cells by DAC + GEM *in vivo*. In particular, the construction of PDX models can more truly reflect the original characteristics of tumors and more accurately reflect the drug sensitivity and tolerance of tumor patients. Secondly, although this study suggests that DAC + GEM may inhibit the proliferation of NK/T-cell lymphoma cells through apoptosis or ferroptosis, we still need more evidence to prove whether these two mechanisms play a major inhibitory role or play a joint inhibitory role. This study demonstrates that the combination of DAC and GEM is promising for inhibiting NK/T cell lymphoma cells and provides new ideas for the clinical treatment of NK/T cell lymphoma.

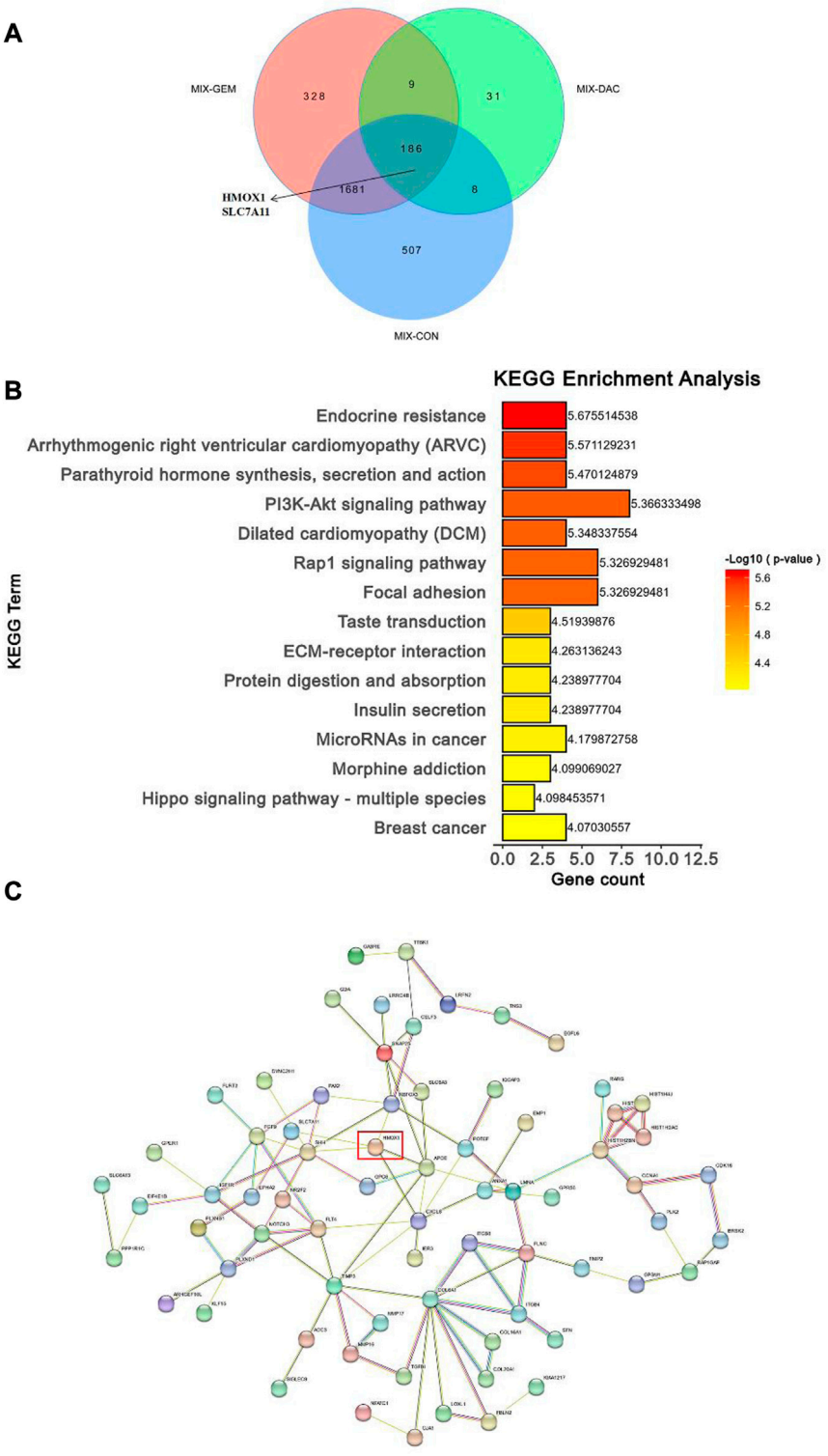

FIGURE 5
Combination of DAC and GEM induced transcriptome level changes. **(A)** The Venn diagrams showed the DEGs in the combination group when compared with each single drug group and control group in NK92MI cells. **(B)** The primary signal transduction pathways of DEGs in the combination group compared with each single drug group and control group in NK92MI cells. **(C)** The protein-protein interaction network topology analysis of DEGs in the combination group compared with each single drug group and control group in NK92MI cells.

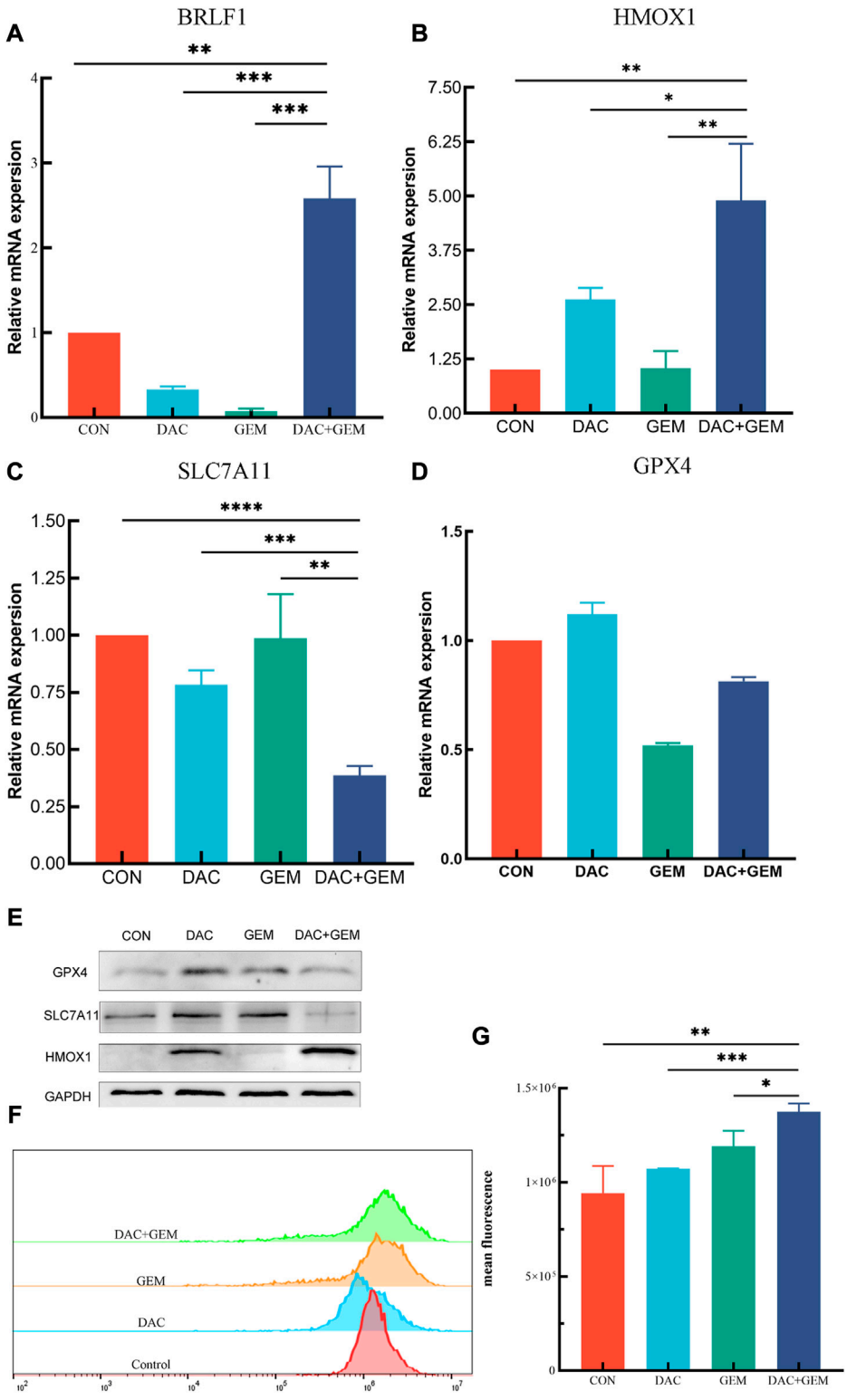

FIGURE 6
Combined treatment of DAC and GEM assists ferroptosis. **(A)** After treating with the indicated dose of DAC and GEM alone or in combination, BRLF1 mRNA expression was quantified by RT-PCR in NK92MI cells. **(B)** After treating with the indicated dose of DAC and GEM alone or in combination, HMOX1 mRNA expression was quantified by RT-PCR in NK92MI cells. **(C)** After treating with the indicated dose of DAC and GEM alone or in combination, SAL7A11 mRNA expression was quantified by RT-PCR in NK92MI cells. **(D)** After treating with the indicated dose of DAC and GEM alone or in combination, GPX4 mRNA expression was quantified by RT-PCR in NK92MI cells. **(E)** After treatment with the indicated dose of DAC and GEM alone or in combination, HMOX1, SAL7A11, and GPX4 protein expression were immunoblotted in NK92MI cells. **(F, G)** The effects of DAC and GEM on regulating ROS level in NK92MI cells. *$p < 0.05$, **$p < 0.01$, ***$p < 0.001$ versus control group and alone group.

Data availability statement

The raw data generated in this study have been deposited in the SRA database (https://www.ncbi.nlm.nih.gov/sra), under the accession numbers SRR23620573, SRR23620567, SRR23620568, SRR23620570, SRR23620575, SRR23620572, SRR23620569, SRR23620571, SRR23620574, SRR23620577, SRR23620576, SRR23620566.

Author contributions

LKL, HY and XQL: Experiment, data curation, writing—Original draft preparation. HD and KP: Providing experimental guidance. JC and TJ: Supervision and language polishment. CLZ, TJ and XQL: Conceptualization and manuscript revision.

Funding

This work was supported by the National Natural Science Foundation of China (82070930), the Sichuan Science and Technology Program (2022YFS0022, 2023YFS0308), the Chengdu Science & Technology Bureau (2021-YF05-02398-SN), Medico-Engineering Cooperation Funds from University of Electronic Science and Technology of China (ZYGX2021YGLH020) and the Foundation of Sichuan Medical Association (Q16069), Department of Science and Technology of Sichuan Provincial People's Hospital(2017LY15 and 2021LY07).

Conflict of interest

The authors declare that the research was conducted in the absence of any commercial or financial relationships that could be construed as a potential conflict of interest.

Publisher's note

All claims expressed in this article are solely those of the authors and do not necessarily represent those of their affiliated organizations, or those of the publisher, the editors and the reviewers. Any product that may be evaluated in this article, or claim that may be made by its manufacturer, is not guaranteed or endorsed by the publisher.

References

Abdel-Rahman, O., Elsayed, Z., and Elhalawani, H. (2018). Gemcitabine-based chemotherapy for advanced biliary tract carcinomas. *Cochrane Database Syst. Rev.* 4, CD011746. doi:10.1002/14651858.CD011746.pub2

Ashkenazi, A., and Dixit, V. M. (1998). Death receptors: Signaling and modulation. *Science* 281 (5381), 1305–1308. doi:10.1126/science.281.5381.1305

Beltran, B. E., Castillo, J. J., Morales, D., de Mendoza, F. H., Quinones, P., Miranda, R. N., et al. (2011). EBV-Positive diffuse large B-cell lymphoma of the elderly: A case series from Peru. *Am. J. Hematol.* 86 (8), 663–667. doi:10.1002/ajh.22078

Burton, E. M., Voyer, J., and Gewurz, B. E. (2022). Epstein-Barr virus latency programs dynamically sensitize B cells to ferroptosis. *Proc. Natl. Acad. Sci. U. S. A.* 119 (11), e2118300119. doi:10.1073/pnas.2118300119

Chang, M., Xue, J., Sharma, V., and Habtezion, A. (2015). Protective role of hemeoxygenase-1 in gastrointestinal diseases. *Cell. Mol. Life Sci.* 72 (6), 1161–1173. doi:10.1007/s00018-014-1790-1

Chen, M., Jiang, Y., Cai, X., Lu, X., and Chao, H. (2021). Combination of Gemcitabine and Thymosin alpha 1 exhibit a better anti-tumor effect on nasal natural killer/T-cell lymphoma. *Int. Immunopharmacol.* 98, 107829. doi:10.1016/j.intimp.2021.107829

Clouser, C. L., Holtz, C. M., Mullett, M., Crankshaw, D. L., Briggs, J. E., O'Sullivan, M. G., et al. (2012). Activity of a novel combined antiretroviral therapy of gemcitabine and decitabine in a mouse model for HIV-1. *Antimicrob. Agents Chemother.* 56 (4), 1942–1948. doi:10.1128/AAC.06161-11

Cruz, C. R., Gerdemann, U., Leen, A. M., Shafer, J. A., Ku, S., Tzou, B., et al. (2011). Improving T-cell therapy for relapsed EBV-negative Hodgkin lymphoma by targeting upregulated MAGE-A4. *Clin. Cancer Res.* 17 (22), 7058–7066. doi:10.1158/1078-0432.CCR-11-1873

Dalton, T., Doubrovina, E., Pankov, D., Reynolds, R., Scholze, H., Selvakumar, A., et al. (2020). Epigenetic reprogramming sensitizes immunologically silent EBV+ lymphomas to virus-directed immunotherapy. *Blood* 135 (21), 1870–1881. doi:10.1182/blood.2019004126

Dixon, S. J., Lemberg, K. M., Lamprecht, M. R., Skouta, R., Zaitsev, E. M., Gleason, C. E., et al. (2012). Ferroptosis: An iron-dependent form of nonapoptotic cell death. *Cell.* 149 (5), 1060–1072. doi:10.1016/j.cell.2012.03.042

Dong, L. H., Zhang, L. J., Wang, W. J., Lei, W., Sun, X., Du, J. W., et al. (2016). Sequential DICE combined with l-asparaginase chemotherapy followed by involved field radiation in newly diagnosed, stage IE to IIE, nasal and extranodal NK/T-cell lymphoma. *Leuk. Lymphoma* 57 (7), 1600–1606. doi:10.3109/10428194.2015.1108415

Fandy, T. E., Jiemjit, A., Thakar, M., Rhoden, P., Suarez, L., and Gore, S. D. (2014). Decitabine induces delayed reactive oxygen species (ROS) accumulation in leukemia cells and induces the expression of ROS generating enzymes. *Clin. Cancer Res.* 20 (5), 1249–1258. doi:10.1158/1078-0432.CCR-13-1453

Feng, W. H., Hong, G., Delecluse, H. J., and Kenney, S. C. (2004). Lytic induction therapy for Epstein-Barr virus-positive B-cell lymphomas. *J. Virol.* 78 (4), 1893–1902. doi:10.1128/jvi.78.4.1893-1902.2004

Gao, L., Zhang, Y., Wang, S., Kong, P., Su, Y., Hu, J., et al. (2020). Effect of rhG-CSF combined with decitabine prophylaxis on relapse of patients with high-risk MRD-negative AML after HSCT: An open-label, multicenter, randomized controlled trial. *J. Clin. Oncol.* 38 (36), 4249–4259. doi:10.1200/JCO.19.03277

Gesto, D. S., Cerqueira, N. M., Fernandes, P. A., and Ramos, M. J. (2012). Gemcitabine: A critical nucleoside for cancer therapy. *Curr. Med. Chem.* 19 (7), 1076–1087. doi:10.2174/092986712799320682

Gutierrez, W. R., Scherer, A., Rytlewski, J. D., Laverty, E. A., Sheehan, A. P., McGivney, G. R., et al. (2022). Augmenting chemotherapy with low-dose decitabine through an immune-independent mechanism. *JCI Insight* 7, e159419. doi:10.1172/jci.insight.159419

Heslop, H. E., Slobod, K. S., Pule, M. A., Hale, G. A., Rousseau, A., Smith, C. A., et al. (2010). Long-term outcome of EBV-specific T-cell infusions to prevent or treat EBV-related lymphoproliferative disease in transplant recipients. *Blood* 115 (5), 925–935. doi:10.1182/blood-2009-08-239186

Hou, L., Huang, R., Sun, F., Zhang, L., and Wang, Q. (2019). NADPH oxidase regulates paraquat and maneb-induced dopaminergic neurodegeneration through ferroptosis. *Toxicology* 417, 64–73. doi:10.1016/j.tox.2019.02.011

Hu, Z., Negrotto, S., Gu, X., Mahfouz, R., Ng, K. P., Ebrahem, Q., et al. (2010). Decitabine maintains hematopoietic precursor self-renewal by preventing repression of stem cell genes by a differentiation-inducing stimulus. *Mol. Cancer Ther.* 9 (6), 1536–1543. doi:10.1158/1535-7163.MCT-10-0191

Jain, S., Washington, A., Leaf, R. K., Bhargava, P., Clark, R. A., Kupper, T. S., et al. (2017). Decitabine priming enhances mucin 1 inhibition mediated disruption of redox homeostasis in cutaneous T-cell lymphoma. *Mol. Cancer Ther.* 16 (10), 2304–2314. doi:10.1158/1535-7163.MCT-17-0060

Jiang, M., Zhang, H., Jiang, Y., Yang, Q., Xie, L., Liu, W., et al. (2012). Phase 2 trial of "sandwich" L-asparaginase, vincristine, and prednisone chemotherapy with radiotherapy in newly diagnosed, stage IE to IIE, nasal type, extranodal natural killer/T-cell lymphoma. *Cancer* 118 (13), 3294–3301. doi:10.1002/cncr.26629

Jones, R. J., Iempridee, T., Wang, X., Lee, H. C., Mertz, J. E., Kenney, S. C., et al. (2016). Lenalidomide, thalidomide, and pomalidomide reactivate the epstein-barr virus lytic cycle through phosphoinositide 3-kinase signaling and ikaros expression. *Clin. Cancer Res.* 22 (19), 4901–4912. doi:10.1158/1078-0432.CCR-15-2242

Kim, J., Zarjou, A., Traylor, A. M., Bolisetty, S., Jaimes, E. A., Hull, T. D., et al. (2012). *In vivo* regulation of the heme oxygenase-1 gene in humanized transgenic mice. *Kidney Int.* 82 (3), 278–291. doi:10.1038/ki.2012.102

Kishimoto, W., Takiuchi, Y., Nakae, Y., Tabata, S., Fukunaga, A., Matsuzaki, N., et al. (2019). A case of AITL complicated by EBV-positive B cell and monoclonal plasma cell

proliferation and effectively treated with lenalidomide. *Int. J. Hematol.* 109 (4), 499–504. doi:10.1007/s12185-018-02587-6

Kong, Z., Liu, R., and Cheng, Y. (2019). Artesunate alleviates liver fibrosis by regulating ferroptosis signaling pathway. *Biomed. Pharmacother.* 109, 2043–2053. doi:10.1016/j.biopha.2018.11.030

Kwong, Y. L., Kim, W. S., Lim, S. T., Kim, S. J., Tang, T., Tse, E., et al. (2012). SMILE for natural killer/T-cell lymphoma: Analysis of safety and efficacy from the asia lymphoma study group. *Blood* 120 (15), 2973–2980. doi:10.1182/blood-2012-05-431460

Liu, M. K., Sun, X. J., Gao, X. D., Qian, Y., Wang, L., and Zhao, W. L. (2021). Methylation alterations and advance of treatment in lymphoma. *Front. Biosci. Landmark Ed.* 26 (9), 602–613. doi:10.52586/4970

Mi, M., Zhang, C., Liu, Z., Wang, Y., Li, J., and Zhang, L. (2020). Gemcitabine, cisplatin, and dexamethasone and ifosfamide, carboplatin, and etoposide regimens have similar efficacy as salvage treatment for relapsed/refractory aggressive lymphoma: A retrospectively comparative study. *Med. Baltim.* 99 (49), e23412. doi:10.1097/MD.0000000000023412

Mini, E., Nobili, S., Caciagli, B., Landini, I., and Mazzei, T. (2006). Cellular pharmacology of gemcitabine. *Ann. Oncol.* 17 (5), v7–v12. doi:10.1093/annonc/mdj941

Munz, C. (2019). Latency and lytic replication in Epstein-Barr virus-associated oncogenesis. *Nat. Rev. Microbiol.* 17 (11), 691–700. doi:10.1038/s41579-019-0249-7

Munz, C. (2021). The role of lytic infection for lymphomagenesis of human gamma-herpesviruses. *Front. Cell. Infect. Microbiol.* 11, 605258. doi:10.3389/fcimb.2021.605258

Ok, C. Y., Li, L., Xu-Monette, Z. Y., Visco, C., Tzankov, A., Manyam, G. C., et al. (2014). Prevalence and clinical implications of epstein-barr virus infection in de novo diffuse large B-cell lymphoma in Western countries. *Clin. Cancer Res.* 20 (9), 2338–2349. doi:10.1158/1078-0432.CCR-13-3157

Oyama, T., Yamamoto, K., Asano, N., Oshiro, A., Suzuki, R., Kagami, Y., et al. (2007). Age-related EBV-associated B-cell lymphoproliferative disorders constitute a distinct clinicopathologic group: A study of 96 patients. *Clin. Cancer Res.* 13 (17), 5124–5132. doi:10.1158/1078-0432.CCR-06-2823

Patel, A. A., Cahill, K., Saygin, C., and Odenike, O. (2021). Cedazuridine/decitabine: From preclinical to clinical development in myeloid malignancies. *Blood Adv.* 5 (8), 2264–2271. doi:10.1182/bloodadvances.2020002929

Pinto, A., Attadia, V., Fusco, A., Ferrara, F., Spada, O. A., and Di Fiore, P. P. (1984). 5-Aza-2'-deoxycytidine induces terminal differentiation of leukemic blasts from patients with acute myeloid leukemias. *Blood* 64 (4), 922–929. doi:10.1182/blood.v64.4.922.922

Pope, J. H., Horne, M. K., and Scott, W. (1968). Transformation of foetal human keukocytes *in vitro* by filtrates of a human leukaemic cell line containing herpes-like virus. *Int. J. Cancer* 3 (6), 857–866. doi:10.1002/ijc.2910030619

Ramos, C. A., Heslop, H. E., and Brenner, M. K. (2016). CAR-T cell therapy for lymphoma. *Annu. Rev. Med.* 67, 165–183. doi:10.1146/annurev-med-051914-021702

Romero, A., Novoa, B., and Figueras, A. (2015). The complexity of apoptotic cell death in mollusks: An update. *Fish. Shellfish Immunol.* 46 (1), 79–87. doi:10.1016/j.fsi.2015.03.038

Rosemarie, Q., and Sugden, B. (2020). Epstein-Barr virus: How its lytic phase contributes to oncogenesis. *Microorganisms* 8 (11), 1824. doi:10.3390/microorganisms8111824

Seelan, R. S., Mukhopadhyay, P., Pisano, M. M., and Greene, R. M. (2018). Effects of 5-Aza-2'-deoxycytidine (decitabine) on gene expression. *Drug Metab. Rev.* 50 (2), 193–207. doi:10.1080/03602532.2018.1437446

Shannon-Lowe, C., Rickinson, A. B., and Bell, A. I. (2017). Epstein-Barr virus-associated lymphomas. *Philos. Trans. R. Soc. Lond B Biol. Sci.* 372 (1732), 20160271. doi:10.1098/rstb.2016.0271

Sung, H. Y., Choi, B. O., Jeong, J. H., Kong, K. A., Hwang, J., and Ahn, J. H. (2016). Amyloid beta-mediated hypomethylation of heme oxygenase 1 correlates with cognitive impairment in alzheimer's disease. *PLoS One* 11 (4), e0153156. doi:10.1371/journal.pone.0153156

Tse, E., and Kwong, Y. L. (2015). Nasal NK/T-cell lymphoma: RT, CT, or both. *Blood* 126 (12), 1400–1401. doi:10.1182/blood-2015-07-655191

Wang, L., Wang, Z. H., Chen, X. Q., Li, Y. J., Wang, K. F., Xia, Y. F., et al. (2013). First-line combination of gemcitabine, oxaliplatin, and L-asparaginase (GELOX) followed by involved-field radiation therapy for patients with stage IE/IIE extranodal natural killer/T-cell lymphoma. *Cancer* 119 (2), 348–355. doi:10.1002/cncr.27752

Wildeman, M. A., Novalic, Z., Verkuijlen, S. A., Juwana, H., Huitema, A. D., Tan, I. B., et al. (2012). Cytolytic virus activation therapy for Epstein-Barr virus-driven tumors. *Clin. Cancer Res.* 18 (18), 5061–5070. doi:10.1158/1078-0432.CCR-12-0574

Witte, H. M., Merz, H., Biersack, H., Bernard, V., Riecke, A., Gebauer, J., et al. (2020). Impact of treatment variability and clinicopathological characteristics on survival in patients with Epstein-Barr-Virus positive diffuse large B cell lymphoma. *Br. J. Haematol.* 189 (2), 257–268. doi:10.1111/bjh.16342

Wu, J., Li, Y., Wu, J., Song, H., Tang, Y., Yan, N., et al. (2021). Decitabine activates type I interferon signaling to inhibit p53-deficient myeloid malignant cells. *Clin. Transl. Med.* 11 (11), e593. doi:10.1002/ctm2.593

Xia, L., Zhang, H. S., Bao, J., Zhao, Y. C., and Xia, H. L. (2021). Successful outcome of programmed death 1 blockade plus GemOx for epstein-barr virus-associated primary nodal T/NK cell lymphoma: A case report. *Front. Oncol.* 11, 706865. doi:10.3389/fonc.2021.706865

Xie, Y., Liu, Y., Wen, C., Li, W., Lu, X., and Deng, L. (2021). Primary colon natural killer (NK)/T-cell lymphoma, nasal type, with perforations: A case report and literature review. *Ann. Palliat. Med.* 10 (11), 12025–12033. doi:10.21037/apm-21-3178

Xu, P. P., Xiong, J., Cheng, S., Zhao, X., Wang, C. F., Cai, G., et al. (2017). A phase II study of methotrexate, etoposide, dexamethasone and pegaspargase sandwiched with radiotherapy in the treatment of newly diagnosed, stage IE to IIE extranodal natural-killer/T-cell lymphoma, nasal-type. *EBioMedicine* 25, 41–49. doi:10.1016/j.ebiom.2017.10.011

Yamaguchi, M., Kita, K., Miwa, H., Nishii, K., Oka, K., Ohno, T., et al. (1995). Frequent expression of P-glycoprotein/MDR1 by nasal T-cell lymphoma cells. *Cancer* 76 (11), 2351–2356. doi:10.1002/1097-0142(19951201)76:11<2351::aid-cncr2820761125>3.0.co;2-1

Zhang, M. C., Fang, Y., Xu, P. P., Dong, L., Shen, R., Huang, Y. H., et al. (2021). Clinical efficacy and tumour microenvironment influence of decitabine plus R-CHOP in patients with newly diagnosed diffuse large B-Cell lymphoma: Phase 1/2 and biomarker study. *Clin. Transl. Med.* 11 (12), e584. doi:10.1002/ctm2.584

Zhang, Y., Chen, L., Hu, G. Q., Zhang, N., Zhu, X. D., Yang, K. Y., et al. (2022). Final overall survival analysis of gemcitabine and cisplatin induction chemotherapy in nasopharyngeal carcinoma: A multicenter, randomized phase III trial. *J. Clin. Oncol.* 40 (22), 2420–2425. doi:10.1200/JCO.22.00327

frontiers | Frontiers in Pharmacology

TYPE Review
PUBLISHED 30 March 2023
DOI 10.3389/fphar.2023.1177068

OPEN ACCESS

EDITED BY
Qin Wang,
Southwest Jiaotong University, China

REVIEWED BY
Sanjun Shi,
Chengdu University of Traditional Chinese Medicine, China
Zhi-Xiang Yuan,
Southwest Minzu University, China
Qing Lin,
Sichuan University, China

*CORRESPONDENCE
Yuxuan Zhu,
zhuyuxuan6688@163.com

†These authors contributed equally to this work

SPECIALTY SECTION
This article was submitted to Pharmacology of Anti-Cancer Drugs, a section of the journal Frontiers in Pharmacology

RECEIVED 01 March 2023
ACCEPTED 20 March 2023
PUBLISHED 30 March 2023

CITATION
Wang Y, Yang Y, Zheng X, Shi J, Zhong L, Duan X and Zhu Y (2023), Application of iron oxide nanoparticles in the diagnosis and treatment of leukemia.
Front. Pharmacol. 14:1177068.
doi: 10.3389/fphar.2023.1177068

Application of iron oxide nanoparticles in the diagnosis and treatment of leukemia

Yiling Wang†, Yan Yang†, Xi Zheng, Jianyou Shi, Lei Zhong, Xingmei Duan and Yuxuan Zhu*

Personalized Drug Therapy Key Laboratory of Sichuan Province, Sichuan Academy of Medical Science & Sichuan Provincial People's Hospital, University of Electronic Science and Technology of China, Chengdu, China

Leukemia is a malignancy initiated by uncontrolled proliferation of hematopoietic stem cell from the B and T lineages, resulting in destruction of hematopoietic system. The conventional leukemia treatments induce severe toxic and a long series of unwanted side-effects which are caused by lack of specificity of anti-leukemic drugs. Recently, nanotechnology have shown tremendous application and clinical impact with respect to diagnosis and treatment of leukemia. According to considerable researches in the context of finding new nanotechnological platform, iron oxide nanoparticles have been gained increasing attention for the leukemia patients use. In this review, a short introduction of leukemia is described followed by the evaluation of the current approaches of iron oxide nanoparticles applied in the leukemia detection and treatment. The enormous advantages of iron oxide nanoparticles for leukemia have been discussed, which consist of the detection of magnetic resonance imaging (MRI) as efficient contrast agents, magnetic biosensors and targeted delivery of anti-leukemia drugs by coating different targeting moieties. In addition, this paper will briefly describe the application of iron oxide nanoparticles in the combined treatment of leukemia. Finally, the shortcomings of the current applications of iron-based nanoparticles in leukemia diagnosis and treatment will be discussed in particular.

KEYWORDS

leukemia, iron oxide nanoparticles, magnetism, drug delivery, targeted therapy

1 Introduction

Leukemia is a tumor of the hematopoietic and lymphoid tissues. Clonal leukemia cells proliferate, accumulate and infiltrate in the bone marrow and other hematopoietic and non-hematopoietic tissues due to abnormal proliferation of differentiated hematopoietic stem cell or progenitor cells, thus affecting the physiological bone marrow of various tissues and organs. Siegel et al. (2019) Symptoms are usually characterized by bleeding, fever, immunosuppression, bone and joint pain, hepatosplenomegaly, and lymphadenopathy, these symptoms are caused by varying degrees of anemia, neutrophil, thrombocytopenia, or tissue infiltration. Chen and Zhou (2012) According to the progression of the disease, leukemia is mainly classified as acute and chronic, while leukemia is mainly classified as lymphoid and myeloid leukemia according to the origin of malignant proliferating cells. Alsalem et al. (2018) Current therapies of leukemia include chemotherapy, radiotherapy, targeted therapy and stem cell transplantation. Kadia et al. (2015) Although, many studies have shown that viruses, genetics, radiation and chemical toxins may cause leukemia, the cause of leukemia is still not a unified answer. Curtis et al. (1992); Lo et al. (2010); Winandy

et al. (1995) The other hand, the clinical characteristics of different types of leukemia are obviously different. Because of the limitation of the above factors, there is no uniform treatment of leukemia at present. Short et al. (2018).

Chemotherapy is the most common treatment for leukemia. Pant and Bhatt (2017) Chemotherapy drugs such as vinblastine, Cytarabine, Vindesine, daunorubicin, northromycin, doxorubicin, and mitoxantrone are often used. Single drug often leads to drug resistance, so combination therapies are used to treat leukemia in order to reduce even eliminate drug resistance. Kantarjian et al. (2010) The "3 + 7 regimen" proposed in the 1970s has become the cornerstone of induction chemotherapy for acute myeloid leukemia (AML), which can achieve a certain remission rate. However, for older patients with leukemia, this regimen can lead to up to 30% early treatment-related mortality and the survival rate is less than 10 percent in 3–5 years Gardin et al. (2020).

Radiotherapy is the treatment of malignant tumors with radionuclide alpha, beta, gamma radiation and X-ray, electron and proton beams produced by various X-ray therapy machines or accelerators. Walter (2022) Radiation inevitably exposes normal cells to ionizing radiation, so there is a risk that cancer may develop again during treatment. Bodet-Milin et al. (2016).

Targeted therapy, as one of the treatment modalities for leukemia, has three main therapeutic mechanisms: small molecule inhibitors that target gene mutations, inhibitors that target key signaling pathways, and antibodies or antibody-coupled drugs that target cell surface molecules. Newell and Cook (2021) Although great progress has been made in the treatment of leukemia with targeted therapy, there are still many problems. For example, treatment of leukemia with FLT 3 inhibitors alone, such as Gilteritinib, is less toxic than conventional chemotherapy, but resistance continues to develop in patients with certain gene mutations. Travis et al. (2000).

Currently, Hematopoietic stem cell transplantation (HSCT) is considered to be an effective treatment for leukemia. Ljungman et al. (2019) HSCT is to kill as many abnormal cells or tumor cells as possible through high-dose chemotherapy or radiotherapy, and then restore hematopoietic and immune functions through intravenous infusion of pre-collected autologous or allogeneic stem cells. Pavlů and Apperley (2013) However, HSCT also cause some adverse reactions. After allogeneic stem cell transplantation, the need for immunosuppressants, may cause low immunity, secondary infection. Zhao et al. (2019) Moreover, some patients may have a graft-versus-host reaction, which not only leads to graft failure, but also to death. Peccatori and Ciceri (2010).

The above-mentioned therapies generally have some disadvantages, such as low drug targeting, high adverse reactions, and drug resistance in patients. Therefore, it is very important to develop an efficient and targeted intelligent drug delivery system in the past decades Wicki et al. (2015) With the continuous progress of nanotechnology, nanotechnology has been widely used in drug delivery, disease diagnosis and treatment (Patra et al., 2018).

Iron oxide nanoparticles (IONPs) in the diagnosis and treatment of cancer has attracted more and more attention. Wang et al. (2018) Furthermore, iron-based nanoparticles have high transverse relaxation rate, good biocompatibility and long circulation *in vivo*, has been widely used as magnetic resonance imaging (MRI) contrast agent for tumor diagnosis. Na et al. (2009); Lee et al. (2012) Iron oxide nanoparticles have unique magnetic properties and can be used as magnetic thermotherapy, photothermal therapy and magnetic targeted drug delivery. Alphandéry (2019); Li et al. (2017) Based on its characteristics, it has been used more and more in hematological tumors in recent years.

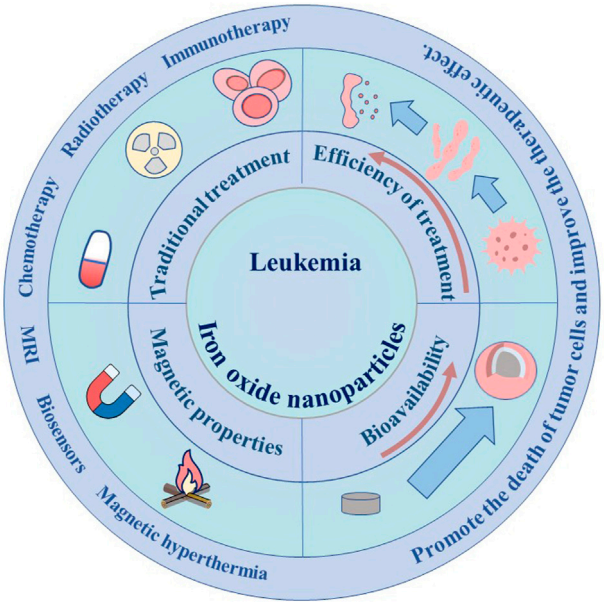

FIGURE 1
Application of IONPs in leukemia.

In this paper, the current status of leukemia treatment, the preparation of iron nanoparticles and their application in leukemia detection and treatment are briefly introduced (Figure 1). This article reviews the great advantages of iron nanoparticles in the treatment of leukemia, including MRI detection as an effective contrast agent, tumor-related iron-based nanoparticle therapy, and targeted drug delivery by coating different targets. In addition, this paper will briefly introduce the application of iron-based nanoparticles in combination therapy of leukemia. Finally, the shortcomings of the current application of iron-based nanoparticles in the diagnosis and treatment of leukemia will be particularly discussed.

2 Iron-based nanoparticles

In recent years, nanotechnology has been widely used in the diagnosis and treatment of various diseases, especially in oncology. El-Sherbiny et al. (2017) Nanomedicine overcomes many disadvantages of traditional cancer treatment methods for cancer treatment, such as low bioavailability, drug resistance and side effects of patients, which provides a new and effective treatment for cancer. Nagaraju et al. (2021) In addition, through the surface modification of nanoparticle structures and the integration of tumor diagnosis and treatment, nanomaterials can also be used for early diagnosis, imaging, precision therapy and smart anti-cancer drugs. Auría-Soro et al. (2019).

TABLE 1 Comparison of the characteristics of different synthesis methods of IONPs.

Method name	Principle	Advantages	Disadvantages	Impact factors	Reference
Thermal decomposition method	The organic metal precursor is decomposed into metal oxide at high temperature or metallic elements	monodisperse and uniform in diameter	The product surface is hydrophobic and needs to be modified	Temperature, heating rate, reaction time	Lu et al. (2007)
Hydrothermal method	The hot solvent is converted into nanoparticles under high temperature and high pressure	simple operation, high crystallinity, good hydrophilicity and no need of surface modification	Reaction equipment is expensive, to the temperature, the pressure, the device request is high	Temperature, reaction time, type of solvent	Li et al., (2013)
Coprecipitation method	Ferric and ferric precipitates in alkaline solutions	Good hydrophilicity, simple procedure and high yield	Product size polydispersity	Temperature, pH, concentration, type of iron salt	Frimpong et al., (2010)
Microemulsion method	Surfactants and bases are added to form a microemulsion system in which the co-precipitation reaction takes place	size controlled, and the product has monodispersety	Toxic Surfactant	Emulsifier, surfactant concentration ratio, reaction temperature and time	Bai et al., (2007)

As an important endogenous trace element, iron is widely distributed in various tissues of human body to maintain biological health. In recent years, iron-based nanomaterials have been widely used in various fields of biomedicine. Xie et al. (2018) Through the precise control and surface modification of magnetic materials, nano-materials such as iron oxide nanoparticles have been widely used in the biomedical research field, as a contrast agent for drug delivery such as magnetic resonance magnetic resonance imaging hyperthermia drug delivery. Shen et al. (2017) Recently, with the development of nanomedicine, more and more IONPs have been used in the diagnosis and treatment of leukemia.

2.1 Preparation and modification of iron oxide nanoparticles

There are many methods for preparing magnetic iron oxide nanoparticles, such as physical methods, chemical methods and microbial technology. Wei and Wang (2013) The physical chemistry properties of the prepared magnetic ferroferric oxide nanoparticles (Fe_3O_4NPs) are closely related to the preparation methods. Laurent et al. (2008) Therefore, it is very important to choose a suitable method to synthesize magnetic nanoparticles; Song et al. (2019) Among the many methods, the most commonly used are chemical methods, which have lower synthesis costs and higher yields; Hu et al. (2018) Chemical methods of preparation of Fe_3O_4NPs include thermal decomposition method, hydrothermal method, co-precipitation method, micro-emulsion method; Sodipo and Aziz, (2016) The most common method for Fe_3O_4NPs preparation is co-precipitation. There are the detailed characteristics of these methods (Table 1).

Although the preparation of Fe_3O_4NPs is mature, there are still several problems in production and application, such as the formation of aggregation due to the instability of nanoparticles. Mohammadi et al. (2013) Therefore, it is necessary to modify the surface of Fe_3O_4NPs. The appropriate surface modification has ability to improve the stability, targeting ability and biocompatibility of Fe_3O_4NPs nanoparticles (Arias et al., 2018). The various materials used to modify IONPs have different advantages and applications (Table 2).

2.2 Iron-based nanoparticles and magnetic resonance imaging

Molecular imaging plays an important role in tumor detection and prognosis monitoring (Gordon et al., 2019). This technology has high accuracy and reliability in elucidating the process of tumor development and monitoring the condition of patients. Current imaging techniques include optical imaging (OI), X-ray computed tomography (CT), Positron emission tomography Single-photon emission computed tomography (PET SPECT) (Fonti et al., 2019), magnetic resonance imaging (MRI) and ultrasound (US) (Mammatas et al., 2015). Compared with other imaging methods, MRI has many advantages, such as non-invasive, high resolution, high soft tissue resolution and fast living imaging. It has become an important tool in clinical imaging diagnosis and disease monitoring (Chandarana et al., 2018).

The contrast agent can shorten the longitudinal and transverse relaxation time of the surrounding hydrogen protons, thus enhancing the signal contrast of the focus and improving the detection sensitivity (Shuvaev et al., 2021). MRI contrast media are usually divided into T_1W_1 and T_2W_1 (Kanda et al., 2015). Currently, most gadolinium-based T_1 contrast agents are used clinically. However, gadolinium-based T_1 contrast agents tend to dissociate *in vivo*, and free gadolinium ions can deposit in the kidneys and central nervous system, causing nephrogenic systemic fibrosis and neurotoxicity (McDonald et al., 2015). Therefore, for patients with renal dysfunction, gadolinium-based contrast agents may aggravate renal toxicity and even cause renal failure. Because of it is reported that iron-based nanoparticles have better biocompatibility than gadolinium-based contrast agents due to its unique magnetism and tiny size (Yang et al., 2012). Neuwelt E A et al. studied the effect of size on IONPs, and the results showed that when the size of ferrite nanoparticles is less than 5 nm, the decrease of magnetic moment can not only suppress the T_2 effect,

TABLE 2 Characteristics of different modifying materials for IONPs.

Classification	Representative	Advantage	Application	Reference
Small molecules	Carboxylic acid, oleic acid	High hydrophilicity	Targeted Drug, vacuum sealing	Reguera et al., (2017)
Biomolecules	Nucleic acid, polypeptide, protein	High targeting	Targeted Drugs, immunotherapy, gene therapy	Banchelli et al., (2014)
Inorganic Materials	Au, AG, MOS2	High stability, simple preparation	Targeted drug delivery, multimodality imaging, and photothermal therapy	Li et al., (2015)
Mesoporous materials	Mesoporous silicon dioxide, organic metal frame MOFs	High hydrophilicity, high drug loading rate	Targeted drug delivery, fluorescence imaging	Fang et al., (2020)
Polymer	PEG, PVP, PEI	Long circulation, high Biocompatibility	Targeted drug delivery, bioimaging	Dehaini et al., (2016)

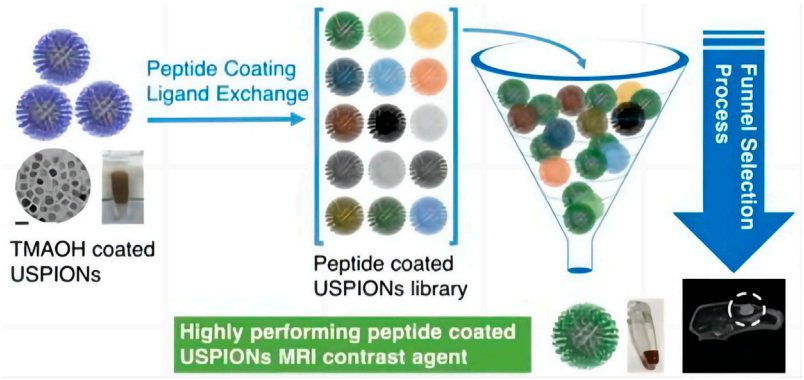

FIGURE 2
Synthesis process and application of 2PG-S*VVVT-PEG4-ol-coated USPIONs (Chee et al., 2018).

but also enhance the T_1 signal effectively, which reflects the high T_1 contrast enhancement performance (Neuwelt et al., 2009).

IONPs can be modified with biological material to improve the biocompatibility of the contrast medium. Chee, H et al. designed a short peptide and ligand library for enhancing MRI Biocompatibility, which was used to prepare 86 different peptide-coated ultra miniature superparamagnetic iron oxide nanoparticles (USPION) (Chee et al., 2018). Diphosphopeptide 2 PG-S *VVVT-PEG 4-OL was screened and found to provide the highest biocompatibility and performance for USPION, with no detectable toxicity or adhesion to living cells, and was comparable to commercially available contrast media, the peptide-coated USPION can be used to target the tumor, improve the contrast of the target site, and show better MRI performance (Figure 2). Compared with conventional MRI contrast agents, this kind of contrast agent with iron oxide nanoparticles has a higher overall safety and targeting function.

At present, MRI is mainly used to evaluate the prognosis of leukemia and to screen the complications caused by the treatment of leukemia (Mayerhoefer et al., 2020). Intracranial infection is a common central nervous system complication of leukemia. Leukemia patients, especially children, can be infected with microorganisms in the central nervous system due to the damage of immune system, damage of immune system caused by chemotherapy and persistent neutrophils (Lim et al., 2021). Previous intracranial infections were mainly diagnosed by clinical manifestations and laboratory examinations such as cerebrospinal fluid (CSF). Because of the similar clinical characteristics of these central nervous system complications, it is sometimes difficult to make a differential diagnosis by clinical laboratory tests, and the location and extent of the lesions can not be determined by CSF smears (Abdalkader et al., 2019). MRI has some advantages over laboratory tests in leukemia with central nervous system infection. Moreover, MRI can identify the location and extent of the lesion, on the other hand, the infection caused by different pathogenic microorganisms has different imaging features, therefore, MRI can help to diagnose infectious brain lesions caused by leukemia and differentiate other central system diseases (Mayerhoefer et al., 2020). Because of the ultra-small size and specific magnetic properties of iron oxide nanoparticles, iron nanoparticles have great potential as MRI contrast agents in the diagnosis of leukemia-related central system complications.

2.3 Magnetic hyperthermia

Magnetic hyperthermia was proposed by Gilchrist in 1957. On the basis of the research on the destruction of dog's lymphoma

tissues by magnetic materials, it was proved that magnetic materials could move and gather in the tumor tissues in a targeted manner, and generate heat to destroy the tumor tissue under the action of alternating magnetic field (Gilchrist et al., 1957). With the rise of nanotechnology, magnetic hyperthermia is developing constantly. Magnetic hyperthermia is based on the principle that tumor cells are different from normal cells in their tolerance to temperature, under the action of alternating magnetic field, magnetic nanoparticles produce magnetic hysteresis and relaxation, which leads to heat generation. Finally, the temperature in the tissue region is increased, and the tumor cells are destroyed (Carrey et al., 2011). Under the action of alternating magnetic field, magnetic nanoparticles produce hysteresis and relaxation, thus generating heat and increasing the temperature of tissue area (Hergt et al., 2009). The raised temperature range of 43°C–46°C induces injury of tumor cells, which undergo physiological changes leading to their apoptosis/necrosis, while normal cells are not affected (Spirou et al., 2018). At present, there are many researches on Magnetic hyperthermia therapy (MHT) in the field of solid tumor treatment, while there are few studies on MHT in the field of non-solid tumor treatment such as leukemia. Magnetic nanomaterials can be modified to functionalize the surface to target the tumor site (Carter et al., 2021). Several studies suggested that epithelial cell adhesion molecule (Ep-CAM) might be a marker reflecting the epithelial state of primary and systemic tumor cells, and the specific expression of Ep-CAM in leukemia cells could be used as an indicator to measure the metastasis of leukemia tumor cells (Zheng et al., 2017). Kim et al. fixed the antibody of epithelial cell adhesion molecule on the surface of magnetic nanoparticles (MNPs) to realize the specificity to leukemia cells. With EpCAM-MNPs hyperthermia in THP 1 cells and AKR mouse models, leukemic cell numbers were reduced by approximately 40% compared with control samples (Al Faruque et al., 2020). This experiment provides favorable supporting evidence for the treatment of leukemia with magnetic thermotherapy, so magnetic nanoparticles-mediated magnetic thermotherapy has a certain prospect in the treatment of leukemia.

3 Application of iron nanoparticles in leukemia

3.1 Iron-oxide nanoparticles and leukemia diagnosis

Unlike other diseases, based on the malignant proliferation and metastasis of cancer cells, one of the most effective treatments for cancer is to diagnose leukemia as early as possible. Traditional methods rely on the patient's clinical symptoms, cytomorphology and cytogenetics to diagnose leukemia. However, traditional methods are less sensitive and leukemia cells can not be detected in the early stages of the disease. Therefore, it is necessary to develop a highly selective and sensitive method for the diagnosis of leukemia. Based on the advantages of good selectivity, high sensitivity, simple equipment and low price, biosensors have been used as diagnostic tools in drug detection, biomedical evaluation, environmental monitoring (Sharifi et al., 2019).

Many studies have shown that the application of nanomaterials in traditional biosensors can improve the detection sensitivity, speed and selectivity. The combination of metal oxide nanoparticles and biosensor can not only increase the sensitivity, but also improve the signal-to-noise ratio (Kaushik et al., 2008). Dinani et al. (2022) constructed the first gold nanoparticle/magnetite/reduced graphene oxide (AuNPs/Fe_3O_4/RGO) adapter sensor for detecting the concentration of the leukemia biomarker miRNA-128. The electrical conductivity and the sensitivity of the sensor have been improved by this nanocomposite. Therefore, the quantitative determination of miRNA-128 by the biosensor is realized for the first time, which can be applied to the diagnosis and prognosis of acute lymphocyte leukemia (ALL). Because of the specific expression of miRNA-128 in ALL, the sensor can also be used for differential diagnosis of different types of leukemia, especially with AML, in which miRNA-128 is not expressed. (Figure 3).

Fe_3O_4 nanomaterials as metal oxide nanomaterials can increase the active surface area of the electrode surface and the electron transfer rate of redox, which leads to higher catalytic activity. Sgc8c linker can specifically bind to PTK7 which overexpresses in leukemia cells (Liu et al., 2019). Khoshfetrat and Mehrgardi (2017) first fixed the thiogenated sgc8c junction on the magnetic Fe_3O_4 nanoparticles (Apt-GMNPs) coated with gold nanoparticles, and then used N-doped graphene nanoplates as the detection electrode, an electrochemical joint sensor was successfully constructed to detect the selectivity and sensitivity of leukemic cells. It is reported that nitrogen-doped graphene had larger functional surface area, more active sites catalytic reactions and higher conductivity compared with graphene nanosheet (Wen et al., 2014). Moreover, gold coated MNPs as a separation tool have ability to decrease the signal-to-noise ratio in complex media. The unique magnetism of MNPs can be used not only in biosensors, but also in combination with gene detection technology to improve the sensitivity of leukemia detection (Manthawornsiri et al., 2016).

Recently, Magnetic separation technology has been discovered and applied to separate substances under magnetic field. Compared with other separation methods, such as centrifugation, electrophoresis and ultrafiltration, the advantages of magnetic separation involved of high specificity, mild reaction conditions, simple operation and low cost (Liu et al., 2020). In 1973, Fe_3O_4 NPs were firstly applied to the field of biological magnetic separation by Robinson et al. (1973). Nowadays, Fe_3O_4 NPs have been widely used in the separation of biological macromolecules such as cells, pathogens, nucleic acids and proteins (You et al., 2019). Rashid et al. (2020) prepared Fe_3O_4 NPs by coprecipitation, and coated the nanoparticles with SiO_2. Finally, Fe_3O_4@SiO_2 was functionalized to obtain Fe_3O_4@SiO_2@PMIDA MNP. The nanocomposite is not only simple and inexpensive to fabricate, but also selectively isolates $CD4^+$ T lymphocytes from human peripheral blood. Quynh et al. (2018) developed a novel Fe_3O_4/AG nanocomposite with core-shell structure and coupled anti-CD34 antibody to magnetic nanoparticles, which can collect CD34 + stem cells from bone marrow samples with high selectivity. The above researches on the application of magnetic separation in the separation of cells, which indicated that it is promising for the diagnosis of leukemia *via* magnetic separation technology.

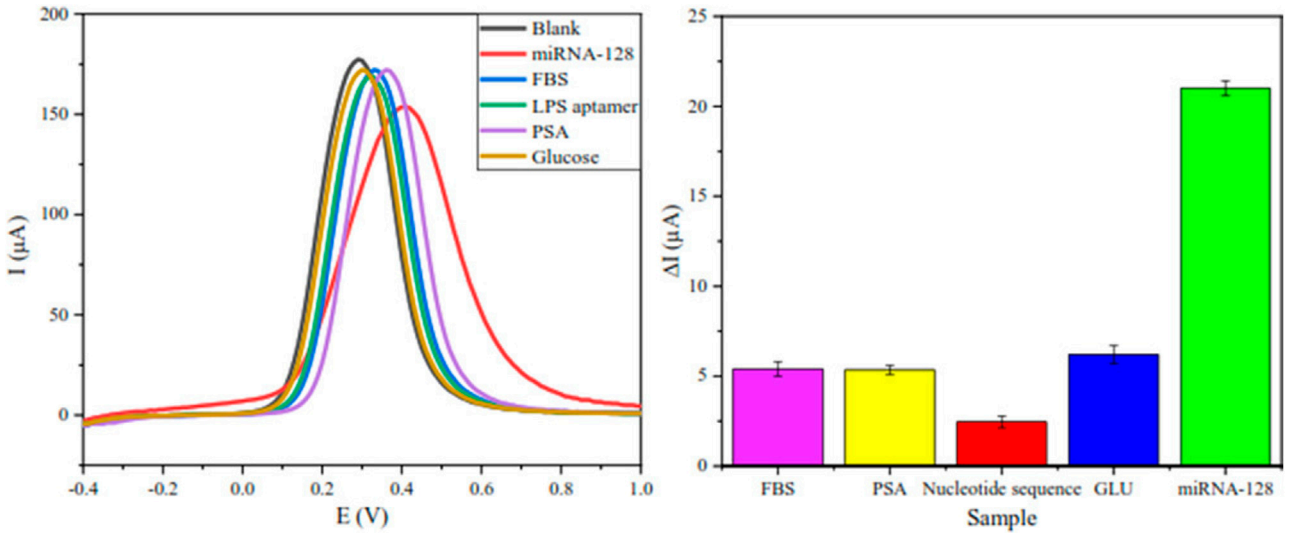

FIGURE 3
To confirm the high selectivity of the biosensor, besides miRNA-128, this biosensor was also documented for four other biomolecules that are in concentration in healthy humans, including LPS aptamer, glucose, PSA and BSA (Dinani et al., 2022).

3.2 Iron-oxide nanoparticles and leukemia treatment

3.2.1 Improve the bioavailability of drugs

It is suggested that oral administration might be often regarded as common administration routes for the treatment of hematologic tumors (Liu, 2021). However, due to low water solubility and low oral absorption of most therapeutic drugs, it is necessary to increase the oral dose of cytotoxic drugs in order to enhance the blood concentration of drugs, which also causing damage of normal cells to a certain extent (Kantarjian et al., 2021). Therefore, it is important to discover a method to improve the bioavailability of drugs.

Homoharringtonine (HHT) can induce apoptosis by activating Caspase-3 and decreasing the expression of BCL-2, which can be used in tyrosine-kinase inhibitor myeloid leukemia (Chen et al., 2019). However, poor water solubility and serious adverse reactions limit its clinical application. In order to improve the bioavailability of HHT and reduce the adverse reactions, HHT-MNP-Fe_3O_4 nanoparticles were prepared as drug delivery nanoparticles (Li et al., 2020). The results showed that HHT delivered by MNP-Fe_3O_4 could not only inhibit the growth of myeloid leukemia cell, but also inhibit the proliferation of leukemia cells *in vivo* and *in vitro*, and induce apoptosis of leukemia cells on a wider range. The reason why HHT-MNP-Fe_3O_4 can improve the curative effect may be that the magnetic nanoparticles downregulate the expression of myeloid leukemia-1, inhibit the activation of cal-pain I and poly-ADP- ribose polymerase, and thus induce apoptosis of leukemia cells. Like HHT, genistein has anti-tumor potential. However, due to its poor water solubility, the effective doses of genistein will have more side effects when used to treat blood tumors. Chouhan et al. (2021); Ghasemi Goorbandi et al. (2020) prepared Fe_3O_4-CMC-genistein by covalently modifying Fe_3O_4 nanoparticles with Genistein. This study showed that the release rate of the synthesized Fe_3O_4-CMC-genistein was very slow, and compared with genistein, the synthesized Fe_3O_4-CMC- genistein showed a higher inhibition rate, especially at 72 h.

Most chemotherapeutic drugs used to treat leukemia have a short half-life and therefore do not reach effective therapeutic concentrations in the bloodstream for long enough to produce a lasting therapeutic effect. For example, the half-life of a chlorambucil is only 1–2 h, and the half-life of a mercaptopurine is 90 min (Sang et al., 2022). Fe_3O_4 nanoparticles can overcome this disadvantage. Chemotherapeutic drugs are encapsulated in nanoparticles to slow or control drug release and thereby improve drug bioavailability. Chloramb is used as an alkylating agent in the chemotherapy of chronic lymph leukemia (CLL) and chronic myeloid leukemia (CML). CS-IONPs with core-shell structure were prepared by Hussein-Al-Ali et al. (2021) Chloramb-CS-IONPs were synthesized by ionic gelation method using CS-IONPs as carriers of chlorambucil with 19% loading rate of chloramb. In this study, Chloramb-loaded IONPs reduced cancer cell viability in a leukemia cell line (WEHI) better than Chloramb. Furthermore, the release of Chloramb from the drug-loaded complex has proved to be a controlled release behavior. Chloramb-CS-IONPs provided a new way to improve the bioavailability of chloramphenylene, thus providing a new idea for the treatment of leukemia with Chloramb. Dorniani et al. (2014) used a co-precipitation method to mercaptopurine iron oxide nanoparticles coated with PEG. By simulating the pH of the stomach and blood, the drug-release behavior of the nanoparticles is controlled, thus the anti-leukemia effect of WEHI-3B can be maintained.

3.2.2 Improve the efficiency of treatment

The clinical use of systemic chemotherapy for leukemia is often hampered by cancer cells and the multiple drug resistance of anticancer drugs. The process of multidrug resistance (MDR) development is very complex, which is related to transporter overexpression, enhanced xenobiotics metabolism, DNA repair ability changes, genetic factors and so on Bukowski et al. (2020).

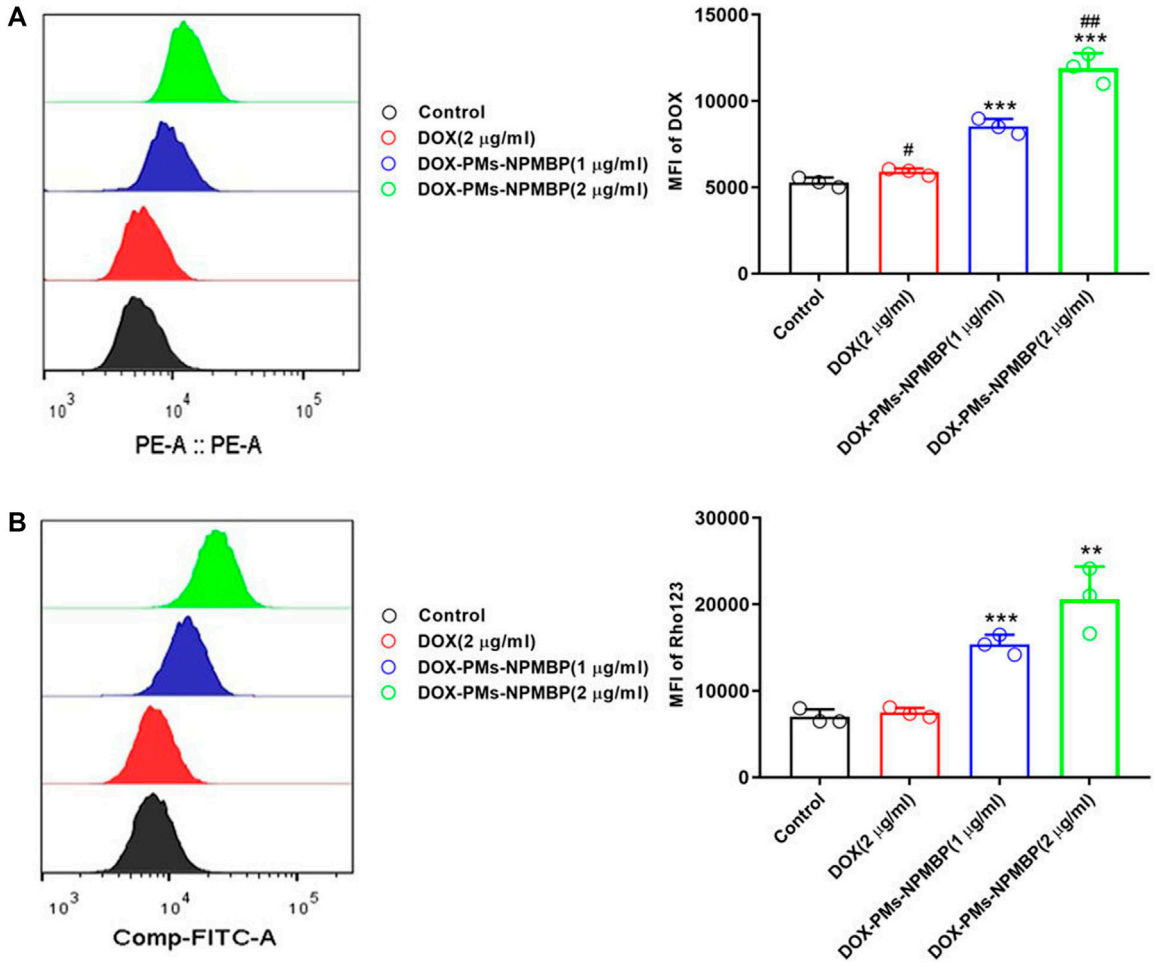

FIGURE 4
DOX-PMs-NPMBP promotes the intracellular retention of DOX in DOX-resistant cells. **(A)** The intracellular retention of DOX was assessed by flow cytometry in Nalm6/DOX cells after different treatments. **(B)** The MFI of Rhodamine123in Nalm123/ADR cells was assessed by flow cytometry analysis through FITC channels (Gan et al., 2021).

Nano-agents will play an important role in the treatment of multi-drug resistant tumors because they can not only carry multiple chemotherapeutic agents and bioactive components, but also overcome multiple mechanisms of MDR.

To reverse MDR and minimize serious adverse effects of systemic chemotherapy, Wang et al. (2011) used oleic acid-coated IONPs as a co-delivery vehicle for DNR and Br Tet, named DNR/Br Tet-MNPs. The effect of the drug-loaded nanoparticles on the apoptosis of drug-resistant human leukemia K562/A02 cells was studied. The study showed that DNR/Br Tet-MNPs could deliver DNR to drug-resistant cells better than DNR and Br Tet Solution. The reason may be that the drug-loaded nanoparticles decrease the expression of BCL-2 and increase the expression of Caspase 3, thus increasing the apoptosis of drug-resistant leukemia cells.

Doxorubicin (DOX) is a commonly used drug to treat acute leukemia, but its application is limited because of drug resistance. Studies have shown that over-expression of NPM can lead to multidrug resistance of ALL, and the engineered recombinant NPM binding protein (NPMBP) can knock out NPM by RNA interference, thus reversing multidrug resistance of leukemia cells (Wang et al., 2015). Gan D and his colleagues (Gan et al., 2021) assembled DOX and NPMBP into polymer nanomicelles called DOX-PMs-NPMBP. Compared with DOX, DOX-PMs-NPMBP could increase the drug retention capacity of DOX-resistant cells and induce G0/G1 phase arrest of drug-resistant cells, thus achieving a more significant anti-leukemia effect. In addition, the study showed that the multidrug resistance mechanism of DOX-PMs-NPMBP nanoparticles system was proved by the Rho123 outflow test by regulating the functional activity of P-glycoprotein (P-gp). Overexpression of P-gp in drug-resistant cells increases drug efflux, resulting in a decrease in intracellular drug concentration. The new DOX-PMs-NPMBP nanoparticle system can significantly regulate the functional activity of P-gp, thus reducing the efflux of Rho123 mediated by drug pump P-gp in drug-resistant ALL cells (Figure 4). These results suggest that the classical MDR phenotype-dependent mechanism is involved in the effect of DOX-PMs-NPMBP on DOX-resistant cells.

IONPs can trigger the Fenton reaction, a chemical reaction in which divalent and/or ferric can convert hydrogen peroxide into hydroxyl radicals. The Fenton reaction produces reactive oxygen species (ROS) and mediates lipid peroxidation, which can lead to

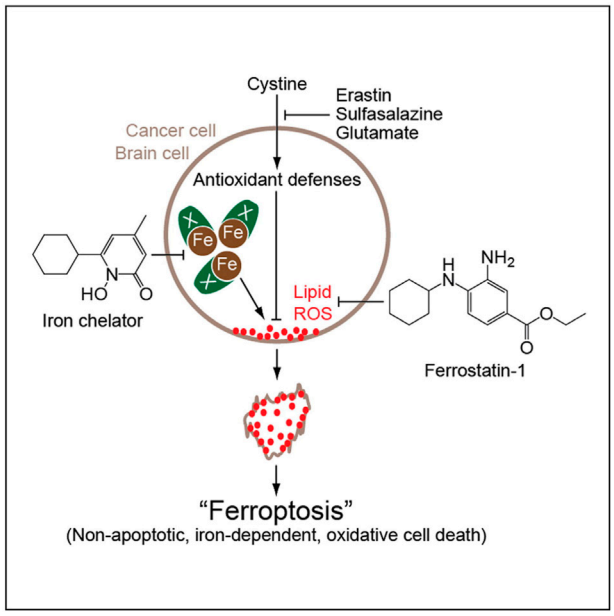

FIGURE 5
Mechanism of action of iron death (Dixon et al., 2012).

ferroptosis. Shen et al. (2018) Ferroptosis, discovered and named by Dixon et al. (2012), is a new form of iron-dependent cell death that differs from apoptosis, cell necrosis, and autophagy (Figure 5). The biochemical mechanisms of ferroptosis include the production of lethal ROS, lipid peroxidation and intracellular iron accumulation, which in turn produce large amounts of oxygen free radicals. When the steady-state imbalance of ROS production and degradation occurs, the cell's own antioxidant capacity decreases to a point where it is not sufficient to clear the excessive accumulation of lipid ROS. Hydroxyl radicals and ROS can attack structures such as DNA, proteins and cell membranes, and thus destroy the structure and function of cells, causing ferroptotic cell death. Chen et al. (2021).

Trujillo-Alonso et al. (2019) found that iron oxide nanoparticles approved by the FDA for the treatment of iron deficiency can be used to treat leukemia with low ferroportin (FPN) expression. Iron oxide nanoparticles can aggravate the reduction of cellular iron efflux and increase intracellular iron content, thus aggravating the increase of intracellular ROS level. Because FPN is highly expressed in normal hematopoietic cells, and iron oxide nanoparticles do not cause severe toxic and side effects in normal hematopoietic cells. Therefore, iron oxide nanoparticles are relatively safe in the treatment of this kind of leukemia.

Dou et al. (2021) found that the combination of Fe_3O_4 nanoparticles with cytarabine (Ara-C) inhibited leukemia stem cell (LSC) more than Ara-C alone. They analyzed changes in ROS-related substances such as gp91-phox and SOD1 by measuring ROS levels in LSC and non-LSC under different conditions. It was demonstrated that IONPs and Ara-C might induce LSC apoptosis due to increased ROS levels. Therefore, iron oxide nanoparticles can regulate the oxidative damage and defense balance of cells through the mechanism of iron death, which has a great prospect in the treatment of leukemia.

4 Conclusion and prospects

With the development of medical science and technology, the traditional way of drug delivery will be innovated. Due to the convenience and biocompatibility of IONPs, it has a broad application prospects in clinical transformation. The rapid development of nanotechnology has laid a solid foundation for the diagnosis and treatment of leukemia, and more and more application of IONPs in the treatment of leukemia. Furthermore, IONPs are widely used in tumor imaging, magnetic hyperthermia and biomacromolecule magnetic separation because of their magnetic properties. More importantly, IONPs can not only achieve synergistic drug delivery, but also combine with other therapeutic methods to achieve better therapeutic effects, which has become one of the hot research directions.

However, the application of iron oxide nanoparticles in the diagnosis and treatment of leukemia still needs to overcome huge obstacles in the clinical transformation process. 1) At present, there is still a lack of high-yield and high-safety methods for the preparation of iron oxide nanoparticles. Although some modified materials have been studied, the synthetic standard of modified materials and whether other new materials can be used for modification are still an urgent problem to be solved. 2) Lack of detailed toxicity test results of iron oxide nanoparticles. Although iron oxide nanoparticles are biocompatible compared to other materials, the long-term side effects of iron oxide nanoparticles on normal cells, tissues and organs need to be further determined, and carefully study the metabolism of this material and degradation of the impact on the body. 3) The detailed mechanism of iron oxide nanoparticles involved in regulating the metabolism of leukemic cells is not completely clear. 4) For the application of IONPs in the treatment of leukemia, most of current studies are devoted to the examination of the drug-carrying function of IONPs, and there are fewer applications regarding the magnetic properties of IONPs, such as magnetic hyperthermia and magnetic separation. 6) The clinical transformation of iron oxide nanoparticles in leukemia has been very slow, and only a small number of studies have been carried out in clinical trials. 7) The design of iron oxide nanoparticles with imaging, diagnosis and therapy, and the realization of multi-treatment of leukemia, may be one of the hot research directions in the future.

These questions may inspire future research into the development and improvement of IONPs, providing better opportunities for the treatment of leukemia. In summary, combining multidisciplinary knowledge and research tools to explore effective therapies for leukemia and develop highly biocompatibility, highly targeted iron oxide nanoparticles will be the focus. It is believed that with the joint efforts of researchers, IONPs may be further applied in the clinical treatment of leukemia.

Author contributions

YZ conceived and designed the current study. YW and YY search and summarize the data. XZ, JS and XD analyzed the data.

YW and YY drafted the manuscript. All authors have read and approved the final manuscript.

Funding

This work was supported by the Research Program of the Science and Technology Department of Sichuan Province (2022NSFSC0630); Research Program of the Science and Technology Department of Chengdu (2021-YF05-01034-SN); Open Project of Central Nervous System Drug Key Laboratory of Sichuan Province (230015-01SZ); Research Program of Science and Technology Department of Sichuan Province (2021YJ0189); National Key Research and Development Program of China (2020YFC2005500).

Conflict of interest

The authors declare that the research was conducted in the absence of any commercial or financial relationships that could be construed as a potential conflict of interest.

Publisher's note

References

Abdalkader, M., Xie, J., Cervantes-Arslanian, A., Takahashi, C., and Mian, A. Z. (2019). Imaging of intracranial infections. *Seminars Neurology* 39, 322–333. Thieme Medical Publishers. doi:10.1055/s-0039-1693161

Al Faruque, H., Choi, E.-S., Lee, H.-R., Kim, J.-H., Park, S., and Kim, E. (2020). Targeted removal of leukemia cells from the circulating system by whole-body magnetic hyperthermia in mice. *Nanoscale* 12, 2773–2786. doi:10.1039/c9nr06730b

Alphandéry, E. (2019). Biodistribution and targeting properties of iron oxide nanoparticles for treatments of cancer and iron anemia disease. *Nanotoxicology* 13, 573–596. doi:10.1080/17435390.2019.1572809

Alsalem, M. A., Zaidan, A. A., Zaidan, B. B., Hashim, M., Madhloom, H. T., Azeez, N. D., et al. (2018). A review of the automated detection and classification of acute leukaemia: Coherent taxonomy, datasets, validation and performance measurements, motivation, open challenges and recommendations. *Comput. methods programs Biomed.* 158, 93–112. doi:10.1016/j.cmpb.2018.02.005

Arias, L. S., Essan, J. P., Vieira, A. P. M., Lima, T. M. T., Delbem, A. C. B., and Monteiro, D. R. (2018). Iron oxide nanoparticles for biomedical applications: A perspective on synthesis, drugs, antimicrobial activity, and toxicity. *Antibiotics* 7, 46. doi:10.3390/antibiotics7020046

Auría-Soro, C., Nesma, T., Juanes-Velasco, P., Landeira-Viñuela, A., Fidalgo-Gomez, H., Acebes-Fernandez, V., et al. (2019). Interactions of nanoparticles and biosystems: Microenvironment of nanoparticles and biomolecules in nanomedicine. *Nanomaterials* 9, 1365. doi:10.3390/nano9101365

Bai, F., Wang, D., Huo, Z., Chen, W., Liu, L., Liang, X., et al. (2007). A versatile bottom-up assembly approach to colloidal spheres from nanocrystals. *Angew. Chem.* 119, 6650–6653. doi:10.1002/anie.200701355

Banchelli, M., Nappini, S., Montis, C., Bonini, M., Canton, P., Berti, D., et al. (2014). Magnetic nanoparticle clusters as actuators of ssDNA release. *Phys. Chem. Chem. Phys.* 16, 10023–10031. doi:10.1039/c3cp55470h

Bodet-Milin, C., Kraeber-Bodéré, F., Eugène, T., Guérard, F., Gaschet, J., Bailly, C., et al. (2016). Radioimmunotherapy for treatment of acute leukemia. *Seminars Nucl. Med.* 46, 135–146. Elsevier. doi:10.1053/j.semnuclmed.2015.10.007

Bukowski, K., Kciuk, M., and Kontek, R. (2020). Mechanisms of multidrug resistance in cancer chemotherapy. *Int. J. Mol. Sci.* 21, 3233. doi:10.3390/ijms21093233

Carrey, J., Mehdaoui, B., and Respaud, M. (2011). Simple models for dynamic hysteresis loop calculations of magnetic single-domain nanoparticles: Application to magnetic hyperthermia optimization. *J. Appl. Phys.* 109, 083921. doi:10.1063/1.3551582

Carter, T. J., Agliardi, G., Lin, F.-Y., Ellis, M., Jones, C., Robson, M., et al. (2021). Potential of magnetic hyperthermia to stimulate localized immune activation. *Small* 17, 2005241. doi:10.1002/smll.202005241

Chandarana, H., Wang, H., Tijssen, R. H. N., and IndraDas, J. (2018). Emerging role of MRI in radiation therapy. *J. Magnetic Reson. Imaging* 48, 1468–1478. doi:10.1002/jmri.26271

Chee, H. L., Gan, C. R. R., Ng, M., Low, L., Fernig, D. G., KishoreBhakoo, K., et al. (2018). Biocompatible peptide-coated ultrasmall superparamagnetic iron oxide nanoparticles for *in vivo* contrast-enhanced magnetic resonance imaging. *ACS Nano* 12, 6480–6491. doi:10.1021/acsnano.7b07572

Chen, S.-J., and Zhou, G.-B. (2012). Targeted therapy: The new lease on life for acute promyelocytic leukemia, and beyond. *IUBMB life* 64, 671–675. doi:10.1002/iub.1055

Chen, X., Kang, R., Guido, K., and Tang, D. (2021). Broadening horizons: The role of ferroptosis in cancer. *Nat. Rev. Clin. Oncol.* 18, 280–296. doi:10.1038/s41571-020-00462-0

Chen, X.-J., Zhang, W.-N., Chen, B., Xi, W.-D., Lu, Y., Huang, J.-Y., et al. (2019). Homoharringtonine deregulates MYC transcriptional expression by directly binding NF-κB repressing factor. *Proc. Natl. Acad. Sci.* 116, 2220–2225. doi:10.1073/pnas.1818539116

Chouhan, R. S., Horvat, M., Ahmed, J., Alhokbany, N., Alshehri, S. M., and Gandhi, S. (2021). Magnetic nanoparticles—a multifunctional potential agent for diagnosis and therapy. *Cancers* 13, 2213. doi:10.3390/cancers13092213

Curtis, R. E., Boice, J. D., Jr, Stovall, M., Bernstein, L., Greenberg, R. S., Flannery, J. T., et al. (1992). Risk of leukemia after chemotherapy and radiation treatment for breast cancer. *N. Engl. J. Med.* 326, 1745–1751. doi:10.1056/NEJM199206253262605

Dehaini, D., Fang, R. H., Luk, B. T., Pang, Z., Hu, C. M., Kroll, A. V., et al. (2016). Ultra-small lipid–polymer hybrid nanoparticles for tumor-penetrating drug delivery. *Nanoscale* 8, 14411–14419. doi:10.1039/c6nr04091h

Dinani, H. S., Pourmadadi, M., Yazdian, F., Rashedi, H., Ebrahimi, S. A. S., Shayeh, J. S., et al. (2022). Fabrication of Au/Fe3O4/RGO based aptasensor for measurement of miRNA-128, a biomarker for acute lymphoblastic leukemia (ALL). *Eng. Life Sci.* 22, 519–534. doi:10.1002/elsc.202100170

Dixon, S. J., Lemberg, K. M., Lamprecht, M. R., Skouta, R., Zaitsev, E. M., Gleason, C. E., et al. (2012). Ferroptosis: An iron-dependent form of nonapoptotic cell death. *Cell* 149, 1060–1072. doi:10.1016/j.cell.2012.03.042

Dorniani, D., Kura, A. U., Hussein-Al-Ali, S. H., bin Hussein, M. Z., Fakurazi, S., Shaari, A. H., et al. (2014). Release behavior and toxicity profiles towards leukemia (WEHI-3B) cell lines of 6-mercaptopurine-PEG-coated magnetite nanoparticles delivery system. *Sci. World J.* 2014, 972501. doi:10.1155/2014/972501

Dou, J., Li, L., Guo, M., Mei, F., Zheng, D., Xu, H., et al. (2021). Iron oxide nanoparticles combined with cytosine arabinoside show anti-leukemia stem cell effects on acute myeloid leukemia by regulating reactive oxygen species. *Int. J. nanomedicine* 16, 1231–1244. doi:10.2147/IJN.S278885

El-Sherbiny, I.M., Elbaz, N. M., Sedki, M., Elgammal, A., and Yacoub, M. H. (2017). Magnetic nanoparticles-based drug and gene delivery systems for the treatment of pulmonary diseases. *Nanomedicine* 12, 387–402. doi:10.2217/nnm-2016-0341

Fang, C., Deng, Z., Cao, G., Chu, Q., Wu, Y., Xiang, L., et al. (2020). Co–ferrocene MOF/glucose oxidase as cascade nanozyme for effective tumor therapy. *Adv. Funct. Mater.* 30, 1910085. doi:10.1002/adfm.201910085

Fonti, R., Conson, M., and Del Vecchio, S. (2019). PET/CT in radiation oncology. *Seminars Oncol.* 46, 202–209. Elsevier. doi:10.1053/j.seminoncol.2019.07.001

Frimpong, R. A., Dou, J., Pechan, M., and Hilt, J. Z. (2010). Enhancing remote controlled heating characteristics in hydrophilic magnetite nanoparticles via facile co-precipitation. *J. Magnetism Magnetic Mater.* 322, 326–331. doi:10.1016/j.jmmm.2009.09.050

Gan, D., Chen, Y., Wu, Z., Luo, L., Yirga, S. K., Zhang, N., et al. (2021). Doxorubicin/Nucleophosmin binding protein-conjugated nanoparticle enhances anti-leukemia activity in acute lymphoblastic leukemia cells *in vitro* and *in vivo*. *Front. Pharmacol.* 12, 607755. doi:10.3389/fphar.2021.607755

Gardin, C., Pautas, C., Fournier, E., Itzykson, R., Lemasle, E., Bourhis, J.-H., et al. (2020). Added prognostic value of secondary AML-like gene mutations in ELN intermediate-risk older AML: ALFA-1200 study results. *Blood Adv.* 4, 1942–1949. doi:10.1182/bloodadvances.2019001349

Ghasemi Goorbandi, R., Mohammadi, M. R., and Malekzadeh, K. (2020). Synthesizing efficacious genistein in conjugation with superparamagnetic Fe3O4 decorated with bio-compatible carboxymethylated chitosan against acute leukemia lymphoma. *Biomaterials Res.* 24, 9–13. doi:10.1186/s40824-020-00187-2

Gilchrist, R. K., Medal, R., Shorey, W. D., Hanselman, R. C., Parrott, J. C., and Taylor, C. B. (1957). Selective inductive heating of lymph nodes. *Ann. Surg.* 146, 596–606. doi:10.1097/00000658-195710000-00007

Gordon, O., Ruiz-Bedoya, C. A., Ordonez, A. A., Tucker, E. W., and Jain, S. K. (2019). Molecular imaging: A novel tool to visualize pathogenesis of infections *in situ*. *MBio* 10, e00317–e00319. doi:10.1128/mBio.00317-19

Hergt, R., Dutz, S., and Zeisberger, M. (2009). Validity limits of the Néel relaxation model of magnetic nanoparticles for hyperthermia. *Nanotechnology* 21, 015706. doi:10.1088/0957-4484/21/1/015706

Hu, Y., Mignani, S., Majoral, J.-P., Shen, M., and Shi, X. (2018). Construction of iron oxide nanoparticle-based hybrid platforms for tumor imaging and therapy. *Chem. Soc. Rev.* 47, 1874–1900. doi:10.1039/c7cs00657h

Hussein-Al-Ali, S. H., Hussein, M. Z., Bullo, S., and Arulselvan, P. (2021). Chlorambucil-iron oxide nanoparticles as a drug delivery system for leukemia cancer cells. *Int. J. nanomedicine* 16, 6205–6216. doi:10.2147/IJN.S312752

Kadia, T. M., Ravandi, F., Cortes, J., and Kantarjian, H. (2015). Toward individualized therapy in acute myeloid leukemia: A contemporary review. *JAMA Oncol.* 1, 820–828. doi:10.1001/jamaoncol.2015.0617

Kanda, T., Fukusato, T., Matsuda, M., Toyoda, K., Oba, H., Kotoku, J., et al. (2015). Gadolinium-based contrast agent accumulates in the brain even in subjects without severe renal dysfunction: Evaluation of autopsy brain specimens with inductively coupled plasma mass spectroscopy. *Radiology* 276, 228–232. doi:10.1148/radiol.2015142690

Kantarjian, H., Kadia, T., DiNardo, C., Daver, N., Borthakur, G., Jabbour, E., et al. (2021). Acute myeloid leukemia: Current progress and future directions. *Blood cancer J.* 11, 41. doi:10.1038/s41408-021-00425-3

Kantarjian, H., Ravandi, F., O'Brien, S., Cortes, J., Faderl, S., Garcia-Manero, G., et al. (2010). Intensive chemotherapy does not benefit most older patients (age 70 years or older) with acute myeloid leukemia. *Blood, J. Am. Soc. Hematol.* 116, 4422–4429. doi:10.1182/blood-2010-03-276485

Kaushik, A., Khan, R., Solanki, P. R., Pandey, P., Alam, J., Ahmad, S., et al. (2008). Iron oxide nanoparticles–chitosan composite based glucose biosensor. *Biosens. Bioelectron.* 24, 676–683. doi:10.1016/j.bios.2008.06.032

Khoshfetrat, S. M., and Mehrgardi, M. A. (2017). Amplified detection of leukemia cancer cells using an aptamer-conjugated gold-coated magnetic nanoparticles on a nitrogen-doped graphene modified electrode. *Bioelectrochemistry* 114, 24–32. doi:10.1016/j.bioelechem.2016.12.001

Laurent, S., Forge, D., Port, M., Roch, A., Robic, C., Vander Elst, L., et al. (2008). Magnetic iron oxide nanoparticles: Synthesis, stabilization, vectorization, physicochemical characterizations, and biological applications. *Chem. Rev.* 108, 2064–2110. doi:10.1021/cr068445e

Lee, D.-E., Koo, H., Kwon, I. C., Ryu, J. H., Kim, K., and Kwon, I. C. (2012). Multifunctional nanoparticles for multimodal imaging and theragnosis. *Chem. Soc. Rev.* 41, 2656–2672. doi:10.1039/c2cs15261d

Li, C., Dong, L., Su, R., Bi, Y., Qing, Y., Deng, X., et al. (2020). Homoharringtonine exhibits potent anti-tumor effect and modulates DNA epigenome in acute myeloid leukemia by targeting SP1/TET1/5hmC. *Haematologica* 105, 148–160. doi:10.3324/haematol.2018.208835

Li, J., Hu, Y., Jia, Y., Wei, P., Sun, W., Shen, M., et al. (2015). Hyaluronic acid-modified Fe3O4@ Au core/shell nanostars for multimodal imaging and photothermal therapy of tumors. *Biomaterials* 38, 10–21. doi:10.1016/j.biomaterials.2014.10.065

Li, J., Zheng, L., Cai, H., Sun, W., Shen, M., Zhang, G., et al. (2013). Polyethyleneimine-mediated synthesis of folic acid-targeted iron oxide nanoparticles for *in vivo* tumor MR imaging. *Biomaterials* 34, 8382–8392. doi:10.1016/j.biomaterials.2013.07.070

Li, K., Nejadnik, H., and Daldrup-Link, H. E. (2017). Next-generation superparamagnetic iron oxide nanoparticles for cancer theranostics. *Drug Discov. today* 22, 1421–1429. doi:10.1016/j.drudis.2017.04.008

Lim, E. A., Gnanadurai, R., Ruffle, J. K., Lee, H., Miller, R. F., and Hyare, H. (2021). Neuroimaging of CNS infection in haematological malignancy: Important signs and common diagnostic pitfalls. *Clin. Radiol.* 76, 470.e1–470.e12. doi:10.1016/j.crad.2021.01.009

Liu, H. (2021). Emerging agents and regimens for AML. *J. Hematol. Oncol.* 14, 49. doi:10.1186/s13045-021-01062-w

Liu, M., Ma, W., Li, Q., Zhao, D., Shao, X., Huang, Q., et al. (2019). Aptamer-targeted DNA nanostructures with doxorubicin to treat protein tyrosine kinase 7-positive tumours. *Cell Prolif.* 52, e12511. doi:10.1111/cpr.12511

Liu, S., Yu, B., Wang, S., Shen, Y., and Cong, H. (2020). Preparation, surface functionalization and application of Fe3O4 magnetic nanoparticles. *Adv. colloid Interface Sci.* 281, 102165. doi:10.1016/j.cis.2020.102165

Ljungman, P., de la Camara, R., Robin, C., Crocchiolo, R., Hermann, E., Hill, J. A., et al. (2019). Guidelines for the management of cytomegalovirus infection in patients with haematological malignancies and after stem cell transplantation from the 2017 European Conference on Infections in Leukaemia (ECIL 7). *Lancet Infect. Dis.* 19, e260–e272. doi:10.1016/S1473-3099(19)30107-0

Lo, S.-C., Pripuzova, N., Li, B., Komaroff, A. L., Hung, G.-C., Wang, R., et al. (2010). Detection of MLV-related virus gene sequences in blood of patients with chronic fatigue syndrome and healthy blood donors. *Proc. Natl. Acad. Sci.* 107, 15874–15879. doi:10.1073/pnas.1006901107

Lu, A.-H., Salabas, E., and Schüth, F. (2007). Magnetic nanoparticles: Synthesis, protection, functionalization, and application. *Angew. Chem. Int. Ed.* 46, 1222–1244. doi:10.1002/anie.200602866

Mammatas, L. H., Verheul, H. M. W., Harry Hendrikse, N., Yaqub, M., Lammertsma, A. A., and Menke-van der Houven van Oordt, C. W. (2015). Molecular imaging of targeted therapies with positron emission tomography: The visualization of personalized cancer care. *Cell. Oncol.* 38, 49–64. doi:10.1007/s13402-014-0194-4

Manthawornsiri, Y., Polpanich, D., Yamkamon, V., Thiramanas, R., Hongeng, S., Rerkamnuaychoke, B., et al. (2016). Magnetic nanoparticles PCR enzyme-linked gene assay for quantitative detection of BCR/ABL fusion gene in chronic myelogenous leukemia. *J. Clin. Laboratory Analysis* 30, 534–542. doi:10.1002/jcla.21899

Mayerhoefer, M. E., Archibald, S. J., Messiou, C., Staudenherz, A., Berzaczy, D., and Schöder, H. (2020). MRI and PET/MRI in hematologic malignancies. *J. Magnetic Reson. Imaging* 51, 1325–1335. doi:10.1002/jmri.26848

McDonald, R. J., McDonald, J.r S., Kallmes, D. F., Jentoft, M. E., Murray, D. L., KentThielen, R., et al. (2015). Intracranial gadolinium deposition after contrast-enhanced MR imaging. *Radiology* 275, 772–782. doi:10.1148/radiol.15150025

Mohammadi, A., Barikani, M., and Barmar, M. (2013). Effect of surface modification of Fe 3 O 4 nanoparticles on thermal and mechanical properties of magnetic polyurethane elastomer nanocomposites. *J. Mater. Sci.* 48, 7493–7502. doi:10.1007/s10853-013-7563-7

Na, H. B., Song, C., and Hyeon, T. (2009). Inorganic nanoparticles for MRI contrast agents. *Adv. Mater.* 21, 2133–2148. doi:10.1002/adma.200802366

Nagaraju, G. P., Srivani, G., Dariya, B., Chalikonda, G., Farran, B., Kumar Behera, S., et al. (2021). Nanoparticles guided drug delivery and imaging in gastric cancer. *Seminars Cancer Biol.* 69, 69–76. Elsevier. doi:10.1016/j.semcancer.2020.01.006

Neuwelt, E. A., Hamilton, B. E., Varallyay, C. G., Rooney, W. R., Edelman, R. D., Jacobs, P. M., et al. (2009). Ultrasmall superparamagnetic iron oxides (USPIOs): A future alternative magnetic resonance (MR) contrast agent for patients at risk for nephrogenic systemic fibrosis (NSF)? *Kidney Int.* 75, 465–474. doi:10.1038/ki.2008.496

Newell, L. F., and Cook, R. J. (2021). Advances in acute myeloid leukemia. *Bmj* 375, n2026. doi:10.1136/bmj.n2026

Pant, M., and Bhatt, V. R. (2017). Early mortality and survival in older adults with acute myeloid leukemia. *Future Med.* 6 (3), 61–63. doi:10.2217/ijh-2017-0013

Patra, J. K., Das, G., Fernandes Fraceto, L., Campos, E. V. R., Rodriguez-Torres, M. P., Acosta-Torres, L. S., et al. (2018). Nano based drug delivery systems: Recent developments and future prospects. *J. nanobiotechnology* 16, 71–33. doi:10.1186/s12951-018-0392-8

Pavlů, J., and Apperley, J. F. (2013). Allogeneic stem cell transplantation for chronic myeloid leukemia. *Curr. Hematol. malignancy Rep.* 8, 43–51. doi:10.1007/s11899-012-0149-7

Peccatori, J., and Ciceri, F. (2010). Allogeneic stem cell transplantation for acute myeloid leukemia. *Haematologica* 95, 857–859. doi:10.3324/haematol.2010.023184

Quynh, L. M., Dung, C. T., Mai, B. T., Huy, H. V., Loc, N. Q., Hoa, N. Q., et al. (2018). Development of Fe3O4/Ag core/shell-based multifunctional immunomagnetic nanoparticles for isolation and detection of CD34+ stem cells. *J. Immunoass. Immunochem.* 39, 308–322. doi:10.1080/15321819.2018.1488725

Rashid, Z., Shokri, F., Abbasi, A., Khoobi, M., and Zarnani, A.-H. (2020). Surface modification and bioconjugation of anti-CD4 monoclonal antibody to magnetic nanoparticles as a highly efficient affinity adsorbent for positive selection of peripheral blood T CD4+ lymphocytes. *Int. J. Biol. Macromol.* 161, 729–737. doi:10.1016/j.ijbiomac.2020.05.264

Reguera, J., de Aberasturi, D. J., Henriksen-Lacey, M., Langer, J., Espinosa, A., Szczupak, B., et al. (2017). Janus plasmonic–magnetic gold–iron oxide nanoparticles as contrast agents for multimodal imaging. *Nanoscale* 9, 9467–9480. doi:10.1039/c7nr01406f

Robinson, P. J., Dunnill, P., and Lilly, M. D. (1973). The properties of magnetic supports in relation to immobilized enzyme reactors. *Biotechnol. Bioeng.* 15, 603–606. doi:10.1002/bit.260150318

Sang, L., Li, J., Zhang, F., Jia, J., Zhang, J., Ding, P., et al. (2022). Glycyrrhetinic acid modified chlorambucil prodrug for hepatocellular carcinoma treatment based on DNA replication and tumor microenvironment. *Colloids Surfaces B Biointerfaces* 220, 112864. doi:10.1016/j.colsurfb.2022.112864

Sharifi, M., Reza Avadi, M., Attar, F., Dashtestani, F., Ghorchian, H., Rezayat, S. M., et al. (2019). Cancer diagnosis using nanomaterials based electrochemical nanobiosensors. *Biosens. Bioelectron.* 126, 773–784. doi:10.1016/j.bios.2018.11.026

Shen, Y., Wu, C., Uyeda, T.Q. P., Plaza, G. R., Liu, B., Han, Yu, et al. (2017). Elongated nanoparticle aggregates in cancer cells for mechanical destruction with low frequency rotating magnetic field. *Theranostics* 7, 1735–1748. doi:10.7150/thno.18352

Shen, Z., Song, J., Bryant, C. Y., Zhou, Z., Wu, A., and Chen, X. (2018). Emerging strategies of cancer therapy based on ferroptosis. *Adv. Mater.* 30, 1704007. doi:10.1002/adma.201704007

Short, N. J., Rytting, M. E., and Cortes, J. E. (2018). Acute myeloid leukaemia. *Lancet* 392, 593–606. doi:10.1016/S0140-6736(18)31041-9

Shuvaev, S., Akam, E., and Peter, C. (2021). Molecular MR contrast agents. *Investig. Radiol.* 56, 20–34. doi:10.1097/RLI.0000000000000731

Siegel, R. L., Miller, K. D., and Jemal, A. (2019). Cancer statistics, 2019. *CA a cancer J. Clin.* 69, 7–34. doi:10.3322/caac.21551

Sodipo, B. K., and Aziz, A. A. (2016). Recent advances in synthesis and surface modification of superparamagnetic iron oxide nanoparticles with silica. *J. Magnetism Magnetic Mater.* 416, 275–291. doi:10.1016/j.jmmm.2016.05.019

Song, C., Sun, W., Xiao, Y., and Shi, X. (2019). Ultrasmall iron oxide nanoparticles: Synthesis, surface modification, assembly, and biomedical applications. *Drug Discov. today* 24, 835–844. doi:10.1016/j.drudis.2019.01.001

Spirou, S. V., Basini, M., Lascialfari, A., Sangregorio, C., and Innocenti, C. (2018). Magnetic hyperthermia and radiation therapy: Radiobiological principles and current practice. *Nanomaterials* 8, 401. doi:10.3390/nano8060401

Travis, L. B., Andersson, M., Gospodarowicz, M., Van Leeuwen, F. E., Bergfeldt, K., Lynch, C. F., et al. (2000). Treatment-associated leukemia following testicular cancer. *J. Natl. Cancer Inst.* 92, 1165–1171. doi:10.1093/jnci/92.14.1165

Trujillo-Alonso, V., Pratt, E. C., Zong, H., Lara-Martinez, A., Kaittanis, C., Rabie, M. O., et al. (2019). FDA-approved ferumoxytol displays anti-leukaemia efficacy against cells with low ferroportin levels. *Nat. Nanotechnol.* 14, 616–622. doi:10.1038/s41565-019-0406-1

Walter, R. B. (2022). Where do we stand with radioimmunotherapy for acute myeloid leukemia? *Expert Opin. Biol. Ther.* 22, 555–561. doi:10.1080/14712598.2022.2060735

Wang, J., Chen, B., Cheng, J., Cai, X., Xia, G., Liu, R., et al. (2011). Apoptotic mechanism of human leukemia K562/A02 cells induced by magnetic iron oxide nanoparticles co-loaded with daunorubicin and 5-bromotetrandrin. *Int. J. nanomedicine* 6, 1027–1034. doi:10.2147/IJN.S18023

Wang, L., Chen, B., Lin, M., Cao, Y., Chen, Y., Chen, X., et al. (2015). Decreased expression of nucleophosmin/B23 increases drug sensitivity of adriamycin-resistant Molt-4 leukemia cells through mdr-1 regulation and Akt/mTOR signaling. *Immunobiology* 220, 331–340. doi:10.1016/j.imbio.2014.10.015

Wang, S., Luo, J., Zhang, Z., Dong, D., Shen, Y., Fang, Y., et al. (2018). Iron and magnetic: New research direction of the ferroptosis-based cancer therapy. *Am. J. Cancer Res.* 8, 1933–1946.

Wei, H., and Wang, E. (2013). Nanomaterials with enzyme-like characteristics (nanozymes): Next-generation artificial enzymes. *Chem. Soc. Rev.* 42, 6060–6093. doi:10.1039/c3cs35486e

Wen, Q., Wang, S., Yan, J., Cong, L., Chen, Y., and Xi, H. (2014). Porous nitrogen-doped carbon nanosheet on graphene as metal-free catalyst for oxygen reduction reaction in air-cathode microbial fuel cells. *Bioelectrochemistry* 95, 23–28. doi:10.1016/j.bioelechem.2013.10.007

Wicki, A., Witzigmann, D., Balasubramanian, V., and Huwyler, J. (2015). Nanomedicine in cancer therapy: Challenges, opportunities, and clinical applications. *J. Control. release* 200, 138–157. doi:10.1016/j.jconrel.2014.12.030

Winandy, S., Wu, P., and Georgopoulos, K. (1995). A dominant mutation in the Ikaros gene leads to rapid development of leukemia and lymphoma. *Cell* 83, 289–299. doi:10.1016/0092-8674(95)90170-1

Xie, W., Guo, Z., Gao, F., Gao, Q., Wang, D., Liaw, B., et al. (2018). Shape-size- and structure-controlled synthesis and biocompatibility of iron oxide nanoparticles for magnetic theranostics. *Theranostics* 8, 3284–3307. doi:10.7150/thno.25220

Yang, L., Krefting, I., Gorovets, A., Marzella, L., Kaiser, J., Boucher, R., et al. (2012). Nephrogenic systemic fibrosis and class labeling of gadolinium-based contrast agents by the Food and Drug Administration. *Radiology* 265, 248–253. doi:10.1148/radiol.12112783

You, N., Wang, X.-F., Li, J.-Y., Fan, H.-T., Shen, H., and Zhang, Q. (2019). Synergistic removal of arsanilic acid using adsorption and magnetic separation technique based on Fe3O4@ graphene nanocomposite. *J. Industrial Eng. Chem.* 70, 346–354. doi:10.1016/j.jiec.2018.10.035

Zhao, Y., Chen, X., and Feng, S. (2019). Autologous hematopoietic stem cell transplantation in acute myelogenous leukemia. *Biol. Blood Marrow Transplant.* 25, e285–e292. doi:10.1016/j.bbmt.2019.04.027

Zheng, X., Fan, X., Fu, B., Zheng, M., Zhang, A., Zhong, K., et al. (2017). EpCAM inhibition sensitizes chemoresistant leukemia to immune surveillance. *Cancer Res.* 77, 482–493. doi:10.1158/0008-5472.CAN-16-0842

frontiers | Frontiers in Bioengineering and Biotechnology

TYPE Original Research
PUBLISHED 05 May 2023
DOI 10.3389/fbioe.2023.1176369

OPEN ACCESS

EDITED BY
Chao Yin,
Nanjing University of Posts and Telecommunications, China

REVIEWED BY
Chen Xie,
Nanjing University of Posts and Telecommunications, China
Kunyu Zhang,
South China University of Technology, China
Zhen Yang,
Fujian Normal University, China
Cao Cui,
Xiangyang Central Hospital, China

*CORRESPONDENCE
Fei Lin,
linfei@gxmu.edu.cn

†These authors have contributed equally to this work

RECEIVED 02 March 2023
ACCEPTED 24 April 2023
PUBLISHED 05 May 2023

CITATION
He X, Li Z, Ye M, Zhao C, Wu S, Qin Y, Guo Y, Zhang L and Lin F (2023), Near-infrared laser-irradiated upconversion nanoparticles with dexamethasone precise released for alleviating lung ischemia-reperfusion injury.
Front. Bioeng. Biotechnol. 11:1176369.
doi: 10.3389/fbioe.2023.1176369

Near-infrared laser-irradiated upconversion nanoparticles with dexamethasone precise released for alleviating lung ischemia-reperfusion injury

Xiaojing He[1,2,3,4†], Zhining Li[1†], Mengling Ye[1,3,4], Chen Zhao[1,2,3,4], Siyi Wu[1,2,3,4], Yi Qin[1,2,3,4], Youyuan Guo[1,2,3,4], Lu Zhang[1,2,3,4] and Fei Lin[1,2,3,4*]

[1]Guangxi Medical University Cancer Hospital, Nanning, China, [2]Guangxi Clinical Research Center for Anesthesiology, Nanning, China, [3]Guangxi Engineering Research Center for Tissue & Organ Injury and Repair Medicine, Nanning, China, [4]Guangxi Key Laboratory for Basic Science and Prevention of Perioperative Organ Disfunction, Nanning, China

Introduction: Dexamethasone (DEX), as an important enduring-effect glucocorticoid (GC), holds great promise in the field of lung ischemia-reperfusion injury (LIRI) comprehensive therapy owing to its immunomodulatory properties, such as inducing apoptosis and cell cycle distribution. However, its potent anti-inflammatory application is still restricted because of multiple internal physiologic barriers.

Methods: Herein, we developed upconversion nanoparticles (UCNPs) coated with photosensitizer/capping agent/fluorescent probe-modified mesoporous silica (UCNPs@mSiO$_2$[DEX]-Py/β-CD/FITC, USDPFs) for precise DEX release synergistic LIRI comprehensive therapy. The UCNPs were designed by covering an inert YOF:Yb shell on the YOF:Yb, Tm core to achieve high-intensity blue and red upconversion emission upon Near-Infrared (NIR) laser irradiation.

Results: Under suitable compatibility conditions, the molecular structure of photosensitizer can be damaged along with capping agent shedding, which endowed USDPFs with an outstanding capability to carry out DEX release controlling and fluorescent indicator targeting. Furthermore, the hybrid encapsulating of DEX significantly increased utilization of nano-drugs, improving the water solubility and bioavailability, which was conducive to developing the anti-inflammatory performance of USDPFs in the complex clinical environment.

Discussion: The response-controlled release of DEX in the intrapulmonary microenvironment can reduce normal cell damage, which can effectively avoid the side effects of nano-drugs in anti-inflammatory application. Meanwhile, the multi-wavelength of UCNPs endowed nano-drugs with the fluorescence emission imaging capacity in an intrapulmonary microenvironment, providing precise guidance for LIRI.

KEYWORDS

dexamethasone, upconversion nanoparticles, near-infrared, response-controlled release, inflammation, lung ischemia-reperfusion injury

1 Introduction

Arising after lung transplantation surgery, the pathogenesis of local acute inflammation such as lung ischemia-reperfusion injury (LIRI) is extremely complex, including an inflammatory cascade, programmed cell death, and oxidative stress(Ng et al., 2005; Ng et al., 2006). Besides, inflammatory cells (e.g., alveolar macrophages and neutrophils) are activated to secrete large amounts of inflammatory factors, which will lead to excessive uncontrolled inflammation and tissue damage(Fiser et al., 2002). Glucocorticoids (GC) are potent anti-inflammatory agents with the ability to provide a variety of anti-inflammatory, anti-edematous and pulmonary vasodilatory effects through genomic and non-genomic mechanisms(Peter et al., 2008; Coutinho and Chapman, 2011; Zhang et al., 2015). Dexamethasone (DEX), one of the most commonly used glucocorticoids, has been shown in clinical data to reduce tissue injury by decreasing the secretion of pro-inflammatory factors and inhibiting apoptosis (Aktas et al., 2017). Postoperative studies in LIRI have shown that DEX not only reduces sepsis-related lung damage (Kuwajima et al., 2019), but also reduces inflammation by attenuating the activity of the JAK2/STAT3 signaling pathway and increasing the expression of ICAM-1, thereby protecting lungs from severe acute pancreas inflammation-related lung injury (Han et al., 2016). For this reason, DEX is one of the good alternative drugs used to ameliorate the local acute inflammation generated after LIRI. However, the clinical application of DEX is due to its poor water solubility, low bioavailability and side effects on the body (Caplan et al., 2017). Therefore, it is urgent to address the issue of DEX precise release for therapeutic use in the intrapulmonary microenvironment after LIRI.

To overcome the multiple adverse effects arising from the release of drugs *in vivo* prior to treatment, various mesoporous silica ($mSiO_2$)-based nano-drug delivery approaches have been widely reported (Spahn et al., 2015; Tian et al., 2015; Eskandari et al., 2019). However, the practical application of these protocols remains limited due to the lack of control over the trace images displayed *in vivo*, as well as the amount and time of drug release. Recently, upconversion nanoparticles (UCNPs) accompanied by rare earth element (Ln) doping have shown promising prospects due to their applications in bioimaging and optical therapy features (Yuan et al., 2014; Song et al., 2022). As a suitable host material for hexagonal crystalline systems, YOFs convert near-infrared light to UV-visible light by doping with Yb^{3+}/Tm^{3+} ionic couples (Yi et al., 2011; Suo et al., 2016; Lee et al., 2017).

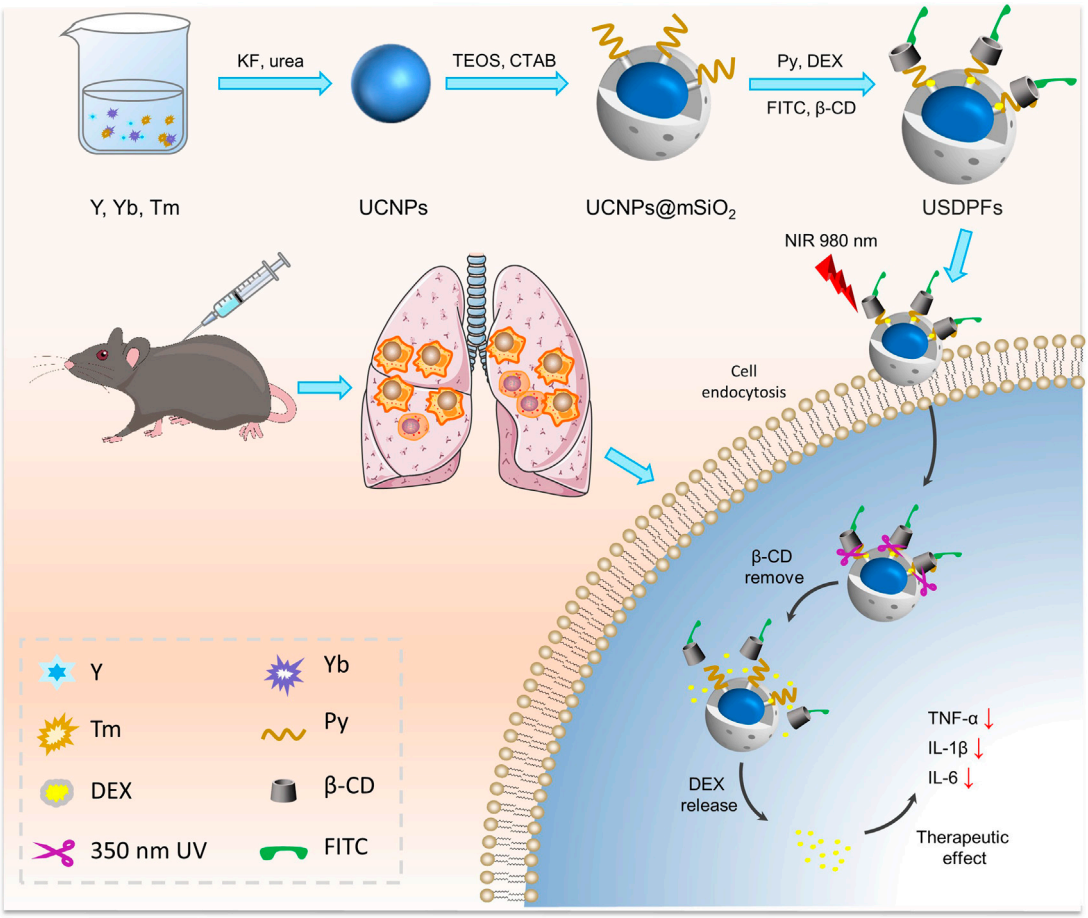

FIGURE 1
Schematic synthesis process and theranostic mechanism of nano-drugs for LIRI comprehensive therapy.

Meanwhile, the surface inert layer can further reduce the defect quenching and enhance the luminescence quality (Ma et al., 2018; Lu et al., 2019). Further, the good biocompatibility of UCNPs guarantees for biomedical applications such as drug delivery and cancer therapy (Xiang et al., 2018; Yan et al., 2021). The $mSiO_2$ can be effectively coated on the surface of upconversion nanoparticles (UCNPs), which is very beneficial to achieve surface functionalization of particles and optimize their properties for biomedical applications (Liu et al., 2019). The terminal methyl pyrrole of pyrene conjugated β-cyclodextrin (β-CD), as a pair of molecular capping agent couple, is often used to seal the pores of $mSiO_2$ (Indrajit et al., 2010; Wang et al., 2017). In the presence of near-infrared light absorption, the ester bond adjoining the pyrene chromophore is broken and accompanied by the shedding of β-CD, resulting in the release of drugs from the $mSiO_2$ pores (Liu et al., 2019). The photoswitching effect can play a significant role in the controlled release of nano-drugs and localization imaging.

In this study, YOF:Yb^{3+}/Tm^{3+} UCNPs were encapsulated in $mSiO_2$, then modified by γ-Oxo-1-pyrenebutyricacid (Py) and loaded with DEX, and finally capped with β-CD, which was labeled with fluorescein isothiocyanate (FITC), to construct YOF:Yb^{3+}/Tm^{3+}@YOF:Yb^{3+}@$mSiO_2$(DEX)-Py/β-CD/FITC nanohybrids (USDPFs). Under NIR irradiation, UV light from UCNPs upconversion emission breaks the ester bond adjoining the pyrene chromophore bond and promotes the detachment of nanovalve β-CD for encapsulated drug release. As a fluorescent marker, FITC can be employed to label and trace nanoparticles *in vivo* and *in vitro*. In addition, $mSiO_2$ coating and β-CD coupling can also improve the biocompatibility of nanocomposites, providing security for anti-inflammatory therapy after LIRI.

2 Materials and methods

2.1 Materials

Yttrium oxide (Y_2O_3), Ytterbium oxide (Yb_2O_3), Thulium oxide (Tm_2O_3), Potassium fluoride (KF), Urea (CH_4N_2O), Anhydrous ethanol, Tetraethylorthosilicate (TEOS), Cetyltrimethylammonium bromide (CTAB), N,N-Dimethylformamide (DMF), (3-dimethylaminopropyl)ethyl-carbodiimidmonohydrochloride (EDC), Beta-cyclodextrin (β-CD), Fluorescein isothiocyanate (FITC), Dexamethasone (DEX), γ-Oxo-1-pyrenebutyricacid (Py), and 3-Aminopropyltriethoxysilane (ATPES) were purchased from Aladdin Biochemical Technology Co. Ltd. Concentrated nitric acid, Ammonium Hydroxide ($NH_3{\cdot}H_2O$), and Acetone were bought from Sinopharm Chemical Reagent Co. Ltd. All reagents were analytical grade, and the deionized water was obtained by ultrapure water mechanism (Vent Filter MPK01, Merck Millipore).

Cell Counting Kit-8 was ordered from Beyotime. Mounting Medium, antifading (with DAPI), Calcein-AM/PI live cell/dead cell double staining kit, Triton X-100, Hematoxylin-Eosin/HE Staining Kit were obtained from Solarbio Life Sciences. Enzyme-linked immunosorbent assay (ELISA) kits for the detection of inflammatory factors (IL-1β, IL-6 and TNF-α) were obtained from Elabscience Biotechnology. Dulbecco's Modified Eagle Medium (DMEM, with or without high glucose, L-glutamine, phenol red, sodium pyruvate), Fetal bovine serum (FBS), were purchased from Gibco. RAW264.7, mouse mononuclear macrophage leukemia cells, tissue source of male Abelson mouse leukemia virus-induced tumors, were purchased from Procell Life Science&Technology Co. Ltd.

C57BL/6 mice, clean grade, 7–9 weeks old, weighing about 20–25 g, were purchased from the Experimental Animal Center of Guangxi Medical University. The mice were housed in an SPF-grade animal laboratory, with normal feeding, free access to water, and an ambient temperature of about 23°C. All animal protocols conformed to the animal guidelines of the Institutional Animal Care and Use Committee of Guangxi Medical University.

2.2 Characterization

Transmission electron microscopy (TEM) images were observed on an electron microscope (JEM-3010, JEOL). UV/Vis spectra were acquired with a UV/Vis spectrophotometer (UV-2600, Shimadzu). Fourier transform infrared (FT-IR) spectrum was recorded on a FT-IR spectrometer (Nicolet iS10, Thermo Fisher Scientific). Cell viability was obtained by a microplate reader (Infinite M Plex, Tecan). Fluorescence

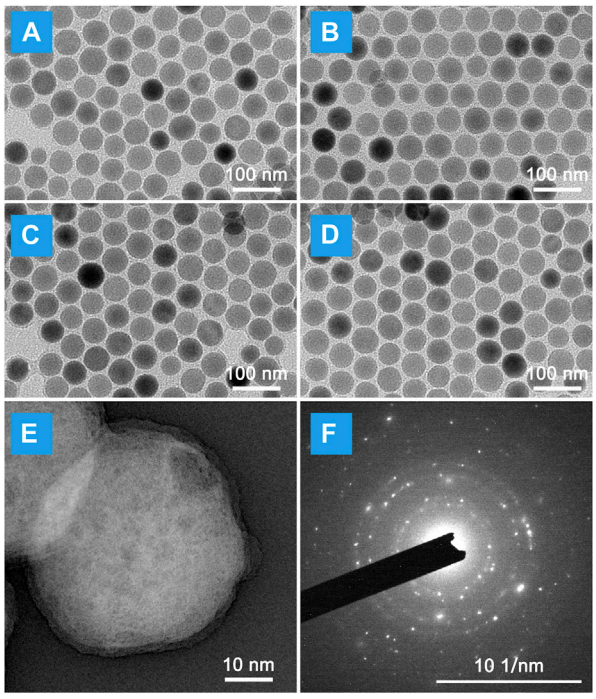

FIGURE 2
Micromorphology of LIRI comprehensive therapeutic nano-drugs at each synthesis process. TEM images of **(A)** UCNPs; **(B)** UCNPs@$mSiO_2$; **(C)** UCNPs@$mSiO_2$-Py; **(D)** UCNPs@$mSiO_2$(DEX)-Py/β-CD/FITC (USDPFs). **(E)** STEM image and **(F)** Selected area electron diffraction (SAED) of USDPFs.

microscopy results were evaluated by fluorescence microscopy (LSM 980, ZEISS).

2.3 Synthesis of $Y(OH)_x(CO_3)_yF_z$:Yb/Tm@ $Y(OH)_x(CO_3)_yF_z$:Yb precursors

Y_2O_3 (0.695 mmol), Yb_2O_3 (0.30 mmol), Tm_2O_3 (0.005 mmol), nitric acid, and ultrapure water were prepared for rare earth nitrate solution. Then, 1 ml of $Y(NO_3)_3$, 1 ml of $Yb(NO_3)_3$, 1 ml of $Tm(NO_3)_3$, 0.0581 g (1 mmol) of KF, and 3 g (0.05 mmol) of urea were added to a beaker. The beaker was volume fixed with ultrapure water to 50 ml and stirred for 5 min until the powder was completely dissolved. The beaker was placed in a constant temperature water bath and maintained at 90°C for 3 h. After the co-precipitation reaction, white flocculent precipitates were obtained at the bottom of the vessel. Then the beaker was taken out and cooled to room temperature. Afterwards, the precipitates were thoroughly cleaned 3 times with ultra-pure water and anhydrous ethanol, respectively. After drying overnight, the precursor $Y(OH)_x(CO_3)_yF_z$:Yb/Tm@$Y(OH)_x(CO_3)_yF_z$:Yb was finally obtained.

2.4 Synthesis of YOF:Yb/Tm@YOF:Yb@ $mSiO_2$ (UCNPs@$mSiO_2$)

The precursor polymer was calcined at 700°C for 3 h to obtain YOF:Yb/Tm@YOF:Yb (UCNPs) for particle size analysis and long-range stability experiments. 0.2 g of precursor polymer, diluted with 50 ml absolute ethanol and 70 ml ultra-pure water. Add 0.3 g of cetyltrimethylammonium bromide (CTAB), 300 μL of ethyl orthosilicate (TEOS), and 1 ml of concentrated ammonia to the mixture in turn. The mixture was stirred until the substance was completely dissolved, followed by magnetic stirring at 25°C for 6 h. After centrifugation, the precipitates were cleaned with ultrapure water and anhydrous ethanol. Subsequently, the dried product was calcined at 700°C for 3 h to produce the core-shell structure product UCNPs@$mSiO_2$.

2.5 Synthesis of UCNPs@$mSiO_2$-Py

1.8 g of UCNPs@$mSiO_2$ was dissolved in 20 ml of NaOH solution (1 M), stirred continuously for 8 h, and dried in an oven (60 °C) overnight. Afterwards, the products were dispersed in a mixed solution of 70 ml deionized water and 20 ml APTES and stirred for 8 h at 55°C. The precipitate was gathered by centrifugation, and the precipitate was alternately cleaned with anhydrous ethanol and ultrapure water for 3 times. Finally, the product UCNPs@$mSiO_2$-NH_2 was obtained after drying at 60°C for 12 h. UCNPs@$mSiO_2$-NH_2 was added to an ethanol solution containing Py (10 mM) and EDC (50 mM), then stirred for 12 h at 50°C. The precipitation was recovered by centrifugation and washed thoroughly with ethanol to attained UCNPs@$mSiO_2$-Py.

2.6 UCNPs@$mSiO_2$-Py was loaded with DEX and modified by FITC-β-CD

50 mg β-CD was dissolved in 5 ml of anhydrous DMF, followed by adding 0.3 mM fluorescein isothiocyanate (FITC) and stirring at 30°C for 12 h. Acetone was added to the above solution to precipitate the precipitate and then precipitated by ethanol solution. After acetone was added, FITC/β-CD was collected by centrifugation and thoroughly cleaned with anhydrous ethanol.

DEX solution (10 ml, 1 mM) was added to a beaker containing UCNPs@$mSiO_2$-Py (100 mg). The mixture was dispersed by ultrasonic for 30 min and stirred continuously for 24 h to diffuse the drug into the nanopores of UCNPs@$mSiO_2$-Py. After that, the precipitates UCNPs@$mSiO_2$(DEX)-Py and supernatant were respectively gathered by centrifugation. Then, UCNPs@$mSiO_2$(DEX)-Py and FITC/β-CD (1 g) were added to a beaker and stirred continuously for 12 h. The precipitates UCNPs@$mSiO_2$(DEX)-Py/β-CD/FITC (USDPFs) were recovered by centrifugation, purified with ultrapure water, and dried in a drying oven. The amount of DEX in the supernatant was converted from the UV-Vis spectrum of DEX (absorbance at 291 nm).

2.7 DEX loading and releasing tests in USDPFs

DEX was dissolved in ultrapure water and diluted into different concentration gradients (500, 250, 125, 62.5, 31.25, 15.6, 0 μg ml^{-1}). The absorbance corresponding to each concentration gradient at 240 nm wavelength was detected with a UV spectrophotometer, and a standard curve for DEX was drawn.

Aspirate the supernatant in step 2.6, dilute it with ultrapure water, use an ultraviolet spectrophotometer to detect the absorbance at the wavelength of 240 nm, and calculate the concentration of free DEX in the supernatant according to the standard curve of DEX: Drug loading rate (%) = (Amount of drug added - The amount of drug in the supernatant)/Amount of nanocarriers. An appropriate amount of USDPFs was made into a suspension in ultrapure water. After irradiating it with 980 nm NIR for different gradient time, the absorbance at 240 nm wavelength was detected by ultraviolet spectrophotometer (UV/Vis spectrometer). Similarly, the content of DEX in the supernatant was figured out based on the standard curve of DEX, and the DEX release curve with the change of NIR irradiation time was drawn.

2.8 Biocompatibility of USDPFs evaluation

RAW264.7 cells with good growth status were incubated into 96~ well plates (seeding density: 2×10^3 cells/well) and cultured in an incubator (37°C, 5% CO_2) for 4 h. The cell culture medium in the corresponding wells was replaced with the medium containing different concentrations of USDPFs, so that the final concentration of USDPFs in each well plate decreased gradually (500, 250, 125, 62.5, 31.25, 15.625, 7.8125 μg ml^{-1}) and incubated for 24 h. Then, CCK-8 solution (10 μL per well) was added, and the cells were continued to be cultured for 3 h. Use a microtiter plate reader to read the absorbance (OD value) of each group of samples at 450 nm.

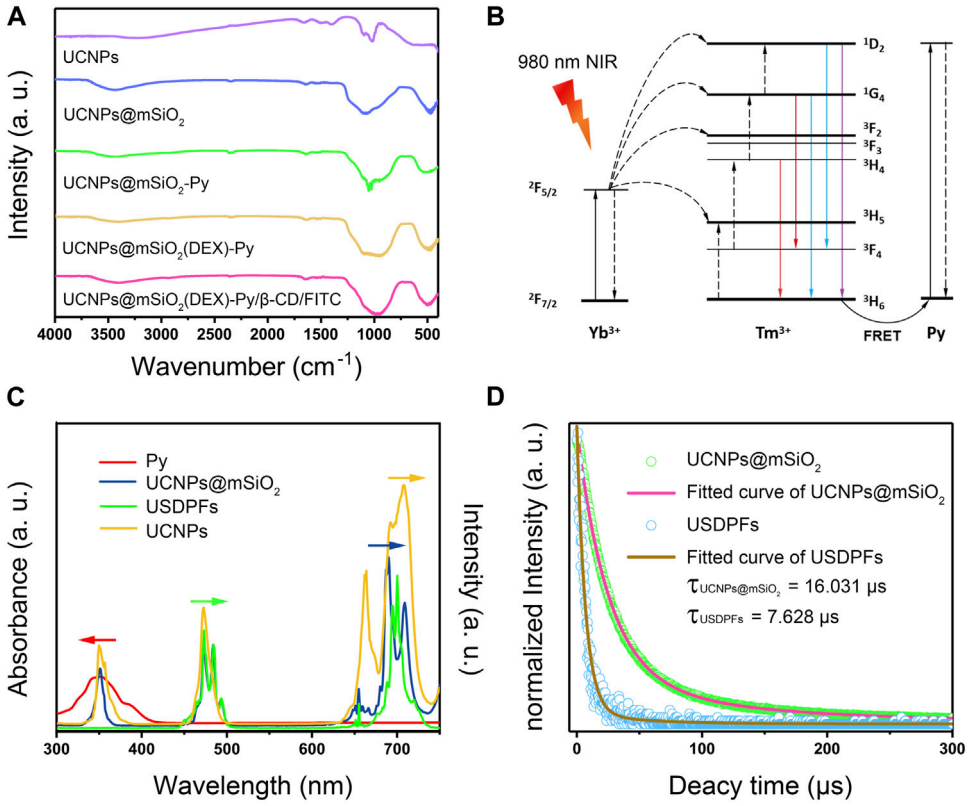

FIGURE 3
(A) FT-IR spectra of specimens in different synthesis steps; **(B)** Energy transfer mechanism between upconversion nanoparticles and light-responsive molecule Py; **(C)** UV-Vis absorption spectra of Py overlapped fluorescence emission spectra of UCNPs, UCNPs@mSiO$_2$ and USDPFs; **(D)** Fluorescence lifetime curve of UCNPs@mSiO$_2$ and USDPFs at 695 nm.

2.9 Hemolysis assay of USDPFs

Human whole blood was purified by centrifugation and washed with 1% normal saline several times to obtain red blood cells. Dilute red blood cells with PBS solution (pH 7.4), and add 200 μL USDPFs solution prepared in PBS solution, with a total volume of 4 ml. The concentrations of USDPFs were 7.8125 μg ml^{-1}, 15.625 μg ml^{-1}, 31.25 μg ml^{-1}, 62.5 μg ml^{-1}, 125 μg ml^{-1}, 250 μg ml^{-1}, and 500 μg ml^{-1}, respectively. The erythrocytes were cultured with USDPFs for 2 h at 37°C and centrifuged to obtain the supernatant. Then, read the absorbance of the supernatant of each group of samples at 541 nm. The equation Hemolysis % = (OD_{sample} − $OD_{control(-)}$)/($OD_{control(+)}$ − $OD_{control(-)}$) was employed on calculating the percent hemolysis of red blood cells, where OD presents the absorbance values of supernatants at 541 nm, $OD_{control(-)}$ means the negative control (RBC dissolved in PBS solution), and $OD_{control(+)}$ means the positive control (RBCs dissolved in ultrapure H_2O).

2.10 Cellular uptake of USDPFs sample

UCNPs, UCNPs@mSiO$_2$, and USDPFs were prepared with DMEM medium at a concentration of 50 μg ml^{-1}. RAW264.7 cells were co-cultured with these three solutions for 6 h. Then the cells were washed with PBS solution, labeled by adding DAPI fluorescent dye and observed under a confocal microscope.

2.11 *In vivo* safety evaluation of USDPFs

Normal saline and USDPFs (5 mg kg^{-1}) was injected into healthy male C57BL/6 mice by intratracheal administration, and the mice were sacrificed 2 weeks later. The main organs (heart, lung, liver, spleen, kidney) were collected for hematoxylin and eosin (H&E) staining. USDPFs (5 mg kg^{-1}) was injected into mice through intratracheal administration. After 1 day, 3 days, 7 days, 14 days, and 21 days, the mice were euthanized and lung tissues were collected for H&E staining. The morphological changes of organ tissues were observed under an optical microscope. Inject USDPFs (5 mg kg^{-1}) into the tail vein of mice for pharmacokinetic testing.

2.12 *In vivo* imaging effects of USDPFs

Normal saline, USDPFs (5 mg kg^{-1}) were injected into healthy C57BL/6 mice by intratracheal administration. *In vivo* fluorescence

imaging of USDPFs was recorded by taking pictures of mice with a small animal imager.

2.13 Anti-inflammatory effect of USDPFs in LIRI *in vitro* model

Referring to previous research (Wang et al., 2020), an oxygen-glucose deprivation and reperfusion (OGD/R) model was developed to simulate *in vitro* lung I/R. RAW264.7 cells were divided into a control group, USDPFs group, USDPFs + NIR group, OGD/R group, OGD/R + USDPFs group, and OGD/R + USDPFs + NIR group. OGD/R group: cells were incubated in a Whitley H35 Hypoxystation containing 1% O_2, 5% CO_2, and 94% N_2 at 37°C (Don Whitley Scientific, Bingley, UK) for 1 h. The used medium was then removed and a medium containing serum, high sugar and no antibiotics was added. Cells were continued to be cultured in a normal incubator for 6 h. Cells in all groups were precultured with USDPFs (50 μg ml^{-1}) for 6 h in addition to the control and OGD/R groups. After that, cells in the USDPFs + NIR group were irradiated with 980 nm NIR (10 min, 0.5 W cm^{-2}), and cells in the OGD/R + USDPFs + NIR group were irradiated with 980 nm NIR (10 min, 0.5 W cm^{-2}) after OGD/R. Biological transmission electron microscopy (Bio-TEM) of RAW264.7 Cells.

RAW264.7 cells in each group were collected, fixed with glutaraldehyde (3%) overnight and osmic acid (1%) for 2 h. The cells were subsequently dehydrated with acetone and embedded in resin. The samples were cut into ultra-thin slices and observed under a Bio-TEM (Hitachi H-7560, Tokyo, Japan).

2.13.1 Live/dead cell staining

RAW264.7 cells were seeded in 24-well plates (seeding density: 1×10^5 cells/well) and cultured for 4 h. Incubation was continued for 6 h after the addition of USDPFs (50 μg ml^{-1}). Then, the USDPFs that were not taken up by the cells were removed, and the cells were cultured for 24 h. After washing the cells three times with PBS buffer, add 50 μL of FDA (labeled live cells, green fluorescence, 8 μg ml^{-1}) and PI (labeled dead cells, red fluorescence, 20 μg ml^{-1} in PBS buffer to the cells) for 5 min. Discard the staining solution, add freshly prepared PBS buffer, and observe the cells under a fluorescence microscope.

2.13.2 Detection of inflammatory factors in cell supernatant by ELISA

The cell supernatants of each group were retained, and the expression of inflammatory factors (IL-1β, IL-6 and TNF-α) in the cell supernatant was measured separately by ELISA kits.

2.14 Anti-inflammatory effect of USDPFs in LIRI *in vivo* model

Thirty healthy clean-grade male C57BL/6 mice at 7–9 weeks, weighing about 20–25 g, were randomly divided into 6 groups (n = 5): Control group, USDPFs group, USDPFs + NIR group, I/R + USDPFs group, I/R + USDPFs + NIR group. Ischemia/reperfusion (I/R) group (based on a previous study (Liang et al., 2021)): the chest cavity was opened from the left chest of mice, and the left hilum was clamped for 1 h by a non-invasive vascular clamp (maintaining the state of ischemia and hypoxia). Then released the hemostatic clamp, opened the left hilum, and reperfusion for 6 h. Except for the control group and the I/R group, the mice in the other groups were given USDPFs suspension (5 mg kg^{-1}) by intratracheal injection 1 h before the operation. The mice in the USDPFs + NIR group were irradiated by 980 nm NIR (3 × 10 min, 1 W cm^{-2}) after 2 h of administration. The mice in the I/R + USDPFs + NIR group were irradiated by 980 nm NIR (3 × 10 min, 1 W cm^{-2}) after suturing the incision. After 6 h, mice were sacrificed by exsanguination. Serum and left lung tissue were collected. Similarly, after intratracheal injection of USDPFs (5 mg kg^{-1})

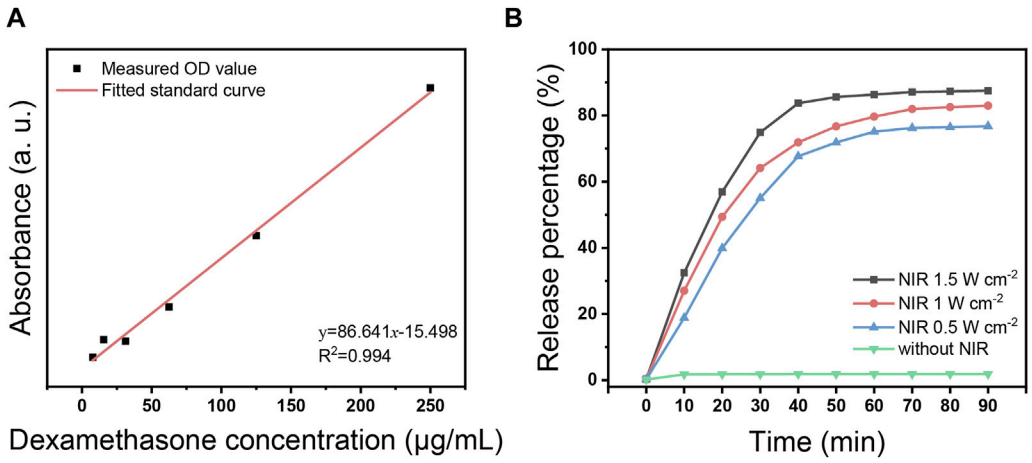

FIGURE 4
(A) Fitted standard curve of DEX in different concentrations; **(B)** DEX release curve with time under 980 nm NIR laser irradiation at different power.

and use of dexamethasone aerosol (DEX-A) in mice, pathological changes in lung tissue were observed.

2.14.1 H&E staining

Lung tissue samples were fixed with 4% paraformaldehyde, embedded in paraffin, sectioned, stained with H&E, and explored with a fluorescence microscope. Lung tissue damage was scored as described below, based on the accumulation or infiltration of inflammatory cells in the vessel wall or in the air spaces [1 = vessel wall only, 2 = small amount in alveolar space, 3 = moderate amount, 4 = severe (alveolar space congestion)], presenting alveolar hyaline and interstitial congestion [1 = normal, 2 = mild (>25% of the field), 3 = moderate (25–50% of the field) and 4 = severe (>50% of the field)], and with (1) or without (0) hemorrhage (Murray and Wynn, 2011). The scores of the above items were added to obtain the lung injury score of the sample.

2.14.2 Wet to dry weight ratio

The lung wet-to-dry (W/D) ratio was recorded to assess the degree of pulmonary edema. Fresh left lung tissue was gathered and weighed as wet weight instantly. Then, lung tissue samples were dried in a desiccator at 60°C for 48 h to a constant weight, recorded as dry weight, and the W/D ratio was calculated.

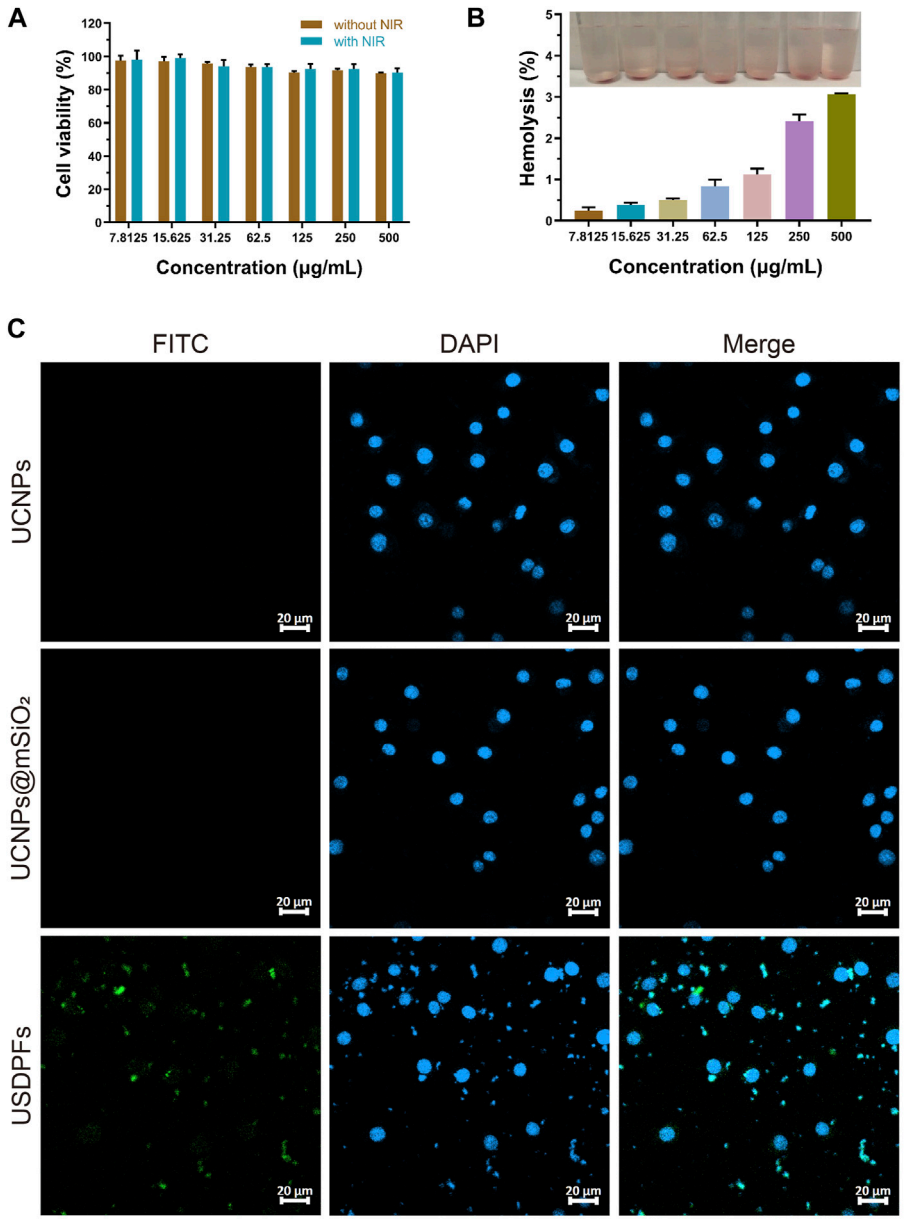

FIGURE 5
(A) Cell viability measurement of USDPFs with different concentrations; **(B)** Hemolysis test of USDPFs *in vitro*; **(C)** Cellular uptake of USDPFs (50 μg ml^{-1}) under CLSM observation (× 400, scale bar 20 μm).

2.14.3 Detection of inflammatory factors in serum and lung tissue by ELISA

Lung tissue was prepared as a tissue homogenate and serum was extracted from whole blood. The expressions of IL-1β, IL-6 and TNF-α in serum and lung tissue were detected by ELISA kits, respectively.

2.15 Statistical analysis

All data were dealt with the average of three independent experiments ± the standard deviation of the mean, Student's t-test or one-way analysis of variance (SPSS 22.0), which could be employed on analysing the significant difference between the means of the groups was statistically significant. Statistically significant differences existed between groups when $^{*}p < 0.05$.

3 Results and discussion

3.1 Preparation and analysis of the upconversion nanoparticles

The schematic of NIR laser-irradiated upconversion nanoparticles with DEX precise released for LIRI comprehensive therapy was shown in Figure 1. It can be interpreted that the key to the precise release of DEX *in vivo* depends on the design and synthesis of nano-drugs. As illustrated in Supplementary Figure S1, UCNPs have a uniform particle size distribution and good stability, and do not decompose and modify over a long resting period. As images observed in Figures 2A, B, there was no obvious change in morphology, although particle size increased slightly (~10 nm) after UCNPs coated $mSiO_2$, indicating that $mSiO_2$ layer was successfully tightly attached to UCNPs core. In Figures 2C, D, amorphous matter is obviously present on the surface of nanoparticles, which verifies that inorganic UCNPs@$mSiO_2$ can be wrapped by polymer layers. The resulting nanohybrid UCNPs@$mSiO_2$(DEX)-Py/β-CD/FITC (USDPFs) has a spherical morphology with a size of about 45–50 nm, uniform size and good monodispersity. In order to further investigate its crystallographic properties, STEM and SAED were measured simultaneously (Figures 2E, F). The results exhibited that the cladding structure was symmetry and the crystallinity was excellent.

Figure 3A proves the changes of functional groups on the surface of nanoparticles at different synthesis stages, indicating the successful coating and accurate synthesis of layer, which is consistent with the TEM results. The excellent coating effect provides a close enough distance for the interlayer fluorescence resonance energy transfer, energy level transition process was designed in Figure 3B. Yb^{3+} ions in UCNPs absorb 980 nm light and transmit photons to Er^{3+} ions for visible light emission. Meanwhile, by collaborating Förster resonance energy transfer (FRET) effect, some of the blue emission light is absorbed by Py, which can break the ester bond adjoining the pyrene chromophore bond. As explored in Figure 3C, the strongest emission of blue and red light is at 475 nm and 695 nm, corresponding to $^{1}G_4 \rightarrow {}^{3}H_6$ and $^{1}G_4 \rightarrow {}^{3}F_4$ transition emissions separately. (Pengpeng et al., 2019). Since Py is strongly absorbed around 350 nm, the absorption peak of USDPFs relative to UCNPs@$mSiO_2$ disappears in blue light emissions. Also, the visible emission intensity of fluorescence decreased slightly due to the increase of layer thickness on the nanohybrids. Moreover, the fluorescence lifetime of USDPFs was less than UCNPs@$mSiO_2$, which was consistent with the results of fluorescence intensity.

3.2 DEX loading and release of USDPFs nano-drugs

Figure 4A indicates the fitted standard curve of absorbance at 240 nm for different concentration gradients of DEX. Based on the absorbance of free DEX released from USDPFs, the drug loading rate was calculated to be 11.46%.

Figure 4B demonstrates the release of DEX from USDPFs after NIR irradiation. In the absence of NIR irradiation, the amount of DEX in the solution was almost zero; after NIR initiation, the release of DEX gradually increased with increasing irradiation time and irradiation power. The increase in DEX concentration was

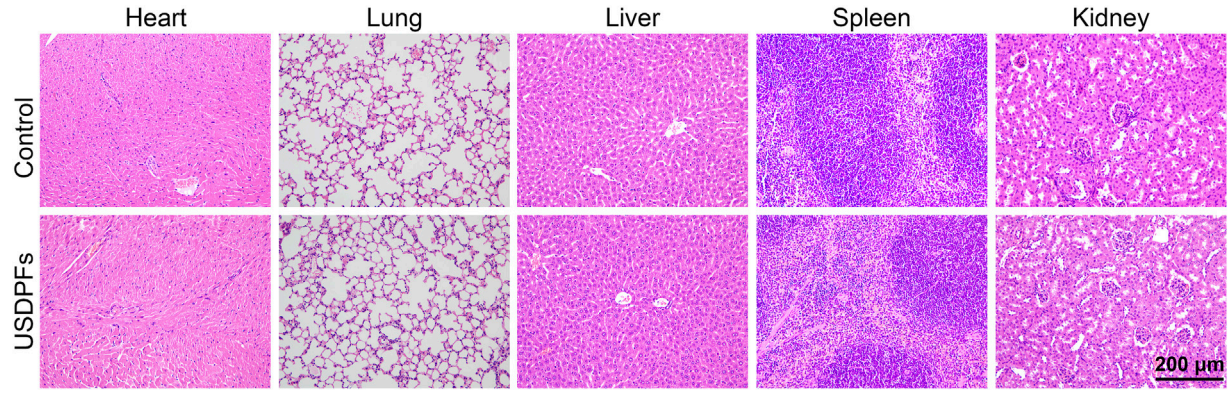

FIGURE 6
H&E staining of the heart, lung, liver, spleen and kidney of C57B/L6 mice 2 weeks after intratracheal injection of USDPFs (5 mg kg^{-1}) (× 200, scale bar 200 μm).

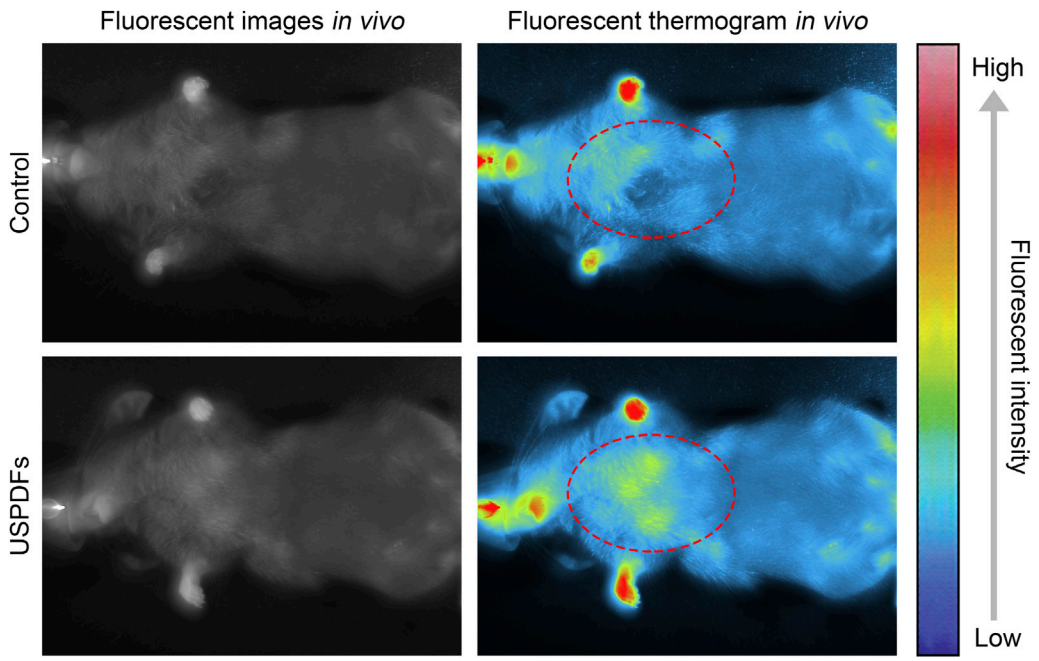

FIGURE 7
Small animal imager to observe the fluorescence imaging of USDPFs (5 mg kg^{-1}) in mice after intratracheal administration.

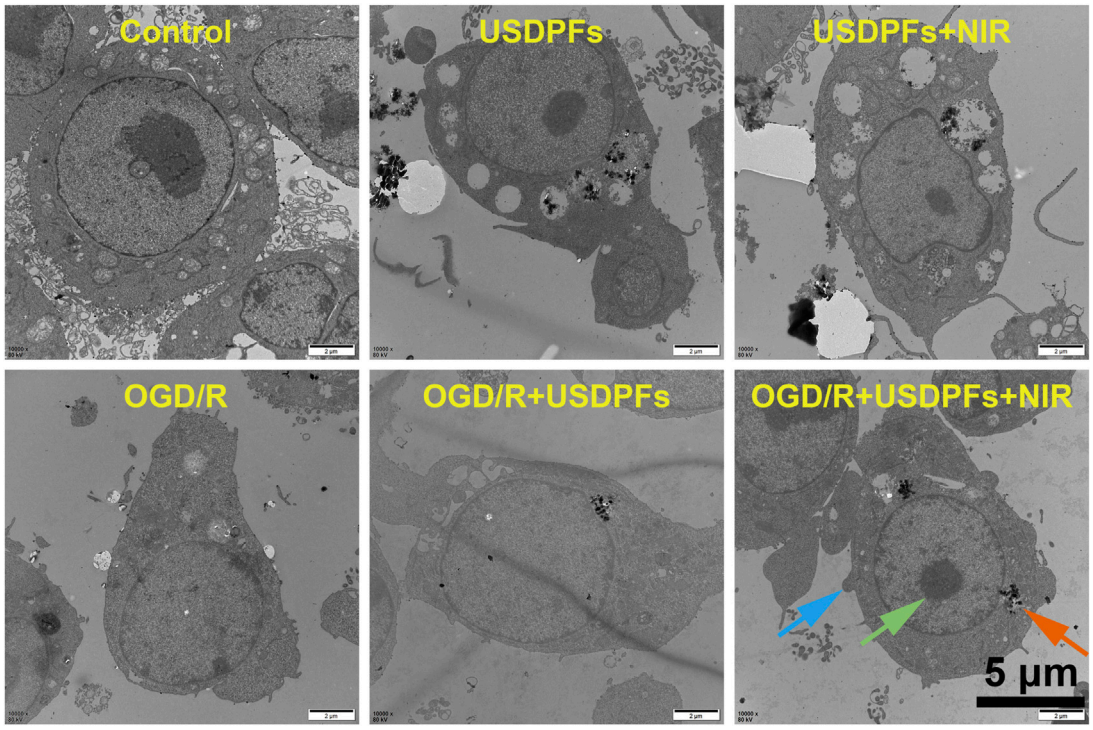

FIGURE 8
Ultrastructural changes of RAW264.7 cells in each group (×10000, scale bar 5 μm) (Cell processes are indicated by blue arrows, phagocytosis vesicles are indicated by orange arrows, and nucleoli are indicated by green arrows).

most pronounced when the irradiation time accumulated to 30 min, at which point the amount released was more than half. After the irradiation time accumulated to 40 min, the release was close to the peak; the release was up to 87.5% when accumulated to 90 min.

3.3 *In vitro* evaluation of biocompatibility, hemolysis, and cellular uptake of USDPFs

RAW264.7 cells were co-cultured with USDPFs and then subjected to CCK-8 assay to detect cell viability. The cell viability of each group decreased with increasing concentration of USDPFs, as explained in Figure 5A. To further test the biocompatibility of USDPFs, USDPFs were co-cultured with human erythrocytes for hemolysis assay. Figure 5B illustrates that the lysis of erythrocytes increased as the concentration of USDPFs increased. The above results indicate that the silica-coated and β-CD-modified USDPFs have high biosafety.

Figure 5C exhibits the results of the cellular uptake of USDPFs under confocal microscopy. DAPI stains the nuclei bright blue. A large number of USDPFs modified with FITC appear green under the microscope and surround the nucleus. Compared to UCNPs and UCNPs@mSiO_2, the biggest difference of USDPFs is the presence of polymer coating (β-CD). The encapsulation of β-CD resulted in better water solubility, lower cytotoxicity, and better biocompatibility of the nanomaterials (Liu et al., 2019). Both USDPFs (encapsulated with β-CD) and cell membranes are organic components. Therefore, USDPFs are more compatible with cell membranes and facilitate cell phagocytosis. These results further indicate that USDPFs have good cytocompatibility and can be largely endocytosed by RAW264.7 cells for stable coexistence and fusion.

3.4 *In vivo* safety evaluation and prolonged blood circulation of USDPFs

To evaluate the safety of USDPFs *in vivo*, healthy adult C57B/L6 mice were injected intratracheally with USDPFs. After 2 weeks, the major organs (heart, lung, liver, spleen, and kidney) of mice were collected for H&E staining. As given in Figure 6, the mice in the USDPFs group did not have inflammatory cell infiltration and tissue necrosis in the heart, lung, liver, spleen, and kidney compared with the control group. As shown in Supplementary Figure S2, after intratracheal administration of USDPFs for 1 day, 3 days, 7 days, 14 days, and 21 days, no significant damage was observed in the lung tissue pathology of the mice, indicating that the intratracheal administration of nanoparticles does no damage to lung tissues. These results indicated that USDPFs were not significantly toxic to some vital organs of mice and had good *in vivo* safety.

According to the references (Hu et al., 2019; Hu et al., 2021; Lu et al., 2023), an *in vivo* pharmacokinetics study of USDPFs (5 mg kg^{-1}) was conducted to demonstrate the prolonged blood circulation of the nanoplatform for exerting the enhanced permeability and retention (EPR) effect. As shown in Supplementary Figure S3, after intravenous injection, USDPFs remain for about 10 h and gradually decrease, indicating that the blood circulation time of USDPFs in the body is prolonged, exerting the EPR effect.

3.5 *In vivo* imaging evaluation of USDPFs

Healthy adult C57B/L6 mice were intratracheally injected with USDPFs, and fluorescence imaging of USDPFs in mice was observed under 980 nm NIR irradiation (Figure 7). The fluorescence in mice appeared bright white, and USDPFs showed stronger fluorescence in mice compared to controls. This strong fluorescence contrast is

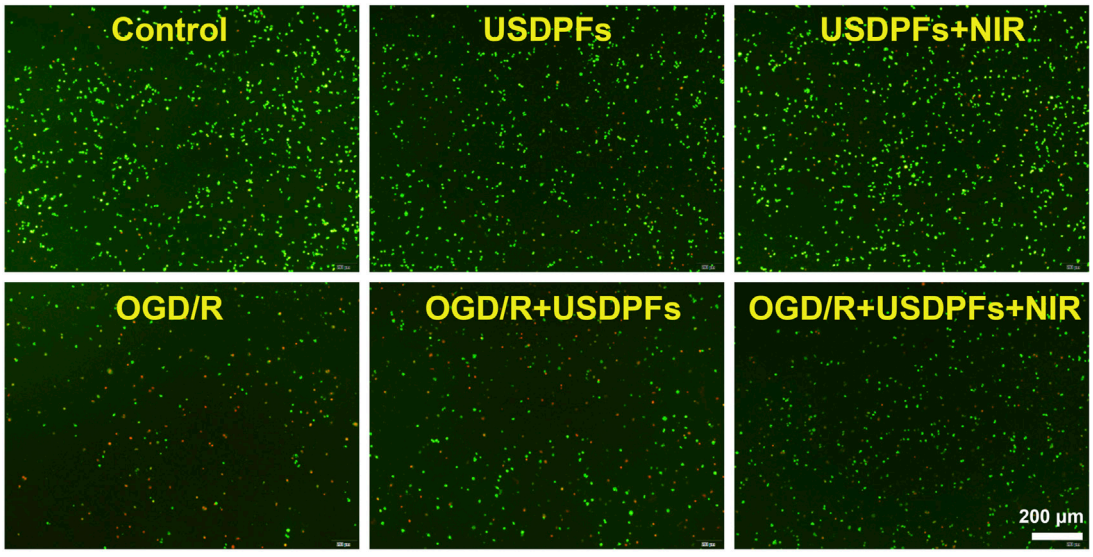

FIGURE 9
Cell viability/cytotoxicity detection of RAW264.7 cells in each group (×40, scale bar 200 μm) (Green fluorescence represents live cells, red fluorescence represents dead cells).

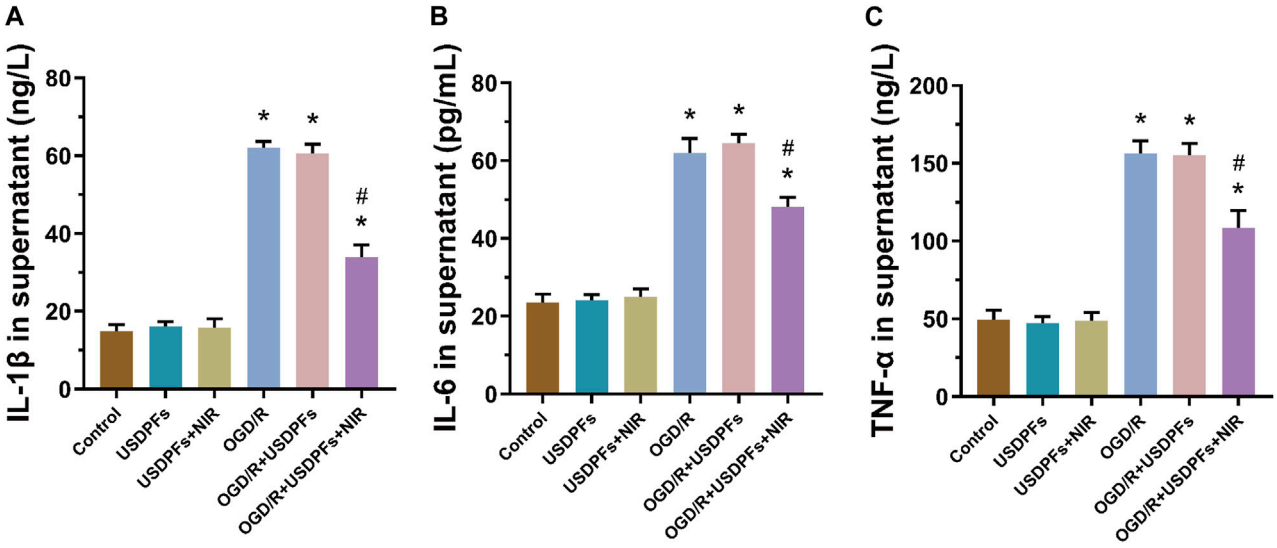

FIGURE 10
Expression of IL-1β **(A)**, IL-6 **(B)** and TNF-α **(C)** in the supernatant of RAW264.7 cells in each group (n = 5 per group,compared with the control group, $^{*}p < 0.05$; Compared with the OGD/R group, $^{\#}p < 0.05$).

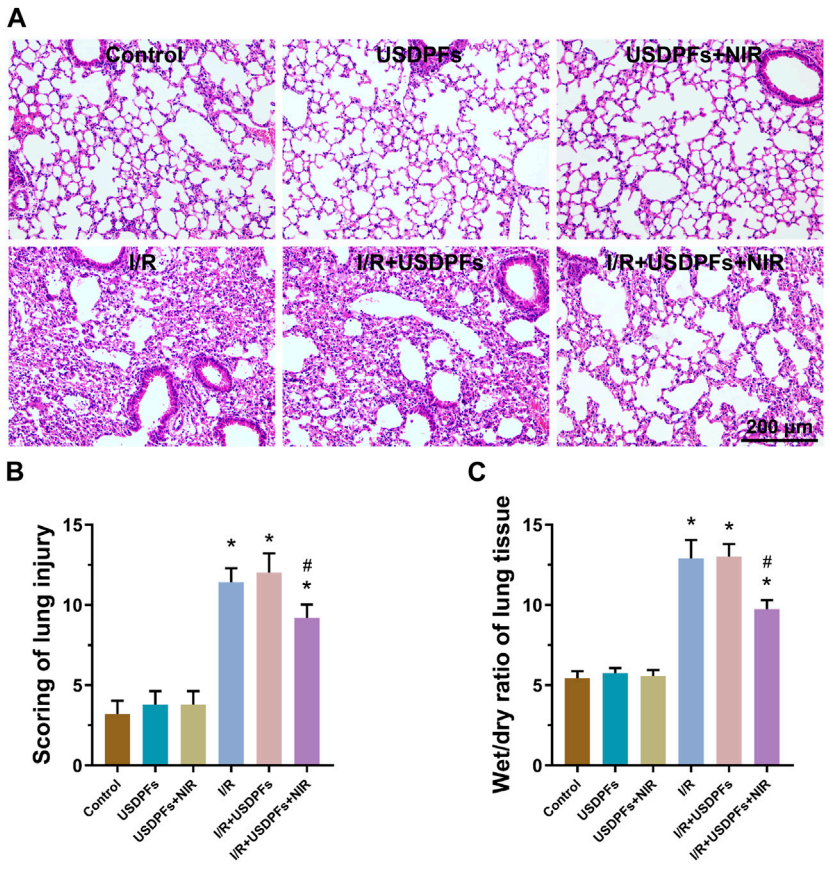

FIGURE 11
(A) H&E staining of lung tissue of mice in each group (×200, scale bar 200 μm); **(B)**. Pathological lung injury scores of mice in each group; **(C)**. Wet/dry ratio of lung tissue of mice in each group (n = 5 per group, compared with the control group, $^{*}p < 0.05$; Compared with the I/R group, $^{\#}p < 0.05$).

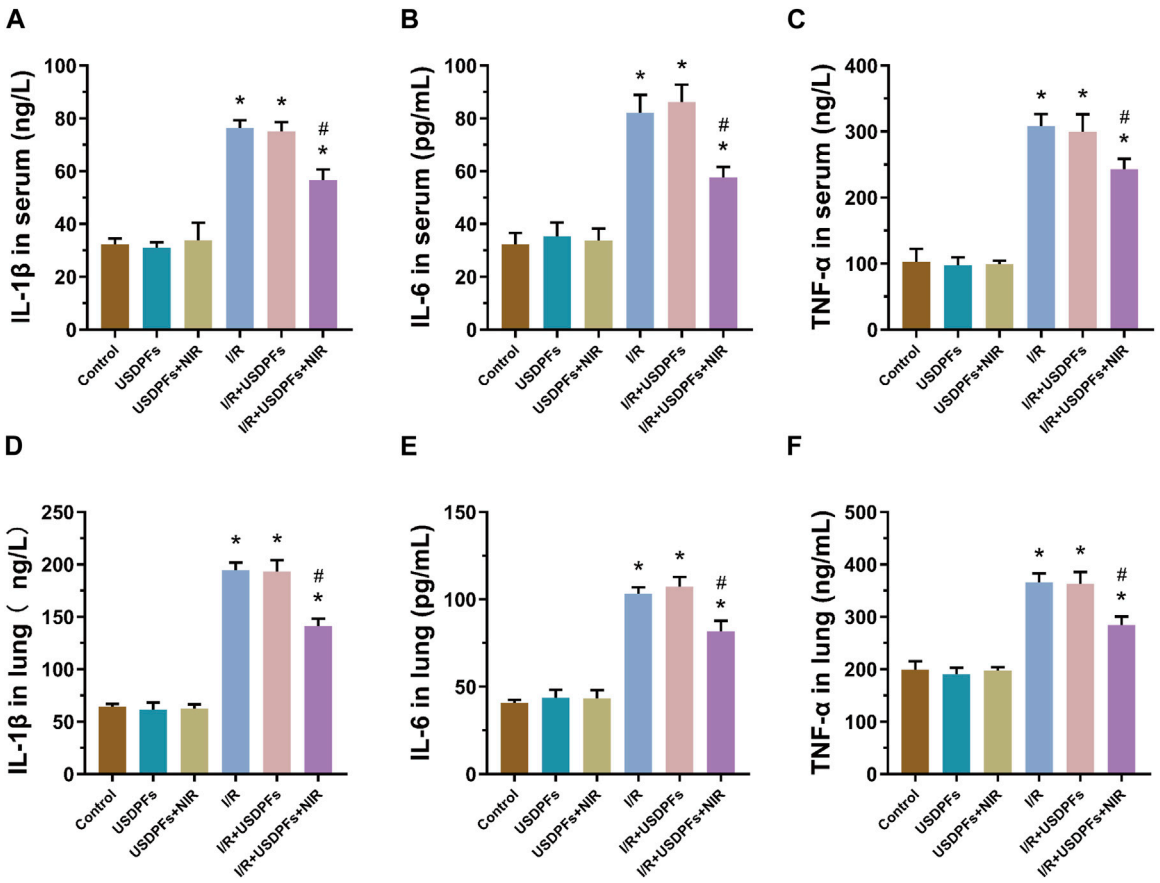

FIGURE 12
(A–C) Expression of IL-1β **(A)**, IL-6 **(B)** and TNF-α **(C)** in serum. **(D–F)** Expression of IL-1β **(D)**, IL-6 **(E)** and TNF-α **(F)** in lung tissue. (n = 5 per group, compared with the control group, $^{*}p < 0.05$; Compared with the OGD/R group, $^{\#}p < 0.05$).

more pronounced in thermogram images and is mainly concentrated in the lungs (marked by red dashed circles). These results suggest that USDPFs are mainly distributed in lung tissue after intratracheal injection and have effective *in vivo* imaging properties.

3.6 Evaluation of the *in vitro* anti-inflammatory effect of USDPFs

The ultrastructural changes of the cells in each group were detected by transmission electron microscopy (Figure 8). The control RAW264.7 cells apparently had a large number of protrusions on the cell membrane, intact intracellular organelles, and a large number of phagocytic vesicles. The ultrastructure of the ODG/R and OGD/R + USDPFs groups was severely damaged, with fewer protrusions or even disappearances. In addition, there were fewer phagocytic vesicles, reduced chromatin border set, and disappeared nucleoli. The cell damage in the OGD/R + USDPFs + NIR group was improved, and a small amount of organelles, such as phagocytic vesicles and nucleoli, were present.

The apoptosis of the cells in each group was observed by double staining of live/dead cells. Figure 9 implies that the number of cells in the control, USDPFs, and USDPFs + NIR groups were essentially similar, with only a minimal number of apoptotic cells (stained in red). The difference is that the OGD/R and OGD/R + USDPFs groups have significantly fewer surviving cells (stained in green) and even a large number of apoptotic cells. The OGD/R + USDPFs + NIR group had more surviving cells and fewer apoptotic cells.

The expression of inflammatory mediators (IL-1β, IL-6 and TNF-α) in cell culture supernatants was measured by ELISA to assess the degree of inflammatory damage in each group of cells (Figure 10). First, there was no significant difference in cell damage in the USDPFs and USDPFs + NIR groups compared with the control group; cell damage was severe in both the OGD/R and OGD/R + USDPFs groups. Importantly, cellular inflammatory damage was significantly improved in the OGD/R + USDPFs + NIR group compared to the OGD/R and OGD/R + USDPFs groups.

The above results further suggest that NIR irradiation at 980 nm triggered the release of DEX, which ameliorated the cell damage induced by OGD/R.

3.7 Evaluation of the *in vivo* anti-inflammatory effect of USDPFs

Histopathological changes in C57B/L6 mice lung tissues in each group were observed under light microscopy. As explicated in Figure 11A, in control, USDPFs, and USDPFs+NIR groups, the lung tissue structure was clear and uniform in thickness, without congestion and inflammatory cell infiltration. In contrast, the alveolar walls of the I/R group and I/R+USDPFs group were thickened, with interstitial edema, and filled with a large number of erythrocytes and inflammatory cells. Compared with the I/R group, the I/R+USDPFs+NIR group had more apparent lung tissue contours, reduced edema, and fewer inflammatory cells and erythrocytes. The pathological changes after intratracheal injection of USDPFs (5 mg kg^{-1}) and use of dexamethasone aerosol in mice are shown in Supplementary Figure S4. The effect of USDPFs is similar to that of dexamethasone aerosols, which can alleviate lung tissue damage after I/R.

Figure 11B illustrates the pathology score of lung injury. Compared to the control group, there was no significant difference between the USDPFs and USDPFs + NIR groups, and the scores of the I/R and I/R + USDPFs groups were significantly increased. Unexpectedly, the I/R + USDPFs + NIR group had significantly lower scores than the I/R and I/R + USDPFs groups.

The W/D values of the lung tissue represent the degree of pulmonary edema and inflammatory exudation. There was no difference in pulmonary edema between the USDPFs group and USDPFs + NIR group mice compared to the control group (Figure 11C). Encouragingly, the lung edema of mice in the I/R + USDPFs + NIR group improved compared to the I/R group and the I/R + USDPFs group.

Inflammatory factors (IL-1β, IL-6 and TNF-α) were measured in mouse serum and lung tissue by ELISA to assess inflammatory damage in each group (Figure 12). Compared with the control group, the degree of inflammatory injury was not significantly different between the USDPFs and USDPFs+NIR groups of mice. In contrast, the inflammatory injury was more severe in mice's I/R and I/R+USDPFs groups. Significantly, the mice in the I/R+USDPFs+NIR group had significantly lower inflammatory injury than those in the I/R and I/R+USDPFs groups.

The above results suggest that USDPFs has better biosafety, and 980 nm NIR irradiation triggers the release of DEX, which reduces the inflammatory damage and edema of lung tissue caused by I/R.

4 Conclusion

In this work, we construct a multi-functional upconversion nano-drug delivery system USDPFs for LIRI. First, DEX can be efficiently and accurately released from USDPFs in the intrapulmonary microenvironment after 980 nm laser irradiation, which can be directly applied to improve I/R-induced lung injury. Meanwhile, USDPFs have good upconversion fluorescence emission ability, biocompatibility, and hemolysis, supporting their excellent multiple fluorescence imaging performance *in vitro* and *vivo*.

Data availability statement

The original contributions presented in the study are included in the article/Supplementary Materials, further inquiries can be directed to the corresponding author.

Ethics statement

The animal study was reviewed and approved by The Institutional Animal Care and Use Committee of Guangxi Medical University.

Author contributions

XH and ZL: Designed the project and conducted the experiments. MY, CZ, SW, YQ, YG, and LZ: Analyzed the data, performed statistical analyses, and wrote the manuscript. FL: Provided scientific support, critically reviewed the manuscript and experimental design. All authors read and approved the final manuscript.

Funding

This study was supported by the National Natural Science Foundation of China (81560018, 81960022, and 81900234), Guangxi Natural Science Foundation Special Project (2020GXNSFAA159123), Guangxi Science and Technology Base Talent Special Project (AD22035047), China Postdoctoral Science Foundation Project (2021M700911), Guangxi Postgraduate Education Innovation Project (YCSW2021126), the Guangxi Thousand Young and Middle-aged Backbone Teachers Training Program, Guangxi Medical HighLevel Talents Training Program (G201903011), and Advanced Innovation Teams and Xinghu Scholars Program of Guangxi Medical University.

Conflict of interest

The authors declare that the research was conducted in the absence of any commercial or financial relationships that could be construed as a potential conflict of interest.

Publisher's note

Supplementary material

The Supplementary Material for this article can be found online at: https://www.frontiersin.org/articles/10.3389/fbioe.2023.1176369/full#supplementary-material

References

Aktas, M. S., Kandemir, F. M., Ozkaraca, M., Hanedan, B., and Kirbas, A. (2017). Protective effects of rutin on acute lung injury induced by oleic acid in rats. *Kafkas Univ. Vet. Fak.* 23 (3), 445–451. doi:10.9775/kvfd.2016.16977

Caplan, A., Fett, N., Rosenbach, M., Werth, V. P., and Micheletti, R. G. (2017). Prevention and management of glucocorticoid-induced side effects: A comprehensive review. *J. Am. Acad. Dermatol* 76 (2), 201–207. doi:10.1016/j.jaad.2016.02.1241

Coutinho, A. E., and Chapman, K. E. (2011). The anti-inflammatory and immunosuppressive effects of glucocorticoids, recent developments and mechanistic insights. *Mol. Cell Endocrinol.* 335 (1), 2–13. doi:10.1016/j.mce.2010.04.005

Eskandari, P., Bigdeli, B., Porgham Daryasari, M., Baharifar, H., Bazri, B., Shourian, M., et al. (2019). Gold-capped mesoporous silica nanoparticles as an excellent enzyme-responsive nanocarrier for controlled doxorubicin delivery. *J. Drug Target* 27 (10), 1084–1093. doi:10.1080/1061186x.2019.1599379

Fiser, S. M., Tribble, C. G., Long, S. M., Kaza, A. K., Kern, J. A., Jones, D. R., et al. (2002). Ischemia-reperfusion injury after lung transplantation increases risk of late bronchiolitis obliterans syndrome. *Ann. Thorac. Surg.* 73 (4), 1041–1048. doi:10.1016/S0003-4975(01)03606-2

Han, X., Wang, Y., Chen, H., Zhang, J., Xu, C., Li, J., et al. (2016). Enhancement of ICAM-1 via the JAK2/STAT3 signaling pathway in a rat model of severe acute pancreatitis-associated lung injury. *Exp. Ther. Med.* 11 (3), 788–796. doi:10.3892/etm.2016.2988

Hu, X., Chen, Z., Jin, A. J., Yang, Z., Gan, D., Wu, A., et al. (2021). Rational design of all-organic nanoplatform for highly efficient MR/NIR-II imaging-guided cancer phototheranostics. *Small* 17 (12), e2007566. doi:10.1002/smll.202007566

Hu, X., Tang, Y., Hu, Y., Lu, F., Lu, X., Wang, Y., et al. (2019). Gadolinium-chelated conjugated polymer-based nanotheranostics for photoacoustic/magnetic resonance/NIR-II fluorescence imaging-guided cancer photothermal therapy. *Theranostics* 9 (14), 4168–4181. doi:10.7150/thno.34390

Indrajit, S., Masaki, U., and Imane, T. (2010). Sensitizing of pyrene fluorescence by β-cyclodextrin-modified TiO_2 nanoparticles. *J. Colloid Interf. Sci.* 352 (2), 12–237. doi:10.1016/j.jcis.2010.08.055

Kuwajima, K., Chang, K., Furuta, A., Bougaki, M., Uchida, K., Sawamura, S., et al. (2019). Synergistic cytoprotection by co-treatment with dexamethasone and rapamycin against proinflammatory cytokine-induced alveolar epithelial cell injury. *J. Intensive Care* 7, 12. doi:10.1186/s40560-019-0365-5

Lee, J., Yoo, B., Lee, H., Cha, G. D., Lee, H. S., Cho, Y., et al. (2017). Ultra-wideband multi-dye-sensitized upconverting nanoparticles for information security application. *Adv. Mater* 29 (1), 1603169. doi:10.1002/adma.201603169

Liang, F., Liu, H., He, X., Liu, C., Wu, S., Qin, Y., et al. (2021). Role and regulatory mechanism of triggering receptor expressed on myeloid cells 2 in mice lung ischemia/reperfusion injury. *Zhonghua Wei Zhong Bing Ji Jiu Yi Xue* 33 (8), 933–937. doi:10.3760/cma.j.cn121430-20201013-00669

Liu, Z., Shi, J., Wang, Y., Gan, Y., and Wang, P. (2019). Facile preparation of pyrenemethyl ester-based nanovalve on mesoporous silica coated upconversion nanoparticle for NIR light-triggered drug release with potential monitoring capability. *Colloid Surf. A* 568, 436–444. doi:10.1016/j.colsurfa.2019.02.027

Lu, H., Yang, J., Huang, D., Zou, Q., Yang, M., Zhang, X., et al. (2019). Ultranarrow NIR bandwidth and temperature sensing of YOF:Yb^{3+}/Tm^{3+} phosphor in low temperature range. *J. Lumin* 206, 613–617. doi:10.1016/j.jlumin.2018.10.091

Lu, Y., Luo, Q., Jia, X., Tam, J. P., Yang, H., Shen, Y., et al. (2023). Multidisciplinary strategies to enhance therapeutic effects of flavonoids from Epimedii Folium: Integration of herbal medicine, enzyme engineering, and nanotechnology. *J. Pharm. Anal.* 13 (3), 239–254. doi:10.1016/j.jpha.2022.12.001

Ma, T., List, T., and Donnelly, V. M. (2018). Comparisons of NF_3 plasma-cleaned Y_2O_3, YOF, and YF_3 chamber coatings during silicon etching in Cl_2 plasmas. *J. Vac. Sci. Technol. A* 36 (3), 031305. doi:10.1116/1.5026777

Murray, P. J., and Wynn, T. A. (2011). Protective and pathogenic functions of macrophage subsets. *Nat. Rev. Immunol.* 11 (11), 723–737. doi:10.1038/nri3073

Ng, C. S. H., Wan, S., Arifi, A. A., and Yim, A. P. C. (2006). Inflammatory response to pulmonary ischemia-reperfusion injury. *Surg. Today* 36 (3), 205–214. doi:10.1007/s00595-005-3124-2

Ng, C. S., Wan, S., and Yim, A. P. (2005). Pulmonary ischaemia-reperfusion injury: Role of apoptosis. *Eur. Respir. J.* 25 (2), 356–363. doi:10.1183/09031936.05.00030304

Pengpeng, D., Jing, S., Juanjuan, C., Zou, X., and Liao, L. (2019). Fast responsive photo-switchable dual-color fluorescent cyclodextrin nanogels for cancer cell imaging. *Carbohyd Polym.* 210, 379–388. doi:10.1016/j.carbpol.2019.01.086

Peter, J. V., John, P., Graham, P. L., Moran, J. L., George, I. A., and Bersten, A. (2008). Corticosteroids in the prevention and treatment of acute respiratory distress syndrome (ARDS) in adults: Meta-analysis. *BRIT Med. J.* 336 (7651), 1006–1009. doi:10.1136/bmj.39537.939039

Song, Y., Sun, R., Sun, G., Xie, Y., and Sun, L. (2022). Upconversion/downshifting multimode luminescence of lanthanide-doped nanocrystals for multidimensional information encoding security. *Chem-Asian J.* 17 (17), e202200537. doi:10.1002/asia.202200537

Spahn, J. H., Li, W., Bribriesco, A. C., Liu, J., Shen, H., Ibricevic, A., et al. (2015). DAP12 expression in lung macrophages mediates ischemia/reperfusion injury by promoting neutrophil extravasation. *J. Immunol.* 194 (8), 4039–4048. doi:10.4049/jimmunol.1401415

Suo, H., Guo, C., Zheng, J., Zhou, B., Ma, C., Zhao, X., et al. (2016). Sensitivity modulation of upconverting thermometry through engineering phonon energy of a matrix. *ACS Appl. Mater Interfaces* 8(44), 229–233. doi:10.1021/acsami.6b12176

Tian, X. X., Wang, B. L., Cao, Y. Z., Zhong, Y. X., Tu, Y. Y., Xiao, J. B., et al. (2015). Comparison of protective effects of safflor injection and extract of Ginkgo biloba on lung ischemia/reperfusion injury in rabbits. *Chin. J. Integr. Med.* 21(3), 229–233. doi:10.1007/s11655-013-1513-8

Wang, N., Yu, X., Zhang, K., Mirkin, C. A., and Li, J. (2017). Upconversion nanoprobes for the ratiometric luminescent sensing of nitric oxide. *J. Am. Chem. Soc.* 139 (36), 12354–12357. doi:10.1021/jacs.7b06059

Wang, T., Liu, C., Pan, L. H., Liu, Z., Li, C. L., Lin, J. Y., et al. (2020). Inhibition of p38 MAPK mitigates lung ischemia reperfusion injury by reducing blood-air barrier hyperpermeability. *Front. Pharmacol.* 11, 569251. doi:10.3389/fphar.2020.569251

Xiang, J., Tong, X., Shi, F., Yan, Q., Yu, B., and Zhao, Y. (2018). Near-infrared light-triggered drug release from UV-responsive diblock copolymer-coated upconversion nanoparticles with high monodispersity. *J. Mater Chem. B* 6 (21), 3531–3540. doi:10.1039/c8tb00651b

Yan, H., Dong, J., Huang, X., and Du, X. (2021). Protein-gated upconversion nanoparticle-embedded mesoporous silica nanovehicles via diselenide linkages for drug release tracking in real time and tumor chemotherapy. *ACS Appl. Mater Interfaces* 13 (24), 29070–29082. doi:10.1021/acsami.1c04447

Yi, G., Peng, Y., and Gao, Z. (2011). Strong red-emitting near-infrared-to-visible upconversion fluorescent nanoparticles. *Chem. Mater* 23 (11), 18018–18025.doi:10.1021/cm103175s

Yuan, C., Chen, G., Li, L., Damasco, J. A., Ning, Z., Xing, H., et al. (2014). Simultaneous multiple wavelength upconversion in a core-shell nanoparticle for enhanced near infrared light harvesting in a dye-sensitized solar cell. *ACS Appl. Mater Interfaces* 6 (20), 18018–18025. doi:10.1021/am504866g

Zhang, Z., Chen, L., and Ni, H. (2015). The effectiveness of corticosteroids on mortality in patients with acute respiratory distress syndrome or acute lung injury: A secondary analysis. *Sci. Rep.* 5, 17654. doi:10.1038/srep17654

frontiers | Frontiers in Oncology

TYPE Review
PUBLISHED 14 July 2023
DOI 10.3389/fonc.2023.1178092

OPEN ACCESS

EDITED BY
Arif Gulzar,
University of Queensland, Australia

REVIEWED BY
Hojjat Farahmandnia,
Kerman University of Medical Sciences, Iran
Hamid Safarpour,
Medical University of Ilam, Iran

*CORRESPONDENCE
Miao Huang
miaohuangsc@gmail.com

RECEIVED 02 March 2023
ACCEPTED 15 May 2023
PUBLISHED 14 July 2023

CITATION
Wang W, Li H and Huang M (2023) A literature review on the impact of disasters on healthcare systems, the role of nursing in disaster management, and strategies for cancer care delivery in disaster-affected populations.
Front. Oncol. 13:1178092.
doi: 10.3389/fonc.2023.1178092

A literature review on the impact of disasters on healthcare systems, the role of nursing in disaster management, and strategies for cancer care delivery in disaster-affected populations

Wen Wang, Hui Li and Miao Huang*

Department of Hematology, Sichuan Provincial People's Hospital, University of Electronic Science and Technology of China, Chengdu, China

This review article highlights the critical role of nurses in disaster management, with a specific focus on addressing blood tumors in disaster-affected populations. Disasters have a significant impact on healthcare systems and populations, and nurses play a crucial role in disaster preparedness, response, and recovery. The article provides case studies and successful examples of nursing interventions in disaster settings and tumor management, emphasizing the challenges and opportunities in providing cancer care in disaster settings. Recommendations for future research and practice in disaster nursing and blood tumor care are also presented. This information is essential for healthcare professionals and policymakers involved in disaster management, as well as researchers and clinicians working in the field of cancer care.

KEYWORDS

disaster, nursing, tumor, healthcare delivery, cancer care

1 Introduction

Background information on disasters and their impact on healthcare systems.

Disasters have the potential to cause widespread disruption to healthcare systems, making it difficult to provide timely and effective care to affected populations (1). Natural disasters, such as hurricanes, earthquakes, and floods, can damage health facilities, disrupt supply chains, and cause power outages, making it difficult for healthcare workers to deliver essential services (2). Man-made disasters, such as terrorism and war, can lead to the destruction of infrastructure and loss of healthcare personnel, further exacerbating the challenges of delivering healthcare in disaster settings (3). As healthcare systems face an

ever-increasing threat of disasters, it is crucial to understand the impact of disasters on healthcare delivery and to identify strategies to mitigate these impacts (4). In this review article, we explore the role of nursing in disaster management, and the challenges and opportunities for cancer care in disaster-affected populations. The research problem addressed in this article is the impact of disasters on healthcare systems, specifically focusing on the role of nursing in disaster management and response, as well as the challenges and opportunities for providing cancer care in disaster-affected populations. Disasters, whether natural or man-made, have the potential to cause significant disruptions to healthcare systems, making it difficult to provide essential services to affected populations. Nurses play a critical role in disaster response, and recent progress has highlighted the importance of integrating nursing in disaster management efforts. Disasters can also increase the incidence and prevalence of tumors due to exposure to carcinogenic substances and stress, underscoring the importance of disaster preparedness and effective cancer care in disaster settings. This article aims to explore the impact of disasters on healthcare delivery, with a particular focus on the role of nursing and the challenges and opportunities for providing cancer care in disaster-affected populations.

2 Importance of nursing in disaster management and response

Recent progress has highlighted the crucial role of nursing in disaster management and response (5). Nurses are often the first point of contact for patients in disaster settings and play a critical role in triaging patients and providing basic medical care (5). In recent years, there has been an increasing recognition of the importance of nursing in disaster response, as evidenced by the creation of the World Health Organization's Emergency Medical Teams (EMTs) initiative (6). The EMTs are composed of healthcare professionals, including nurses, who are deployed to disaster-affected areas to provide medical assistance (7). Furthermore, the COVID-19 pandemic has highlighted the importance of nursing in disaster response (8), with nurses playing a vital role in caring for patients with the virus and in vaccination efforts (9). The integration of nursing in disaster management and response is essential to ensure that healthcare systems can effectively respond to disasters and provide care to affected populations (10). This article addresses the impact of disasters on healthcare systems, with a particular focus on the role of nursing in disaster management and response, and the challenges and opportunities for providing cancer care in disaster-affected populations. Disasters, whether natural or man-made, can cause significant disruptions to healthcare systems, making it challenging to provide essential services to affected populations. Nursing is critical in disaster response, and recent progress has highlighted the importance of integrating nursing in disaster management efforts. Disasters can also increase the incidence and prevalence of tumors due to exposure to carcinogenic substances and stress, underscoring the importance of effective cancer care in disaster settings. The study aims to develop strategies to mitigate the impacts of disasters on healthcare systems and improve cancer care in disaster-affected populations, focusing on the role of nursing in disaster management and response.

3 Prevalence and significance of tumors in disaster-affected populations

Recent progress has shed light on the prevalence and significance of tumors in disaster-affected populations (11). Studies have shown that disasters can increase the incidence and prevalence of tumors due to factors such as exposure to carcinogenic substances and stress (12). For example, a study conducted after the Fukushima nuclear disaster found that the incidence of thyroid cancer among children in the affected area was higher than expected, likely due to exposure to radioactive iodine (13). Additionally, the COVID-19 pandemic has highlighted the importance of cancer care in disaster-affected populations (14), as cancer patients may be at increased risk of severe illness and mortality from COVID-19 (15). Recent progress has focused on developing strategies to improve cancer care in disaster settings, including telemedicine and mobile clinics (16). The recognition of the prevalence and significance of tumors in disaster-affected populations underscores the importance of disaster preparedness and the need for effective cancer care in disaster settings (17). Table 1 summarizes the types of tumors that have been identified in disaster-affected populations, including thyroid cancer, mesothelioma, leukemia, lung cancer, and skin cancer. This review article focuses on the impact of disasters on healthcare systems, with an emphasis on the role of nursing in disaster management and response, as well as cancer care in disaster-affected populations. Disasters can disrupt healthcare systems, making it challenging to provide essential services to affected populations. Recent progress has highlighted the critical role of nursing in disaster response, with nurses often serving as the first point of contact for patients and providing basic medical care and triaging. Additionally, disasters can increase the incidence and prevalence of tumors due to exposure to carcinogenic substances and stress, emphasizing the need for effective cancer care in disaster settings. Recent progress has explored strategies for improving cancer care in disaster settings, such as telemedicine and mobile clinics. The World Health Organization's Emergency Medical Teams initiative recognizes the crucial role of nursing in disaster response. Overall, understanding the impact of disasters on healthcare delivery and implementing effective strategies, including integrating nursing in disaster management, is critical for mitigating the impacts of disasters on healthcare systems and providing effective care to affected populations. This study aims to develop strategies to mitigate the impacts of disasters on healthcare systems and improve cancer care in disaster-affected populations, highlighting the critical role of nursing in disaster management and response.

TABLE 1 Types of tumors in disaster-affected populations.

Type of Tumor	Examples of Disasters
Thyroid Cancer	Fukushima Nuclear Disaster
Mesothelioma	9/11 Terrorist Attacks
Leukemia	Chemical Spills
Lung Cancer	Wildfires
Skin Cancer	Sun Exposure During Disasters

4 Methods

This article is a comprehensive literature review that examines the challenges and opportunities related to drug delivery in disaster nursing and blood tumor care. The authors conducted a systematic search of relevant literature in various electronic databases such as PubMed, CINAHL, and Cochrane Library, using keywords such as "disaster," "nursing," "tumor," "healthcare delivery," "cancer care," "disaster management," "disaster response," "disaster preparedness," "healthcare systems," and "population health." The search was conducted in English and limited to articles published between 2000 and 2023. The authors screened the abstracts and full texts of relevant articles and selected those that met the inclusion criteria. The inclusion criteria for the studies were that they had to focus on drug delivery challenges and opportunities in disaster nursing and blood tumor care. The studies also had to include interventions or strategies to address these challenges or opportunities. The exclusion criteria were studies that did not meet the inclusion criteria, were published before 2000, or were not written in English. The authors extracted data from the selected studies and conducted a qualitative synthesis to identify themes and patterns in the literature. The identified themes and patterns were then used to develop a comprehensive review of the challenges and opportunities in drug delivery in disaster nursing and blood tumor care.

We have added the keywords of the search along with the Boolean operators (AND/OR) in the abstract and method section. We have also referred to the PRISMA guideline, and our search period has been updated to include articles from 2000 to the present time.

4.1 Study quality assessment

We have introduced the quality review tool for the final studies extracted based on the PRISMA guideline. The methodological quality of the included studies was assessed using the following tools:

For primary research articles, the Critical Appraisal Skills Programme (CASP) checklist was used.

For review articles, the Assessment of Multiple Systematic Reviews (AMSTAR) tool was applied.

For case studies, the Joanna Briggs Institute (JBI) Critical Appraisal Checklist for Case Studies was utilized.

4.2 Search strategy

A comprehensive literature search was conducted using electronic databases such as PubMed, CINAHL, Web of Science, Scopus, and Cochrane Library. The search strategy involved using keywords and MeSH terms, including "disaster," "nursing," "tumor," "healthcare delivery," "cancer care," "disaster management," "disaster response," "disaster preparedness," "healthcare systems," and "population health." Boolean operators (AND, OR) were employed to combine the search terms. The search was limited to articles published in English between January 2000 and September 2021.

4.3 Selection of articles and documents

Two independent reviewers (WW and MH) screened the titles and abstracts of the retrieved articles. Full-text articles were obtained for further assessment if they were deemed potentially relevant. Disagreements between the reviewers were resolved through discussion or consultation with a third reviewer.

4.4 Inclusion and exclusion criteria

Inclusion criteria for the articles were as follows:

Primary research articles, review articles, and case studies focusing on the impact of disasters on healthcare systems, nursing in disaster management, and strategies for cancer care delivery in disaster-affected populations.

Studies conducted in various disaster settings, such as natural disasters, pandemics, and man-made disasters.

Articles published in peer-reviewed journals.

4.5 Exclusion criteria for the articles were as follows

Articles not published in English.

Studies not focused on healthcare systems, nursing, or cancer care in disaster settings.

Opinion pieces, editorials, and commentaries.

4.6 Database search

The search was conducted using the following databases:

PubMed
CINAHL
Web of Science
Scopus
Cochrane Library

5 Results

The review article identifies several challenges related to drug delivery in disaster nursing and blood tumor care, including the shortage of essential drugs and medical supplies, limited access to healthcare facilities, and the need for specialized care and equipment. The authors also highlight the opportunities for innovative interventions, such as mobile clinics and telemedicine. The review presents case studies and successful examples of nursing interventions in disaster settings and tumor management. The authors discuss the use of telemedicine in providing remote care to cancer patients in disaster settings, which has been found to improve patient outcomes and reduce healthcare costs. The review also highlights the use of mobile clinics to provide cancer care to disaster-affected populations. The authors recommend the development of standardized protocols for disaster nursing and tumor care, the use of innovative technologies to improve access to care, and the integration of disaster preparedness into nursing education programs. Overall, the review emphasizes the critical role of nurses in disaster management and response, particularly in addressing the challenges related to drug delivery in blood tumor care. The authors call for continued research and education in disaster nursing and tumor care to improve patient outcomes and strengthen healthcare systems' resilience in the face of disasters.

5.1 Nursing in disaster management and response

Role of nurses in disaster preparedness, response, and recovery.

Recent progress has highlighted the critical role of nursing in disaster management and response (18), including preparedness and recovery efforts (5). Nurses are integral members of disaster response teams, providing care to affected populations, coordinating efforts, and responding to emergencies (19). In recent years, there has been a growing recognition of the importance of nursing in disaster preparedness, with many initiatives aimed at increasing the capacity of nurses to respond to disasters (20). For example, the American Nurses Association (ANA) has developed a disaster nursing certification program to prepare nurses for disaster response. Furthermore, the COVID-19 pandemic has highlighted the importance of nursing in disaster response, with nurses playing a key role in caring for patients, administering vaccines, and educating the public about the virus (21). Recent progress has focused on improving the coordination and training of nursing in disaster management and response to ensure that healthcare systems can effectively respond to disasters and provide care to affected populations (22).

5.2 Challenges and opportunities for nursing in disaster settings

Recent progress has identified several challenges and opportunities for nursing in disaster settings (5). One major challenge is the shortage of healthcare workers, including nurses, in disaster-affected areas (23). Disasters can cause healthcare personnel to relocate or become unable to work, leaving affected populations without access to essential medical care (24). Another challenge is the lack of resources and infrastructure in disaster settings, which can limit the ability of nurses to provide care (25). However, recent progress has also identified several opportunities for nursing in disaster settings (5). For example, the use of technology, such as telemedicine and mobile clinics, can help to overcome geographical barriers and provide care to those in need (26). Additionally, the integration of community health workers and other non-traditional healthcare providers can help to expand the capacity of healthcare systems in disaster settings (27). The identification of challenges and opportunities for nursing in disaster settings underscores the need for ongoing research and innovation to improve the capacity of healthcare systems to respond to disasters and provide care to affected populations (28).

5.3 Best practices for nursing in disaster management

Recent progress has identified several best practices for nursing in disaster management (29). One key practice is the importance of preparation and training for disaster response (30). Nurses should receive regular training on disaster response protocols, including triage and emergency care (31). Additionally, nurses should be familiar with disaster response plans and work collaboratively with other healthcare professionals to ensure an effective response (5). Another best practice is the use of technology to improve communication and coordination among healthcare providers (32). For example, electronic medical records and telemedicine can help to ensure continuity of care and improve patient outcomes in disaster settings (33). Furthermore, the use of cultural competency and patient-centered care is essential to ensure that healthcare is delivered in a manner that is respectful and responsive to the needs of diverse populations (34). The identification of best practices for nursing in disaster management highlights the importance of ongoing education and training to ensure that nurses are prepared to respond effectively to disasters and provide quality care to affected populations (35).

6 Tumors in disaster-affected populations

6.1 Types and prevalence of tumors in disaster-affected populations

Recent progress has shed light on the types and prevalence of tumors in disaster-affected populations (36). Studies have shown that

disasters can increase the incidence and prevalence of certain types of tumors due to exposure to carcinogenic substances and stress (37). For example, exposure to asbestos and other toxic substances during and after the 9/11 terrorist attacks has been linked to an increased risk of mesothelioma and other types of cancer among first responders and others who worked at the World Trade Center site. Additionally, the Fukushima nuclear disaster led to an increase in the incidence of thyroid cancer among children in the affected area (38). Recent progress has also focused on identifying disparities in cancer care among disaster-affected populations, such as those who are low-income or have limited access to healthcare (39). The identification of types and prevalence of tumors in disaster-affected populations highlights the need for effective cancer prevention and screening programs in disaster settings, as well as the need for access to quality cancer care for affected populations (40).

6.2 Factors that contribute to the development and progression of tumors in disaster settings

Recent progress has identified several factors that contribute to the development and progression of tumors in disaster settings (41). One major factor is exposure to carcinogenic substances, such as radiation, asbestos, and other toxic chemicals (42). Disasters can lead to the release of these substances into the environment, putting affected populations at risk of developing cancer (43). Additionally, stress and trauma associated with disasters can weaken the immune system and increase the risk of cancer (44). Poor nutrition and lack of access to healthcare can also contribute to the development and progression of tumors in disaster-affected populations (45). Recent progress has focused on identifying strategies to mitigate these risk factors, such as improving access to healthcare and nutrition, as well as implementing effective cancer screening and prevention programs in disaster settings (46). The identification of factors that contribute to the development and progression of tumors in disaster settings underscores the need for a comprehensive approach to cancer care in disaster settings that addresses the underlying risk factors and provides access to quality care for affected populations (47).

6.3 Challenges and opportunities for cancer care in disaster settings

Recent progress has identified several challenges and opportunities for cancer care in disaster settings (48). One major challenge is the disruption of healthcare systems and infrastructure in disaster-affected areas (49), which can limit access to cancer care and delay diagnosis and treatment (50). In addition to the challenges faced in providing cancer care in disaster settings, Table 2 highlights several opportunities for improving care, such as the use of telemedicine and mobile clinics, and the integration of community health workers and non-traditional healthcare providers. Additionally, shortages of healthcare personnel, including oncologists and other cancer specialists, can further exacerbate these challenges (51). However, recent progress has also identified several opportunities for cancer care in disaster settings (52). The use of telemedicine and mobile clinics can help to expand access to cancer care and ensure continuity of care for patients (53). Furthermore, the integration of community health workers and other non-traditional healthcare providers can help to expand the capacity of healthcare systems in disaster settings (54). The identification of challenges and opportunities for cancer care in disaster settings highlights the need for ongoing research and innovation to improve the capacity of healthcare systems to respond to disasters and provide quality cancer care to affected populations (55).

7 Case studies and examples

7.1 Examples of successful nursing interventions in disaster settings

Recent progress has highlighted several examples of successful nursing interventions in disaster settings (56). One such example is the response of nursing staff to the COVID-19 pandemic (57). Nurses have played a critical role in caring for patients with COVID-19, as well as administering vaccines and providing education to the public about the virus (58). Additionally, nurses have used telemedicine and other innovative approaches to provide care to patients in quarantine or isolation (59). Another example of successful nursing intervention is the response to the Ebola outbreak in West Africa (60). Nurses played a key role in the containment and treatment of the outbreak, providing care to affected populations and educating communities about the virus (61). Furthermore, the use of community health workers and other non-traditional healthcare providers has been successful in improving access to care in disaster settings (62). These examples of successful nursing interventions in disaster settings demonstrate the importance of nursing in disaster management and response, as

TABLE 2 Challenges and opportunities for cancer care in disaster settings.

Challenges	Opportunities
Limited access to healthcare and cancer specialists	Use of telemedicine and mobile clinics
Disruption of healthcare systems and infrastructure	Integration of community health workers and non-traditional healthcare providers
Shortages of healthcare personnel	Development of effective cancer screening and prevention programs
Increased risk of exposure to carcinogenic substances	Increased awareness of cancer prevention and risk reduction strategies
Lack of resources and infrastructure	Use of innovative approaches to care

well as the need for ongoing education and innovation to improve the capacity of healthcare systems to respond to disasters and provide care to affected populations (63).

7.2 Case studies of tumor management in disaster-affected populations

Recent progress has identified several case studies of tumor management in disaster-affected populations (64). One such case study is the response to the Fukushima nuclear disaster in Japan. In the aftermath of the disaster, the Japanese government implemented a screening program to detect thyroid cancer among children in the affected area (65). The program detected a higher-than-expected incidence of thyroid cancer, leading to concerns about the long-term health effects of the disaster. Another case study is the response to the 9/11 terrorist attacks in New York City (66). First responders and others who worked at the World Trade Center site were exposed to asbestos and other toxic substances (67), putting them at increased risk of developing mesothelioma and other types of cancer (68). Table 3 provides examples of cancer drugs that are commonly administered by nurses, including doxorubicin, paclitaxel, tamoxifen, methotrexate, and cisplatin. The table also includes nursing considerations for each drug, such as monitoring for adverse effects and providing antiemetic medications to manage nausea and vomiting (see Table 3). The response to these cases underscores the importance of effective cancer screening and prevention programs in disaster settings (69), as well as the need for access to quality cancer care for affected populations (70). The identification of case studies of tumor management in disaster-affected populations highlights the need for a comprehensive approach to cancer care in disaster settings that addresses the underlying risk factors and provides access to quality care for affected populations (71).

7.3 Lessons learned and future directions for disaster nursing and tumor care

Recent progress has identified several key lessons learned and future directions for disaster nursing and tumor care (72). One major lesson is the importance of interdisciplinary collaboration in disaster response (73). Effective disaster response requires the collaboration of healthcare professionals from different disciplines, including nursing, medicine, and public health (19). Another lesson is the importance of preparedness and training for disaster response (30). Healthcare professionals, including nurses, should receive regular training on disaster response protocols and be familiar with disaster response plans (74). Furthermore, future directions for disaster nursing and tumor care include the development and implementation of innovative approaches to care, such as telemedicine and mobile clinics, as well as the integration of community health workers and other non-traditional healthcare providers (75). Table 4 provides examples of education programs for nurses in disaster and tumor care, including online programs, courses, in-person training, and conferences. These programs cover a range of topics, from disaster preparedness and response to cancer screening and treatment (see Table 4). Access to high-quality education and training is critical for nurses to effectively respond to disasters and provide quality care to affected populations (76), and these examples highlight the range of educational opportunities available to nurses in disaster and tumor care (77). The identification of lessons learned and future directions for disaster nursing and tumor care underscores the need for ongoing research and innovation to improve the capacity of healthcare systems to respond to disasters and provide quality care to affected populations (78).

8 Discussion

The discussion of the review article emphasizes the importance of nurses in disaster management and response, particularly in addressing the challenges related to drug delivery in blood tumor care. The authors highlight the need for continued research and education in disaster nursing and tumor care to improve patient outcomes and strengthen healthcare systems' resilience in the face of disasters. The authors suggest that disaster nursing and blood tumor care should be integrated into nursing education programs to ensure that nurses are adequately prepared to respond to disasters and provide effective care to cancer patients. They also recommend

TABLE 3 Examples of cancer drugs administered by nurses.

Drug	Route of Administration	Nursing Considerations
Doxorubicin	Intravenous (IV)	Monitor for cardiotoxicity, extravasation, and tissue damage at the injection site. Provide antiemetic medications to manage nausea and vomiting.
Paclitaxel	Intravenous (IV)	Monitor for hypersensitivity reactions and infusion-related reactions. Premedicate with corticosteroids and antihistamines as appropriate.
Tamoxifen	Oral	Monitor for adverse effects, such as hot flashes, vaginal discharge, and menstrual irregularities. Educate patients on the importance of taking the medication at the same time each day.
Methotrexate	Intravenous (IV) or oral	Monitor for bone marrow suppression, hepatotoxicity, and nephrotoxicity. Administer folic acid and vitamin B12 to reduce the risk of adverse effects.
Cisplatin	Intravenous (IV)	Monitor for nephrotoxicity, ototoxicity, and electrolyte imbalances. Provide antiemetic medications to manage nausea and vomiting.

TABLE 4 Examples of disaster and tumor care education programs for nurses.

Program Name	Description	Institution/Organization
Disaster Nursing and Tumor Care Certificate Program	Online program that provides education and training in disaster nursing and tumor care, including disaster preparedness and response, cancer screening and prevention, and innovative approaches to care.	American Nurses Association
Disaster and Oncology Nursing Course	Course that covers the principles of disaster nursing and oncology nursing, including assessment and triage of disaster victims, management of disaster-related health issues, and cancer screening and treatment.	Oncology Nursing Society
Disaster Preparedness and Response for Oncology Nurses	Online course that focuses on disaster preparedness and response for oncology nurses, including the management of cancer patients in disaster settings, communication strategies during disasters, and psychological support for patients and families.	Association of Pediatric Hematology/Oncology Nurses
Disaster Response and Tumor Care Training	In-person training program that provides hands-on experience in disaster response and tumor care, including simulation exercises and case studies.	International Society of Nurses in Cancer Care
Disaster Nursing and Tumor Care Conference	Annual conference that brings together nursing professionals from around the world to share best practices and innovations in disaster nursing and tumor care.	Global Network of WHO Collaborating Centres for Nursing and Midwifery

the development of standardized protocols for disaster nursing and tumor care to improve the consistency and quality of care provided in disaster settings. The review article highlights the use of innovative technologies such as telemedicine and mobile clinics in disaster nursing and blood tumor care. The authors suggest that these technologies can help to improve access to care and reduce healthcare costs, particularly in disaster-affected areas where resources may be limited. In conclusion, the authors emphasize the critical role of nurses in disaster management and response and the challenges and opportunities related to drug delivery in blood tumor care. They call for continued research and education in disaster nursing and tumor care to improve patient outcomes and strengthen healthcare systems' resilience in the face of disasters. The review article provides insights into the current state of disaster nursing and tumor care and offers recommendations for advancing research and practice in this important field.

9 Conclusion

In conclusion, this review emphasizes the critical role of nurses in disaster management, specifically in addressing blood tumors in disaster-affected populations. Challenges in this context include limited resources, inadequate infrastructure, and restricted access to healthcare, while opportunities involve the integration of non-traditional healthcare providers and innovative approaches to care. Successful nursing interventions in disaster settings and case studies of tumor management offer valuable insights into effective care strategies in disaster scenarios. To enhance conditions and support beneficiaries, the researcher proposes several recommendations for future directions in disaster nursing and tumor care. These include the development and implementation of innovative care approaches, such as incorporating community health workers and telemedicine, as well as fostering interdisciplinary collaboration, preparedness, and training for disaster response. Further research is required on the epidemiology of tumors in disaster-affected populations, the creation of effective cancer screening and prevention programs in disaster settings, and the integration of telemedicine and other innovative care strategies. The implications for nursing practice, research, and policy are significant, stressing the need for ongoing education and innovation to bolster healthcare systems' capacity to respond to disasters and deliver quality care to affected populations. Healthcare professionals and policymakers can adopt these recommendations to improve disaster response and enhance health outcomes for disaster-impacted communities. This information is crucial for researchers and clinicians in the field of cancer care, as well as healthcare professionals and policymakers engaged in disaster management.

Systematic review flow diagram. Caption: the PRISMA flow diagram for the systematic review detailing the database searches, the number of abstracts screened and the full texts retrieved.

Author contributions

HL: acquisition funding and review, revise the manuscript; WW: Writing, concept. MH: Manage, supervision, review, editing. All authors contributed to the article and approved the submitted version.

Funding

Sichuan Provincial Natural Science Foundation Project (No23NSFSC0607): The role and mechanism of ion channels in the migration ofacute lymphoblastic leukemia.

Conflict of interest

The authors declare that the research was conducted in the absence of any commercial or financial relationships that could be construed as a potential conflict of interest.

Publisher's note

References

1. Davis JR, Wilson S, Brock-Martin A, Glover S, Svendsen ER. The impact of disasters on populations with health and health care disparities. *Disaster Med Public Health Prep* (2010) 4:30–8. doi: 10.1017/S1935789300002391

2. Casey JA, Fukurai M, Hernández D, Balsari S, Kiang MV. Power outages and community health: a narrative review. *Curr Environ Health Rep* (2020) 7:371–83. doi: 10.1007/s40572-020-00295-0

3. Khilji FUR, Raziq A, Shoaib M, Baloch NS, Raza S. "Expecting the unexpected:" nurses' response and preparedness of terrorism-related disaster events in quetta city, Pakistan. *Front Public Health* (2021) 9:695143–3.

4. Pourhosseini SS, Ardalan A, Mehrolhassani MH. Key aspects of providing healthcare services in disaster response stage. *Iran J Public Health* (2015) 44:111–8.

5. Al Harthi M, Al Thobaity A, Al Ahmari W, Almalki M. Challenges for nurses in disaster management: a scoping review. *Risk Manag Healthc Policy* (2020) 13:2627–34. doi: 10.2147/RMHP.S279513

6. Amberson T, Wells C, Gossman S. Increasing disaster preparedness in emergency nurses: a quality improvement initiative. *J Emergency Nurs* (2020) 46:654–665.e621. doi: 10.1016/j.jen.2020.05.001

7. Hamilton ARL, Södergård B, Liverani M. The role of emergency medical teams in disaster response: a summary of the literature. *Natural Hazards* (2022) 110:1417–26. doi: 10.1007/s11069-021-05031-x

8. Shin H, Kim K.h., Kim J-s, Kwak Y-h. Nurses' duty to care during the COVID-19 pandemic: a cross-sectional survey. *BMC Nurs* (2022) 21:293. doi: 10.1186/s12912-022-01064-0

9. Barría P RM. Nursing and its essential role in the vaccination against COVID-19: new challenge in a pandemic scenario. *Invest Educ Enferm* (2021) 39:e01. doi: 10.17533/udea.iee.v39n3e01

10. Lim HW, Li Z, Fang D. Impact of management, leadership, and group integration on the hospital response readiness for earthquakes. *Int J Disaster Risk Reduction* (2020) 48:101586. doi: 10.1016/j.ijdrr.2020.101586

11. Liu T, Liu X, Li Y, Liu S, Cao C. Evolving trends and research hotspots in disaster epidemiology from 1985 to 2020: a bibliometric analysis. *BMJ Open* (2021) 9. doi: 10.3389/fpubh.2021.720787

12. Yu P, Xu R, Yang Z, Ye T, Liu Y, Li S, et al. Cancer and ongoing climate change: who are the most affected? *ACS Environ Au* (2023) 3:5–11. doi: 10.1021/acsenvironau.2c00012

13. Yamashita S, Suzuki S, Suzuki S, Shimura H, Saenko V. Lessons from fukushima: latest findings of thyroid cancer after the fukushima nuclear power plant accident. *Thyroid* (2018) 28:11–22. doi: 10.1089/thy.2017.0283

14. Al-Quteimat OM, Amer AM. The impact of the COVID-19 pandemic on cancer patients. *Am J Clin Oncol* (2020) 43:452–5. doi: 10.1097/COC.0000000000000712

15. Gupta K, Gandhi S, Mebane A III, Singh A, Vishnuvardhan N, Pateld E, et al. Cancer patients and COVID-19: mortality, serious complications, biomarkers, and ways forward. *Cancer Treat Res Commun* (2021) 26:100285–5. doi: 10.1016/j.ctarc.2020.100285

16. Lewis J, Ray P, Liaw ST. Recent worldwide developments in eHealth and mHealth to more effectively manage cancer and other chronic diseases - a systematic review. *Yearb Med Inform* (2016), 93–108.

17. De Guzman R, Malik M. Global cancer burden and natural disasters: a focus on asia's vulnerability, resilience building, and impact on cancer care. *J Glob Oncol* (2019) 5:1–8. doi: 10.1200/JGO.19.00037

18. Firouzkouhi M, Kako M, Abdollahimohammad A, Balouchi A, Farzi J. Nurses' roles in nursing disaster model: a systematic scoping review. *Iran J Public Health* (2021) 50:879–87. doi: 10.18502/ijph.v50i5.6105

19. Xue C-L, Shu Y-S, Hayter M, Lee A. Experiences of nurses involved in natural disaster relief: a meta-synthesis of qualitative literature. *J Clin Nurs* (2020) 29:4514–31. doi: 10.1111/jocn.15476

20. Veenema T. Global disaster nurse preparedness: moving from reserve to rapid action. *Health Emergency Disaster Nurs* (2016) 3:42–7. doi: 10.24298/hedn.2015-0018

21. Akbar MA, Juniarti N, Yamin A. The roles of community health nurses' in covid-19 management in Indonesia: a qualitative study. *Int J Community Based Nurs Midwifery* (2022) 10:96–109.

22. Putra A, Petpichetchian W, Maneewat K. Review: public health nurses' roles and competencies in disaster management. *Nurse Media J Nurs* (2010) 1.

23. Razu SR, Yasmin T, Arif TB, Islam S, Islam SMS, Gesesew HA, et al. Challenges faced by healthcare professionals during the COVID-19 pandemic: a qualitative inquiry from Bangladesh. *Semin Oncol Nurs* (2021) 9. doi: 10.3389/fpubh.2021.647315

24. Civaner MM, Vatansever K, Pala K. Ethical problems in an era where disasters have become a part of daily life: a qualitative study of healthcare workers in Turkey. *PloS One* (2017) 12:e0174162–e0174162. doi: 10.1371/journal.pone.0174162

25. Zhong S, Clark M, Hou X-Y, Zang Y, FitzGerald G. Progress and challenges of disaster health management in China: a scoping review. *Global Health Action* (2014) 7:24986. doi: 10.3402/gha.v7.24986

26. Haleem A, Javaid M, Singh RP, Suman R. Telemedicine for healthcare: capabilities, features, barriers, and applications. *Sens Int* (2021) 2:100117–7. doi: 10.1016/j.sintl.2021.100117

27. Balcazar H, Rosenthal EL, Brownstein JN, Rush CH, Matos S, Hernandez L. Community health workers can be a public health force for change in the united states: three actions for a new paradigm. *Am J Public Health* (2011) 101:2199–203. doi: 10.2105/AJPH.2011.300386

28. Balcazar H, Rosenthal EL, Brownstein JN, Rush CH, Matos S, Hernandez L, et al. Public health emergency preparedness: a framework to promote resilience. *BMC Public Health* (2018) 18:1344. doi: 10.1186/s12889-018-6250-7

29. Fletcher KA, Reddin K, Tait D. The history of disaster nursing: from nightingale to nursing in the 21st century. *J Res Nurs* (2022) 27:257–72. doi: 10.1177/17449871211058854

30. Torani S, Majd PM, Maroufi SS, Dowlati M, Sheikhi RA. The importance of education on disasters and emergencies: a review article. *J Educ Health Promot* (2019) 8:85–5. doi: 10.4103/jehp.jehp_262_18

31. Brinjee D, Al Thobaity A, Almalki M, Alahmari W. Identify the disaster nursing training and education needs for nurses in taif city, Saudi Arabia. *Risk Manag Healthc Policy* (2021) 14:2301–10. doi: 10.2147/RMHP.S312940

32. Manojlovich M, Adler-Milstein J, Harrod M, Sales A, Hofer TP, Saint S, et al. The effect of health information technology on health care provider communication: a mixed-method protocol. *JMIR Res Protoc* (2015) 4:e72–2. doi: 10.2196/resprot.4463

33. Zhang X, Saltman R. Impact of electronic health record interoperability on telehealth service outcomes. *JMIR Med Inform* (2022) 10:e31837–7. doi: 10.2196/31837

34. Stubbe DE. Practicing cultural competence and cultural humility in the care of diverse patients. *Focus (Am Psychiatr Publ)* (2020) 18:49–51. doi: 10.1176/appi.focus.20190041

35. Songwathana P, Timalsina R. Disaster preparedness among nurses of developing countries: an integrative review. *Int Emergency Nurs* (2021) 55:100955. doi: 10.1016/j.ienj.2020.100955

36. D'Souza-Schorey C, Clancy JW. Tumor-derived microvesicles: shedding light on novel microenvironment modulators and prospective cancer biomarkers. *Genes Dev* (2012) 26:1287–99. doi: 10.1101/gad.192351.112

37. Madia F, Worth A, Whelan M, Corvi R. Carcinogenicity assessment: addressing the challenges of cancer and chemicals in the environment. *Environ Int* (2019) 128:417–29. doi: 10.1016/j.envint.2019.04.067

38. Ohtsuru A, Midorikawa S, Ohira T, Suzuki S, Takahashi H, Murakami M, Shimura H, et al. Incidence of thyroid cancer among children and young adults in fukushima, Japan, screened with 2 rounds of ultrasonography within 5 years of the 2011 fukushima daiichi nuclear power station accident. *JAMA Otolaryngol Head Neck Surg* (2019) 145:4–11. doi: 10.1001/jamaoto.2018.3121

39. Esnaola NF, Ford ME. Racial differences and disparities in cancer care and outcomes: where's the rub? *Surg Oncol Clin N Am* (2012) 21:417–viii. doi: 10.1016/j.soc.2012.03.012

40. Shah SC, Kayamba V, Peek RMJr., Heimburger D. Cancer control in low- and middle-income countries: is it time to consider screening? *J Glob Oncol* (2019) 5:1–8. doi: 10.1200/JGO.18.00200

41. Whiteside TL. The tumor microenvironment and its role in promoting tumor growth. *Oncogene* (2008) 27:5904–12. doi: 10.1038/onc.2008.271

42. Carpenter DO, Bushkin-Bedient S. Exposure to chemicals and radiation during childhood and risk for cancer later in life. *J Adolesc Health* (2013) 52:S21–9. doi: 10.1016/j.jadohealth.2013.01.027

43. Pandey G, Madhuri S. Heavy metals causing toxicity in animals and fishes. *J.R.J.o.A. Veterinary Sciences F.* (2014) 2:17–23.

44. Seiler A, Fagundes CP, Christian L. The impact of everyday stressors on the immune system and health. *M.J.S.c. monitoring i.i.s.F.m.t. strategies* (2020), 71–92. doi: 10.1007/978-3-030-16996-1_6

45. El Saghir NS, Soto Pérez de Celis E, Fares JE, Sullivan R. Cancer care for refugees and displaced populations: middle East conflicts and global natural disasters. *J Glob Oncol* (2018) 38:433–40. doi: 10.1200/EDBK_201365

46. Tran KB, Lang JJ, Compton K, Xu R, Acheson AR, Henrikson HJ, et al. The global burden of cancer attributable to risk factors, 2010–19: a systematic analysis for the global burden of disease study 2019. *Lancet* (2022) 400:563–91. doi: 10.1016/S0140-6736(22)01438-6

47. Daly B, Olopade O. A perfect storm: how tumor biology, genomics, and health care delivery patterns collide to create a racial survival disparity in breast cancer and proposed interventions for change. *J Adolesc Health* (2015) 65:221–38. doi: 10.3322/caac.21271

48. De Guzman R, Malik M. Global cancer burden and natural disasters: a focus on asia's vulnerability, resilience building, and impact on cancer care. *J Phys* (2019) 5:1–8. doi: 10.1200/JGO.19.00037

49. Olu O. Resilient health system as conceptual framework for strengthening public health disaster risk management: an African viewpoint. *Stress Challenges and Immunity in Space* (2017) 5:263. doi: 10.3389/fpubh.2017.00263

50. Riera R, Bagattini ÂM, Pacheco RL, Pachito DV, Roitberg F, Ilbawi A. Delays and disruptions in cancer health care due to COVID-19 pandemic: systematic review. *JCO Glob Oncol* (2021) 7:311–23. doi: 10.1200/GO.20.00639

51. Jazieh AR, Akbulut H, Curigliano G, Rogado A, Alsharm AA, Razis ED, et al. Impact of the COVID-19 pandemic on cancer care: a global collaborative study. *JCO Glob Oncol* (2020) 6:1428–38. doi: 10.1200/GO.20.00351

52. Gabrel V, Murat C, Thiele A. Recent advances in robust optimization: an overview. *CA Cancer J Clin* (2014) 235:471–83. doi: 10.1016/j.ejor.2013.09.036

53. Cannon C. Telehealth, mobile applications, and wearable devices are expanding cancer care beyond walls. *Semin Oncol Nurs* (2018) 34:118–25. doi: 10.1016/j.soncn.2018.03.002

54. Lloyd J, Thomas-Henkel C. Integrating community health workers into complex care teams: key considerations. *Risk Manag Healthc Policy* (2017).

55. Lurie N, Carr BG. The role of telehealth in the medical response to disasters. *JCO Glob Oncol* (2018) 178:745–6. doi: 10.1001/jamainternmed.2018.1314

56. de Boer HH, Blau S, Delabarde T, Hackman L. The role of forensic anthropology in disaster victim identification (DVI): recent developments and future prospects. *JCO Glob Oncol* (2019) 4:303–15. doi: 10.1080/20961790.2018.1480460

57. Wood E, King R, Senek M, Robertson S, Taylor B, Tod A, et al. UK Advanced practice nurses' experiences of the COVID-19 pandemic: a mixed-methods cross-sectional study. *Eur J Oper Res* (2021) 11:. doi: 10.1136/bmjopen-2020-044139

58. Goldschmidt K. COVID-19 vaccines for children: the essential role of the pediatric nurse. *Semin Oncol Nurs* (2021) 57:96. doi: 10.1016/j.pedn.2020.12.004

59. Kaye AD, Okeagu CN, Pham AD, Silva RA, Hurley JJ, Arron BL, et al. Economic impact of COVID-19 pandemic on healthcare facilities and systems: international perspectives. *Best Pract Res Clin Anaesthesiol* (2021) 35:293–306. doi: 10.1016/j.bpa.2020.11.009

60. Gee S, Skovdal MJH. Navigating 'riskscapes': the experiences of international health care workers responding to the Ebola outbreak in West Africa. *JAMA Intern Med* (2017) 45:173–80. doi: 10.1016/j.healthplace.2017.03.016

61. Chau JPC, Lo SHS, Saran R, Leung CHY, Lam SKY, Thompson DR. Nurses' experiences of caring for people with COVID-19 in Hong Kong: a qualitative enquiry. *J Pediatr Nurs* (2021) 11:. doi: 10.1136/bmjopen-2021-052683

62. Lloyd J, Davis R, Moses K. Recognizing and sustaining the value of community health workers and promotores. *Front Public Health* (2020) 13.

63. Gowing JR, Walker KN, Elmer SL, Cummings EAJP. Disaster preparedness among health professionals and support staff: what is effective? an integrative literature review. *Health Place* (2017) 32:321–8. doi: 10.1017/S1049023X1700019X

64. Shao Y, Durmus N, Zhang Y, Pehlivan S, Fernandez-Beros M-E, Umana L, et al. The development of a WTC environmental health center pan-cancer database. *BMJ Open* (2021) 18:1646. doi: 10.3390/ijerph18041646

65. Cléro E, Ostroumova E, Demoury C, Grosche B, Kesminiene A, Liutsko L, et al. Lessons learned from Chernobyl and fukushima on thyroid cancer screening and recommendations in case of a future nuclear accident. *Environ Int* (2021) 146:106230. doi: 10.1016/j.envint.2020.106230

66. Li J, Yung J, Qiao B, Takemoto E, Goldfarb DG, Zeig-Owens R, et al. Cancer incidence in world trade center rescue and recovery workers: 14 years of follow-up. *J Natl Cancer Inst* (2022) 114:210–9. doi: 10.1093/jnci/djab165

67. Walker BL. Environments of terror: 9/11, world trade center dust, and the global nature of new york's toxic bodies. (2015), 779–95.

68. Chapple A, Ziebland S, McPherson A. Stigma, shame, and blame experienced by patients with lung cancer: qualitative study. *Environ Int* (2004) 328:1470. doi: 10.1136/bmj.38111.639734.7C

69. Parham GP, Mwanahamuntu MH, Kapambwe S, Muwonge R, Bateman AC, Blevins M, et al. Population-level scale-up of cervical cancer prevention services in a low-resource setting: development, implementation, and evaluation of the cervical cancer prevention program in Zambia. *J Natl Cancer Inst* (2015) 10:. doi: 10.1371/journal.pone.0122169

70. Perin DMP, Christensen T, Burón A, Haas JS, Kamineni A, Pashayan N, et al. Interruption of cancer screening services due to COVID-19 pandemic: lessons from previous disasters. *Prev Med Rep* (2021) 23:101399–9. doi: 10.1016/j.pmedr.2021.101399

71. Gorji HA, Jafari H, Heidari M, Seifi B. Cancer patients during and after natural and man-made disasters: a systematic review. *Asian Pac J Cancer Prev* (2018) 19:2695–700.

72. Rebmann T, English JF, Carrico R. Disaster preparedness lessons learned and future directions for education: results from focus groups conducted at the 2006 APIC conference. *Am J Infect Control* (2007) 35:374–81. doi: 10.1016/j.ajic.2006.09.002

73. Sapat A, Esnard A-M, Kolpakov A. Understanding collaboration in disaster assistance networks: organizational homophily or resource dependency? *Am Rev Public Administration* (2019) 49:957–72. doi: 10.1177/0275074019861347

74. Al Khalaileh MA, Bond E, Alasad J. Jordanian Nurses' perceptions of their preparedness for disaster management. *Asian Pac J Cancer Prev* (2012) 20:14–23. doi: 10.1016/j.ienj.2011.01.001

75. Kichloo A, Albosta M, Dettloff K, Wani F, El-Amir Z, Singh J, et al. Telemedicine, the current COVID-19 pandemic and the future: a narrative review and perspectives moving forward in the USA. *Fam Med Community Health* (2020) 8:e000530. doi: 10.1136/fmch-2020-000530

76. Langan JC, Lavin R, Wolgast KA, Veenema TG. Education for developing and sustaining a health care workforce for disaster readiness. *The American Review of Public Administration* (2017) 41:118–27. doi: 10.1097/NAQ.0000000000000225

77. Veenema TG. Expanding educational opportunities in disaster response and emergency preparedness for nurses. *Nurs Educ Perspect* (2006) 27:93–9.

78. Duffy JR. *Quality caring in nursing and health systems: implications for clinicians, educators, and leaders*. Springer Publishing Company (2022).

Frontiers in Pharmacology

Explores the interactions between chemicals and living beings

The most cited journal in its field, which advances access to pharmacological discoveries to prevent and treat human disease.

Discover the latest Research Topics

See more →

Frontiers

Avenue du Tribunal-Fédéral 34
1005 Lausanne, Switzerland
frontiersin.org

Contact us

+41 (0)21 510 17 00
frontiersin.org/about/contact